Environmental Measurements in the Beaufort Sea, Spring 1986

APL-UW 4-86
January 1987

Informal Document Series

Approved for Public Release; Distribution is Unlimited

Contract N00024-85-C-6264

Environmental Measurements in the Beaufort Sea, Spring 1986

by
G. R. Garrison
T. Wen
R. E. Francois
W. J. Felton
M. L. Welch

APL-UW 4-86
January 1987

Informal Document Series

Applied Physics Laboratory University of Washington
Seattle, Washington 98105

Approved for Public Release; Distribution is Unlimited

Contract N00024-85-C-6264

ACKNOWLEDGMENTS

This research was supported by the Office of Naval Technology (ONT) with technical management provided by the Naval Ocean Research and Development Activity (NORDA).

We appreciate the weather station provided by Ron Lindsay of our Polar Science Center, the satellite images provided by Greta Burger and Kristina Ahlnäs of the Geophysical Institute, University of Alaska, and the NAVSAT transmissions which resulted in excellent positioning data.

CONTENTS

LIST OF FIGURES

LIST OF TABLES

ABSTRACT

Environmental measurements at an ice camp in the Beaufort Sea are reported for the period 20 March to 2 May 1986. The measurements include weather, floe movement, CTD profiles, ice properties, currents relative to the floe, and underwater noise.

I. INTRODUCTION

This report presents environmental data taken in the spring of 1986 at ice camp APLIS in the Beaufort Sea, where research and test activities were conducted by many research organizations as part of ICEX 1-86, a research program sponsored by the U.S. Navy. The environmental measurements were made by personnel from the Applied Physics Laboratory, University of Washington, as part of the APL arctic environmental acoustics program. APL was also responsible for camp logistics, including selection of the site and air transport operations associated with the camp's erection and evacuation as well as day to day operations in support of research activities.

The air search for an ice floe of suitable size and location for the camp was aided by satellite imagery. After the camp was occupied, the location of the floe was monitored by use of a NAVSAT receiver. The rotation of the floe was determined from daily sightings on the sun or moon.

Throughout the occupancy of the camp, weather data (air temperature and pressure, wind velocity and direction) were recorded hourly. The weather records show the high variability of arctic weather, with temperatures from -40°F to +10°F. During setup of the camp, before formal weather recording was begun, overnight temperatures as low as -45° were observed. Occasionally, high winds produced bothersome snow drifts, but no storms were severe enough to shut down normal camp activities.

To study water properties, CTD casts were taken from the camp to a depth of 300 m once or twice each day. The usual 300 m casts were supplemented by a special cast to 1500 m near the end of operations. Some water samples were also taken for salinity and pH analysis. Currents relative to the ice were measured at various depths to 100 m. These results can be compared with similar measurements[1–5] during earlier studies in the Chukchi and Beaufort seas.

To detect biological scattering layers, acoustic pulses were transmitted downward through the water column. The same echo sounder was used as in the fall of 1984, when large populations of acoustic scatterers and fish were observed. This time, in April, no appreciable layers were found.

The underwater noise level during camp operations was monitored every day or so. The noise of snowmobiles and other equipment was obvious, but the general background noise was difficult to relate to specific noise sources. The general stability of the floe and surroundings led to a decrease in the noise level compared with the fall of 1984.

These environmental measurements are discussed in the following sections. Times given in this report are either Greenwich Mean Time (GMT) or Local Civil Time (LCT). At APLIS, LCT equals GMT minus 9 hours. The time reference in use is usually stated.

II. THE ICE FLOE

An ice floe suitable for a 2-month camp and the exercises was found after a considerable air search of an area 100 to 200 miles off the coast between Prudhoe Bay and Barter Island.

A. Locating a Suitable Floe

There were several requirements for the ice floe. With all support by air, the distance from Prudhoe Bay and Barter Island was limited to 250 miles, but an effort was made to keep the distance under about 150 miles. The Navy exercises required a multiyear floe about 5 miles long and 3 miles wide, and an ice thickness of 6 ft was considered necessary for stability and endurance. A refrozen lead, at least 5000 ft long and at least 50 in. thick, was required to develop a landing strip suitable for C-130 aircraft. With a prevailing easterly wind, the site had to be somewhat to the east to allow for an expected drift westward. A requirement for deep water kept the site well away from the coast. In late February through early April, the ice cover in this area was nearly 100%, with very few small cracks observed on aircraft flights from the shore base out to the camp. After the first 50 miles out from land, the ice cover was about one-half old ice (ice from previous seasons) that was estimated (and measured at candidate sites) to be greater than 6 ft thick. The remainder was first-year ice, with a thickness generally less than 4 ft, depending on the date of initial ice formation and deformation history.

In both Fall 1984 and Spring 1986, satellite images (NOAA and LANDSAT) were obtained through the Geophysical Institute at the University of Alaska to help locate a suitable floe. In the fall, the images were very helpful, showing a few scattered old floes surrounded by thin ice or water.[6] In the spring, with the ice cover nearly 100%, the images were not so useful. The relative thickness was difficult to estimate from the LANDSAT images. However, using a careful selection of frequency and enhancement techniques, Geophysical Institute personnel were able to provide some helpful images which allowed differentiation between seasonal and multiyear ice. Figure 1 shows a LANDSAT image of the site taken after the camp was established. At the scale of the images, a 5 x 3 mile floe appeared quite small and there were many of them; thus the search team had a choice of hundreds of floes, one of which appeared much like another. In February and early March, an air search was conducted at low altitude with experienced ice observers to provide a better estimate of ice thickness. Landings were made by a ski-equipped Twin Otter aircraft at seven sites that met general requirements, and the

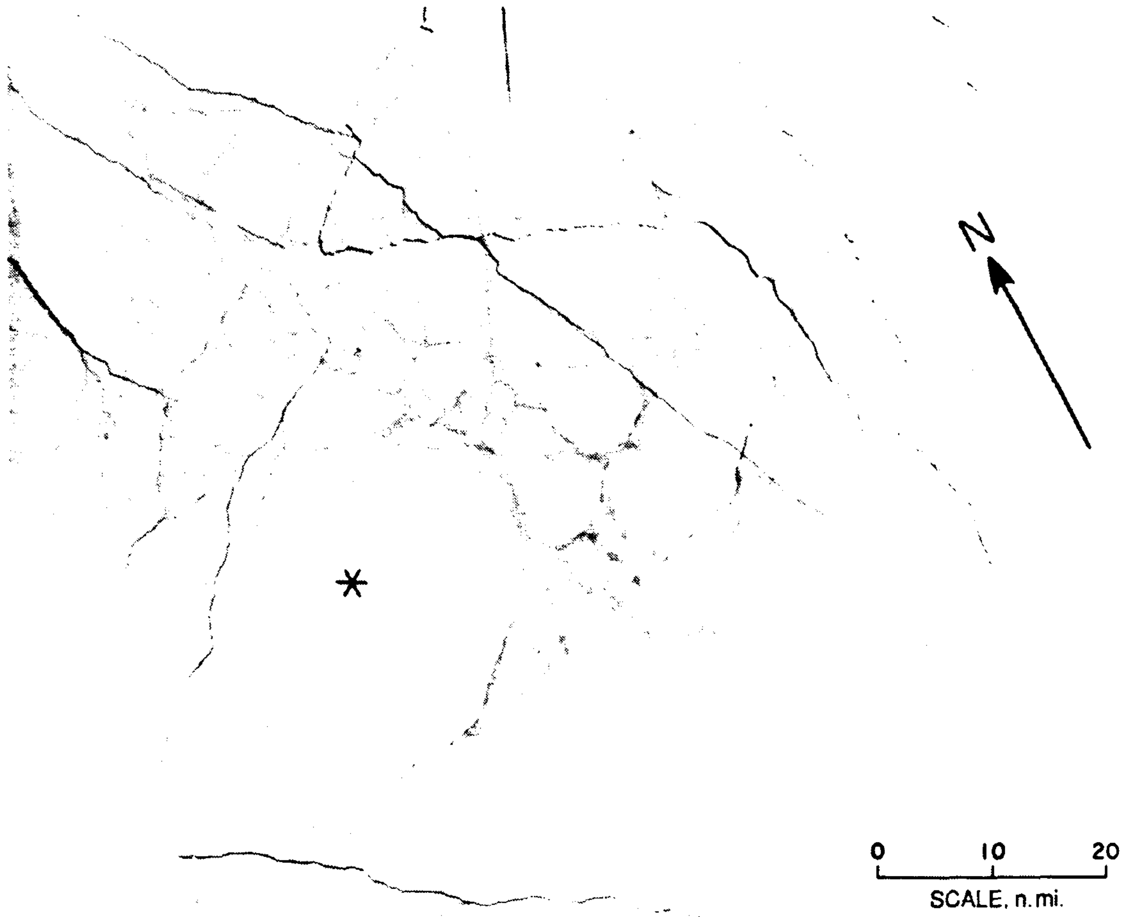

Figure 1. Satellite image of the area surrounding the Spring 1986 ice camp (∗). (LANDSAT-4, band 4, P71, R9, 11 April 1986)

ice thickness was measured by drilling at each site. The APLIS site was selected after considering the suitability of the snow cover for developing a runway and the availability of nearby alternate sites in case of floe failure.

The location and eventual drift of the floe selected are shown in Figure 2 along with the drift of camps in 1984 and 1985 for comparison.

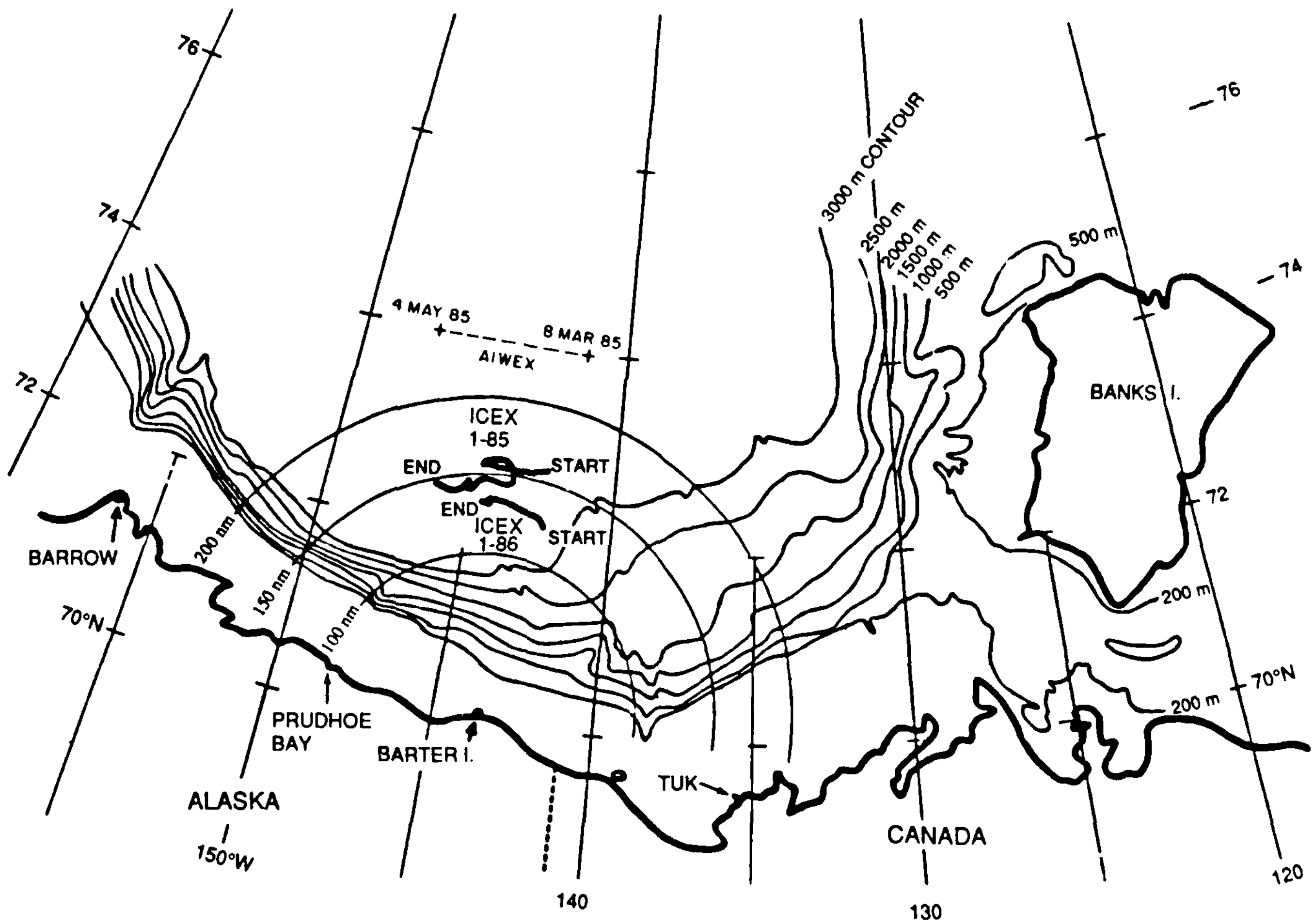

Figure 2. Drift of the ice camp compared with the drift of previous camps.

B. Floe Characteristics

The floe selected for the experiments was 30 n.mi. long and 20 n.mi. wide. The upper surface of the ice near the camp, shown in an aerial view in Figure 3, was fairly smooth and uniform, which was desirable for camp layout and construction. The camp was constructed on ice 14 ft thick. About 400 yd away was a refrozen lead with a uniform thickness of 53 in. ± 2 in. which was used as a landing strip for aircraft.

During various tests, several large holes were drilled through the ice at scattered locations over the floe. The mean depth recorded for these holes was 7.6 ft (standard deviation 2.9 ft), with a maximum hole depth of 20 ft and a minimum of 4 ft. At all of

Figure 3. Aerial view of the camp buildings.

these sites, an attempt was made to drill through the thinnest-looking spot within 50 ft or so of an indicated position. Before 9 April, the ice floe was essentially intact and stationary, although some local cracking took place in the thinner areas around the APLIS floe. In late April, some small cracks occurred in the thicker ice of the main floe. Eventually, several leads opened up in the thinner ice of the runway, which required repositioning and shortening the landing strip.

Many hours of under-ice profiling were performed by two submarines with narrowbeam, upward-looking sonars. These data were recorded digitally and are being processed by the Arctic Submarine Laboratory. (Unfortunately, the data from one of the submarines are probably unusable due to a problem with the recording system.) In addition, submarine personnel noted all keels 35 ft deep or deeper. The location of these keels relative to the grid coordinate system (Figure 4) established at the ice camp is plotted in Figure 5. The ice camp's location is indicated with a symbol at the grid origin. The profiling submarine ran parallel to either the x or y axis of the grid. Runs were not uniformly spaced and did not extend beyond the 4 × 9 mile area of the plotted points. The depth distribution curve shown in Figure 6 includes four keels as deep as 94 ft. Of the 4839 keels observed, 50% had drafts greater than 41 ft, 10% drafts greater than 56 ft, and 1% greater than 75 ft. If we assume that the sample distribution is uniform, the mean distance between the reported keels would be 160 m. The surface topography in the surveyed area was similar to that of the entire floe; thus the distribution of keel depths may be typical of the floe as a whole.

C. Floe Drift

The position of APLIS was obtained from a NAVSAT receiver (Furuno Model FSN-80) which stored data from the preceding 20 satellite passes. Five satellites were in operation. With each orbiting about 14 times per day, there was a possibility of 70 fixes per day. About 40 per day were actually recorded. Every 10 hours or so, the data were copied into a notebook along with the elevation angle of the satellite at the time the data were taken. All the data recorded at the camp were later processed at the Laboratory.

In processing the NAVSAT data, we first checked to determine if outliers corresponded to high satellite elevation angles, a correlation seen in 1984.[6] At that time, data for elevation angles greater than 80° were omitted in the processing. In preliminary plots of the present data, we found that over 80% of the longitude values for satellite elevation angles greater than 60° were outliers. We decided to be more restrictive than in 1984 and discard all data from passes with elevation angles greater than 60°.

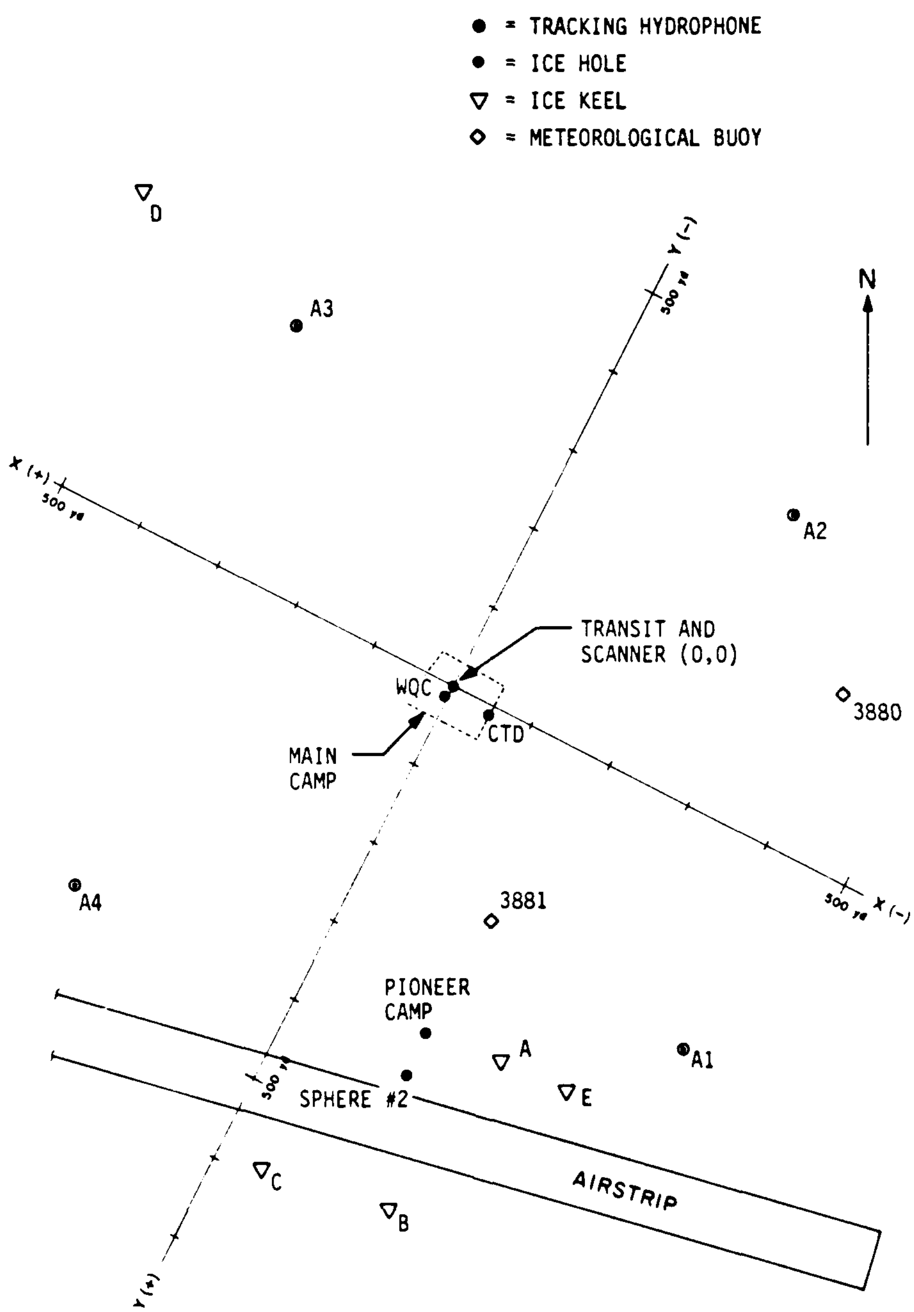

Figure 4. Camp layout, showing grid coordinate system.

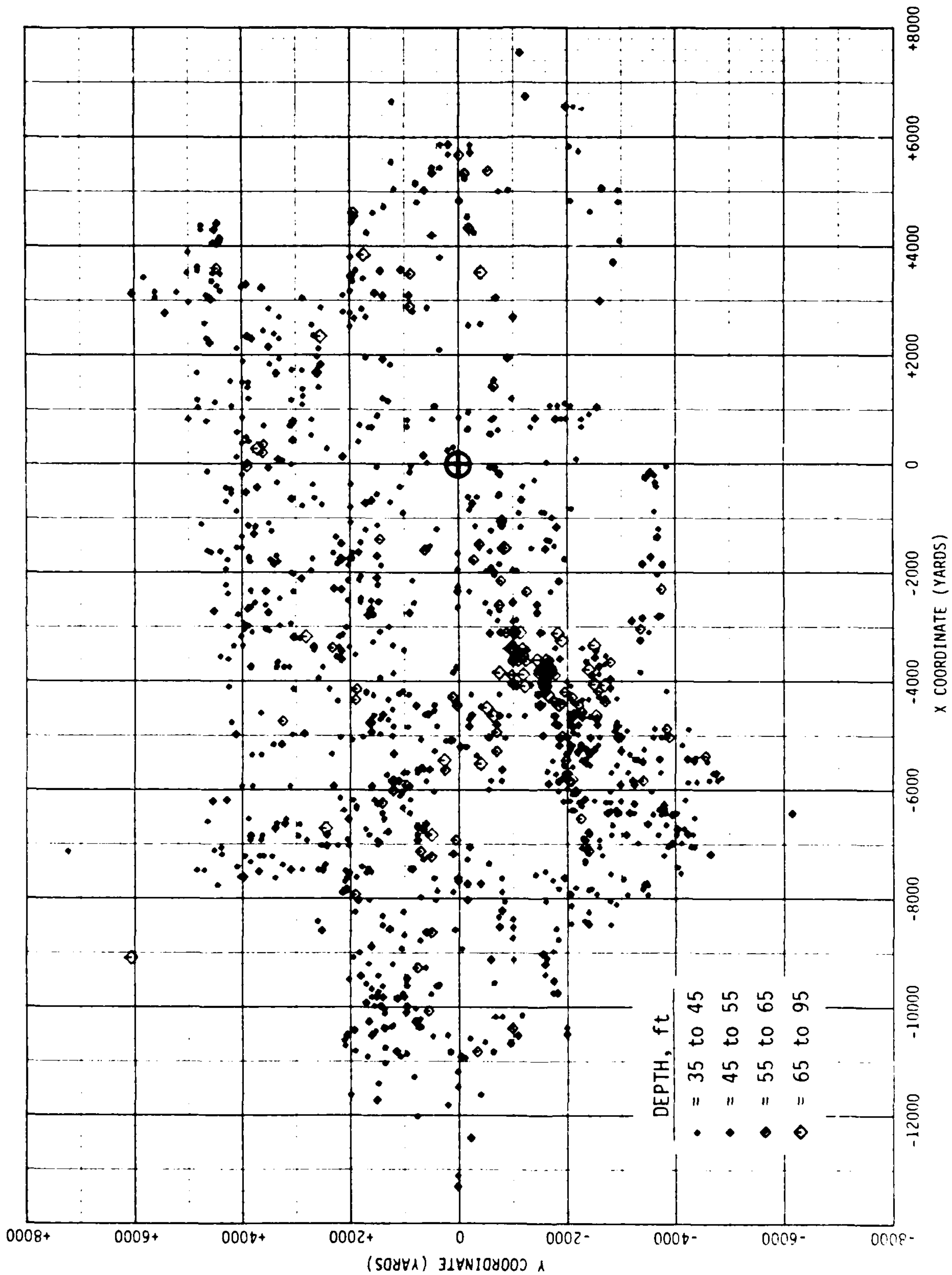

Figure 5. Location of keels reported by a submarine with an under-ice profiler (depths of 35 ft and greater).

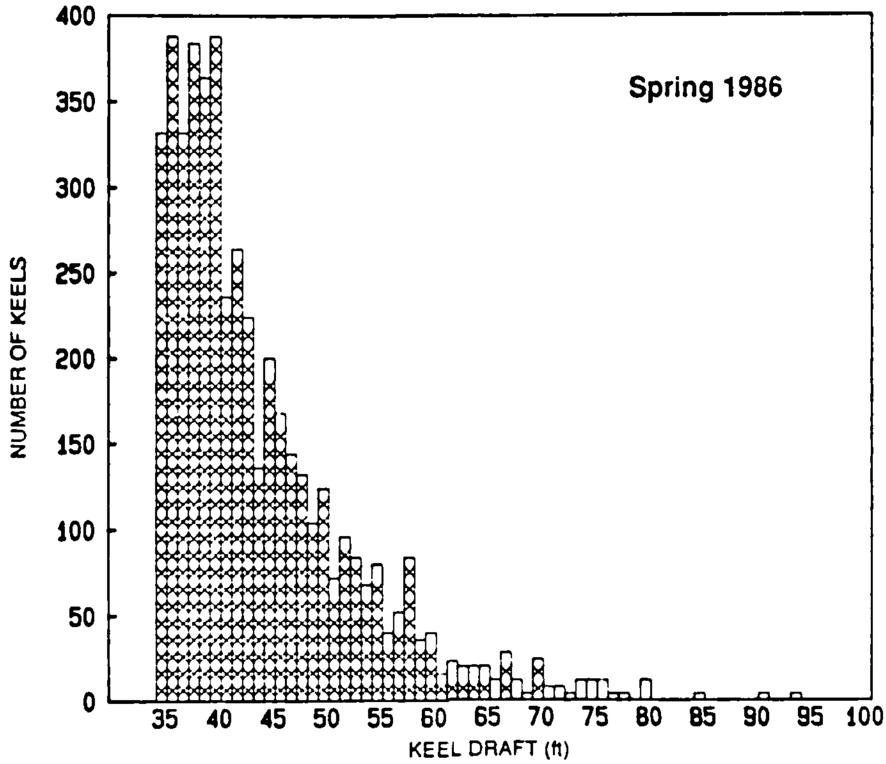

Figure 6. Distribution curve of keel depths reported during under-ice profiling (depths of 35 ft and greater).

The NAVSAT fixes indicated that the camp was virtually stationary from 9 March through 8 April. After the data with high elevation angles were discarded, the mean and standard deviation (σ) of the longitudes and latitudes recorded for this time period were computed to check the accuracy of the data. The values were as follows:

		σ (min. of arc)	σ (n.mi.)
Latitude	72° 8.74′	0.054	0.054
Longitude	142° 11.31′	0.276	0.094

Latitude or longitude values more than 3σ from the computed mean value for this time period were considered to be outliers and were not used in subsequent calculations. For times when the floe was moving, position data were discarded only if their displacement from an average line through adjacent data was decidedly more than the 3σ value computed for the stationary camp. Figure 7 shows a sample plot of the latitude and longitude readings versus time for satellite orbits of 60° or less for one day at the camp. The plots for all days that data were recorded at the final antenna position are presented in Appendix A. (The NAVSAT system was originally set up at a temporary camp adjacent

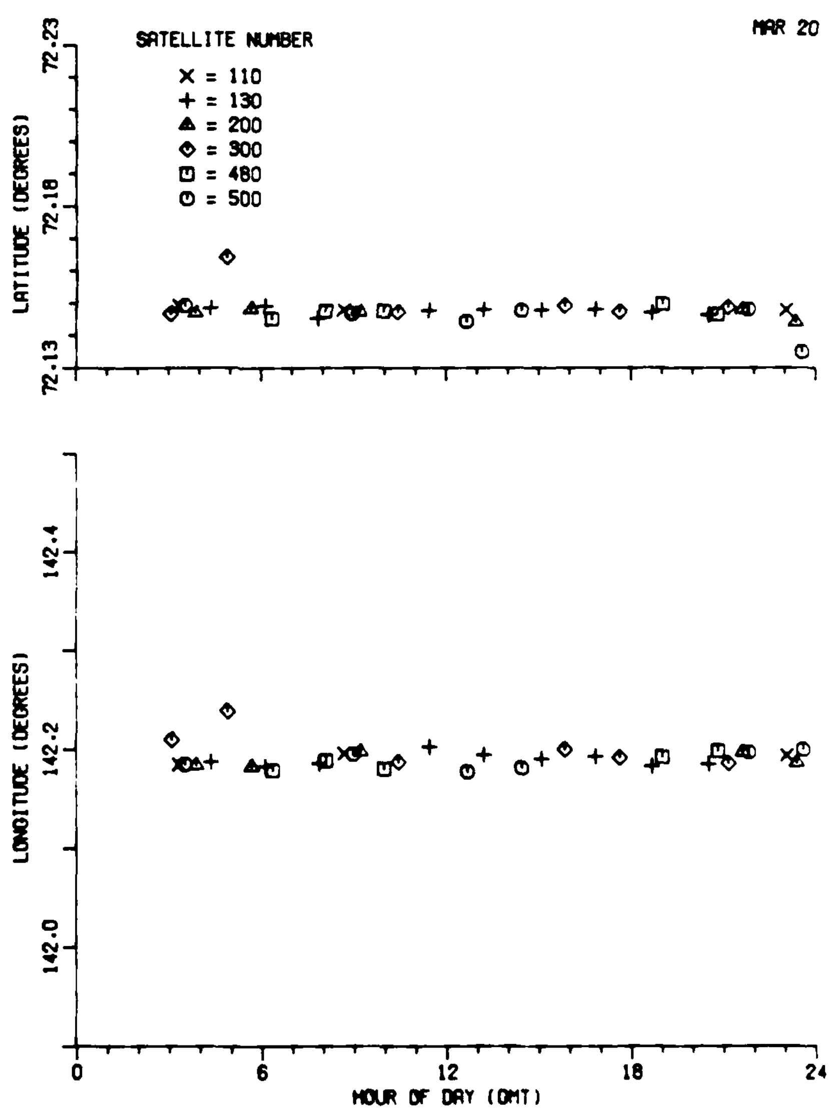

Figure 7.
NAVSAT fixes during one day of the ice camp's occupancy.

to the runway and 400 yd removed from the main APLIS camp; no data have been plotted for this period.) The circled symbols for 25 March through 8 April indicate that either the latitude or the longitude plot showed an outlier (during this time, the camp did not move).

After all elevation angles greater than 60° were discarded to omit outliers, the NAVSAT fixes were used to determine the camp's location and the speed and direction of drift. The average camp coordinates were computed by taking running averages of 12 consecutive fixes, shifting 4 fixes between calculations. The average latitude or longitude was assigned a time equal to the average time for the 12 fixes. This process is illustrated in Figure 8 for the latitude calculations. For each set of 12 fixes, a slope was assigned based on the previous and following 12-fix averages. The slopes from the latitude and longitude calculations for a given 12-fix average were used to calculate speed and direction of drift. (These values were not calculated if the coordinates computed for the previous and following 12-fix sets were less than 0.1 n.mi. apart.)

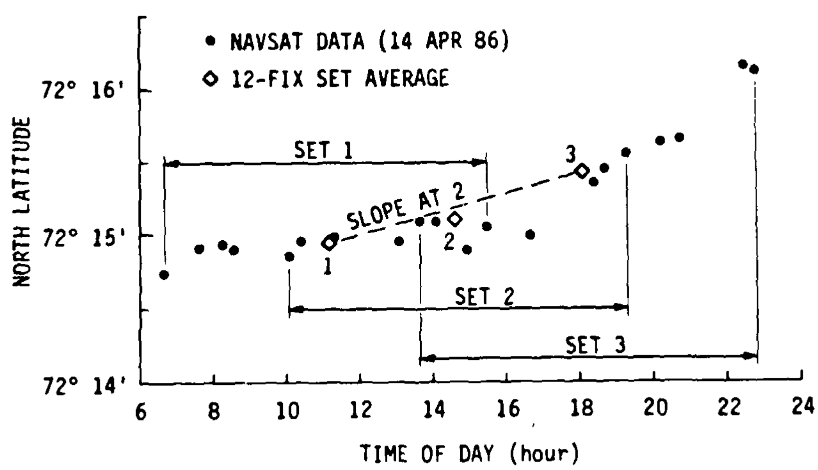

Figure 8. Illustration of the calculation of average values for three overlapping sets of 12 fixes and the average slope assigned to the middle value.

The average camp coordinates, along with speed and direction of drift, are listed in Table I. These coordinates are plotted in Figure 9. The drift of this ice camp is compared with the drift of previous camps in the fall of 1984 and spring of 1985 in Figure 2.

Table I. Average track computed from NAVSAT fixes. Drift speed and direction were not calculated when the apparent movement was less than 0.1 n.mi.

DATE	TIME (GMT)	LATITUDE (DEG)	LATITUDE (MIN)	LONGITUDE (DEG)	LONGITUDE (MIN)	SPEED (KNOT)	DIR. (TRUE)
MAR 20	0620	72	8.86	142	11.27		
MAR 20	0847	72	8.82	142	11.31		
MAR 20	1130	72	8.84	142	11.49		
MAR 20	1436	72	8.86	142	11.40		
MAR 20	1754	72	8.87	142	11.50		
MAR 20	2043	72	8.83	142	11.48		
MAR 20	2334	72	8.82	142	11.47		
MAR 21	0216	72	8.79	142	11.39		
MAR 21	0518	72	8.77	142	11.28		
MAR 21	0848	72	8.73	142	11.38		
MAR 21	1408	72	8.74	142	11.46		
MAR 21	2021	72	8.76	142	11.47		
MAR 22	0204	72	8.76	142	11.31		
MAR 22	0550	72	8.78	142	11.29		
MAR 22	0852	72	8.77	142	11.40		
MAR 22	1142	72	8.79	142	11.46		
MAR 22	1524	72	8.80	142	11.48		
MAR 22	1922	72	8.81	142	11.48		
MAR 22	2325	72	8.81	142	11.48		
MAR 23	0229	72	8.80	142	11.39		
MAR 23	0512	72	8.79	142	11.37		
MAR 23	0815	72	8.78	142	11.35		
MAR 23	1132	72	8.77	142	11.38		
MAR 23	1440	72	8.78	142	11.30		
MAR 23	1733	72	8.78	142	11.34		
MAR 23	2035	72	8.79	142	11.33		
MAR 24	0013	72	8.79	142	11.39		
MAR 24	0326	72	8.79	142	11.36		
MAR 24	0635	72	8.76	142	11.33		
MAR 24	0859	72	8.74	142	11.30		
MAR 24	1125	72	8.75	142	11.31		
MAR 24	1343	72	8.75	142	11.32		
MAR 24	1612	72	8.77	142	11.47		
MAR 24	1859	72	8.78	142	11.50		
MAR 24	2150	72	8.78	142	11.50		
MAR 25	0046	72	8.75	142	11.45		
MAR 25	0411	72	8.72	142	11.46		
MAR 25	0735	72	8.73	142	11.46		
MAR 25	1052	72	8.74	142	11.36		
MAR 25	1322	72	8.75	142	11.36		
MAR 25	1612	72	8.76	142	11.36		
MAR 25	1905	72	8.76	142	11.40		
MAR 25	2210	72	8.76	142	11.34		
MAR 26	0051	72	8.73	142	11.29		
MAR 26	0357	72	8.72	142	11.27		
MAR 26	0706	72	8.73	142	11.31		
MAR 26	1012	72	8.74	142	11.41		
MAR 26	1234	72	8.74	142	11.38		
MAR 26	1444	72	8.74	142	11.37		
MAR 26	1658	72	8.75	142	11.37		
MAR 26	1913	72	8.75	142	11.40		
MAR 26	2133	72	8.75	142	11.38		
MAR 27	0016	72	8.74	142	11.35		
MAR 27	0412	72	8.75	142	11.33		
MAR 27	0853	72	8.76	142	11.35		
MAR 27	1321	72	8.74	142	11.36		
MAR 27	1659	72	8.74	142	11.39		
MAR 27	2015	72	8.72	142	11.38		
MAR 27	2342	72	8.73	142	11.46		
MAR 28	0256	72	8.71	142	11.44		
MAR 28	0545	72	8.72	142	11.42		
MAR 28	0822	72	8.72	142	11.32		
MAR 28	1050	72	8.74	142	11.27		
MAR 28	1314	72	8.74	142	11.21		
MAR 28	1552	72	8.75	142	11.22		
MAR 28	1848	72	8.74	142	11.29		
MAR 28	2152	72	8.75	142	11.38		
MAR 29	0024	72	8.73	142	11.44		
MAR 29	0248	72	8.74	142	11.38		
MAR 29	0511	72	8.74	142	11.28		
MAR 29	0741	72	8.72	142	11.18		
MAR 29	1037	72	8.72	142	11.24		
MAR 29	1354	72	8.70	142	11.43		
MAR 29	1735	72	8.70	142	11.47		
MAR 29	2056	72	8.71	142	11.41		
MAR 29	2356	72	8.73	142	11.26		
MAR 30	0311	72	8.75	142	11.28		
MAR 30	0614	72	8.74	142	11.31		
MAR 30	0923	72	8.73	142	11.37		
MAR 30	1158	72	8.74	142	11.28		
MAR 30	1435	72	8.75	142	11.30		
MAR 30	1705	72	8.74	142	11.27		
MAR 30	1930	72	8.74	142	11.38		
MAR 30	2148	72	8.75	142	11.36		
MAR 31	0001	72	8.76	142	11.30		
MAR 31	0207	72	8.76	142	11.23		
MAR 31	0415	72	8.75	142	11.22		
MAR 31	0644	72	8.76	142	11.38		
MAR 31	0931	72	8.75	142	11.44		
MAR 31	1259	72	8.74	142	11.45		
MAR 31	1716	72	8.73	142	11.31		
MAR 31	2214	72	8.73	142	11.27		
APR 1	0256	72	8.72	142	11.17		
APR 1	0650	72	8.74	142	11.30		
APR 1	0956	72	8.75	142	11.27		
APR 1	1228	72	8.75	142	11.31		
APR 1	1521	72	8.74	142	11.17		
APR 1	1847	72	8.74	142	11.27		
APR 1	2221	72	8.75	142	11.30		
APR 2	0111	72	8.76	142	11.36		
APR 2	0350	72	8.77	142	11.28		
APR 2	0639	72	8.76	142	11.26		
APR 2	0950	72	8.76	142	11.22		
APR 2	1256	72	8.75	142	11.25		
APR 2	1625	72	8.75	142	11.28		
APR 2	2013	72	8.73	142	11.33		
APR 2	2348	72	8.73	142	11.34		
APR 3	0231	72	8.72	142	11.29		
APR 3	0428	72	8.75	142	11.19		
APR 3	0614	72	8.73	142	11.12		
APR 3	0814	72	8.75	142	11.16		
APR 3	1020	72	8.74	142	11.25		
APR 3	1222	72	8.75	142	11.20		
APR 3	1406	72	8.74	142	11.22		
APR 3	1600	72	8.75	142	11.23		
APR 3	1757	72	8.74	142	11.29		
APR 3	2017	72	8.73	142	11.26		
APR 3	2228	72	8.73	142	11.21		
APR 4	0104	72	8.73	142	11.22		
APR 4	0417	72	8.74	142	11.30		
APR 4	0753	72	8.74	142	11.36		
APR 4	1135	72	8.74	142	11.39		
APR 4	1544	72	8.74	142	11.39		
APR 4	2002	72	8.75	142	11.23		
APR 4	2356	72	8.75	142	11.25		
APR 5	0239	72	8.75	142	11.15		
APR 5	0515	72	8.74	142	11.27		
APR 5	0801	72	8.74	142	11.25		
APR 5	1048	72	8.73	142	11.27		
APR 5	1313	72	8.75	142	11.20		
APR 5	1633	72	8.74	142	11.17		
APR 5	2006	72	8.75	142	11.21		
APR 5	2332	72	8.75	142	11.26		
APR 6	0139	72	8.75	142	11.26		
APR 6	0350	72	8.74	142	11.22		
APR 6	0642	72	8.75	142	11.25		
APR 6	1009	72	8.75	142	11.32		
APR 6	1325	72	8.76	142	11.30		
APR 6	1627	72	8.74	142	11.30		
APR 6	1915	72	8.74	142	11.22		
APR 6	2204	72	8.73	142	11.29		
APR 7	0034	72	8.74	142	11.32		
APR 7	0249	72	8.74	142	11.35		
APR 7	0454	72	8.75	142	11.38		
APR 7	0722	72	8.73	142	11.29		
APR 7	0953	72	8.73	142	11.30		
APR 7	1233	72	8.72	142	11.28		
APR 7	1457	72	8.74	142	11.39		
APR 7	1746	72	8.74	142	11.38		
APR 7	2044	72	8.74	142	11.49		
APR 7	2340	72	8.75	142	11.35		
APR 8	0214	72	8.75	142	11.35		
APR 8	0509	72	8.74	142	11.27		
APR 8	0805	72	8.72	142	11.35		
APR 8	1059	72	8.72	142	11.38		
APR 8	1333	72	8.74	142	11.37		
APR 8	1639	72	8.74	142	11.35		
APR 8	2001	72	8.72	142	11.32		
APR 8	2324	72	8.71	142	11.26		
APR 9	0227	72	8.68	142	11.20		
APR 9	0519	72	8.70	142	11.22		
APR 9	0824	72	8.70	142	11.28		
APR 9	1120	72	8.74	142	11.35	.02	317
APR 9	1534	72	8.79	142	11.55	.04	323
APR 9	1923	72	8.97	142	11.92	.07	331
APR 9	2326	72	9.28	142	12.42	.11	332
APR 10	0210	72	9.61	142	13.00	.13	331
APR 10	0458	72	9.90	142	13.52	.12	328
APR 10	0725	72	10.16	142	14.08	.12	321
APR 10	1001	72	10.36	142	14.71	.11	315
APR 10	1226	72	10.56	142	15.37	.10	313
APR 10	1446	72	10.69	142	15.86	.09	313
APR 10	1645	72	10.84	142	16.33	.10	310
APR 10	1850	72	10.97	142	16.91	.11	302

Table I, cont.

DATE	TIME (GMT)	LATITUDE (DEG)(MIN)	LONGITUDE (DEG)(MIN)	SPEED (KNOT)	DIR. (TRUE)
APR 10	2108	72 11.11	142 17.69	.11	302
APR 10	2323	72 11.24	142 18.30	.10	304
APR 11	0119	72 11.33	142 18.76	.08	304
APR 11	0259	72 11.39	142 19.03	.05	293
APR 11	0453	72 11.41	142 19.33	.04	278
APR 11	0714	72 11.42	142 19.51	.03	271
APR 11	1001	72 11.41	142 19.78		
APR 11	1230	72 11.39	142 19.72		
APR 11	1444	72 11.37	142 19.70		
APR 11	1633	72 11.34	142 19.62		
APR 11	1823	72 11.36	142 19.63		
APR 11	2008	72 11.37	142 19.68		
APR 11	2159	72 11.39	142 19.70		
APR 12	0021	72 11.39	142 19.74		
APR 12	0341	72 11.36	142 19.62		
APR 12	0712	72 11.37	142 19.65		
APR 12	1027	72 11.37	142 19.72	.05	300
APR 12	1414	72 11.55	142 20.67	.13	304
APR 12	2033	72 12.08	142 23.19	.16	303
APR 13	0322	72 12.71	142 26.48	.18	300
APR 13	0844	72 13.20	142 29.34	.19	295
APR 13	1118	72 13.35	142 30.81	.18	286
APR 13	1352	72 13.46	142 32.26	.20	283
APR 13	1649	72 13.60	142 34.26	.23	283
APR 13	1954	72 13.78	142 36.59	.27	286
APR 13	2238	72 14.04	142 39.13	.31	290
APR 14	0057	72 14.33	142 41.31	.31	292
APR 14	0317	72 14.60	142 43.49	.29	289
APR 14	0526	72 14.77	142 45.40	.30	280
APR 14	0808	72 14.87	142 48.17	.33	275
APR 14	1111	72 14.96	142 51.63	.38	275
APR 14	1441	72 15.11	142 56.27	.42	279
APR 14	1808	72 15.43	143 .99	.45	286
APR 14	2140	72 15.99	143 6.25	.48	293
APR 15	0128	72 16.83	143 11.57	.47	296
APR 15	0534	72 17.66	143 17.05	.43	295
APR 15	0917	72 18.29	143 21.46	.37	292
APR 15	1209	72 18.60	143 24.55	.33	286
APR 15	1438	72 18.78	143 27.01	.31	281
APR 15	1721	72 18.93	143 29.70	.31	278
APR 15	2004	72 19.05	143 32.46	.32	278
APR 15	2235	72 19.17	143 35.08	.32	279
APR 16	0036	72 19.29	143 37.16	.31	283
APR 16	0245	72 19.46	143 39.21	.28	285
APR 16	0521	72 19.65	143 41.42	.26	285
APR 16	0814	72 19.83	143 43.71	.25	283
APR 16	1105	72 19.98	143 45.92	.23	282
APR 16	1342	72 20.10	143 47.78	.24	278
APR 16	1649	72 20.17	143 50.33	.26	274
APR 16	2028	72 20.24	143 53.64	.29	273
APR 16	2359	72 20.28	143 57.11	.30	272
APR 17	0331	72 20.34	144 .64	.29	271
APR 17	0649	72 20.35	144 3.66	.27	269
APR 17	0955	72 20.32	144 6.34	.25	267
APR 17	1218	72 20.28	144 8.13	.22	266
APR 17	1424	72 20.25	144 9.54	.20	261
APR 17	1651	72 20.14	144 11.16	.21	256
APR 17	1942	72 19.98	144 13.15	.22	254
APR 17	2233	72 19.80	144 15.20	.21	257
APR 18	0108	72 19.74	144 16.84	.15	263
APR 18	0354	72 19.71	144 17.87	.08	267
APR 18	0648	72 19.72	144 18.37	.04	261
APR 18	0929	72 19.68	144 18.60	.02	237
APR 18	1153	72 19.66	144 18.67	.02	210
APR 18	1430	72 19.58	144 18.77	.03	194
APR 18	1757	72 19.48	144 18.83	.04	201
APR 18	2121	72 19.36	144 19.07	.04	209
APR 19	0038	72 19.23	144 19.29	.04	204
APR 19	0320	72 19.16	144 19.37	.03	158
APR 19	0554	72 19.08	144 19.11	.04	128
APR 19	0807	72 19.04	144 18.87	.04	144
APR 19	1006	72 18.96	144 18.81	.04	169
APR 19	1218	72 18.86	144 18.75	.04	171
APR 19	1444	72 18.76	144 18.71	.04	169
APR 19	1706	72 18.67	144 18.64	.04	176
APR 19	1914	72 18.57	144 18.67	.05	189
APR 19	2127	72 18.45	144 18.75	.06	191
APR 20	0028	72 18.26	144 18.88	.05	198
APR 20	0343	72 18.13	144 19.10	.04	212
APR 20	0656	72 18.06	144 19.28	.02	227
APR 20	0930	72 18.05	144 19.40		
APR 20	1151	72 18.03	144 19.33	.02	133
APR 20	1402	72 17.97	144 19.13	.04	132
APR 20	1622	72 17.90	144 18.86	.05	138
APR 20	1859	72 17.78	144 18.57	.05	141
APR 20	2139	72 17.68	144 18.28	.05	129
APR 21	0021	72 17.60	144 17.86	.05	120

DATE	TIME (GMT)	LATITUDE (DEG)(MIN)	LONGITUDE (DEG)(MIN)	SPEED (KNOT)	DIR. (TRUE)
APR 21	0317	72 17.52	144 17.43	.04	118
APR 21	0628	72 17.47	144 17.07	.03	113
APR 21	0939	72 17.44	144 16.78	.02	92
APR 21	1250	72 17.46	144 16.56	.02	68
APR 21	1555	72 17.49	144 16.40		
APR 21	1855	72 17.50	144 16.27		
APR 21	2152	72 17.50	144 16.08	.03	93
APR 22	0052	72 17.49	144 15.78	.02	90
APR 22	0442	72 17.50	144 15.66		
APR 22	0825	72 17.52	144 15.60		
APR 22	1215	72 17.53	144 15.59		
APR 22	1533	72 17.57	144 15.61		
APR 22	1827	72 17.56	144 15.72		
APR 22	2055	72 17.62	144 15.76	.03	6
APR 22	2250	72 17.69	144 15.67	.06	25
APR 23	0041	72 17.81	144 15.46	.06	24
APR 23	0252	72 17.90	144 15.36	.03	23
APR 23	0501	72 17.94	144 15.27	.03	9
APR 23	0715	72 18.02	144 15.29	.04	342
APR 23	0925	72 18.10	144 15.44	.04	335
APR 23	1159	72 18.18	144 15.54	.02	307
APR 23	1528	72 18.18	144 15.76	.03	279
APR 23	1937	72 18.22	144 16.16	.04	291
APR 23	2338	72 18.29	144 16.67	.05	307
APR 24	0301	72 18.43	144 17.11	.05	319
APR 24	0545	72 18.54	144 17.37	.04	317
APR 24	0827	72 18.60	144 17.60	.04	310
APR 24	1057	72 18.66	144 17.85	.03	310
APR 24	1318	72 18.69	144 17.97		
APR 24	1539	72 18.67	144 18.02	.03	163
APR 24	1817	72 18.55	144 17.83	.07	154
APR 24	2102	72 18.35	144 17.52	.09	151
APR 24	2347	72 18.13	144 17.07	.09	151
APR 25	0234	72 17.90	144 16.71	.07	149
APR 25	0542	72 17.75	144 16.35	.05	139
APR 25	0901	72 17.66	144 16.03	.04	110
APR 25	1224	72 17.66	144 15.59	.04	89
APR 25	1532	72 17.67	144 15.14	.04	80
APR 25	1841	72 17.71	144 14.70	.04	73
APR 25	2159	72 17.74	144 14.32	.03	78
APR 26	0143	72 17.75	144 13.95	.03	82
APR 26	0509	72 17.76	144 13.66	.02	94
APR 26	0758	72 17.74	144 13.46		
APR 26	1037	72 17.75	144 13.33		
APR 26	1329	72 17.75	144 13.25		
APR 26	1625	72 17.78	144 13.05	.02	58
APR 26	1851	72 17.81	144 12.96		
APR 26	2118	72 17.77	144 13.03	.02	225
APR 27	0014	72 17.72	144 13.25	.02	226
APR 27	0527	72 17.64	144 13.50	.02	232
APR 27	1244	72 17.59	144 13.82	.02	246
APR 27	1953	72 17.54	144 14.22	.02	255
APR 28	0207	72 17.52	144 14.66	.02	257
APR 28	0625	72 17.50	144 14.92	.02	257
APR 28	1014	72 17.49	144 15.09		
APR 28	1235	72 17.51	144 15.09		
APR 28	1436	72 17.51	144 15.15		
APR 28	1635	72 17.51	144 15.14		
APR 28	1829	72 17.50	144 15.22		
APR 28	2016	72 17.52	144 15.27		
APR 28	2207	72 17.54	144 15.51	.05	288
APR 29	0008	72 17.58	144 15.90	.05	289
APR 29	0310	72 17.62	144 16.27	.03	293
APR 29	0638	72 17.66	144 16.49		
APR 29	1044	72 17.68	144 16.43		
APR 29	1508	72 17.67	144 16.61	.02	269
APR 29	1917	72 17.68	144 16.87	.03	275
APR 29	2256	72 17.70	144 17.41	.05	283
APR 30	0133	72 17.74	144 17.80	.05	293
APR 30	0355	72 17.79	144 18.12	.04	295
APR 30	0629	72 17.83	144 18.37	.02	294
APR 30	0905	72 17.84	144 18.46		
APR 30	1152	72 17.84	144 18.60		
APR 30	1445	72 17.82	144 18.70	.02	264
APR 30	1836	72 17.82	144 19.10	.04	283
APR 30	2255	72 17.89	144 19.67	.05	296
MAY 1	0312	72 18.01	144 20.31	.06	302
MAY 1	0716	72 18.17	144 21.12	.07	302
MAY 1	1058	72 18.28	144 21.75	.06	295
MAY 1	1434	72 18.37	144 22.49	.06	288
MAY 1	1720	72 18.40	144 22.93	.07	283
MAY 1	1955	72 18.45	144 23.61	.09	285
MAY 1	2219	72 18.51	144 24.28	.09	289
MAY 2	0039	72 18.59	144 24.96	.09	293
MAY 2	0254	72 18.67	144 25.49	.06	294
MAY 2	0453	72 18.69	144 25.70		
MAY 2	0657	72 18.69	144 25.80		
MAY 2	0908	72 18.68	144 25.76		

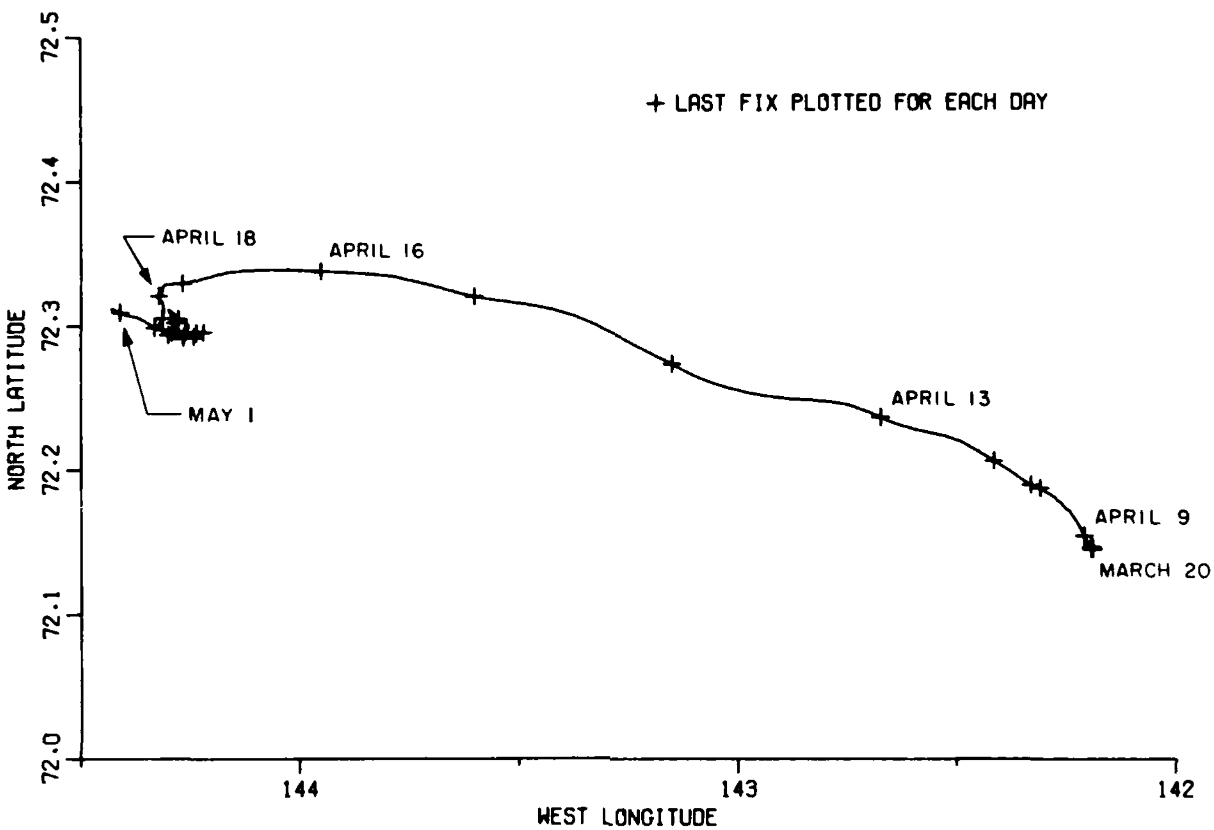

Figure 9. Drift of the ice camp during its occupancy.

D. Floe Orientation

The orientation of the floe was monitored by taking sightings on the sun and moon each day that one or the other was visible. A surveyor's transit was used for the sighting, with 90° set on a marker designating the direction of the x-axis of the grid coordinate system. A nautical almanac was used to determine the true bearing of the sun or moon at the time of the sighting. An HP-85 computer program was developed to expedite the calculations and reduce the chance of error.

In 27 days, we sighted the sun 36 times and the moon 4 times. The results of the two methods agreed to within 0.1°. These measurements of the true bearing of the y-axis are shown in Figure 10.

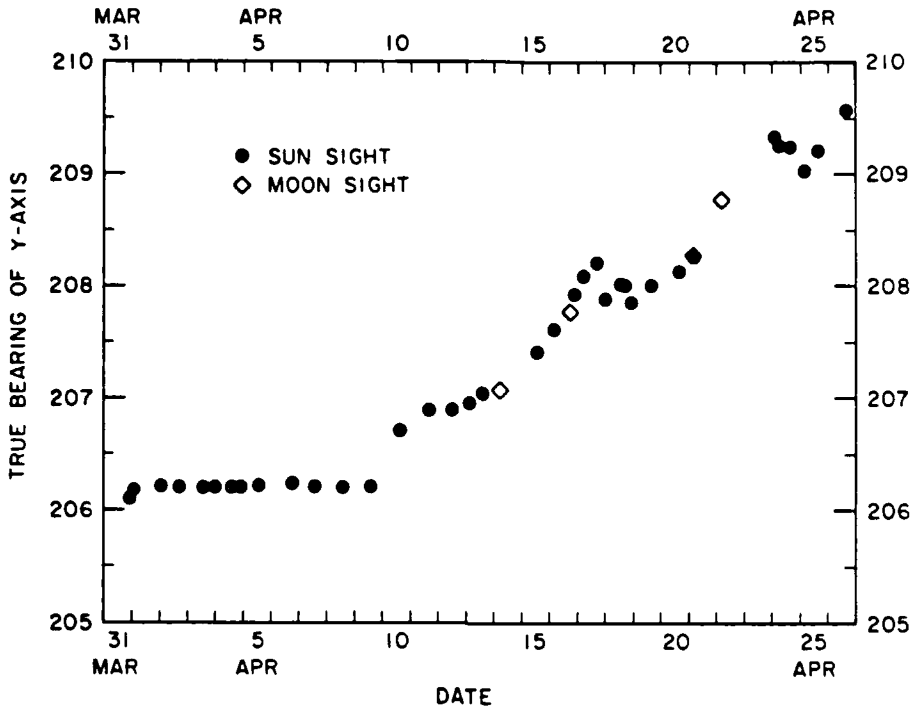

Figure 10. Orientation of the ice floe as determined from sightings on the sun and moon.

III. WEATHER

Weather conditions during the camp's occupancy were monitored by two meteorological buoys which measured wind speed and direction, air temperature, and atmospheric pressure, and transmitted the data via satellite link. The data were processed at Service Argos, Toulouse, France, and sent to the Laboratory on magnetic tape.

Buoy No. 3881 was deployed about 250 yd south of camp (see Figure 4) prior to 16 March. This buoy had a single anemometer and temperature sensor which were mounted on an aluminum mast. The anemometer was clamped to the top of the mast 3 m above the ice, and the temperature sensor was mounted 2.5 m above the ice. The base of the mast was bolted to a wooden 4 x 4 that was set into the ice. A housing next to the base contained a barometer and the satellite transmitter.

Buoy No. 3880 was deployed on 20 March about 400 yd east of the ice camp. It was installed on the tower shown in Figure 11. The anemometer atop the tower was 10 m above the ice. Two anemometers were mounted 3.6 m above the ice, and two temperature sensors (one shielded) were mounted 3 m above the ice. A housing near the tower's base contained a barometer and the satellite transmitter.

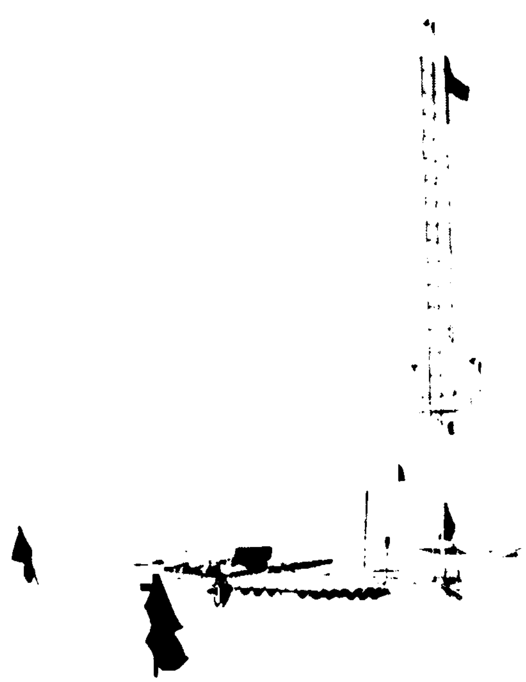

Figure 11.
Meteorological buoy No. 3880 installed at the ice camp.

The data collected by the two buoys are plotted in Figure 12 (English units) and Figure 13 (metric units). The wind and temperature data shown for Buoy No. 3880 are from the 10 m high anemometer and the shielded temperature sensor. No temperature data are plotted for Buoy No. 3881 as the sensor failed during shipment and remained inoperable.

With a few exceptions, camp activities were not adversely affected by the weather. Five days with temperatures approaching -35°F made field operation of equipment troublesome. Three days of 20-30 kn winds resulted in 2- to 4-ft high drifts of hard packed snow. Haze and ice fog at APLIS canceled out flights from the shore base for one day, 22 April.

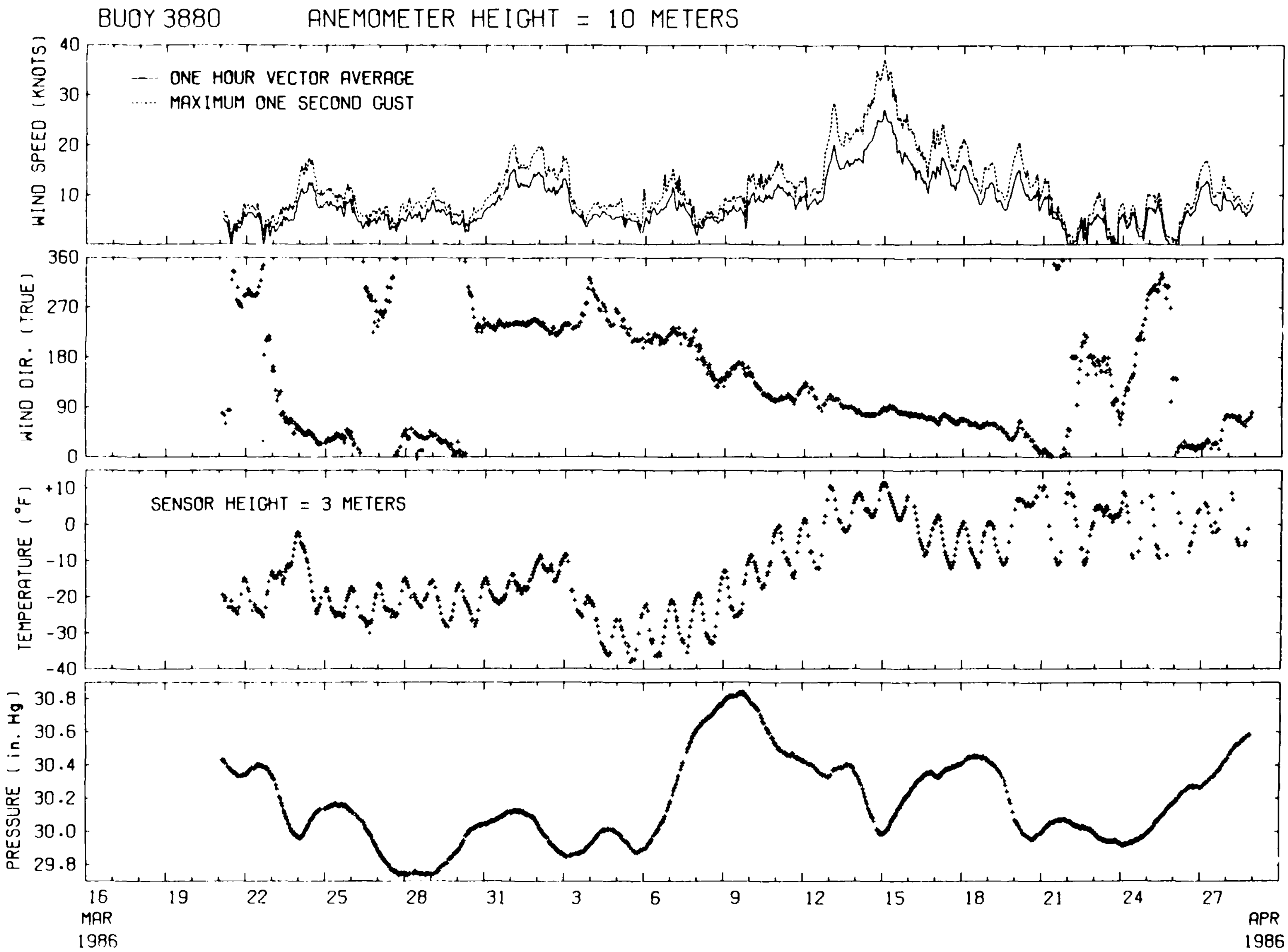

Figure 12a. *Weather measurements taken at APLIS ice camp using meteorological buoy No. 3880 (English units; see Figure 13 for metric units).*

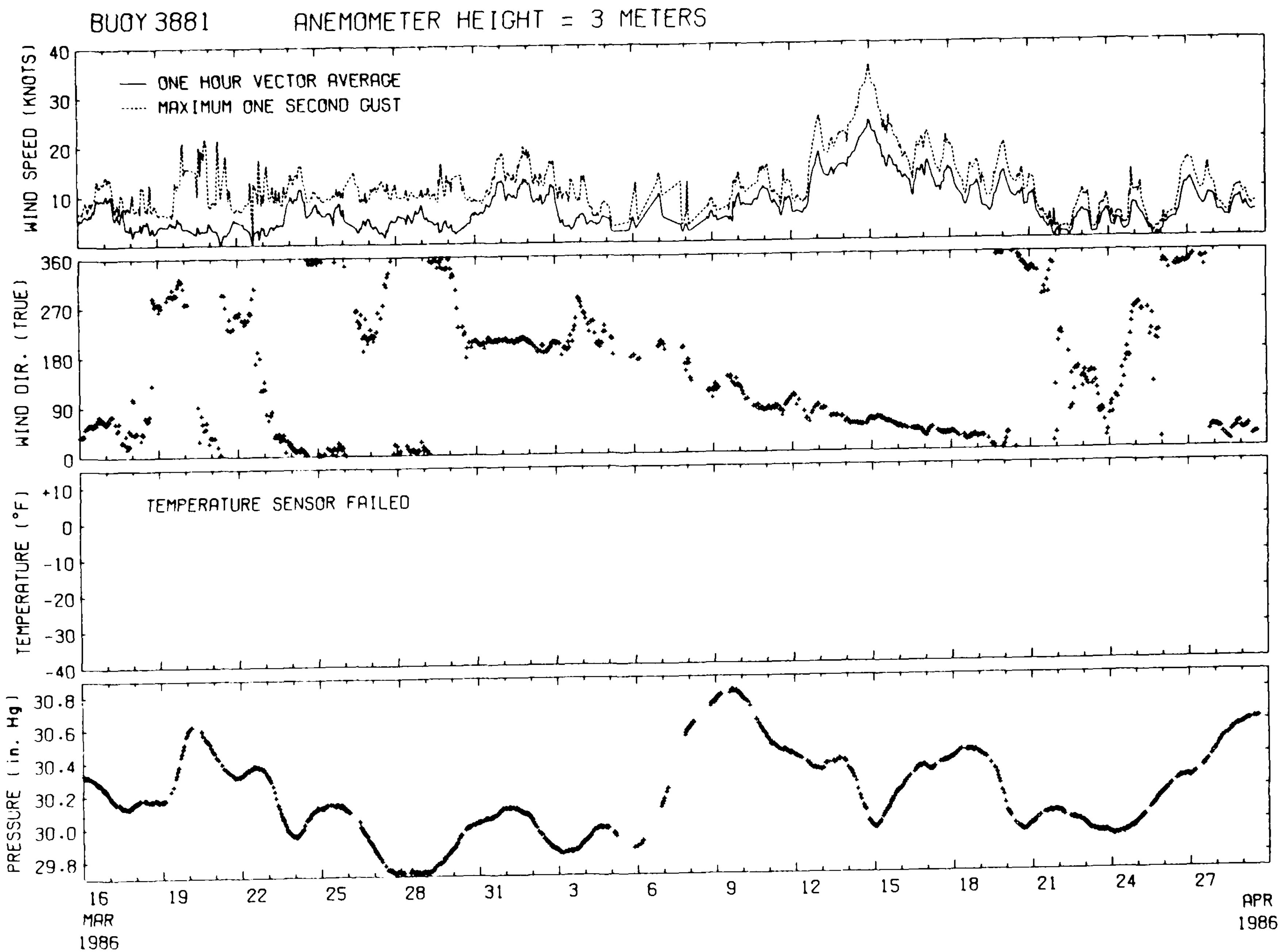

Figure 12b. Weather measurements taken at APLIS ice camp using meteorological buoy No. 3881 (English units; see Figure 13 for metric units).

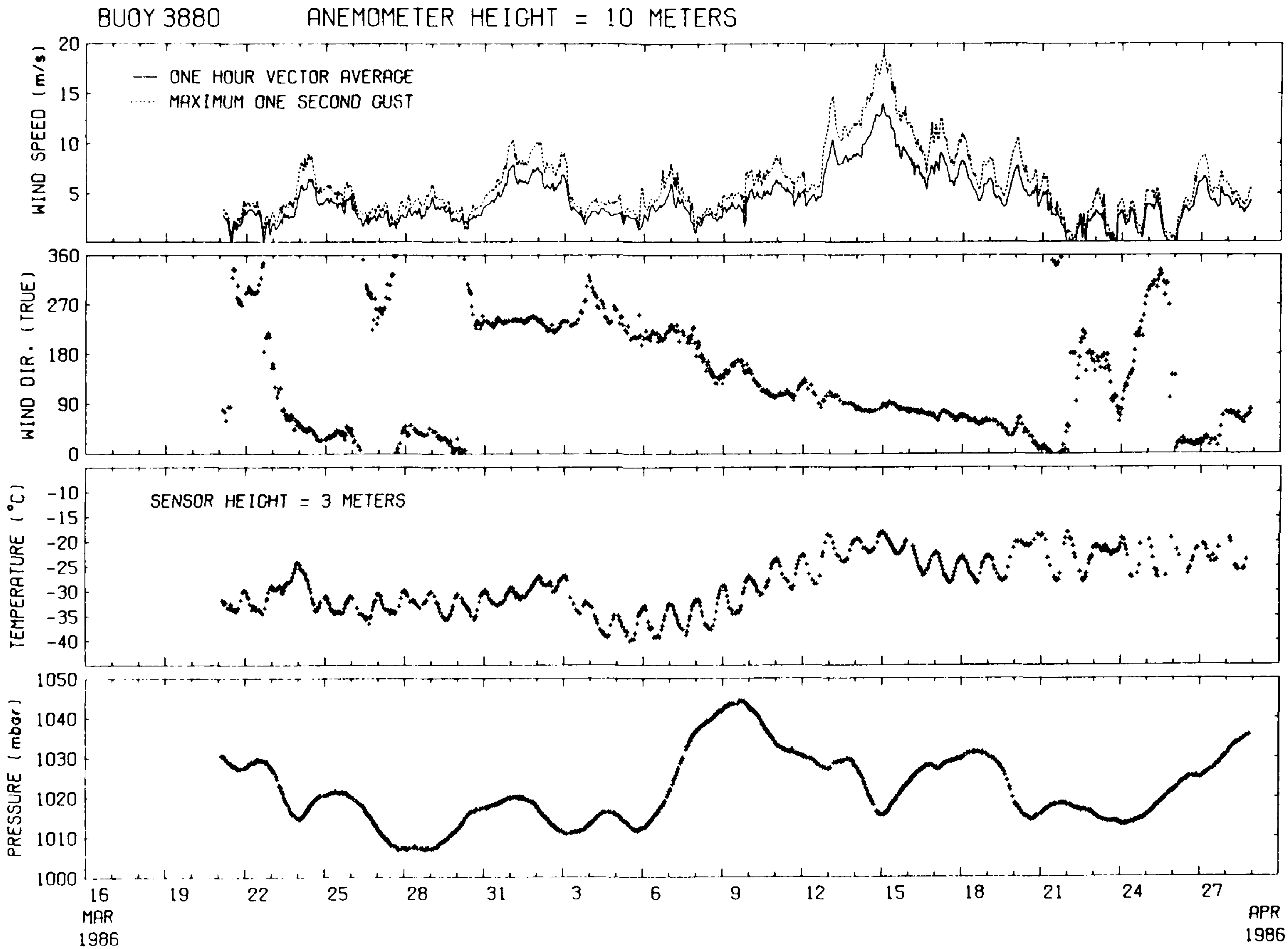

Figure 13a. *Weather measurements taken at APLIS ice camp using meteorological buoy No. 3880 (metric units).*

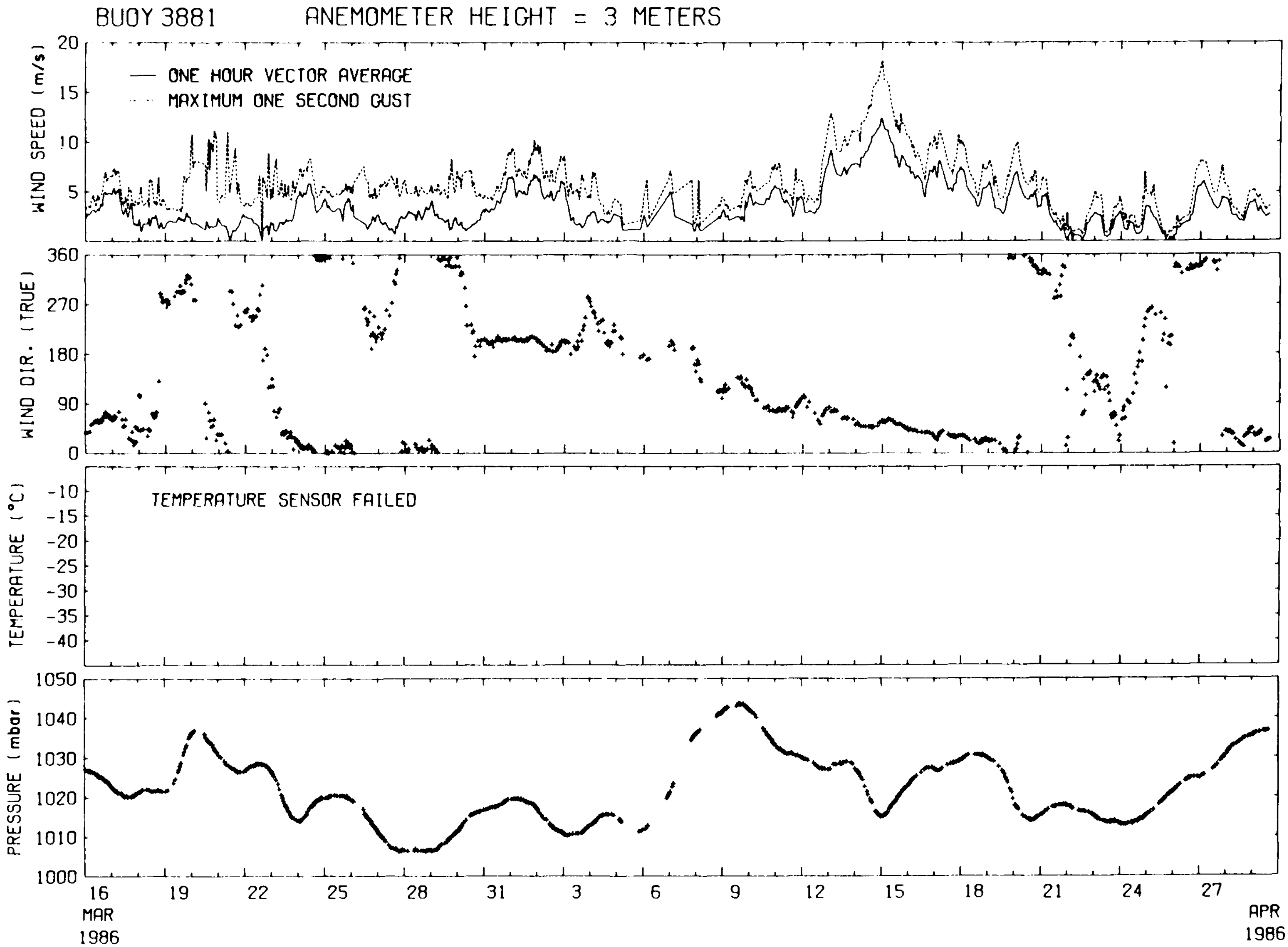

Figure 13b. Weather measurements taken at APLIS ice camp using meteorological buoy No. 3881 (metric units).

IV. VERTICAL PROFILES OF WATER PROPERTIES

A. CTD Measurements at the Ice Camp

To conduct the CTD measurements at the ice camp, we mounted a lightweight profiler[1,2] over a 3-ft diameter hole in the floor of the oceanography hut. A hole was made through the 12 ft of ice near the hut using an ice melter, and the hut slid over the hole so that the two holes coincided. In this profiler, the electronics and tape recorder are mounted in the hub of the cable reel, eliminating the necessity for slip rings. The probes — thermistor, conductivity cell, and pressure sensor — were lowered by hand on the 1/4-in. electric cable, using cranks on each side of the drum. The cable was 300 m long; markers at 10, 100, and 200 m gave a check on depth accuracy when there was no streaming due to current. The sampling rate was 2.8 per second, and the lowering rate was 0.5 to 1 ft per second.

Profiles were obtained once or twice each day, depending on the need and the availability of the operator. The CTD data were processed using an HP-85 desk-top computer to obtain profiles of temperature, salinity, sound speed, and density. These plots were made in the field to monitor the performance of the equipment and to provide investigators with sound speed profiles. Table II lists all CTD profiles measured at the camp. The complete set of profiles is presented in Appendix B. Some noise in the conductivity measurement appears in some of the salinity profiles, most noticeably in that for Station 47. The source of the noise is believed to be instrumental.

An example of the profiles is presented in Figure 14. The glitch at 200 m results from stopping the probe at the 200 m mark on the cable. When lowering resumes, the correct readings continue.

The profiles show a mixed layer in the upper 20 m and a strong halocline below, accompanied by the usual thermal layer at about -1.5°C. This is a remnant of the Bering Sea water that enters the area every summer.[7] The variation in the depth of the halocline is shown in Figure 15. The large changes occurred during the period of greatest movement, 9-18 April.

The last plot in Appendix B is for a 1500 m deep cast made on 25 April. The temperature and salinity data from that cast and a CTD cast made during the fall of 1984 are compared in Figure 16. Below 600 m the data were the same, for the scale of the plot, and are omitted.

Table II. List of CTD measurements at the 1986 ice camp.

Date	Station No.	Local Time	Tape	Sensor Number C	T	D	Max. Depth (m)
Mar 22	3	0600	1	3	429	1653	300
	7	1800					
23	9	0600					
	11	1800					
24	13	0600					
	15	1530					70
	17	1800					300
25	19	0615	2				
	21	1815					
26	23	0600					
27	25	0730					
	27	1644					
28	29	0600					
29	31	0600					
30	33	0600					
	35	1800					
31	37	0600					
	39	1800					
Apr 1	41	0600					
	43	1845					
2	45	0600	3	19	432	1653	
	47	1730					
3	49	1426					
4	51	1430					
5	53	0715	4				
6	55	0645					
7	57	1225					
8	59	0630					
9	61	0630					
10	63	1315					100
11	65	0630					300
12	67	0640					
13	69	0630					
14	71	0645					
15	73	0800	5	19	432	1653	300
16	75	0745					
17	77	0930		3	429	1653	
18	79	0545					
19	81	0845					
20	83	0645					
22	85	0815					
23	87	1730					
24	89	1615					
25	91	0815					
	93	2045					100
	Deep Cast	1200	1	16	432	52	1500

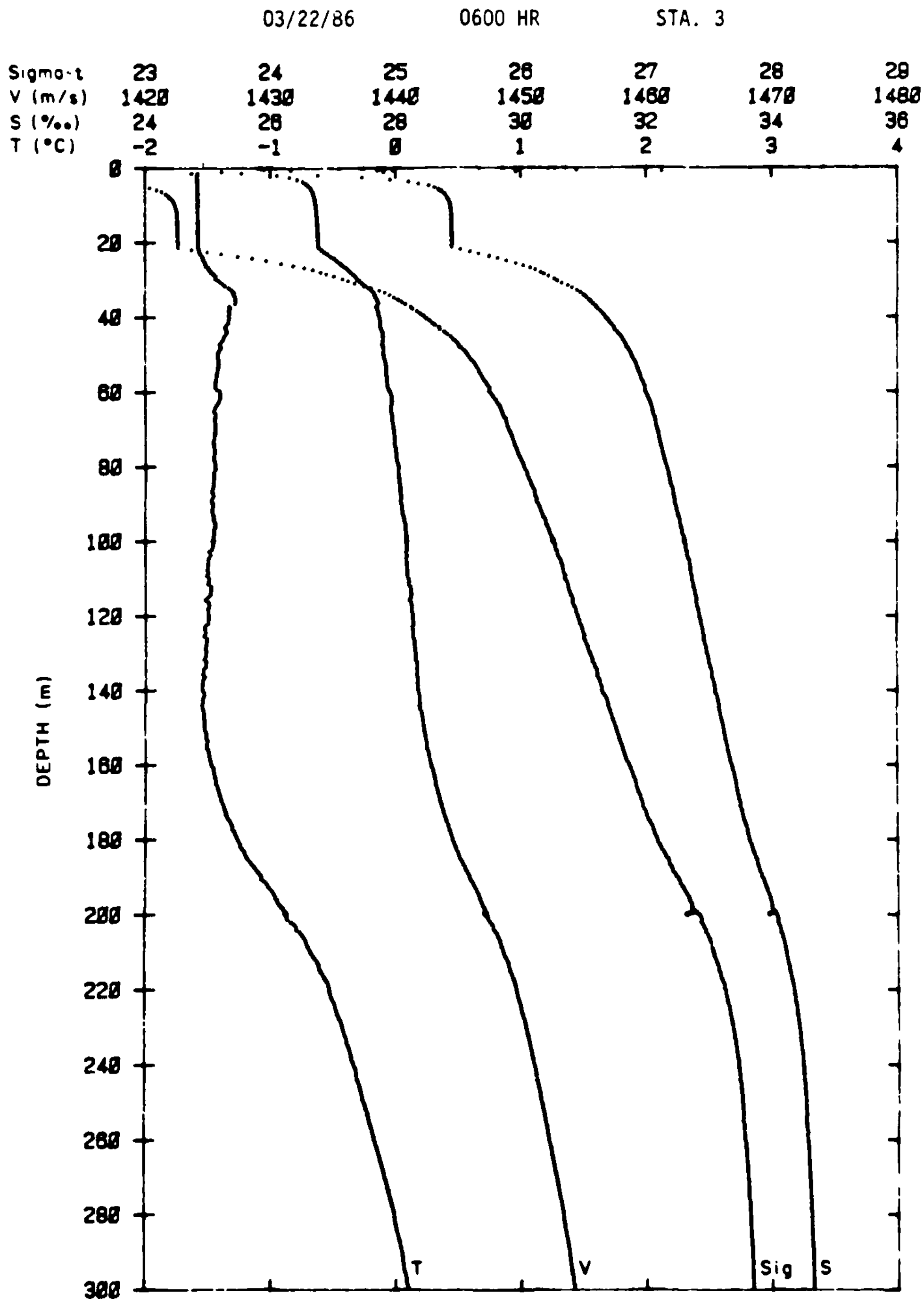

Figure 14. An example of the vertical profiles measured at the ice camp. T refers to temperature, V to sound speed, Sig to σ_t, and S to salinity. A complete set of profiles appears in Appendix B.

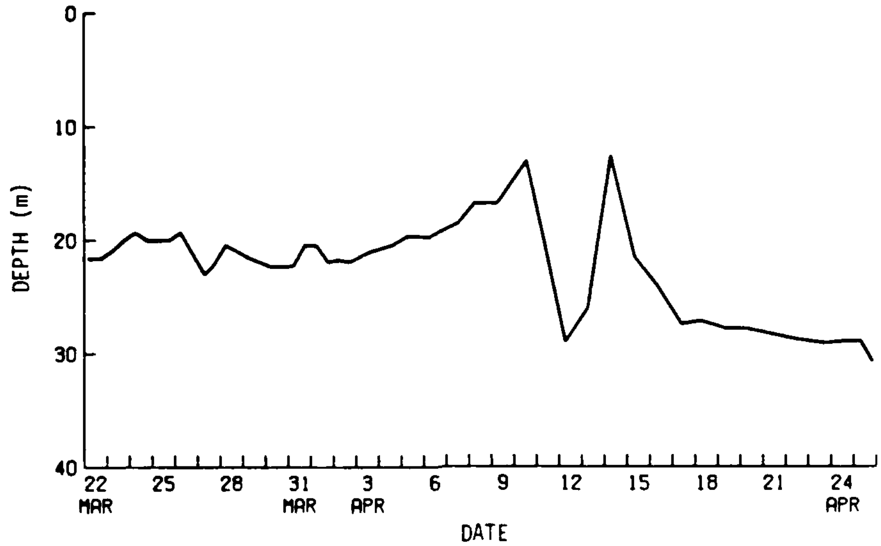

Figure 15. Variation in depth of the major halocline.

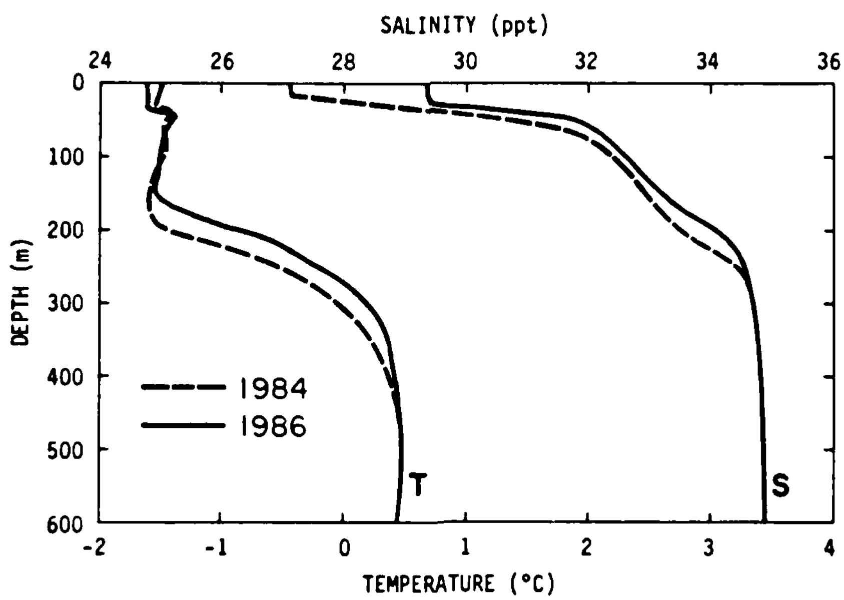

Figure 16. Comparison of temperature and salinity profiles for 25 April 1986 with a CTD cast made in the fall of 1984. For depths 600-1500 m, see the last figure in Appendix B.

B. Water Samples Taken for Salinity and pH Analysis

At seven of the CTD stations, a Niskin bottle sampler was attached to the CTD cable and lowered to the desired sampling depth, where it was tripped and brought back to the surface. Two or three 200 cc samples were then taken from each Niskin bottle for salinity and pH analysis.

The results of the analysis, conducted by conductivity cell at the Northwest Regional Calibration Center (NRCC), are shown in Table III. Examination of pairs of samples from each station shows a maximum difference of 0.011 ppt.

Comparisons of the sampling results and the salinities calculated from the CTD readings can be made by examining the plots for Stations 21, 27, 45, and 91 in Appendix B, where the sample value has been plotted with a circle. The agreement is good to about 0.1 ppt, with the sample analysis usually higher. The discrepancy could result from a calibration error or from some evaporation of the sample.

Table III. Water property analyses for samples taken with a Niskin bottle.

Date	Station	Depth (m)	Salinity[a] (ppt)	pH measured	pH *in situ*
25 March	21	10.0	29.072 29.069	7.9	8.1
27 March	27	190	33.871 33.865	7.8	8.0
2 April	45	290	34.690 34.692	7.9	8.1
25 April	91	10.6	29.363 29.360	8.0	8.2
		70	32.278 32.289	7.8	8.0
		130	33.007 33.013	7.8	8.0
		290	34.720 34.726	8.0	8.2
				average	8.09

[a] Two 200 cc samples were taken from each Niskin bottle sample for salinity analysis, and one for pH analysis.

Some samples were analyzed for pH in the field using a VWR Model 74 pH meter. Corrections were made to give *in situ* pH values; the temperature correction was +0.2 and the depth correction was negligible.

The probe of the pH meter had been replaced before the field trip. This eliminated an objectionable drift in the reading and should have resulted in more accurate readings than in 1984. Readings were taken of standard solutions (pH = 7 and pH = 10) before and after the readings were taken of the samples.

The results do not appear to show a depth dependence for pH. The average of 8.1 is higher than the average of 7.9 obtained in the fall of 1984 in the same area. Some measurements[4] in the fall of 1980 gave an average of 7.5. It seems unlikely that such changes are real; the procedure and meter should be examined for possible errors.

C. Freezing Conditions in Upper Layer

When air temperature is below freezing in the Arctic, a surface layer of nearly uniform temperature and salinity forms in the water. This layer can be tens of meters thick. As the water in contact with the ice freezes, some of the salt is displaced and distributed over this layer, increasing its salinity. This lowers the freezing point, and consequently the temperature of the layer decreases.

The temperature of the surface layer is shown in Figure 17 for three stations taken during April. The computed freezing temperature[8] has also been plotted. In each case, except for the water in the upper portion of the 4 m deep hole in the ice for the CTD, the measured temperature of the surface layer is slightly below the computed freezing temperature. If the salinity were increased by 0.1 ppt, as suggested by the water sample analyses (Section B, above), the computed freezing temperature would be lowered by 0.006°C, only one-third of the difference shown in Figure 17, station 51.

D. Scattering Layer

Acoustic scattering layers have been observed in summer in the Beaufort and Chukchi seas by Feldman et al.[9] and the year around at T-3 by Hunkins.[10] Such layers were also observed from APLIS in the fall of 1984.[6] These layers are suspected of affecting acoustic transmissions that are nearly parallel to them.

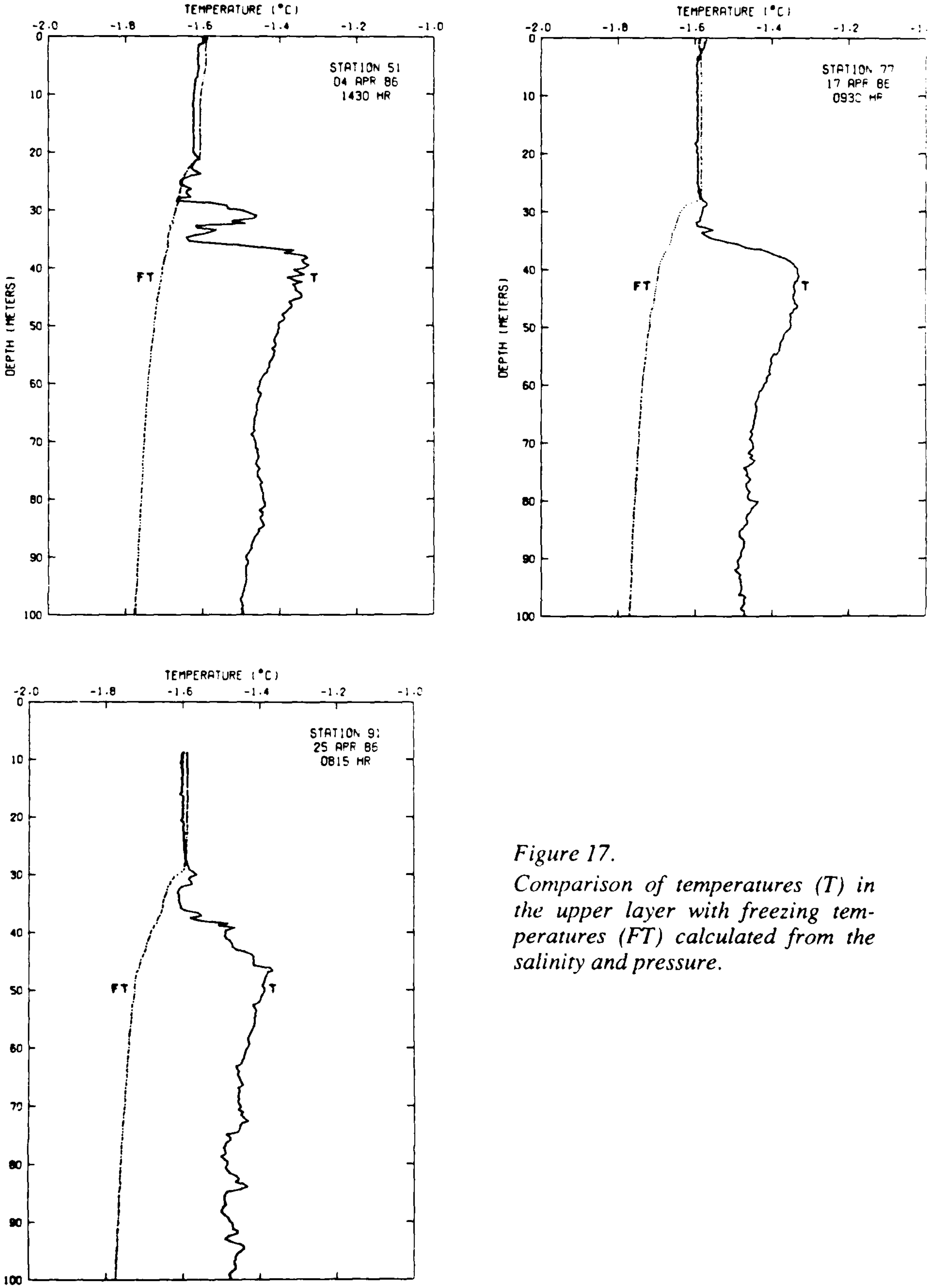

Figure 17.
Comparison of temperatures (T) in the upper layer with freezing temperatures (FT) calculated from the salinity and pressure.

To investigate whether the scattering layers and individual fish found in 1984 were also present in the spring, we installed the same equipment as in 1984. A Ross echo sounder operating at 105 kHz was set up in the oceanography hut, and the transducer lowered 18 ft below the water level through a 3 ft diameter hole in the floor and the underlying ice, which was 12 ft thick with a freeboard of about 2 ft. The transducer was 8 in. in diameter with an 8° beam. Echoes were generally recorded as echograms with a depth scale of 0-50 fathoms.

Although several attempts were made to measure scattering layers, the returns were consistently below the noise level. Objects placed below the ice, such as the CTD probe and dropped weights, appeared as they had in 1984; thus the equipment was working satisfactorily.

We conclude from the 1984 and 1986 measurements that biological layers, which are so prevalent in the summer following the plankton bloom, are still present in the fall but do not last until the following spring.

V. CURRENTS

Measurements of current relative to the floe are important to all experiments that use an ice floe as a base because such currents create streaming in the cables of attached equipment and cause drift in free bodies. For oceanographic studies, absolute currents, which are calculated from the floe's drift and the measured relative currents, are of more concern. In this section, "current" refers to the current measured relative to the floe; "true current" refers to the current with respect to the earth.

A. Equipment

Current was measured with an InterOcean System S4R current meter. This instrument, which is self-contained, is housed in a 10-in. diameter sphere of cast cycloaliphatic epoxy weighing 10 kg in air and 1 kg in water. It measures current by creating a magnetic field and sensing the voltage induced by the movement of water through the field. The orientation of the instrument is obtained from a flux-gate compass, and the direction of the current is computed with respect to magnetic north. Before a measurement, the meter was connected momentarily to an HP-85 computer, through a special interface, and turned on. After the measurement, the HP-85 was reconnected to turn the instrument off and read the data. The meter has a clock which keeps track of the month, day, and time (GMT). The pressure transducer uses a silicon strain gauge. The data interval can be adjusted from the HP-85, which can handle 1000 sets of data.

The current meter was attached 3 m below the CTD probe, and the pair was lowered and raised by hand as was done for the CTD measurements. At 1 kg, the sphere is rather light in the water. A weight was suspended below the meter and a float was attached above it to increase the tension on the meter and reduce the wobble.

B. Measurements

The measurements are summarized in Table IV and plotted in Figure 18. The bars indicate the spread of the readings over a minute or two. This spread represents variations in the current rather than inaccuracies in the measurement.

The true current can be obtained by combining these measurements vectorally with the floe's movement. When the floe started to move on 9 April, it often reached speeds of 0.3 to 0.5 kn, which is about the same magnitude as the currents measured. In some cases, the relative current, especially at the lower depths, may be almost entirely due to the floe's movement over the water.

Table IV. Current "profiles" measured at APLIS-86.

Date	Run	Depth Coverage (m)	Max. Current (kn)
Mar 25	4	60-100	0.4
26	5	50-100	0.3
30	6	20-70	0.2
31	9	15-100	0.3
Apr 1	10	10-100	0.3
4	11	50-250	0.2
9	12	10-70	0.2
13	13	15-100	0.3
16	14	5-220	0.4

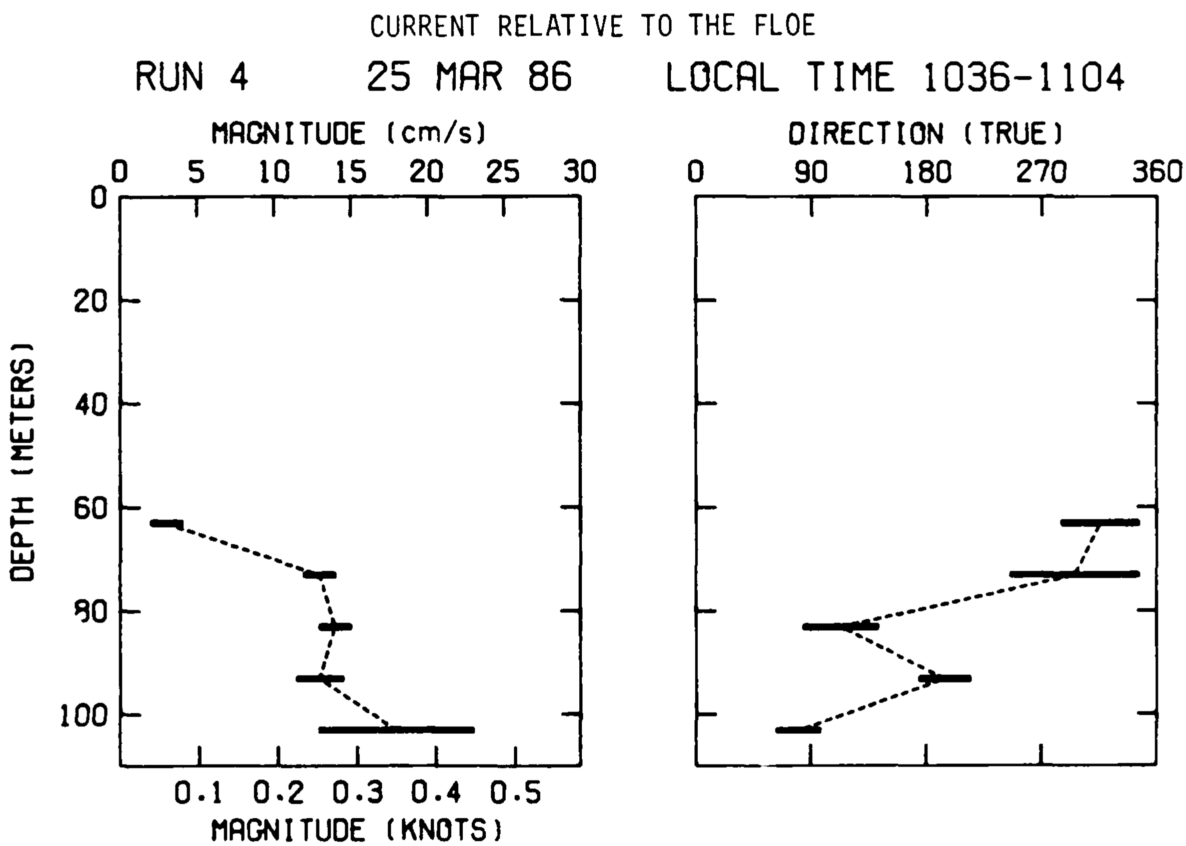

Figure 18. Currents measured during the ice camp's occupancy.

CURRENT RELATIVE TO THE FLOE

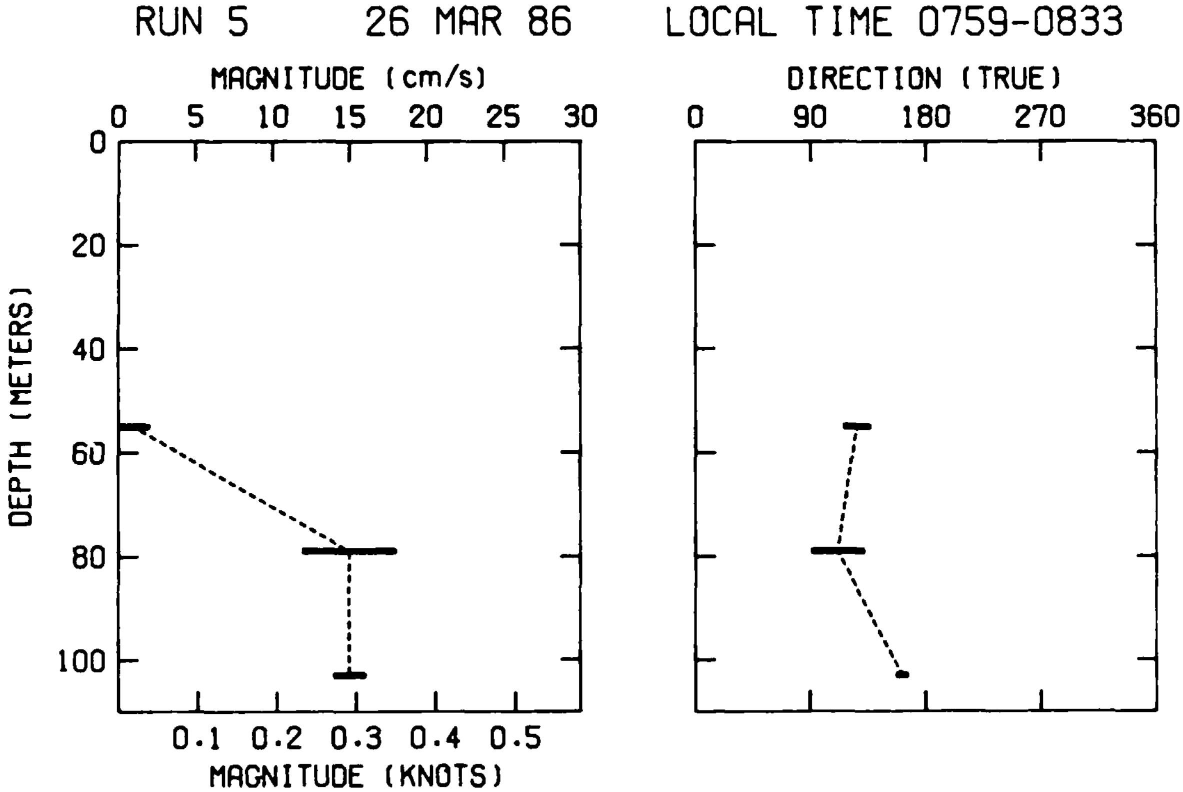

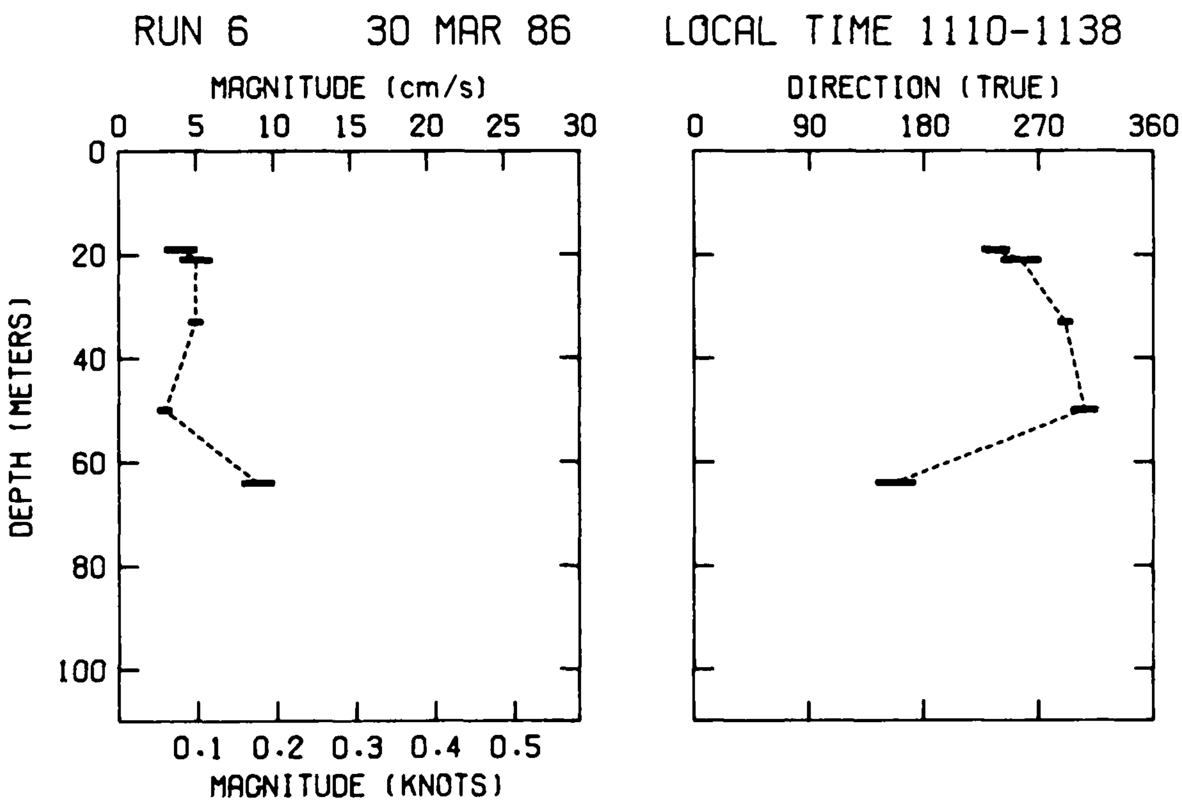

Figure 18, cont.

CURRENT RELATIVE TO THE FLOE

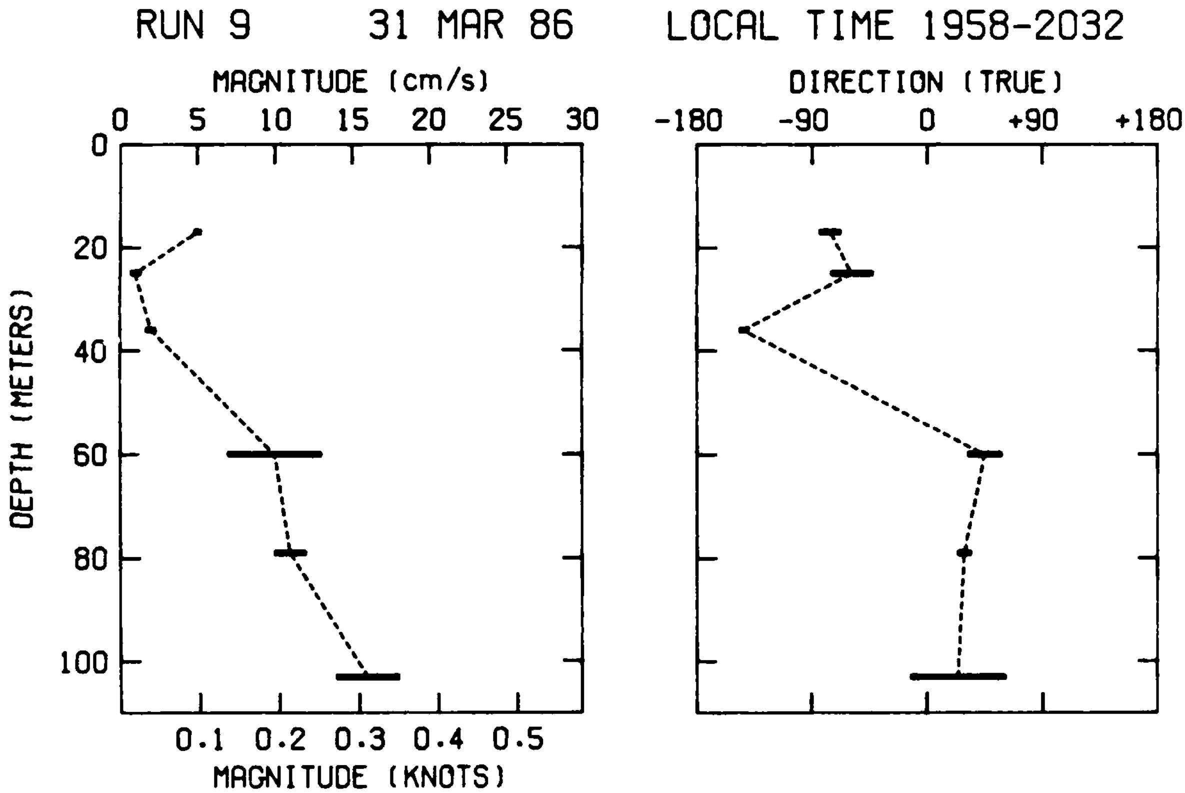

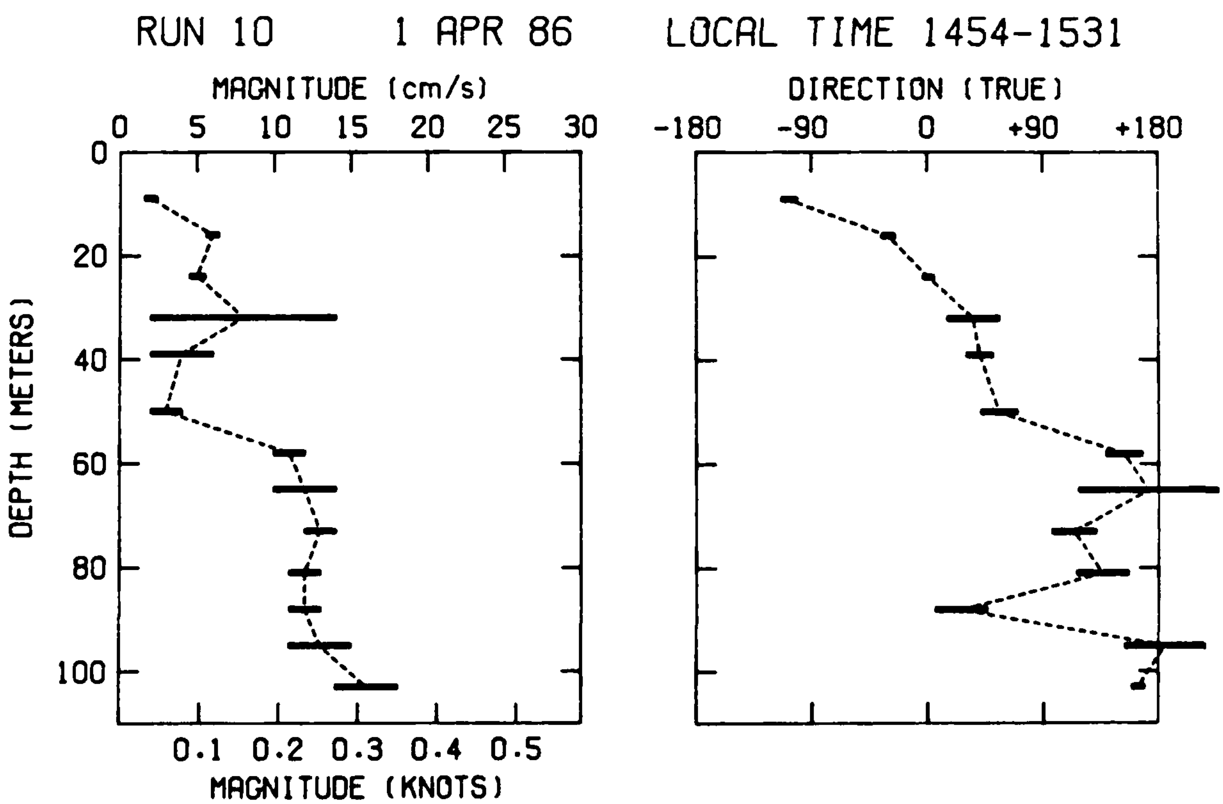

Figure 18, cont.

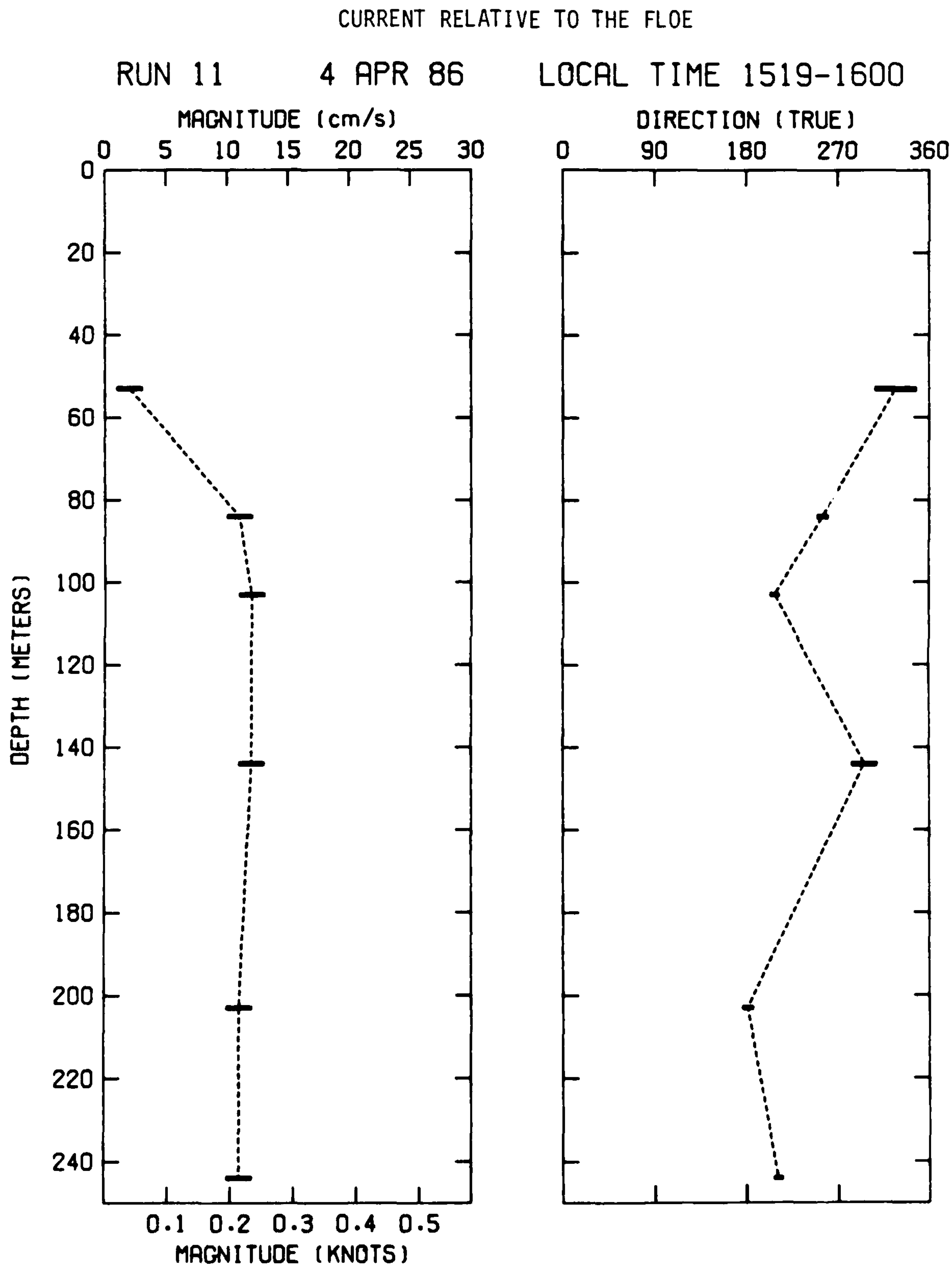

Figure 18, cont.

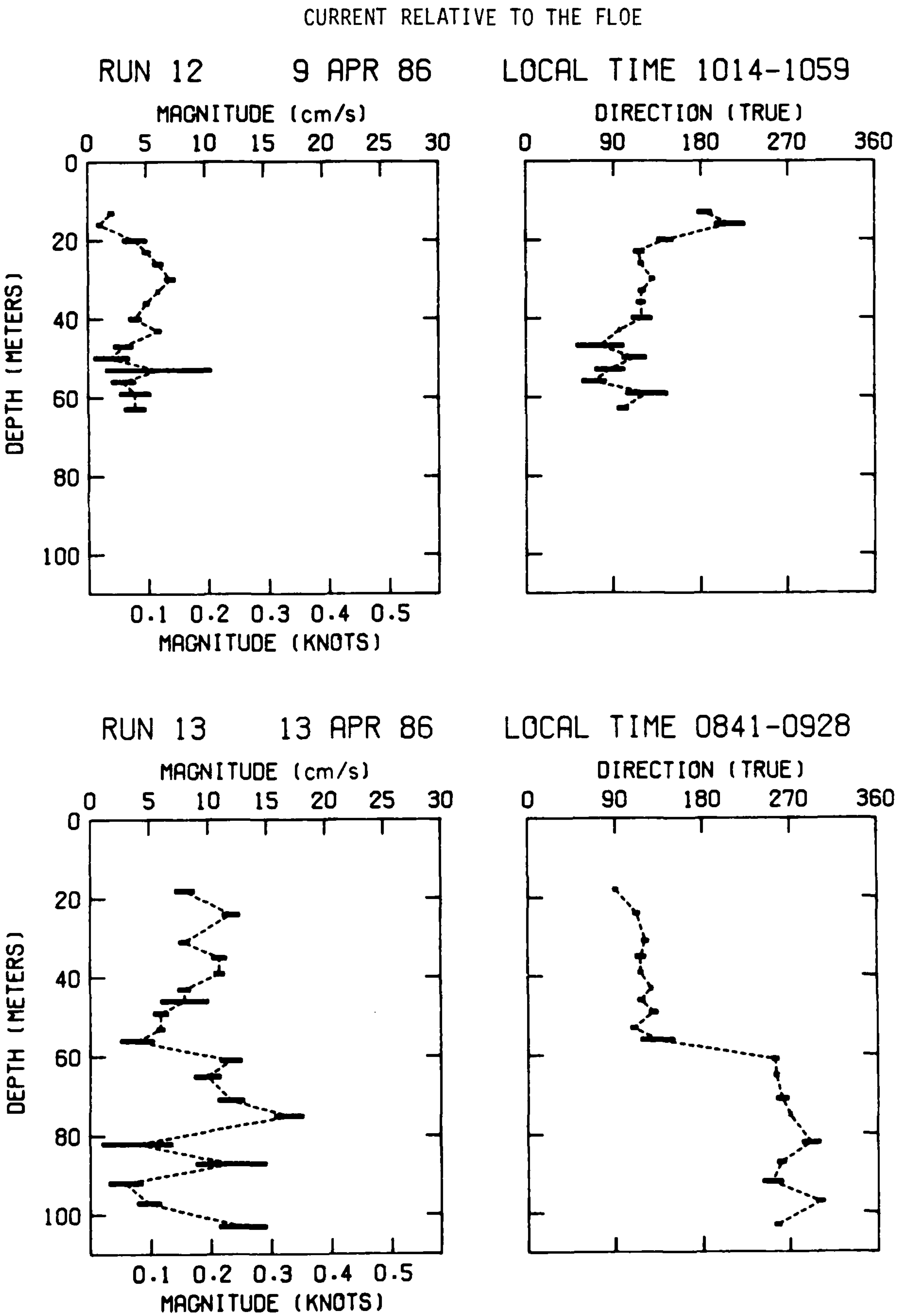

Figure 18, cont.

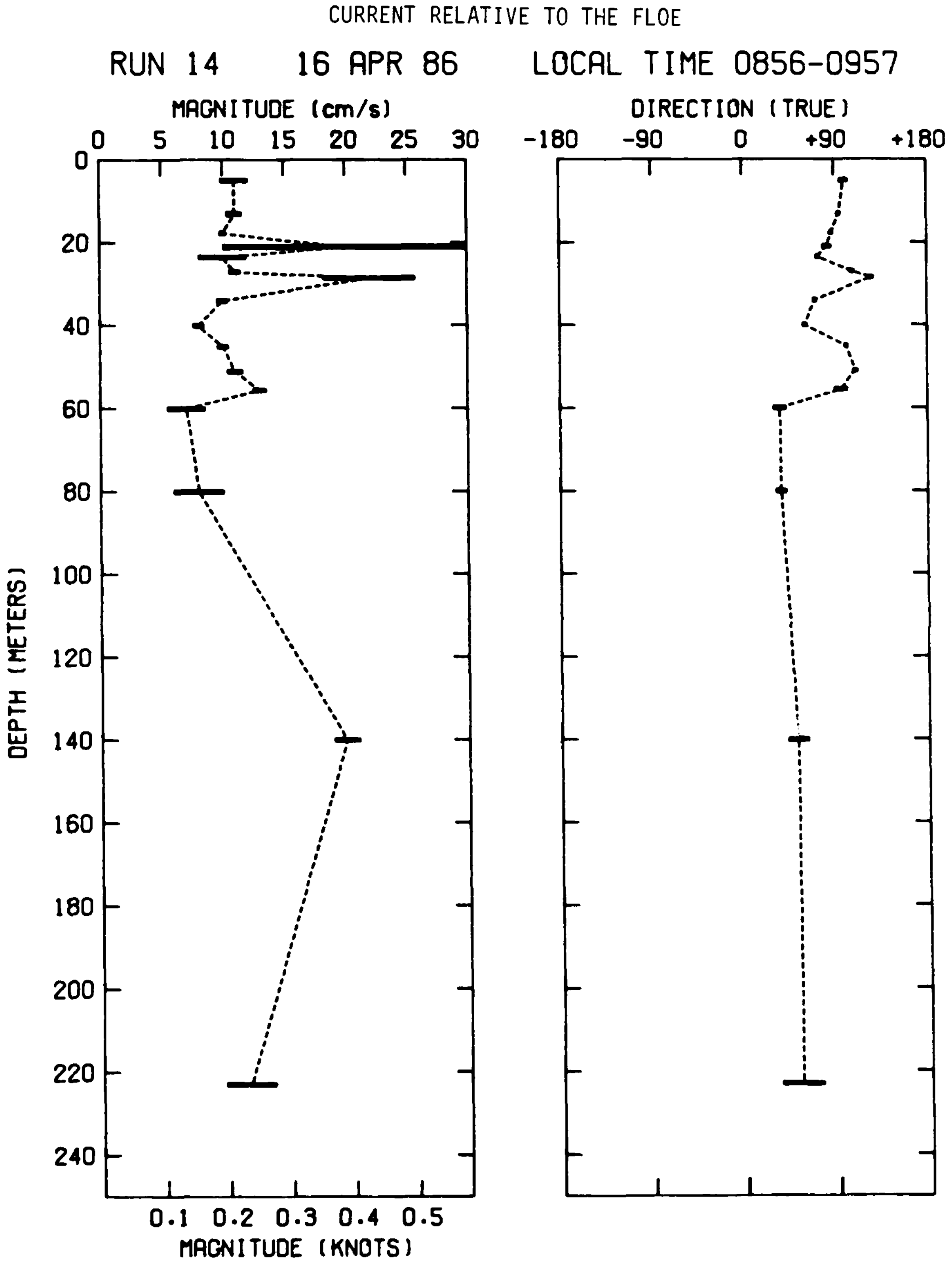

Figure 18, cont.

VI. ICE CORES

Ice cores were obtained with a Sipre corer. As soon as possible after the cores were removed from the coring tube, the temperature was measured at 10 cm intervals. This was done by drilling a 4 cm deep hole in the side of the core and inserting a digital electronic thermometer. After 15-30 s, when the reading was steady, it was recorded. Sections of the core were put in glass bottles and taken to Seattle at the close of the camp. The salinities of the samples were measured at NRCC using a high-accuracy laboratory salinometer.

The densities of the core samples were determined by weighing them in air and then in an oil with a lower density than the ice. The difference gave a measure of the volume. This test was performed at a temperature of about -4°C to avoid any melting. The various properties of the ice core sections are plotted in Figures 19a-19d.

As shown in Figure 19a, the temperature in the ice has a nearly constant gradient between the air temperature at the surface and the water temperature below. In April the air temperature rose, and the temperature profile (Figure 19d) shows a change in slope at about mid-depth in the ice.

The salinity tends to be about 4 ppt except for a few odd values. The single data points with high values in Figures 19a and 19b may be errors or chance inclusion of brine pockets. The low value at the surface in Figure 19d may be from snow, whereas the low value at 150 cm seems to be supported by adjacent low values. The density measurements were made using a method new to us, and we have not investigated the accuracy. The brine and air volumes appear to be reasonable.

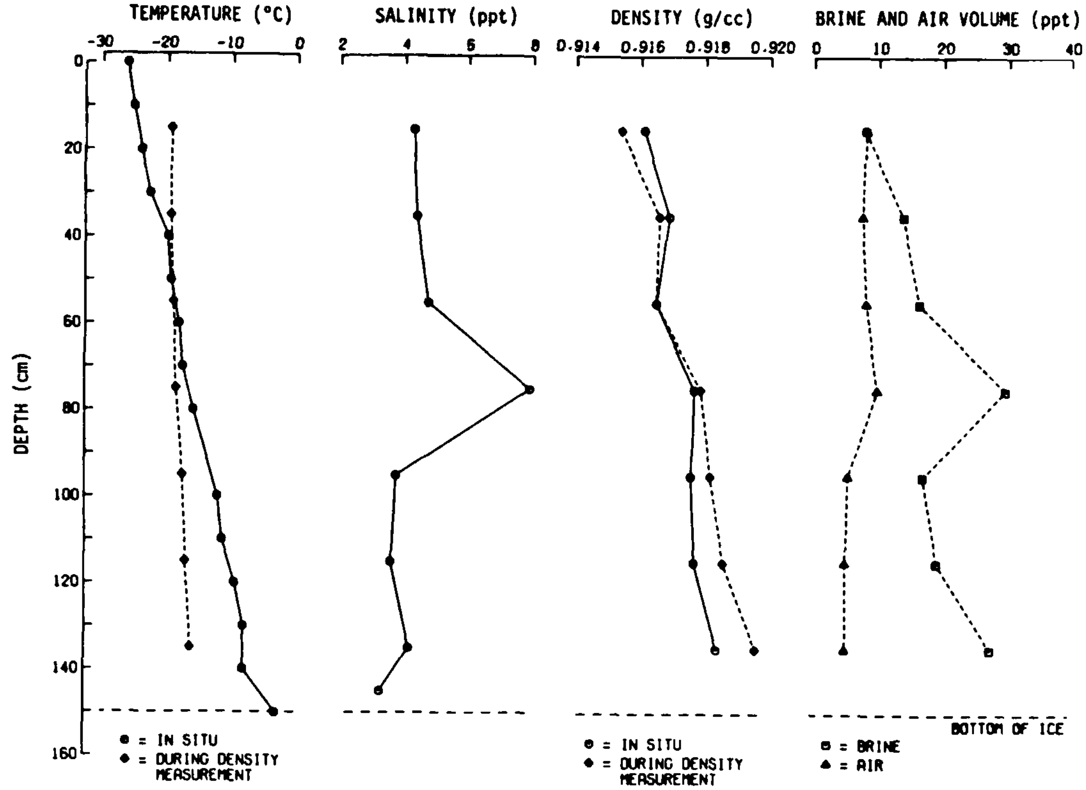

Figure 19a. *Temperature, salinity, and density profiles in the ice, with computed brine and air volumes. Core taken on 27 March at 2322 GMT near sphere #2 in Figure 4.*

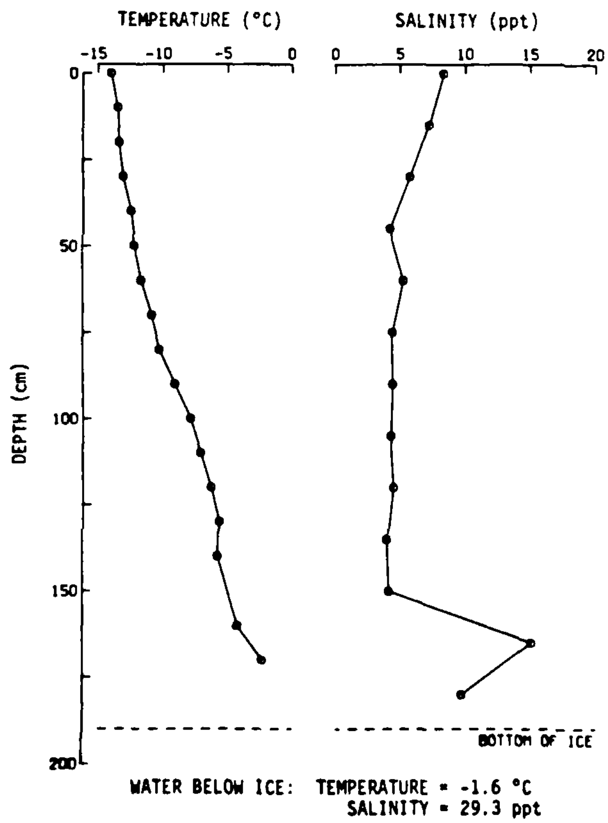

Figure 19b.

Temperature and salinity profiles in the first-year ice of a refrozen lead about 1.3 miles north of camp. Core taken on 26 April at 2242 GMT.

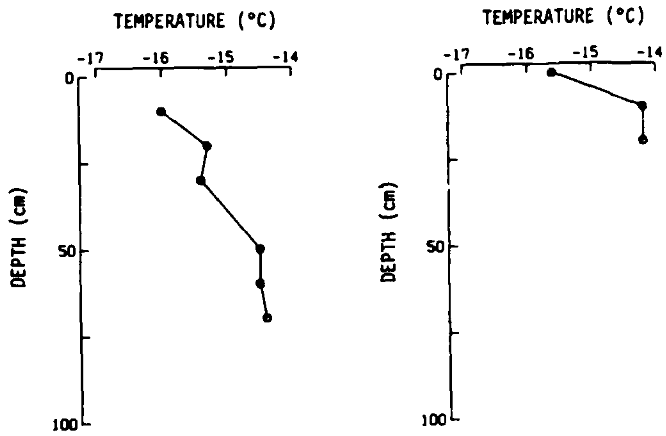

Figure 19c.

Temperature profiles from upper portion of multiyear ice. Cores taken on 27 April at 0330 GMT (left) and 0345 GMT (right).

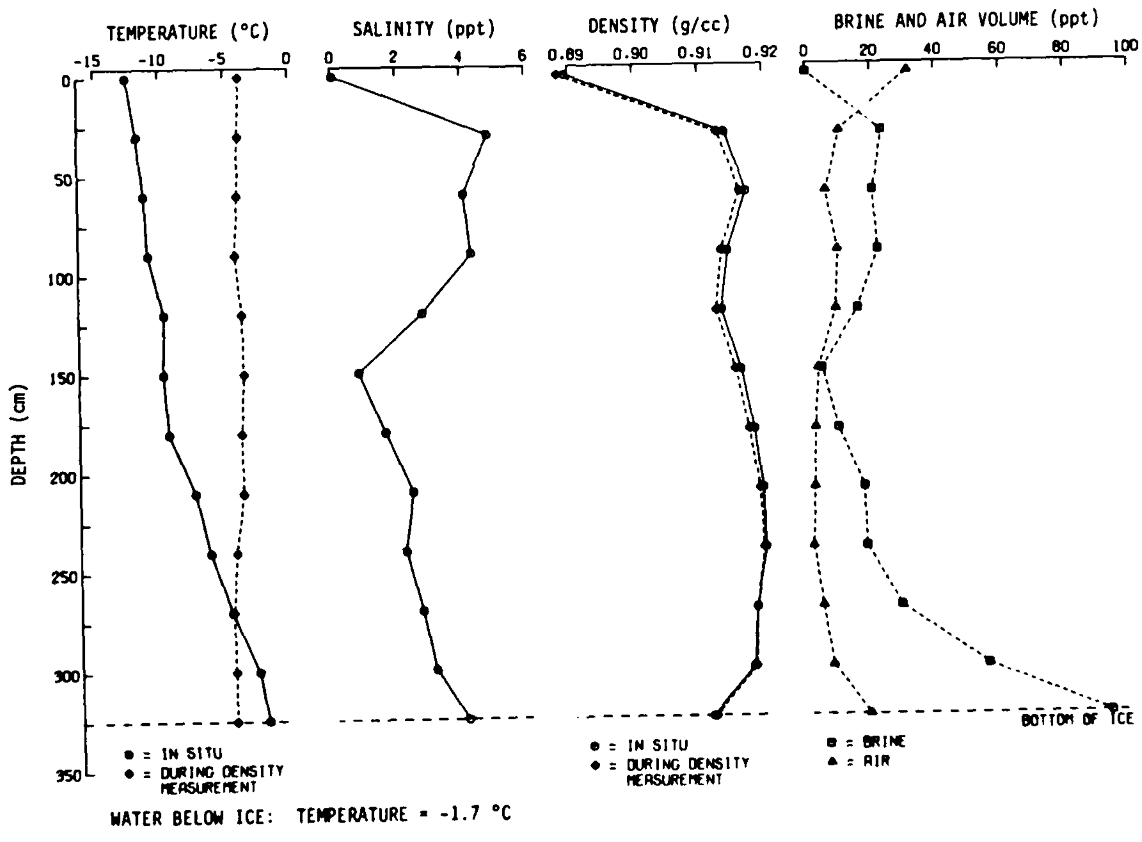

Figure 19d. Temperature, salinity, and density profiles in multiyear ice, with computed brine and air volumes. Core taken on 28 April at 0030 GMT.

VII. UNDERWATER NOISE LEVEL

Underwater noise was measured primarily to determine the noise level in the vicinity of the camp during various exercises. At times the camp was quiet and the natural ambient noise may have predominated. Our measurements provide an upper bound to the ambient noise.

A. Equipment

The noise measurements utilized a Bruel and Kjaer Instruments Inc. Model 8101 omnidirectional hydrophone (serial 693562). The sensitivity of this hydrophone, which is 4 in. long, is given by the manufacturer as -184 dB (re 1 μPa) over a broad frequency range. For the noise measurements, it was suspended by a coaxial cable through the hole in the floor of the oceanography hut. The signal passed through a 60 dB gain amplifier and a high-pass filter and into a Wavetek Rockland Inc. 512 real-time spectrum analyzer. The output spectrum was plotted using an HP-85 desk-top calculator and plotter. At the higher frequencies, the hydrophone pattern is not omnidirectional, which may have reduced the noise somewhat depending on the direction of arrival. No correction was made for the beam pattern.

We generally used the camp ac power to supply the spectrum analyzer and HP-85. When the camp generator was shut down, we used an alternate supply consisting of two 12-V storage batteries and an inverter.

All spectra plotted in this report are an average of 16 samples. The frequency range f_m was variable from 20 Hz to 100,000 Hz. With a 400-line analysis, the resolution was 1/400 of f_m, and the length of the sample in seconds was $400/f_m$. The high-pass filter was set at 12 Hz or 5000 Hz. At frequencies below the filter setting, the spectral levels plotted will be low.

B. Measurements and Results

Noise measurements were made as time permitted, not on a routine schedule. The measurements are summarized in Table V along with a description of conditions at the camp at the time of each measurement. The resulting spectrograms are shown in Figure 20 in the order given in Table V. The Knudsen curve[11] for a zero sea state is shown on each graph for comparison.

Table V. Underwater noise measurements made at the APLIS ice camp at 30 m depth.

No.	Date	Time (local)	High Pass Filter (Hz)	Conditions
2	March 23	0838	12	
5	March 31	1345	12	
6	April 1	1346	12	
7		1400	12	
8		1930	12	
9		1945	12	WQC at 10 kHz
10	April 2	0630	12	
11		1825	12	
12		2140	12	
13	April 3	1530	12	
14	April 4	1240	12	
15		1900	12	
16	April 5	0800	12	
17		0820	12	
18	April 6	1110	12	
19	April 7	0517	5000	
20		1044	5000	
21		1115	5000	
22	April 8	0750	5000	
23		1212	5000	
24	April 9	0650	5000	
25	April 10	0645	5000	Probably thruster
26		0648	5000	20 kHz ping
27		0655	5000	Possibly thruster
28		0800	5000	Possibly thruster
29		0817	5000	
30		0821	5000	
31	April 11	0705	5000	
32		0740	5000	
33	April 12	0600	12	
34	April 13	0903	12	
35	April 14	0827	12	Stormy
36		0900	12	Stormy
38	April 22	0930	12	WQC at 10 kHz
41	April 24	1642	12	
42	April 25	0650	12	
44		0940	12	
46	April 26	0610	12	
48		0620	12	
49		0625	12	
50		1848	12	
51	April 27	0650	12	
52		0653	12	
55		0756	12	dc power supply

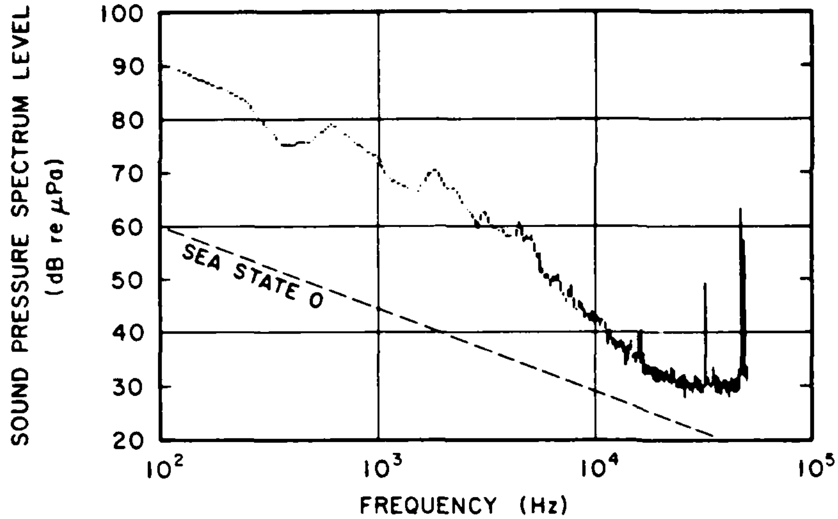

NO. 2
DATE: 23 MAR 86
TIME (LOCAL): 0838

HIGH PASS FILTER: 12 Hz

CONDITIONS:

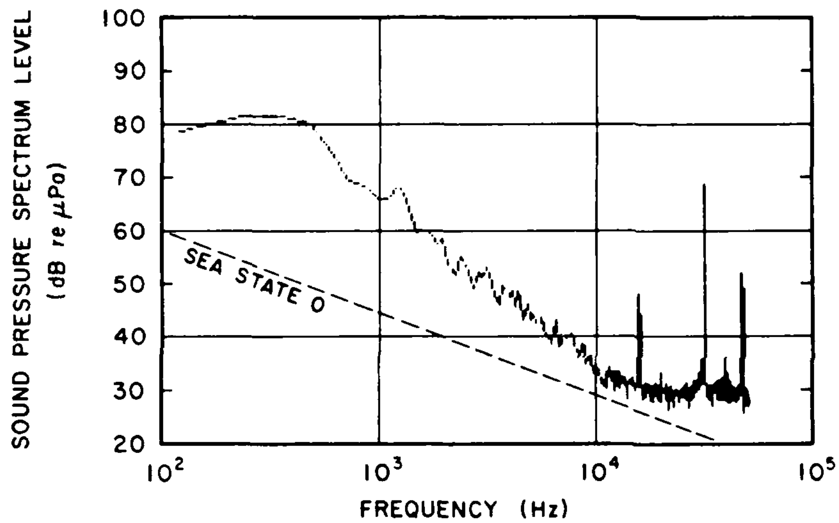

NO. 5
DATE: 31 MAR 86
TIME (LOCAL): 1345

HIGH PASS FILTER: 12 Hz

CONDITIONS:

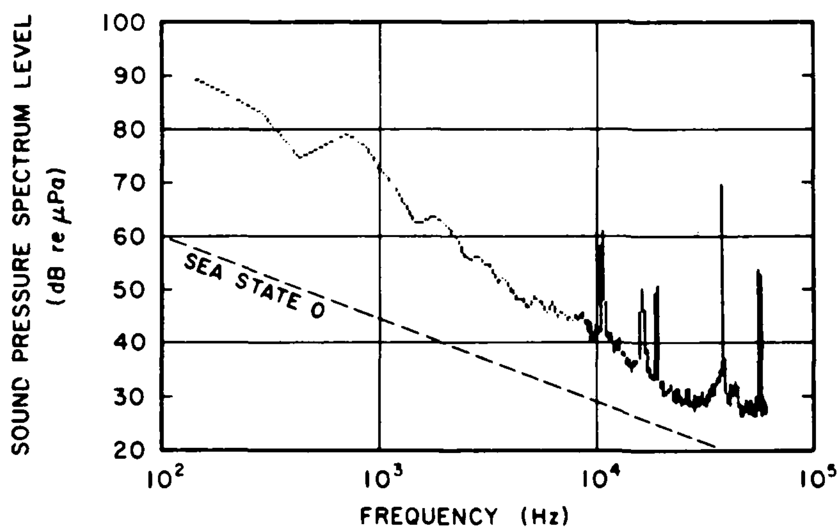

NO. 6
DATE: 1 APR 86
TIME (LOCAL): 1346

HIGH PASS FILTER: 12 Hz

CONDITIONS:

Figure 20. Noise spectra measured during the ice camp's occupancy.

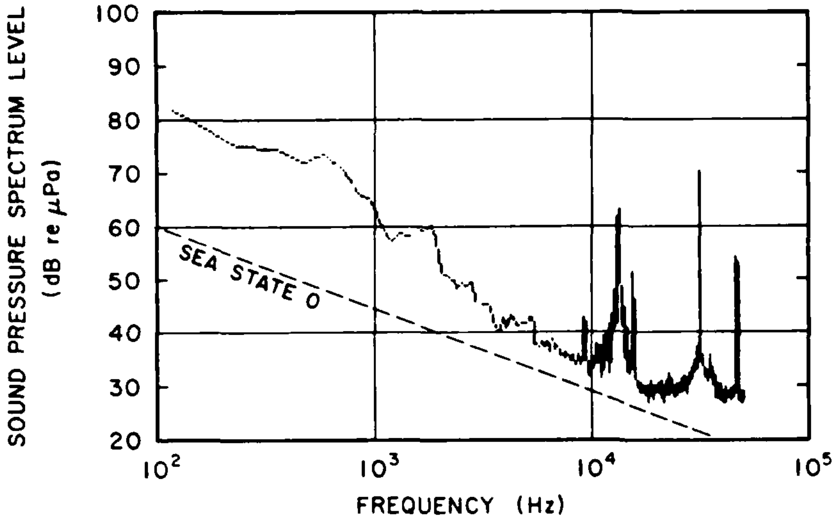

NO. 7
DATE: 1 APR 86
TIME (LOCAL): 1400

HIGH PASS FILTER: 12 Hz

CONDITIONS:

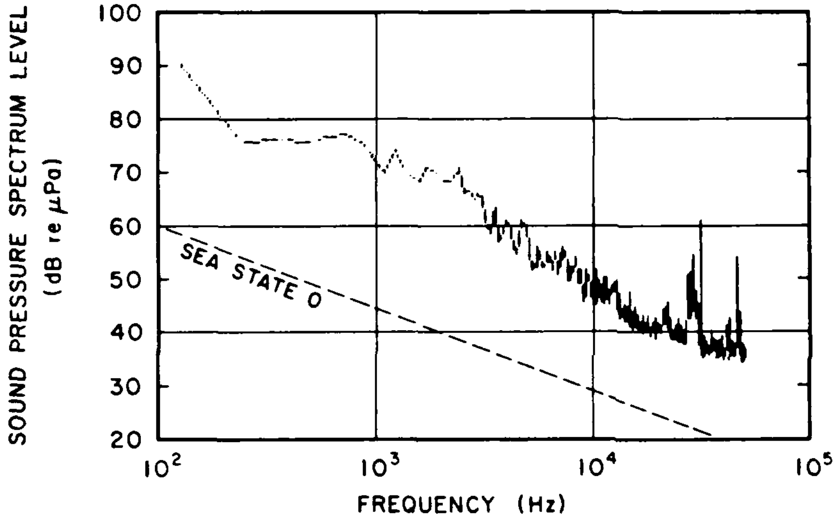

NO. 8
DATE: 1 APR 86
TIME (LOCAL): 1930

HIGH PASS FILTER: 12 Hz

CONDITIONS:

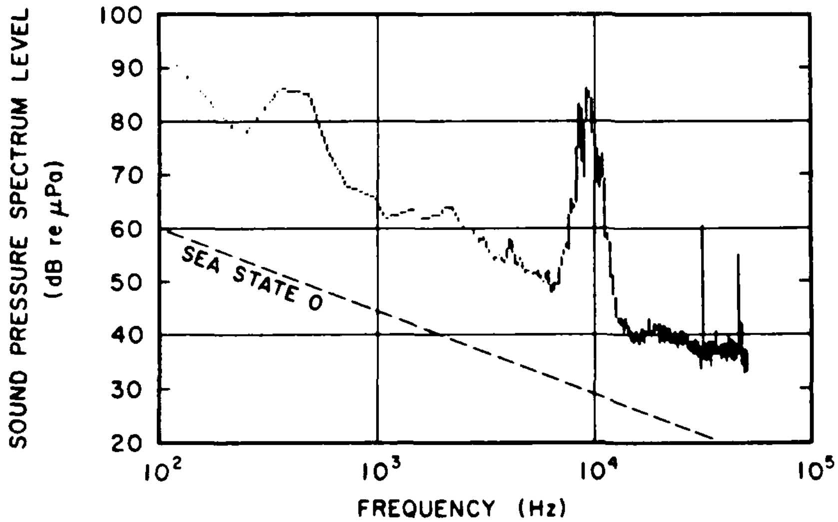

NO. 9
DATE: 1 APR 86
TIME (LOCAL): 1945

HIGH PASS FILTER: 12 Hz

CONDITIONS:

UQC AT 10 kHz

Figure 20, cont.

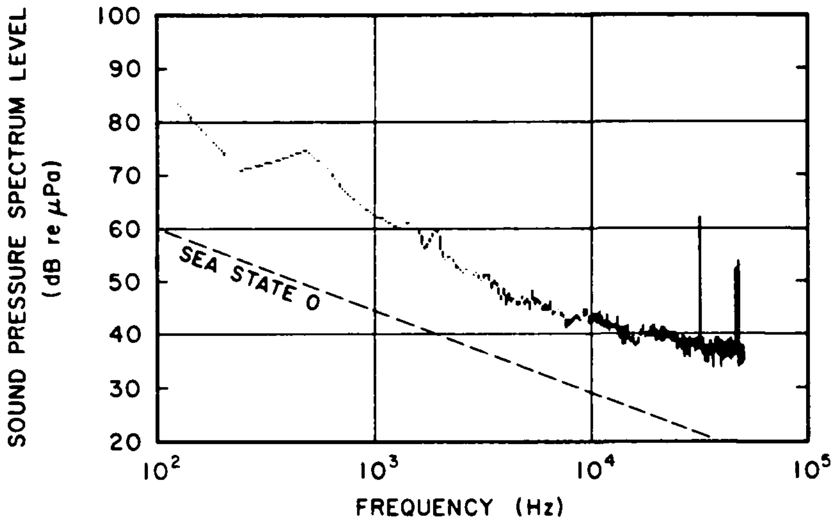

NO. 10
DATE: 2 APR 86
TIME (LOCAL): 0630

HIGH PASS FILTER: 12 Hz

CONDITIONS:

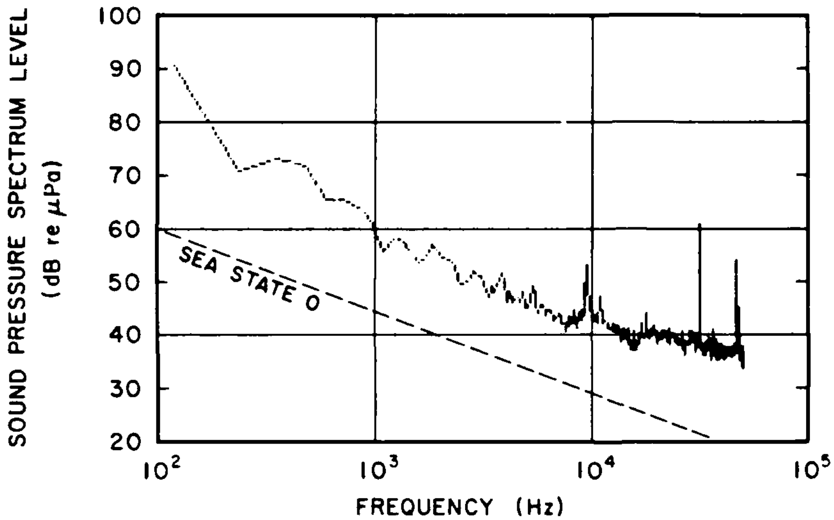

NO. 11
DATE: 2 APR 86
TIME (LOCAL): 1825

HIGH PASS FILTER: 12 Hz

CONDITIONS:

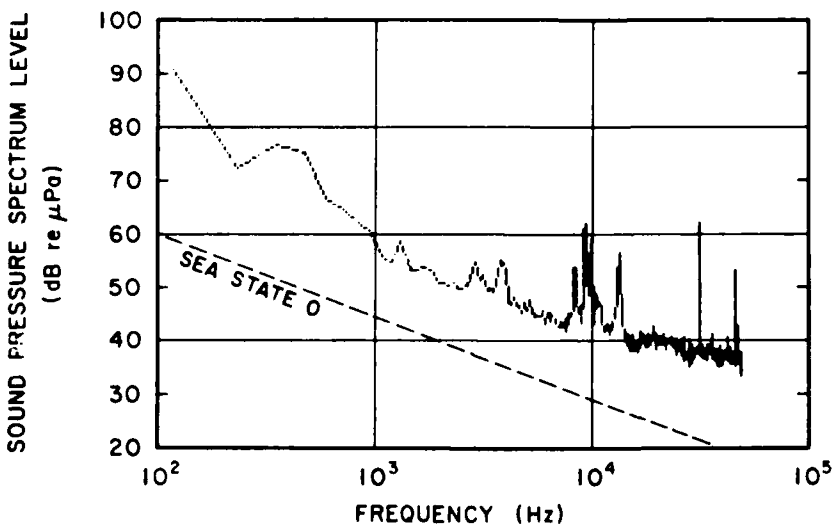

NO. 12
DATE: 2 APR 86
TIME (LOCAL): 2140

HIGH PASS FILTER: 12 Hz

CONDITIONS:

Figure 20, cont.

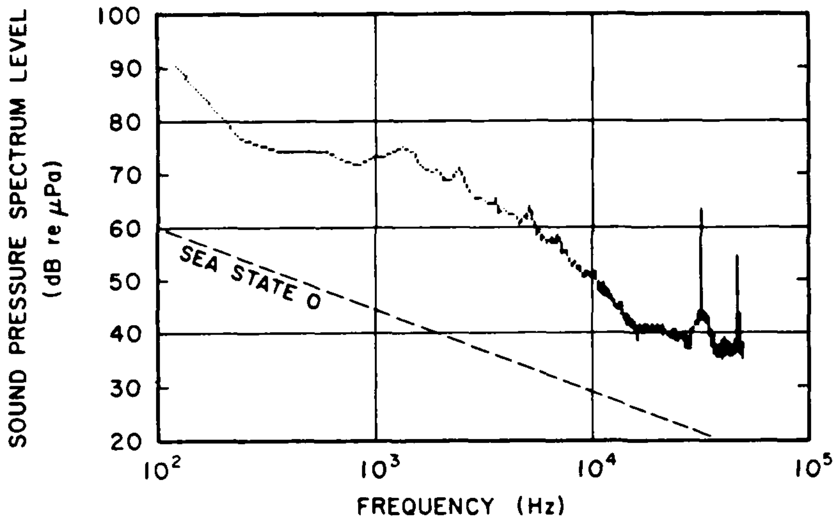

NO. 13
DATE: 3 APR 86
TIME (LOCAL): 1530

HIGH PASS FILTER: 12 Hz

CONDITIONS:

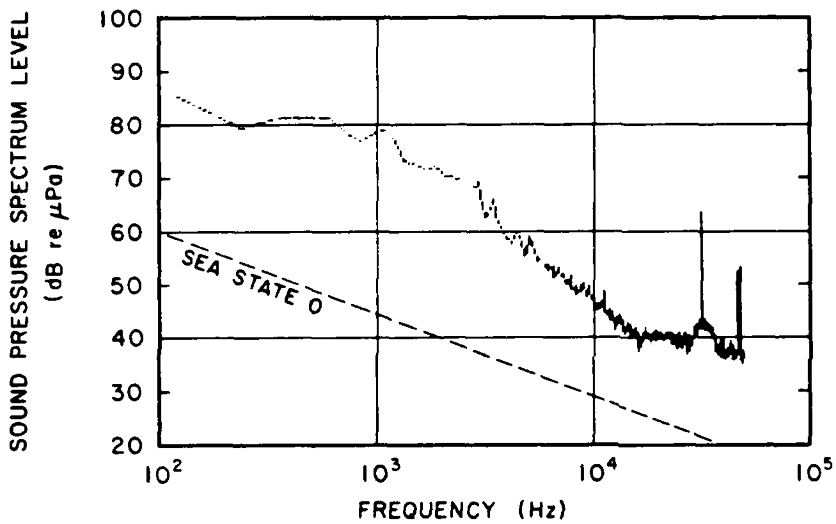

NO. 14
DATE: 4 APR 86
TIME (LOCAL): 1240

HIGH PASS FILTER: 12 Hz

CONDITIONS:

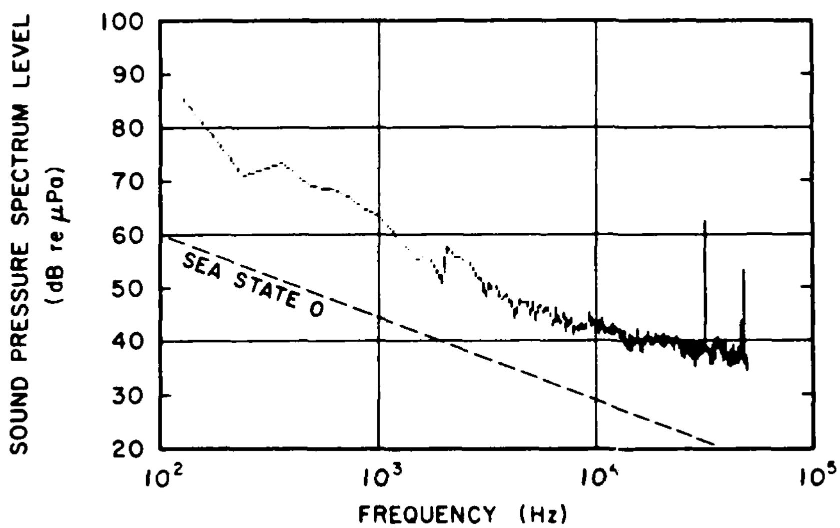

NO. 15
DATE: 4 APR 86
TIME (LOCAL): 1900

HIGH PASS FILTER: 12 Hz

CONDITIONS:

Figure 20, cont.

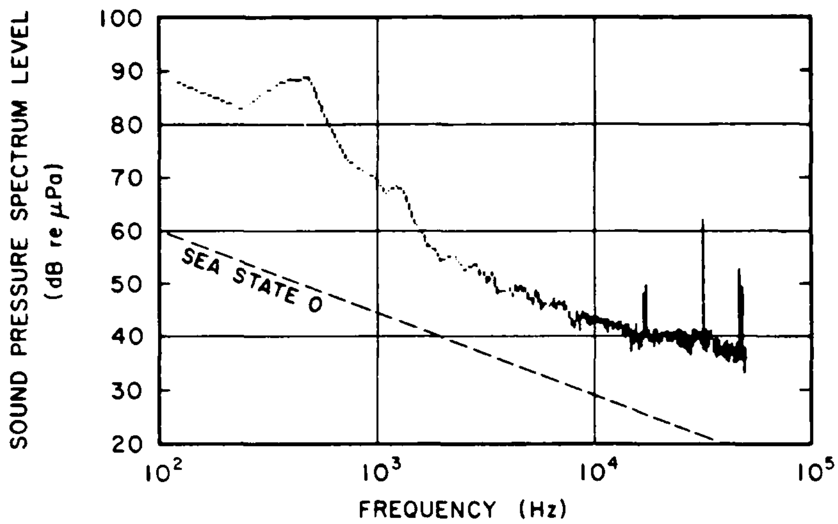

NO. 16
DATE: 5 APR 86
TIME (LOCAL): 0800

HIGH PASS FILTER: 12 Hz

CONDITIONS:

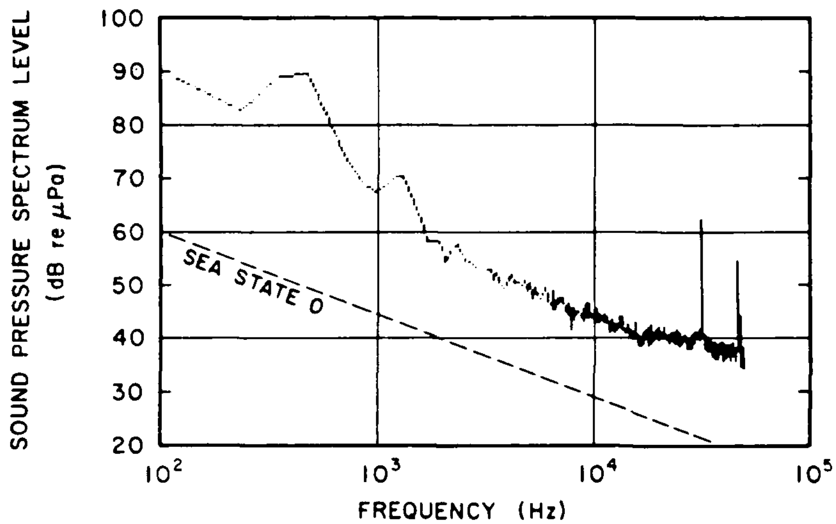

NO. 17
DATE: 5 APR 86
TIME (LOCAL): 0820

HIGH PASS FILTER: 12 Hz

CONDITIONS:

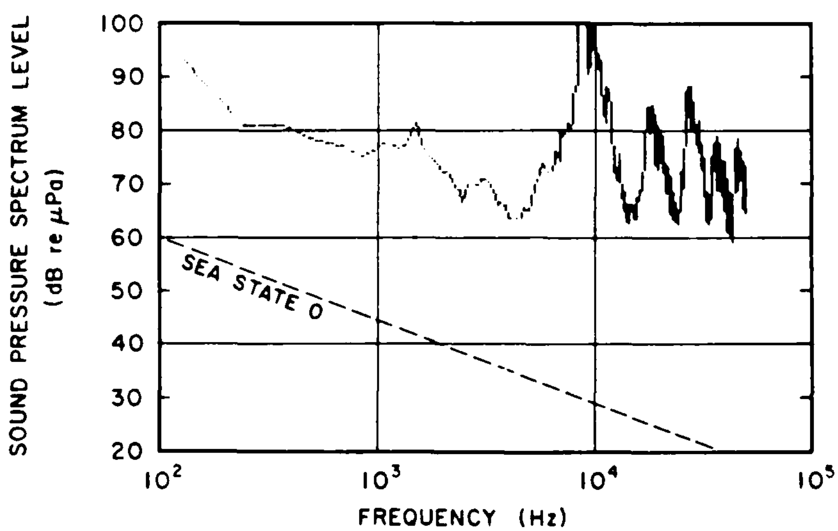

NO. 18
DATE: 6 APR 86
TIME (LOCAL): 1110

HIGH PASS FILTER: 12 Hz

CONDITIONS:

Figure 20, cont.

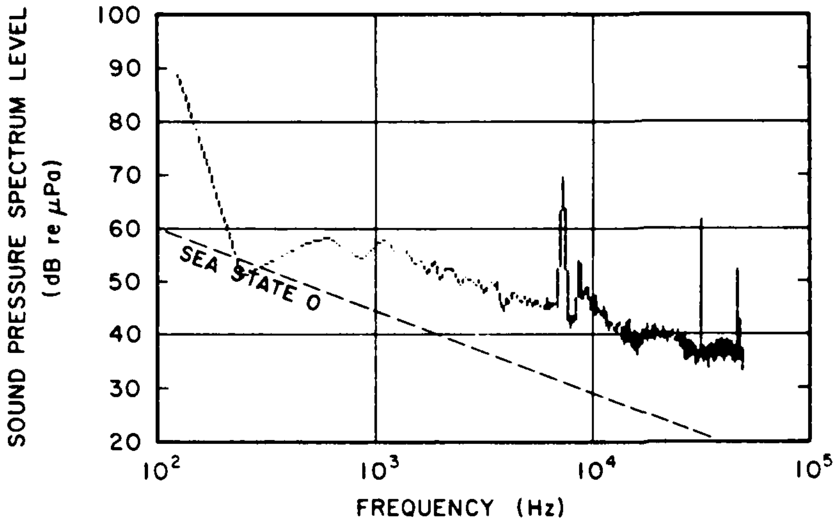

NO. 19
DATE: 7 APR 86
TIME (LOCAL): 0517

HIGH PASS FILTER: 5000 Hz

CONDITIONS:

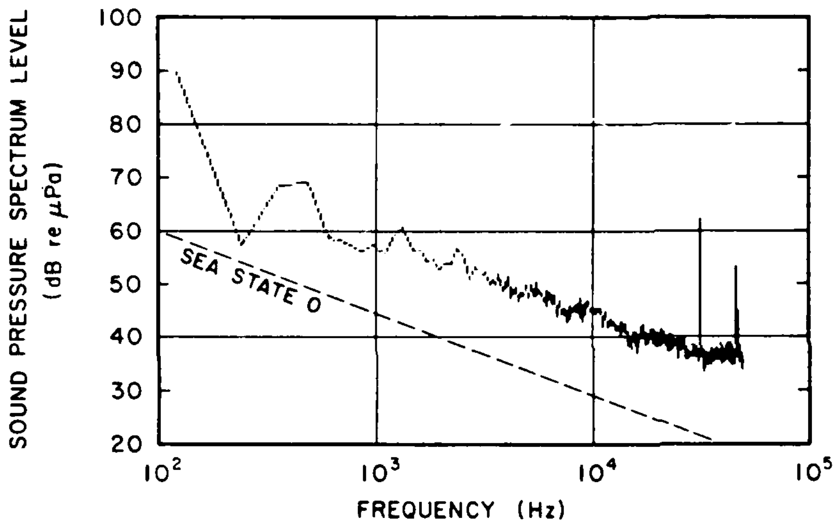

NO. 20
DATE: 7 APR 86
TIME (LOCAL): 1044

HIGH PASS FILTER: 5000 Hz

CONDITIONS:

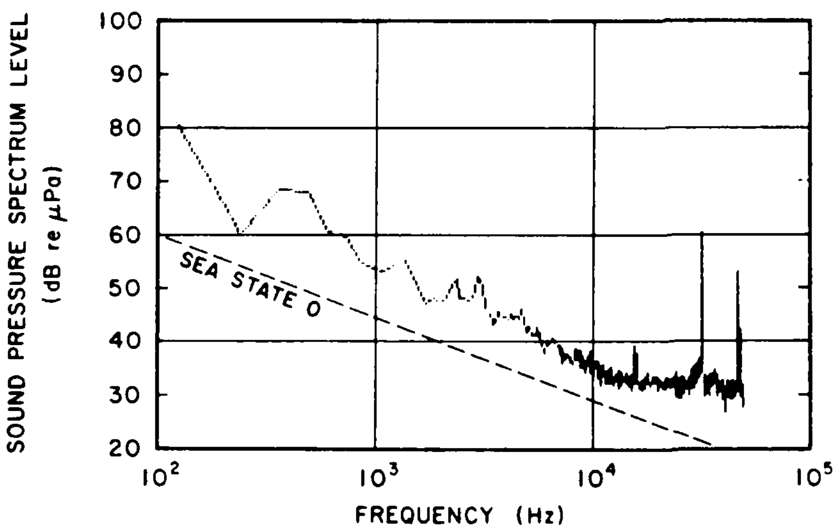

NO. 21
DATE: 7 APR 86
TIME (LOCAL): 1115

HIGH PASS FILTER: 5000 Hz

CONDITIONS:

Figure 20, cont.

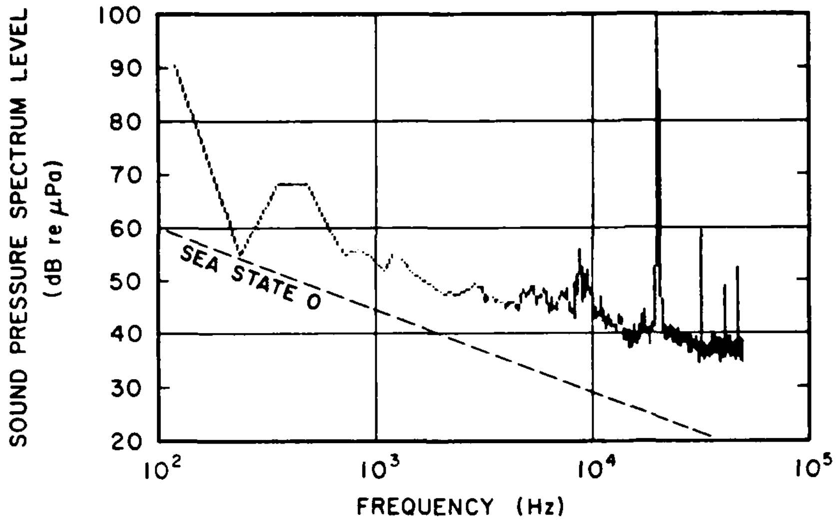

NO. 22
DATE: 8 APR 86
TIME (LOCAL): 0750

HIGH PASS FILTER: 5000 Hz

CONDITIONS:

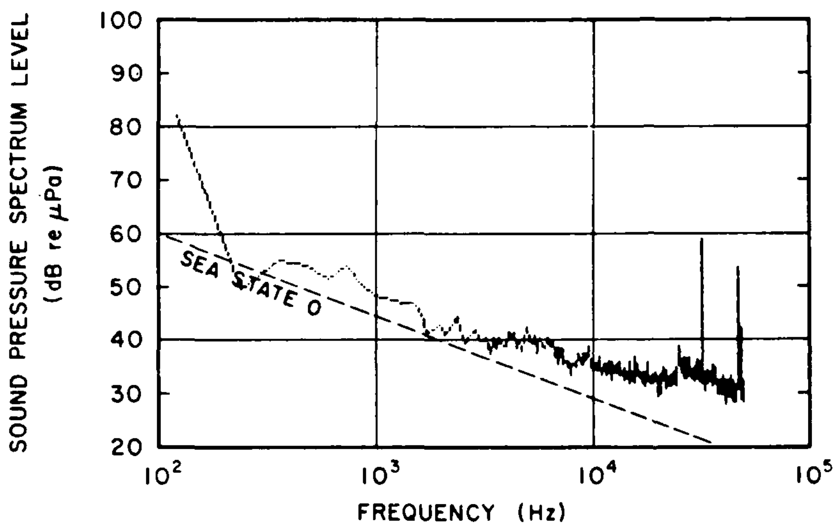

NO. 23
DATE: 8 APR 86
TIME (LOCAL): 1212

HIGH PASS FILTER: 5000 Hz

CONDITIONS:

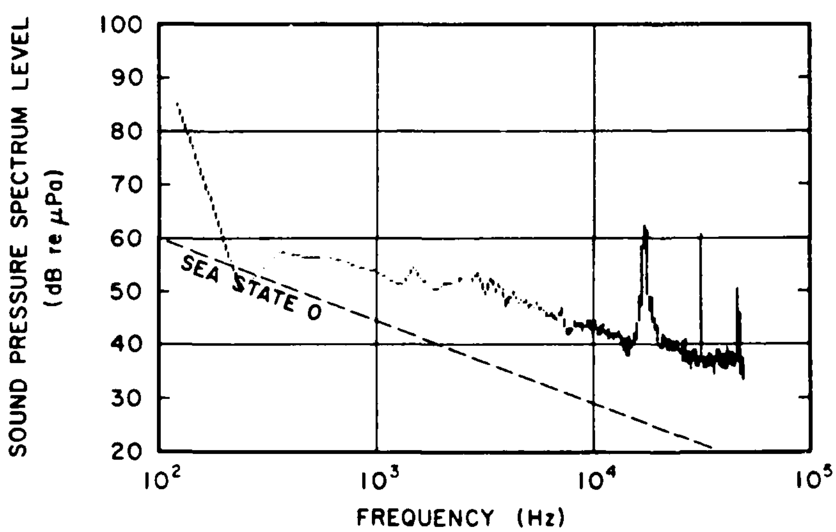

NO. 24
DATE: 9 APR 86
TIME (LOCAL): 0650

HIGH PASS FILTER: 5000 Hz

CONDITIONS:

Figure 20, cont.

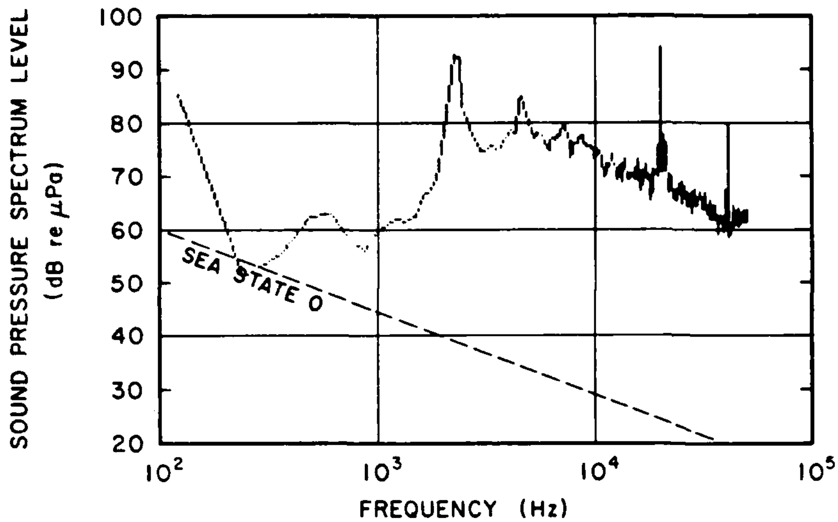

NO. 25
DATE: 10 APR 86
TIME (LOCAL): 0645

HIGH PASS FILTER: 5000 Hz

CONDITIONS:

PROBABLY THRUSTER

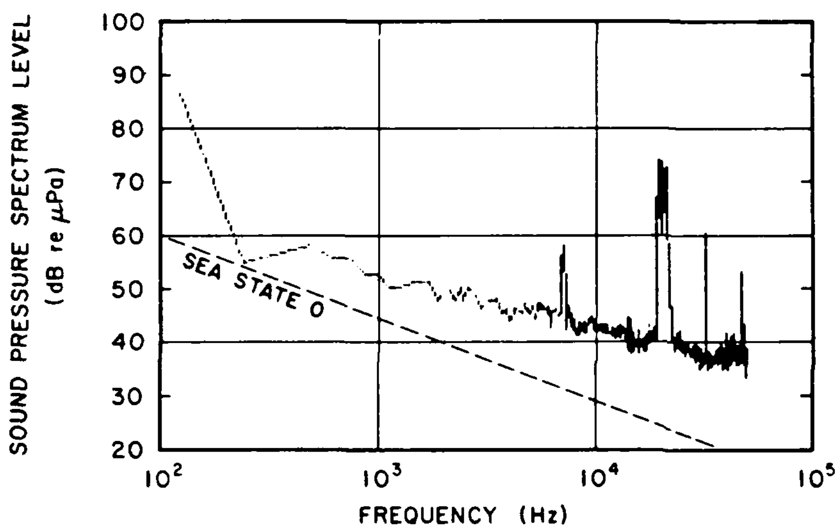

NO. 26
DATE: 10 APR 86
TIME (LOCAL): 0648

HIGH PASS FILTER: 5000 Hz

CONDITIONS:

20 kHz PING

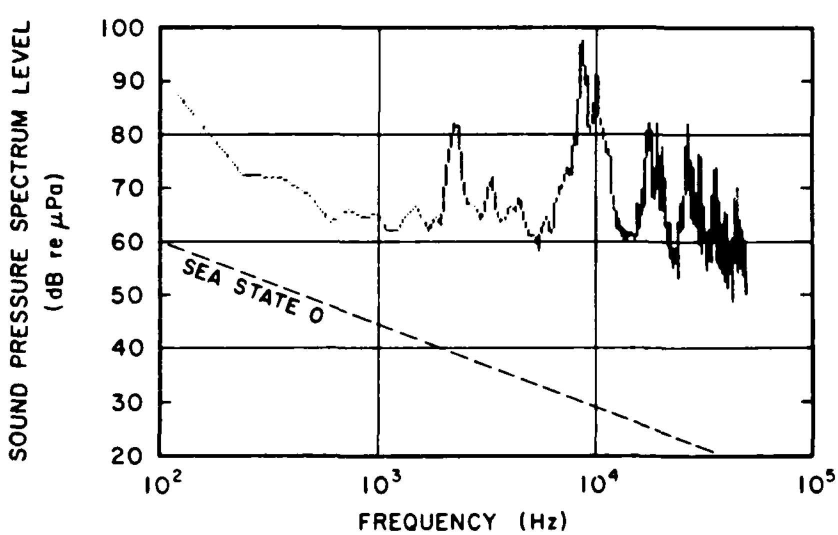

NO. 27
DATE: 10 APR 86
TIME (LOCAL): 0655

HIGH PASS FILTER: 5000 Hz

CONDITIONS:

POSSIBLY THRUSTER

Figure 20, cont.

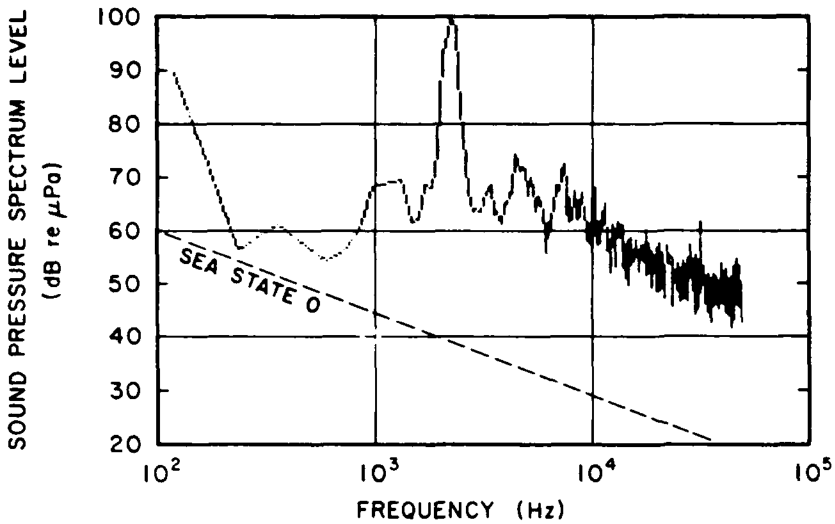

NO. 28
DATE: 10 APR 86
TIME (LOCAL): 0800

HIGH PASS FILTER: 5000 Hz

CONDITIONS:

POSSIBLY THRUSTER

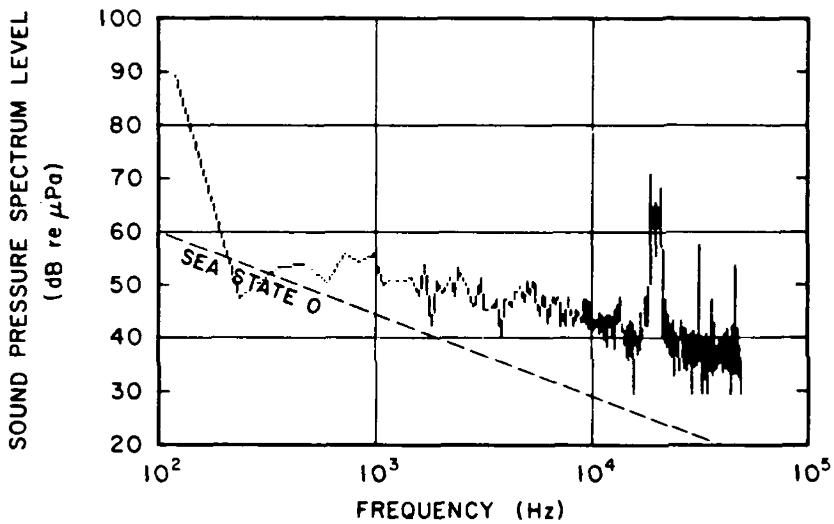

NO. 29
DATE: 10 APR 86
TIME (LOCAL): 0817

HIGH PASS FILTER: 5000 Hz

CONDITIONS:

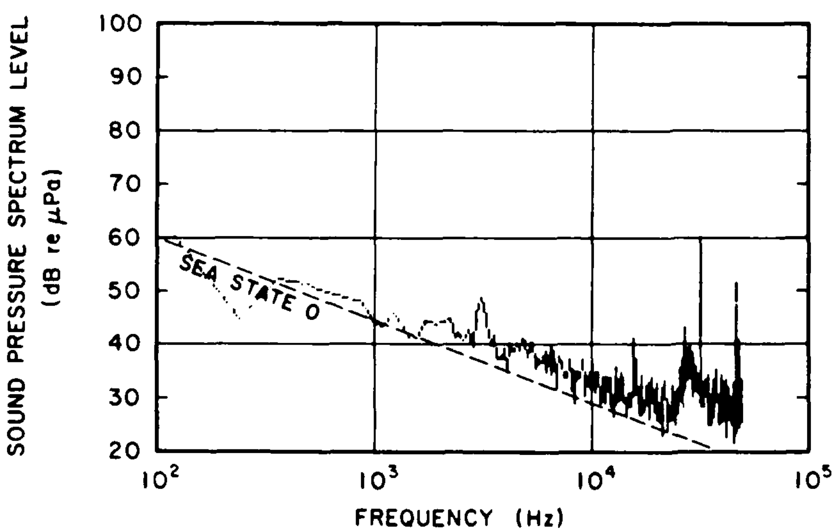

NO. 30
DATE: 10 APR 86
TIME (LOCAL): 0821

HIGH PASS FILTER: 5000 Hz

CONDITIONS:

Figure 20, cont.

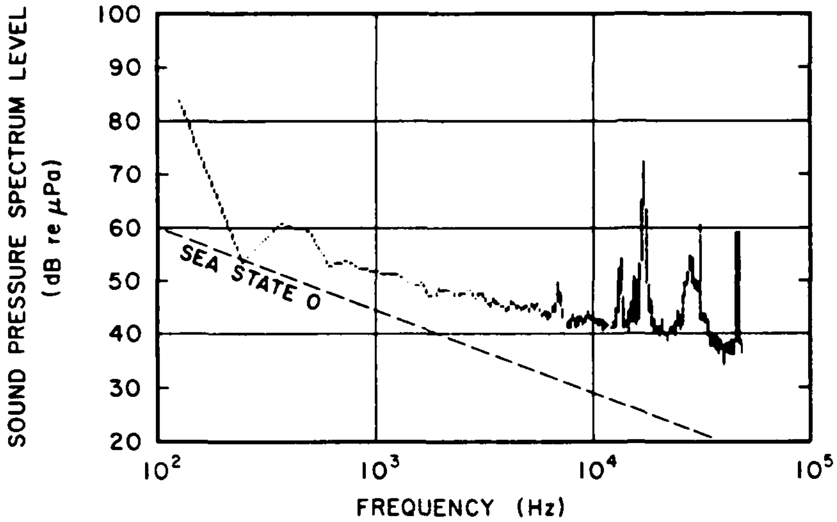

NO. 31
DATE: 11 APR 86
TIME (LOCAL): 0705

HIGH PASS FILTER: 5000 Hz

CONDITIONS:

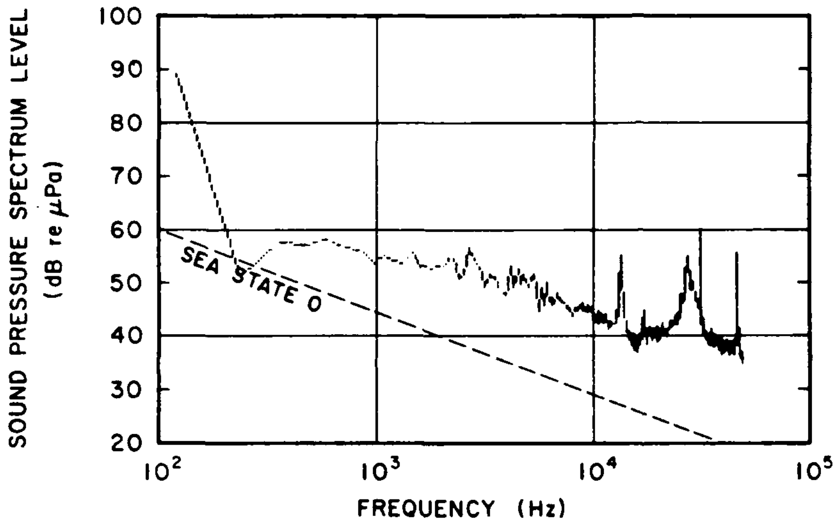

NO. 32
DATE: 11 APR 86
TIME (LOCAL): 0740

HIGH PASS FILTER: 5000 Hz

CONDITIONS:

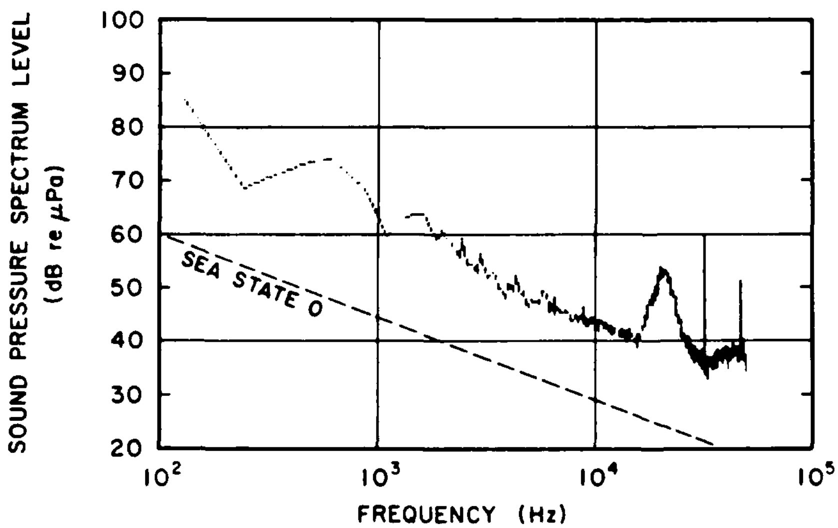

NO. 33
DATE: 12 APR 86
TIME (LOCAL): 0600

HIGH PASS FILTER: 12 Hz

CONDITIONS:

Figure 20, cont.

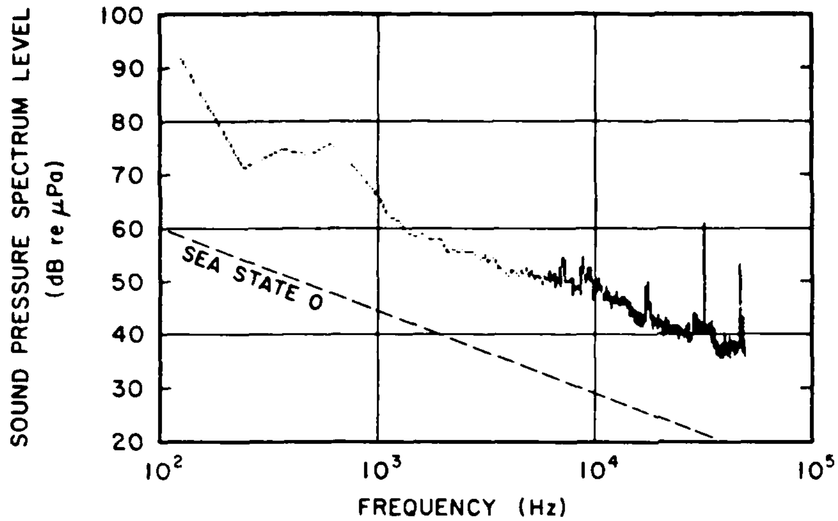

NO. 34
DATE: 13 APR 1986
TIME (LOCAL): 0903

HIGH PASS FILTER: 12 Hz

CONDITIONS:

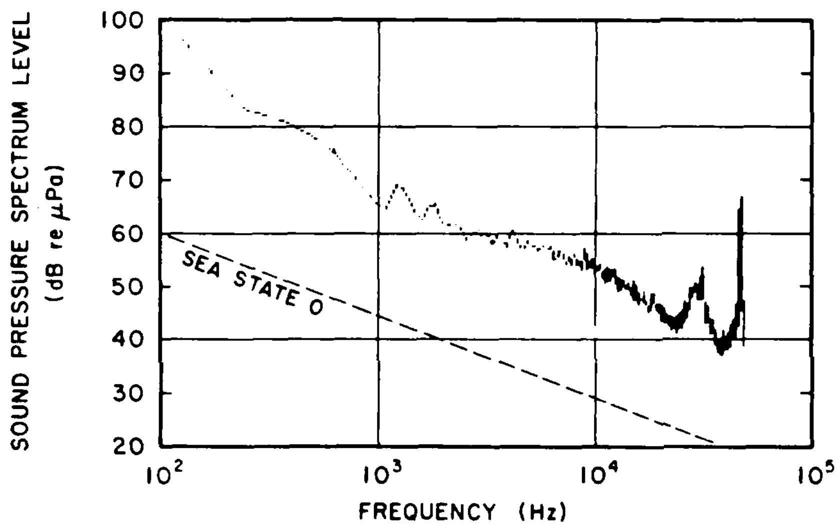

NO. 35
DATE: 14 APR 86
TIME (LOCAL): 0827

HIGH PASS FILTER: 12 Hz

CONDITIONS:

STORMY

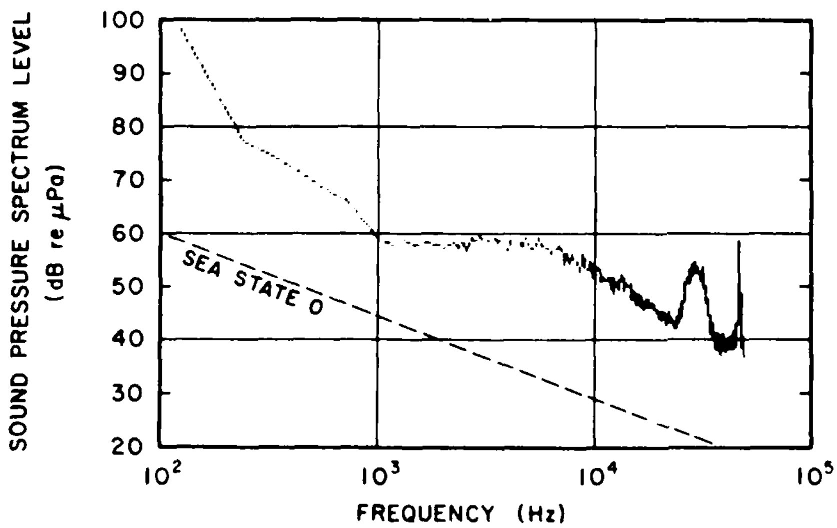

NO. 36
DATE: 14 APR 86
TIME (LOCAL): 0900

HIGH PASS FILTER: 12 Hz

CONDITIONS:

STORMY

Figure 20, cont.

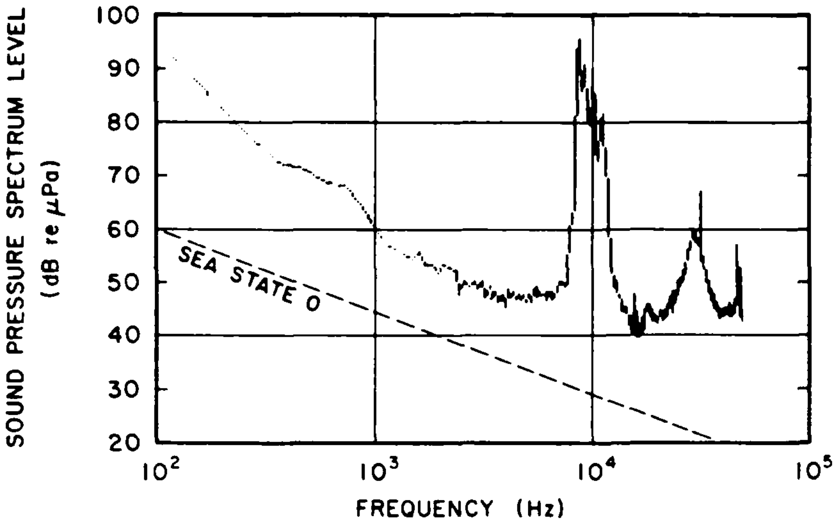

NO. 38
DATE: 22 APR 86
TIME (LOCAL): 0930

HIGH PASS FILTER: 12 Hz

CONDITIONS:

UQC at 10 kHz

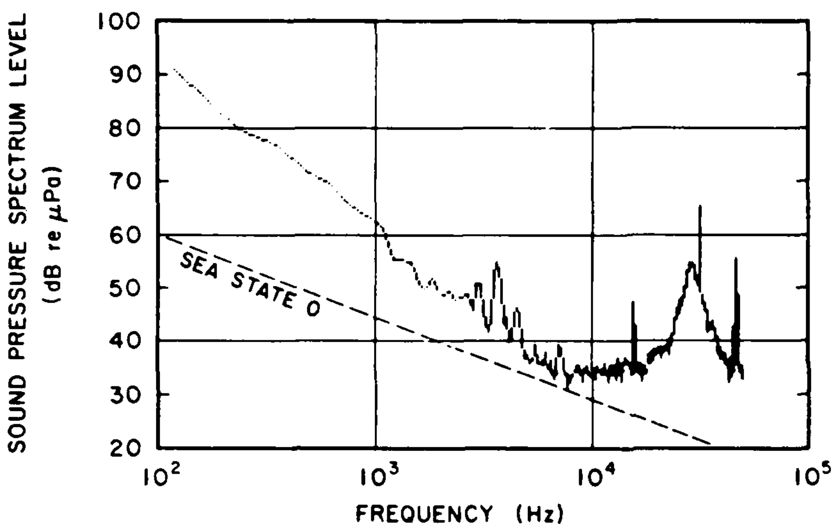

NO. 41
DATE: 24 APR 86
TIME (LOCAL): 1642

HIGH PASS FILTER: 12 Hz

CONDITIONS:

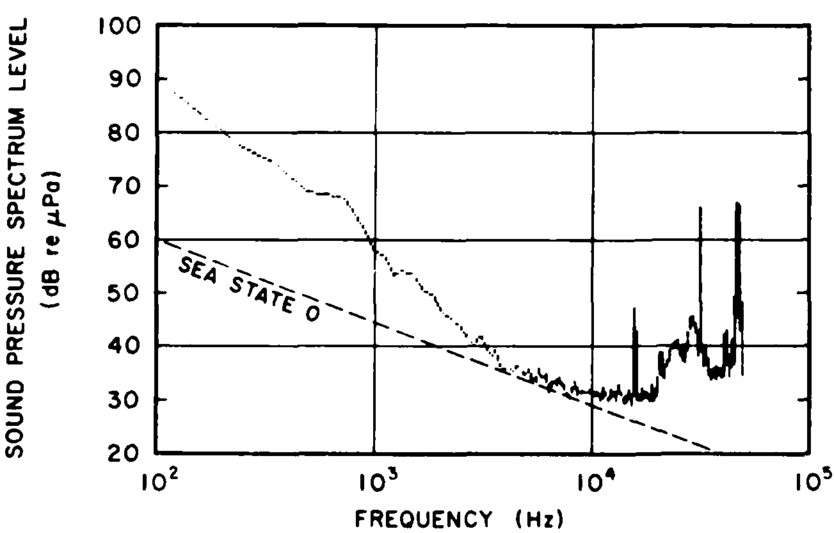

NO. 42
DATE: 25 APR 86
TIME (LOCAL): 0650

HIGH PASS FILTER: 12 Hz

CONDITIONS:

Figure 20, cont.

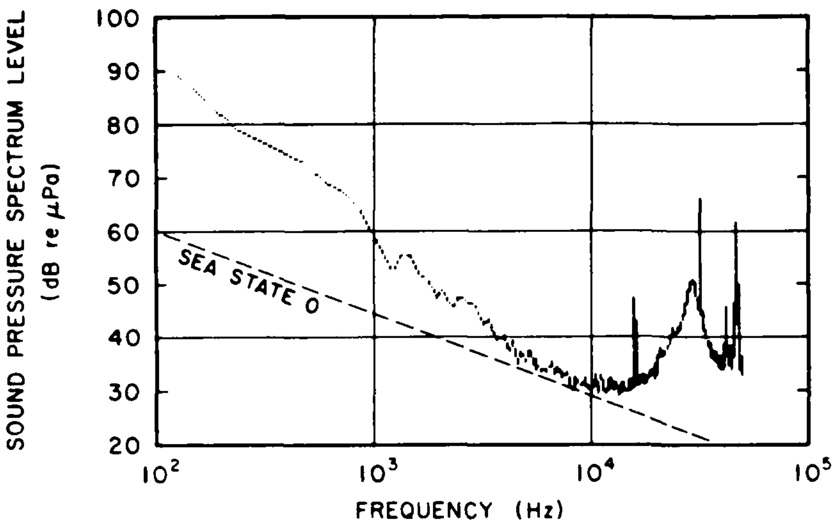

NO. 44
DATE: 25 APR 86
TIME (LOCAL): 0940

HIGH PASS FILTER: 12 Hz

CONDITIONS:

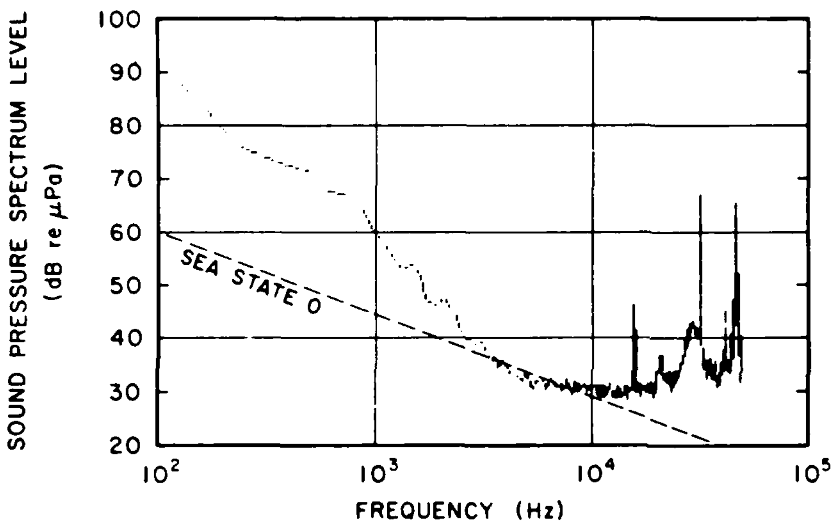

NO. 46
DATE: 26 APR 86
TIME (LOCAL): 0610

HIGH PASS FILTER: 12 Hz

CONDITIONS:

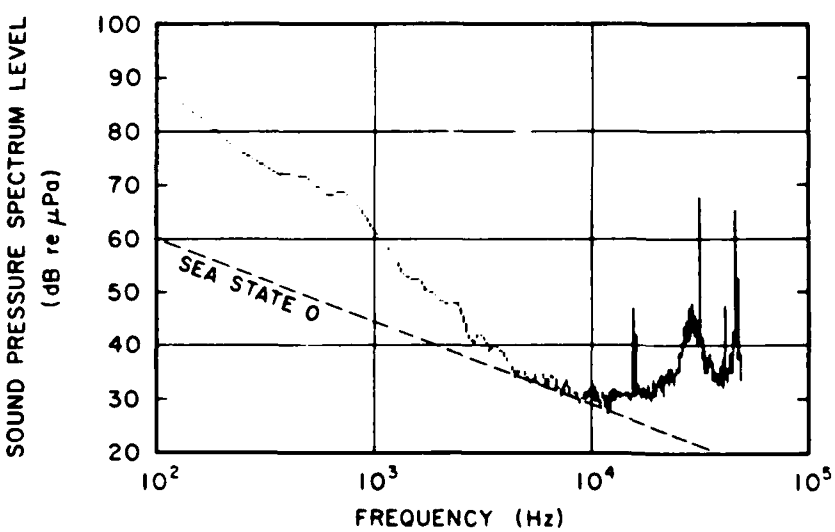

NO. 48
DATE: 26 APR 86
TIME (LOCAL): 0620

HIGH PASS FILTER: 12 Hz

CONDITIONS:

Figure 20, cont.

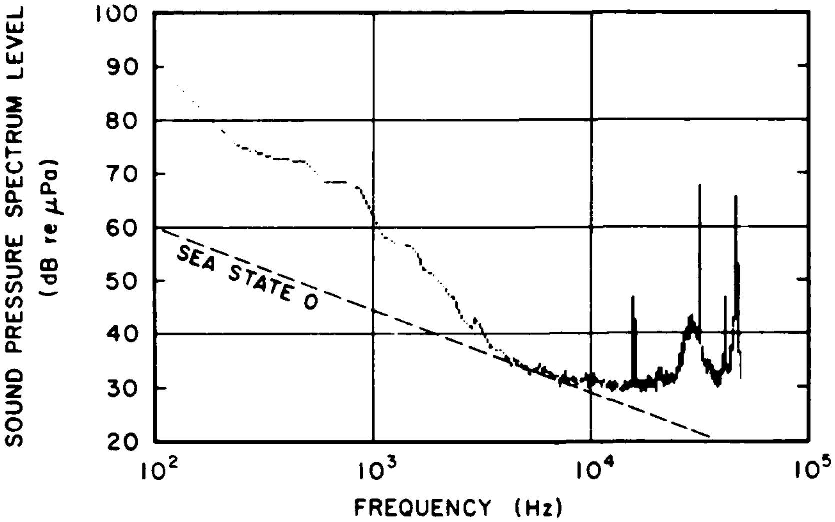

NO. 49
DATE: 26 APR 86
TIME (LOCAL): 0625

HIGH PASS FILTER: 12 Hz

CONDITIONS:

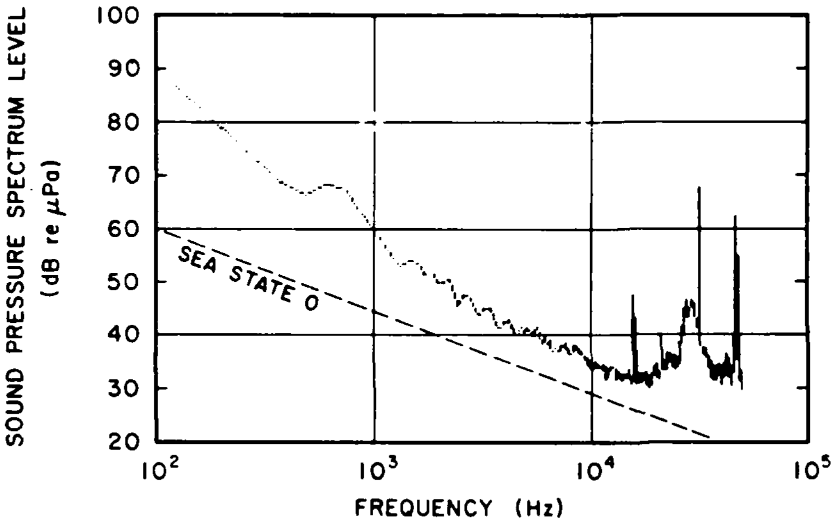

NO. 50
DATE: 26 APR 86
TIME (LOCAL): 1848

HIGH PASS FILTER: 12 Hz

CONDITIONS:

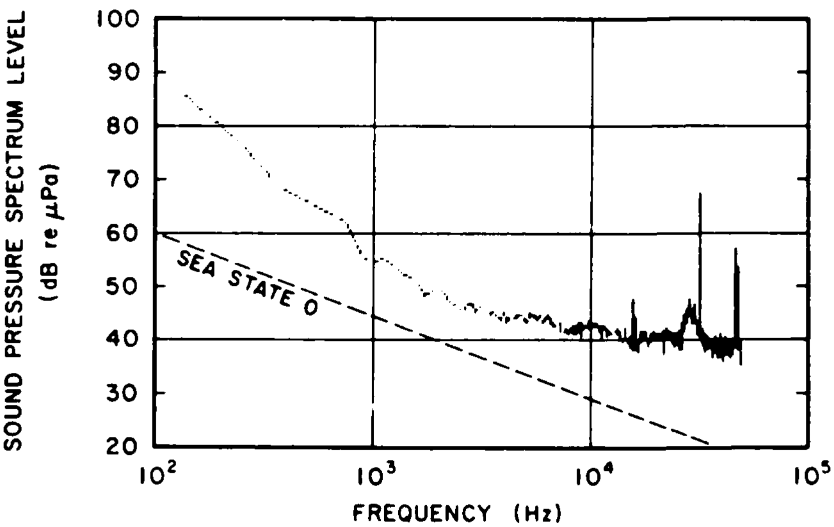

NO. 51
DATE: 27 APR 86
TIME (LOCAL): 0650

HIGH PASS FILTER: 12 Hz

CONDITIONS:

Figure 20, cont.

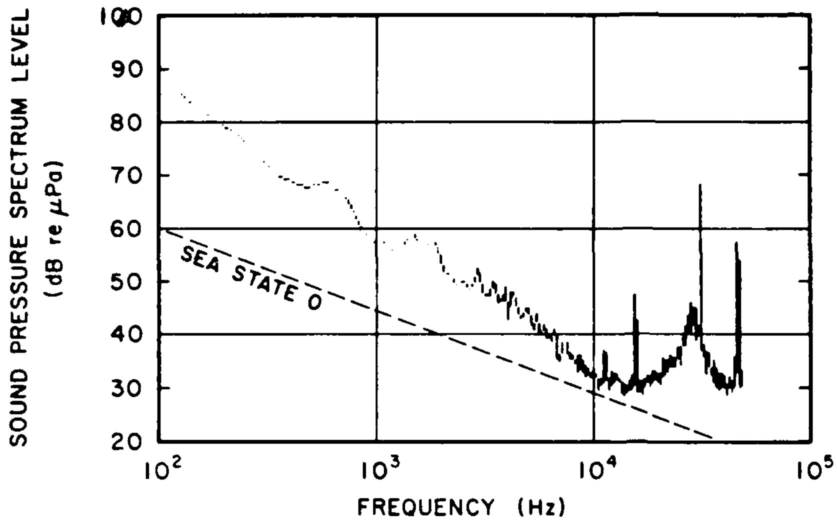

NO. 52
DATE: 27 APR 86
TIME (LOCAL): 0653

HIGH PASS FILTER: 12 Hz

CONDITIONS:

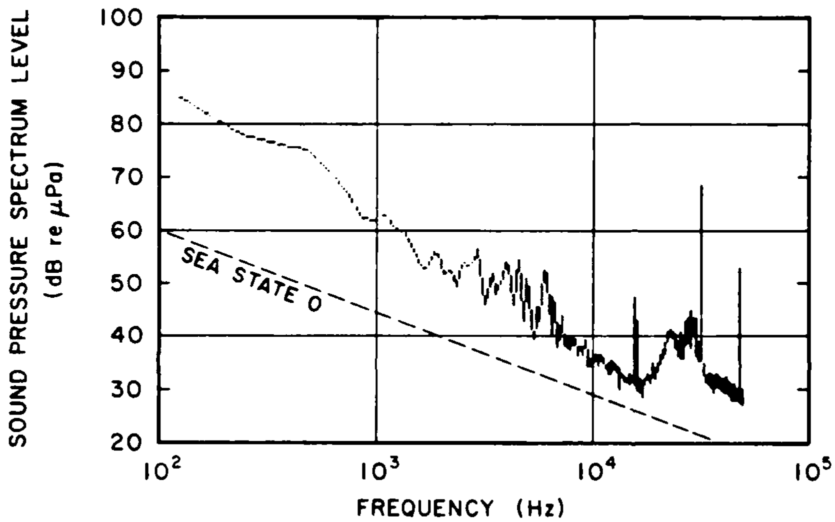

NO. 55
DATE: 27 APR 86
TIME (LOCAL): 0756

HIGH PASS FILTER: 12 Hz

CONDITIONS:

d. c. POWER SUPPLY

Figure 20, cont.

To analyze the noise present at the camp, many noise sources would have to be considered and the appropriate data recorded. The underwater telephone (WQC) was in operation intermittently and created a large disturbance. Tracking pings were often transmitted at 10 s intervals, and several experiments involved sound transmissions into the water. The electric generators powering the camp were generally in operation. Snowmobiles and helicopters were operating near the camp.

Although the "camp quiet" periods should have curtailed some of these man-made noises, no attempt was made to monitor the status of all these noise sources during the brief time of the ambient noise recording. As a result, we have not been able to separate the effects of the various noise sources or to evaluate the contribution of each. The weather was recorded as hourly averages, but any correlation between natural underwater noise and weather was probably masked by man-made camp noise. The stormy periods are noted in Table V.

VIII. REFERENCES

1. G.R. Garrison, "Chukchi Sea oceanography: 1975 measurements and a review of coastal current properties," APL-UW 7614, 27 November 1976.

2. G.R. Garrison and P. Becker, "The Barrow Canyon: a drain for the Chukchi Sea," *J. Geophys. Res.*, **81**: 4444-4453 (1976).

3. G.R. Garrison, M.L. Welch, and J.T. Shaw, "Arctic oceanographic measurements, 1982," APL-UW 4-84, July 1984.

4. G.R. Garrison, J.T. Shaw, and M.L. Welch, "Arctic oceanographic measurements: 1978-1980," APL-UW 8112, June 1982.

5. G.R. Garrison and R.G. Paquette, "Warm water interactions in the Barrow Canyon in winter," *J. Geophys. Res.*, **87**: 5853-5859 (1982).

6. G.R. Garrison, T. Wen, and M.L. Welch, "Environmental measurements in the Beaufort Sea, autumn 1984," APL-UW 3-85, March 1985.

7. L.K. Coachman and C.A. Barnes, "The contribution of Bering Sea water to the Arctic Ocean," *Arctic*, **15**: 251-277 (1961).

8. B.T. Doherty and D.R. Kester, "Freezing point of sea water," *J. Mar. Res.*, **32**: 285-300 (1974).

9. H.R. Feldman, P.H. Moose, and S.R. Shah, "Measurements of the volume scattering strength in the Beaufort and Chukchi seas," *Proc. IEEE Conf. on Eng. in the Ocean Envir., Seattle, 1973*, 508-512.

10. K. Hunkins, "The seasonal variation in the sound-scattering layer observed at Fletcher's Ice Island (T-3) with a 12 kc/s echosounder," *Deep-Sea Res.*, **12**: 879-881 (1965).

11. V.O. Knudsen, R.S. Alford, and J.W. Emling, "Underwater ambient noise," *J. Mar. Res.*, **7**: 410 (1948).

APPENDIX A

NAVSAT Measurements of the Position of the Ice Camp From 20 March to 2 May 1986.

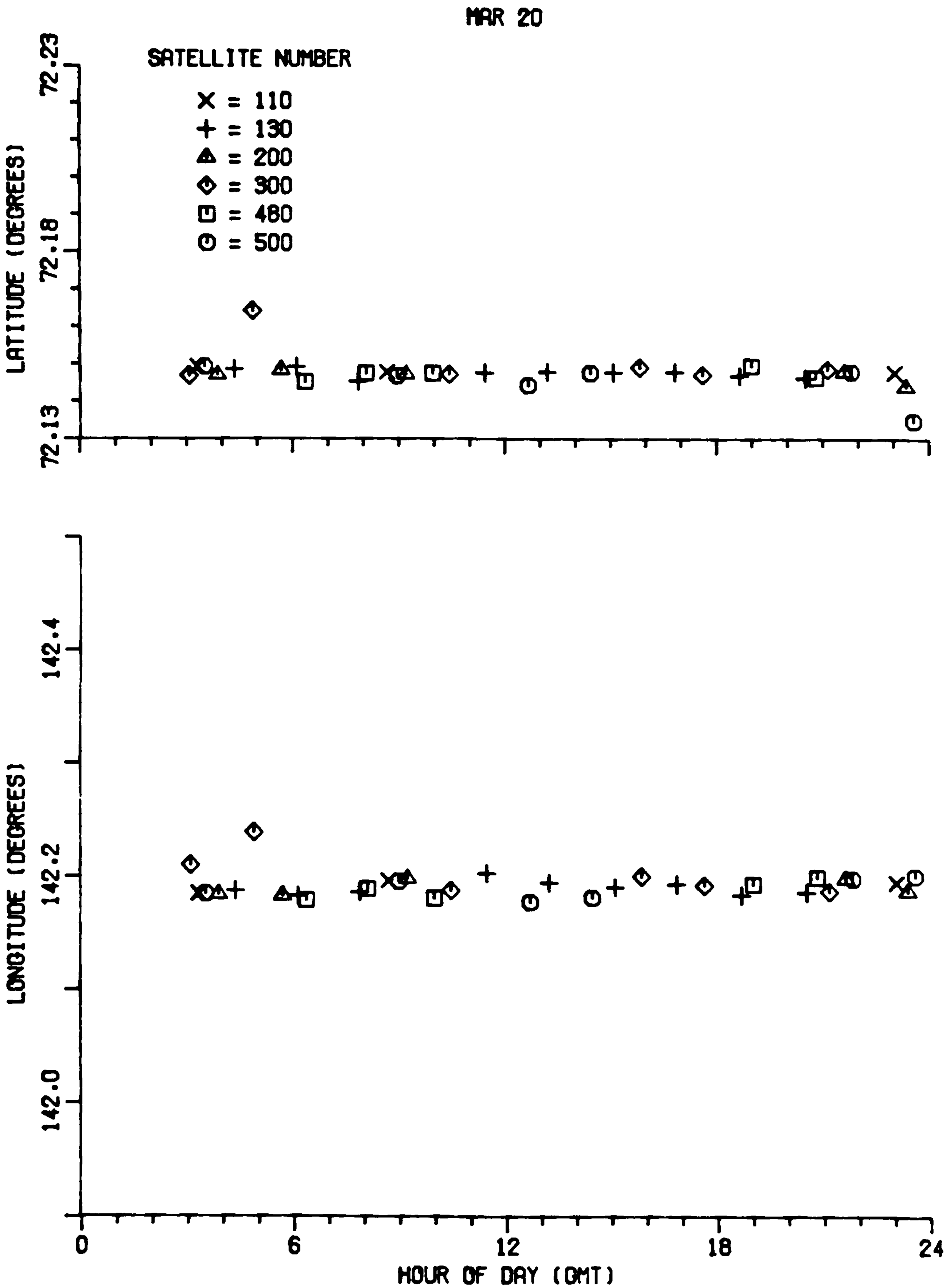
MAR 20
SATELLITE NUMBER
X = 110
+ = 130
Δ = 200
◇ = 300
□ = 480
○ = 500
LATITUDE (DEGREES)
72.23
72.18
72.13
LONGITUDE (DEGREES)
142.4
142.2
142.0
0
6
12
18
24
HOUR OF DAY (GMT)

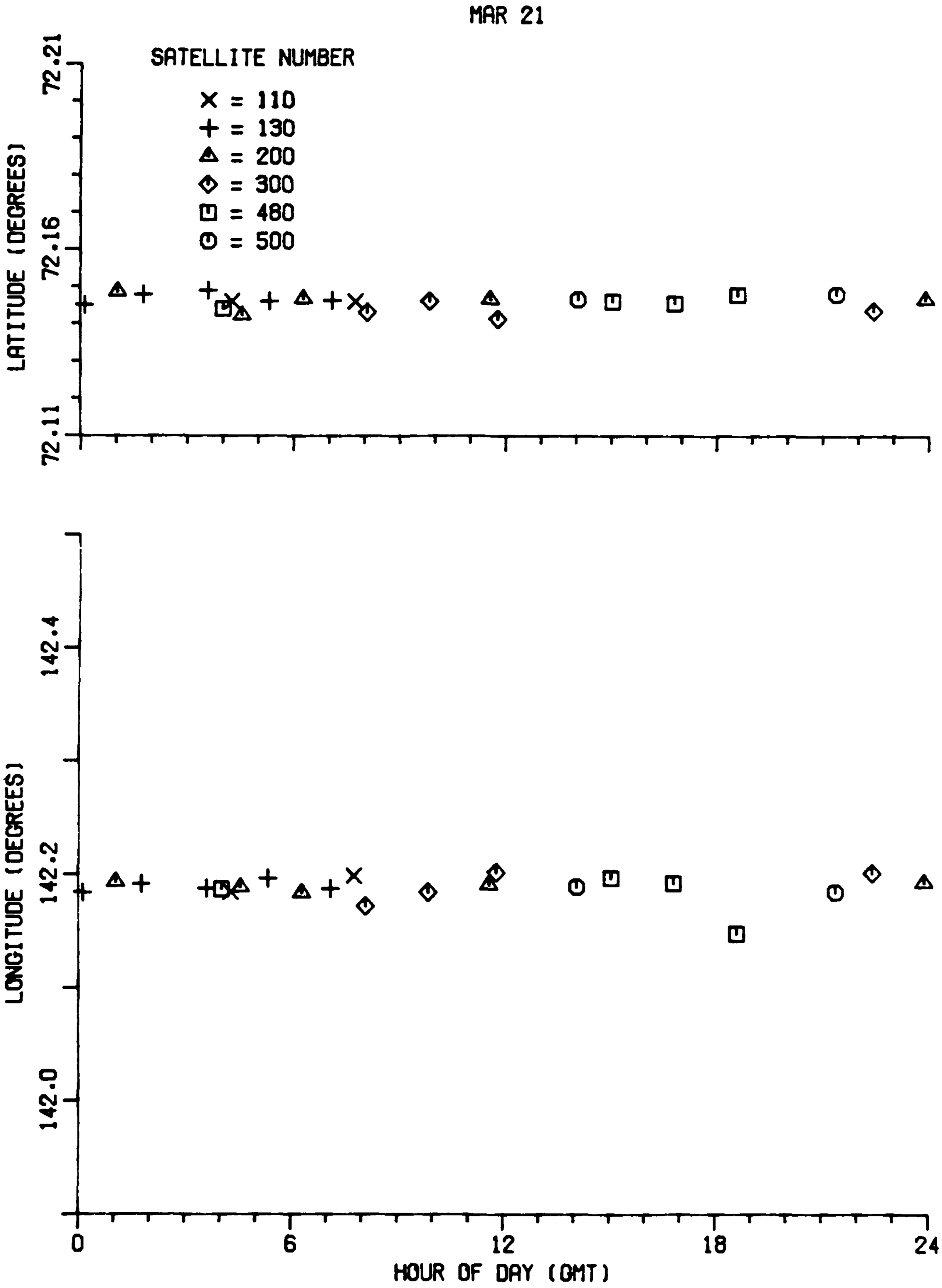
MAR 21
SATELLITE NUMBER
X = 110
+ = 130
Δ = 200
◇ = 300
⊡ = 480
⊙ = 500
LATITUDE (DEGREES)
72.21
72.16
72.11
LONGITUDE (DEGREES)
142.4
142.2
142.0
0
6
12
18
24
HOUR OF DAY (GMT)

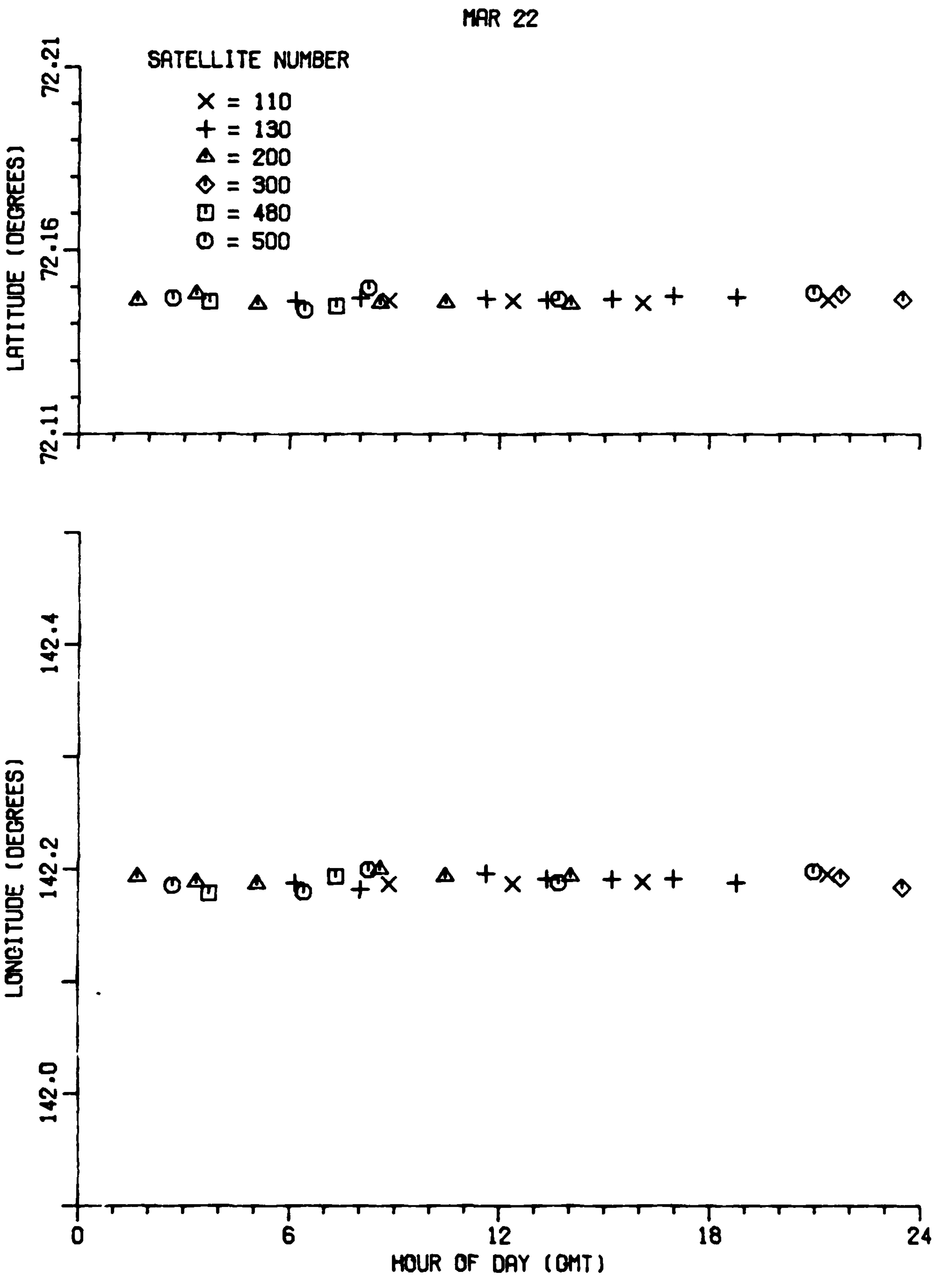

MAR 22
SATELLITE NUMBER
X = 110
+ = 130
Δ = 200
◇ = 300
□ = 480
○ = 500
LATITUDE (DEGREES)
72.21
72.16
72.11
LONGITUDE (DEGREES)
142.4
142.2
142.0
0
6
12
18
24
HOUR OF DAY (GMT)

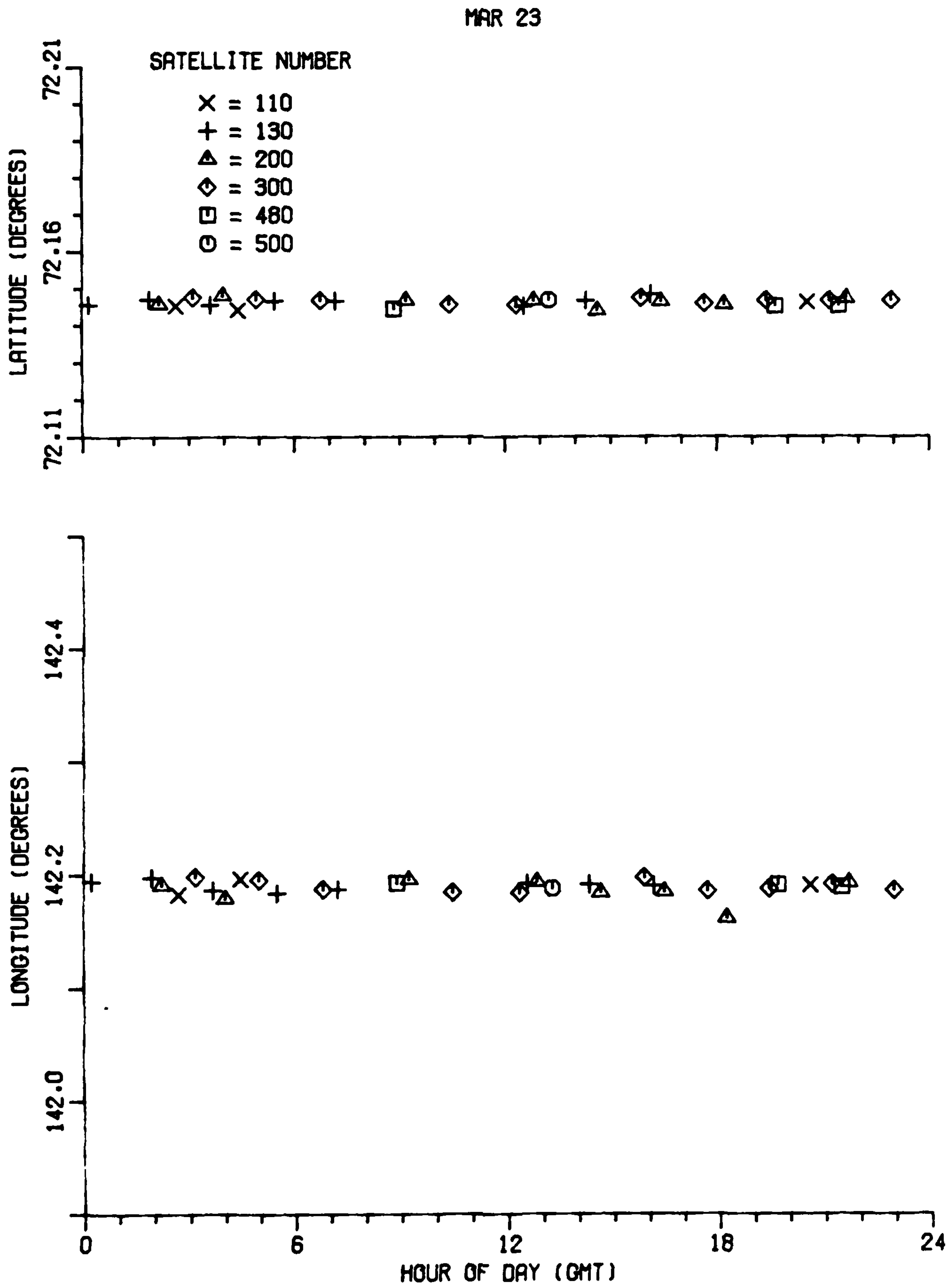
MAR 23
SATELLITE NUMBER
X = 110
+ = 130
△ = 200
◇ = 300
□ = 480
○ = 500
LATITUDE (DEGREES)
72.21
72.16
72.11
LONGITUDE (DEGREES)
142.4
142.2
142.0
0
6
12
18
24
HOUR OF DAY (GMT)

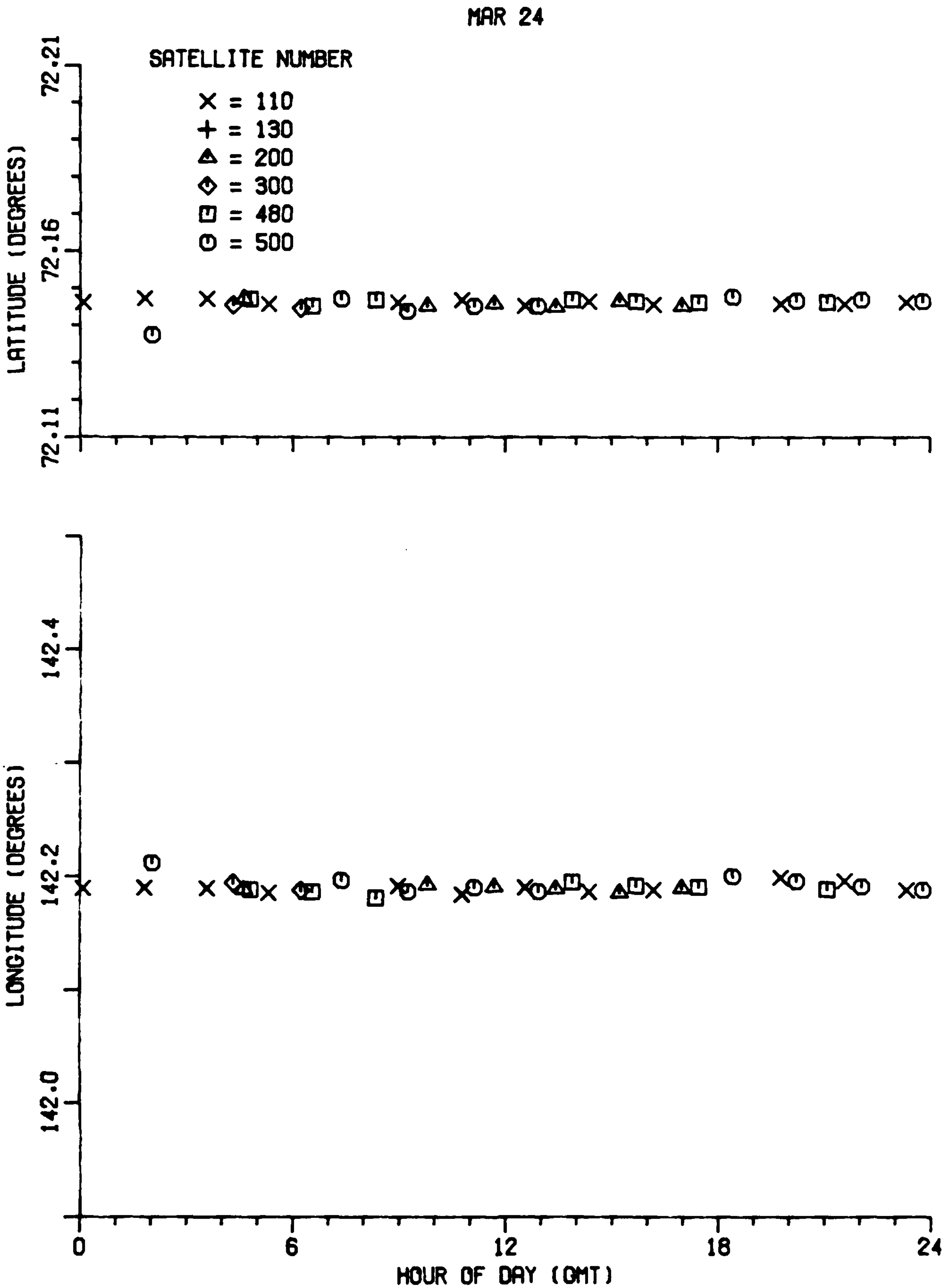

MAR 24
SATELLITE NUMBER
X = 110
+ = 130
△ = 200
◇ = 300
□ = 480
○ = 500
LATITUDE (DEGREES)
72.21
72.16
72.11
LONGITUDE (DEGREES)
142.4
142.2
142.0
0
6
12
18
24
HOUR OF DAY (GMT)

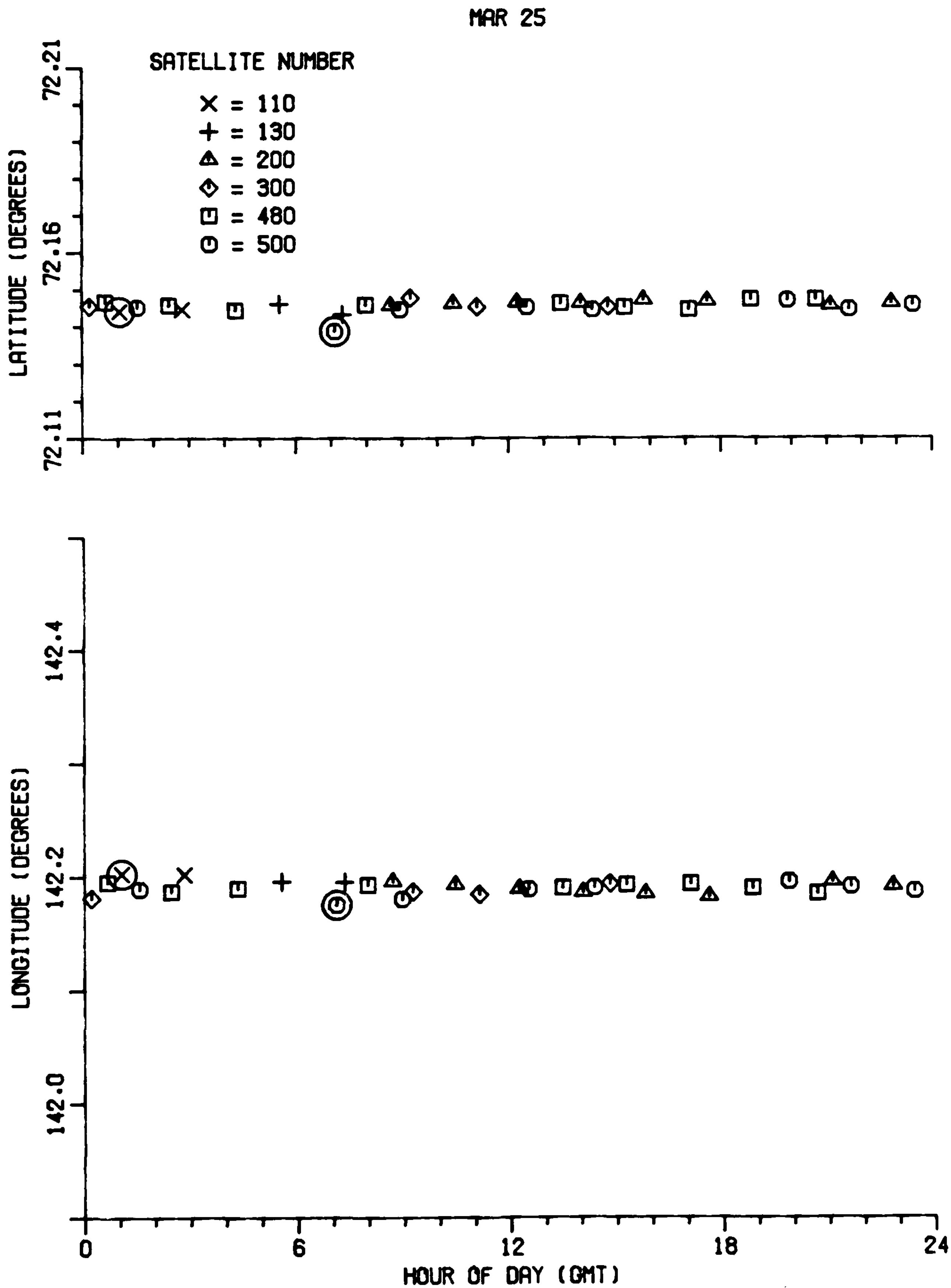
MAR 25
SATELLITE NUMBER
× = 110
+ = 130
△ = 200
◇ = 300
□ = 480
○ = 500
LATITUDE (DEGREES)
72.21
72.16
72.11
LONGITUDE (DEGREES)
142.4
142.2
142.0
0
6
12
18
24
HOUR OF DAY (GMT)

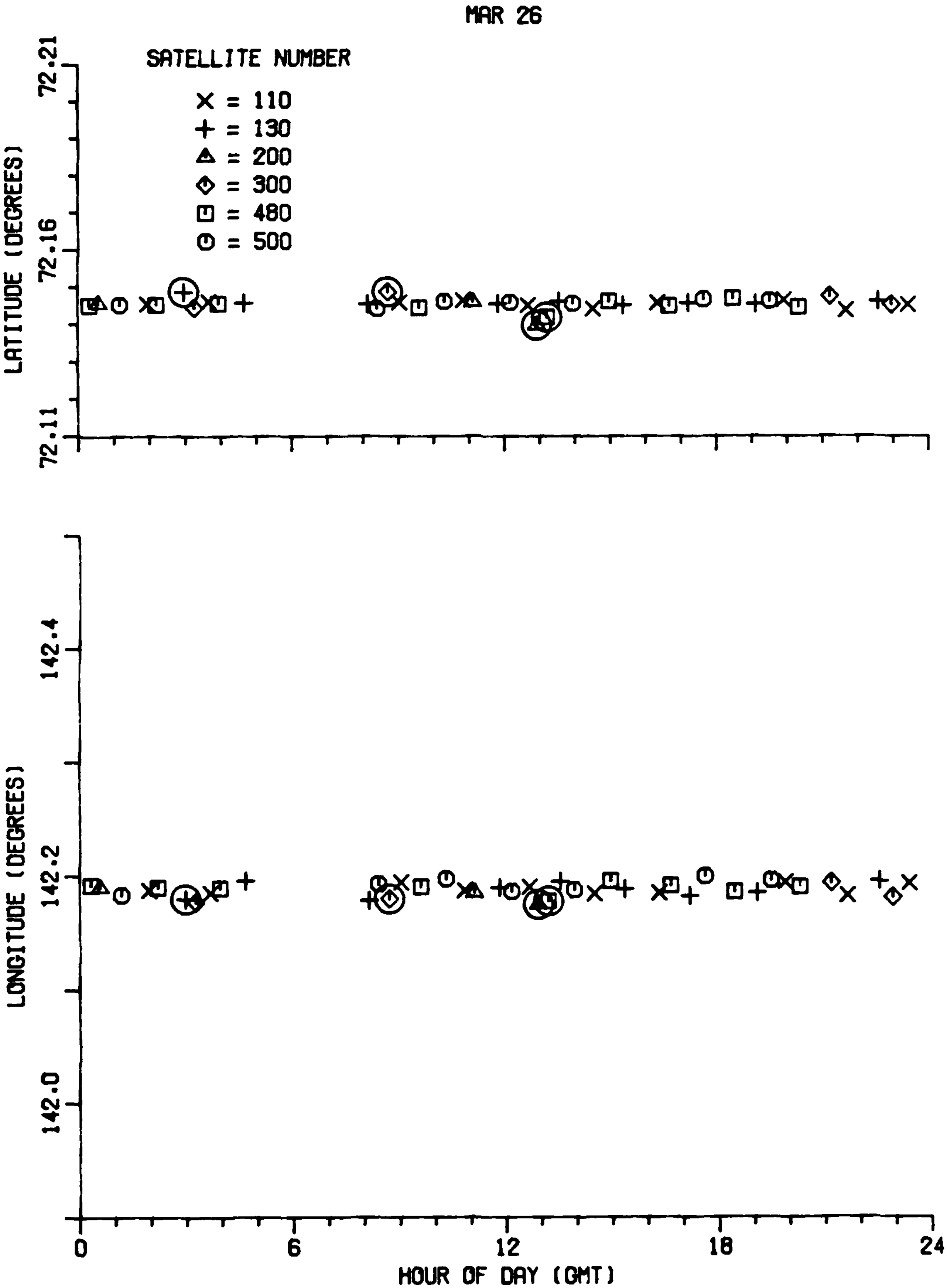
MAR 26
SATELLITE NUMBER
X = 110
+ = 130
△ = 200
◇ = 300
□ = 480
ʘ = 500
LATITUDE (DEGREES)
72.21
72.16
72.11
LONGITUDE (DEGREES)
142.4
142.2
142.0
0
6
12
18
24
HOUR OF DAY (GMT)

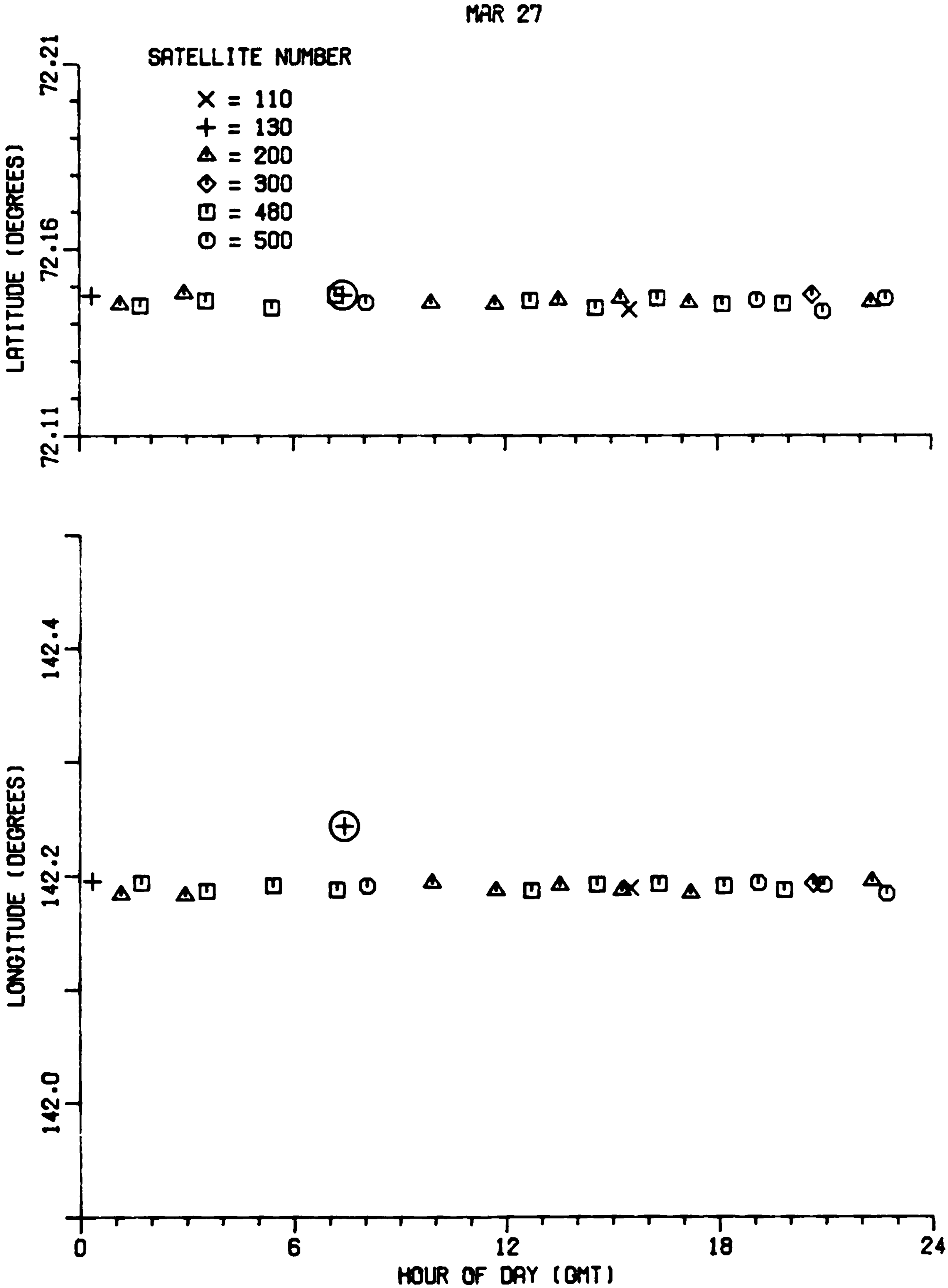
MAR 27
SATELLITE NUMBER
X = 110
+ = 130
Δ = 200
◇ = 300
□ = 480
○ = 500
LATITUDE (DEGREES)
72.21
72.16
72.11
LONGITUDE (DEGREES)
142.4
142.2
142.0
0
6
12
18
24
HOUR OF DAY (GMT)

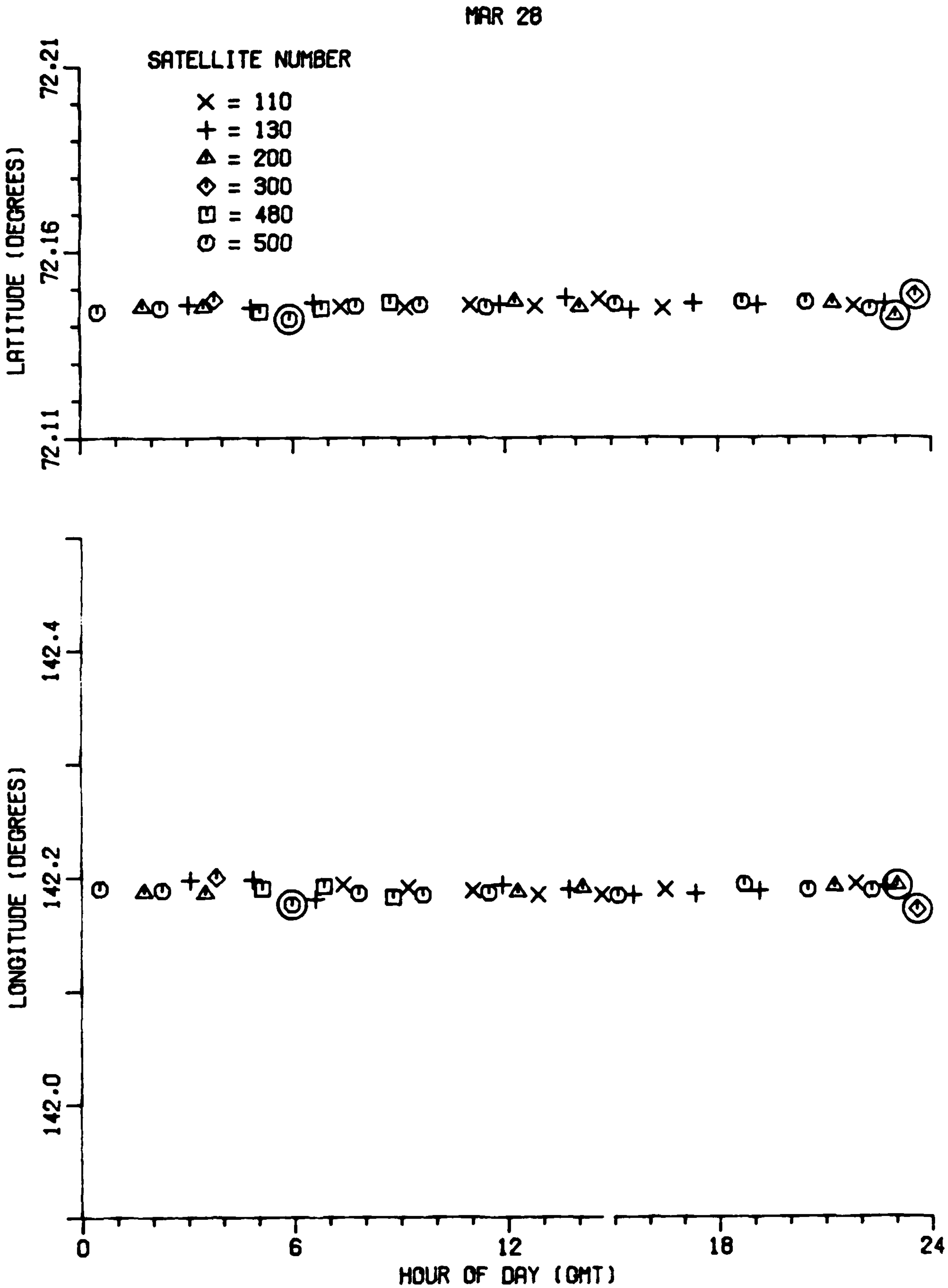
MAR 28
SATELLITE NUMBER
× = 110
+ = 130
△ = 200
◇ = 300
□ = 480
○ = 500
72.21
72.16
72.11
LATITUDE (DEGREES)
142.4
142.2
142.0
LONGITUDE (DEGREES)
0
6
12
18
24
HOUR OF DAY (GMT)

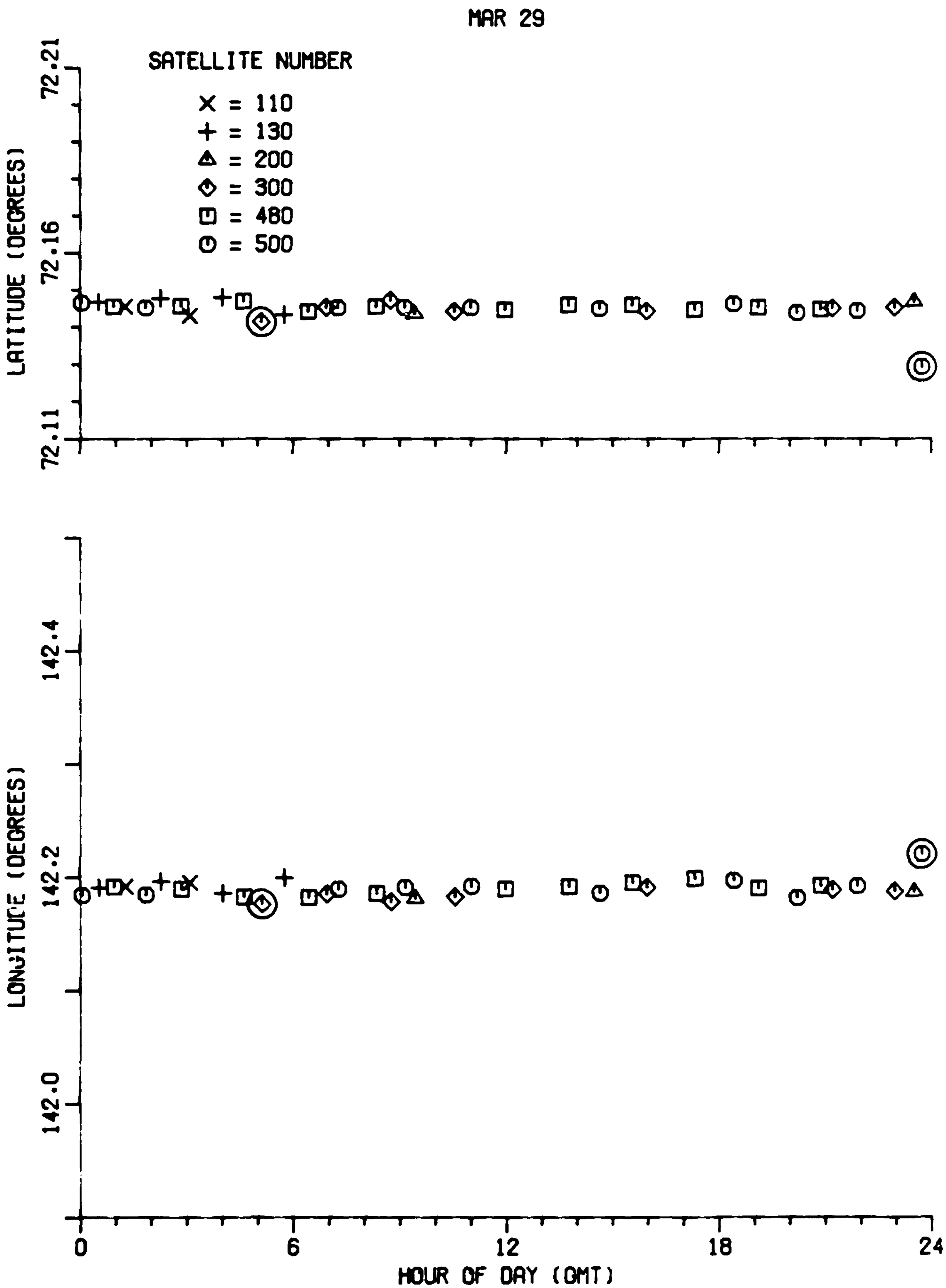
MAR 29
SATELLITE NUMBER
× = 110
+ = 130
△ = 200
◇ = 300
□ = 480
○ = 500
LATITUDE (DEGREES)
72.21
72.16
72.11
LONGITUDE (DEGREES)
142.4
142.2
142.0
0
6
12
18
24
HOUR OF DAY (GMT)

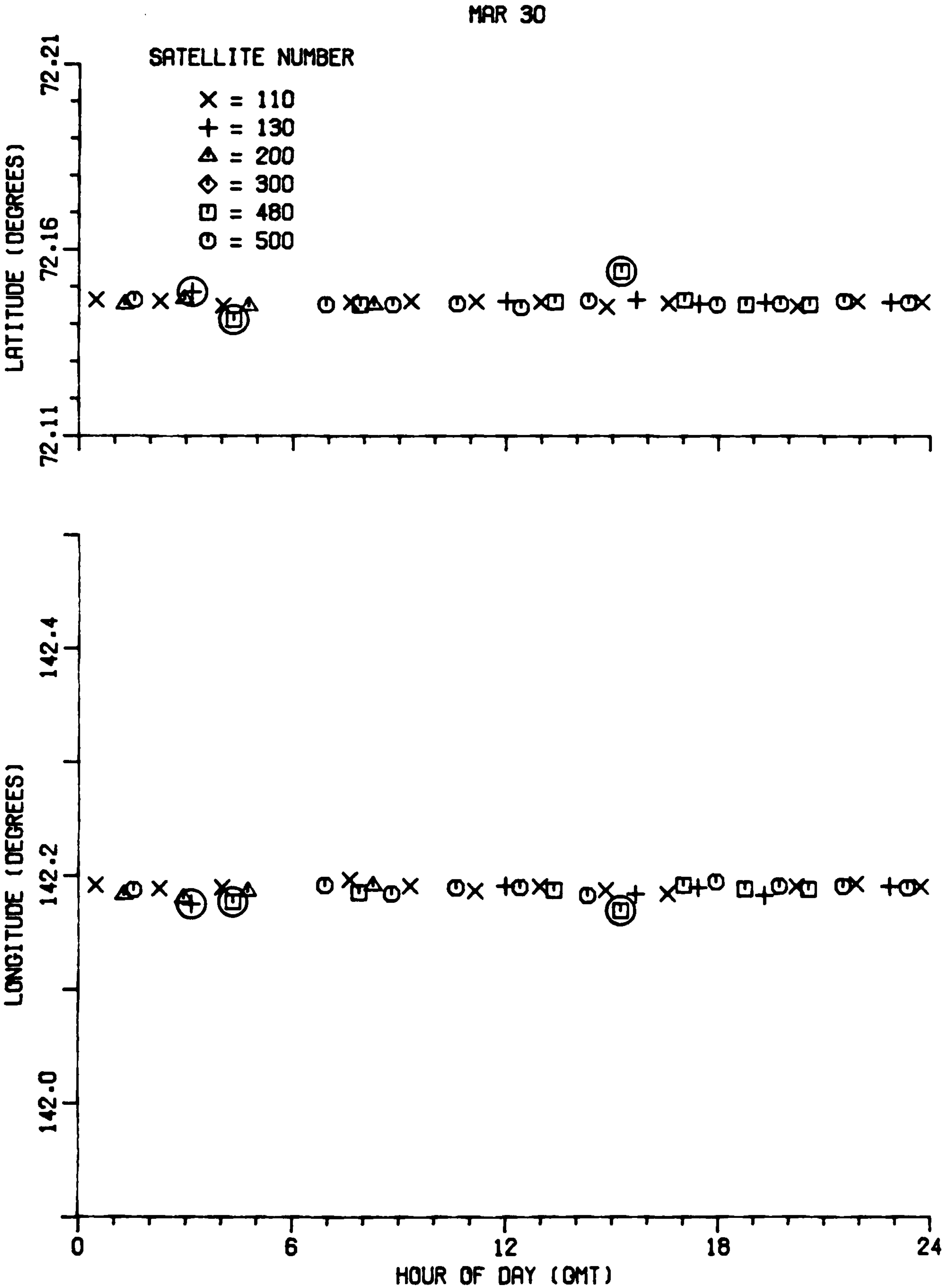
MAR 30
SATELLITE NUMBER
X = 110
+ = 130
Δ = 200
◇ = 300
⊡ = 480
⊙ = 500
72.21
72.16
72.11
LATITUDE (DEGREES)
142.4
142.2
142.0
LONGITUDE (DEGREES)
0
6
12
18
24
HOUR OF DAY (GMT)

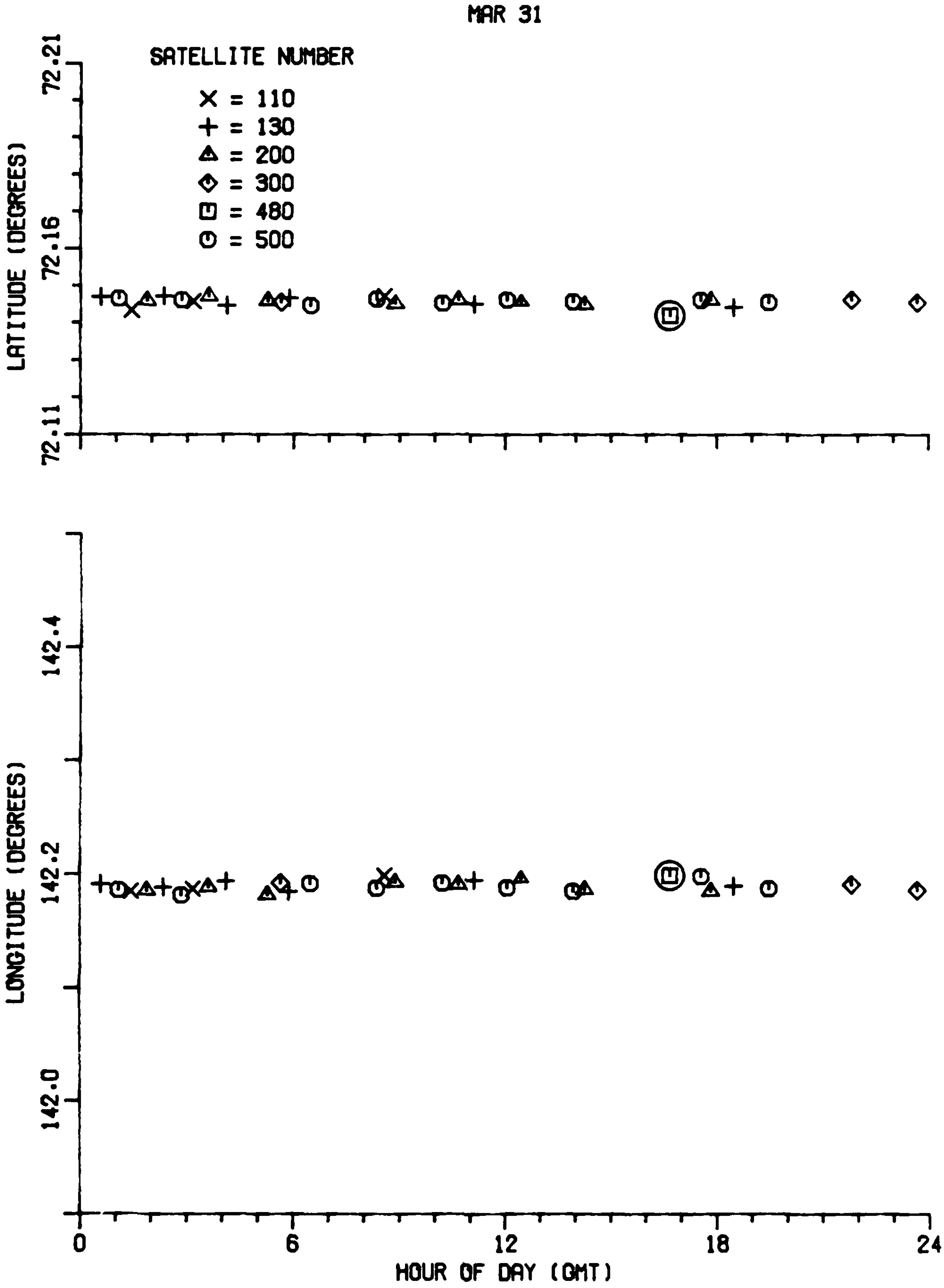
MAR 31
SATELLITE NUMBER
X = 110
+ = 130
△ = 200
◇ = 300
⊡ = 480
⊙ = 500
LATITUDE (DEGREES)
72.21
72.16
72.11
LONGITUDE (DEGREES)
142.4
142.2
142.0
0
6
12
18
24
HOUR OF DAY (GMT)

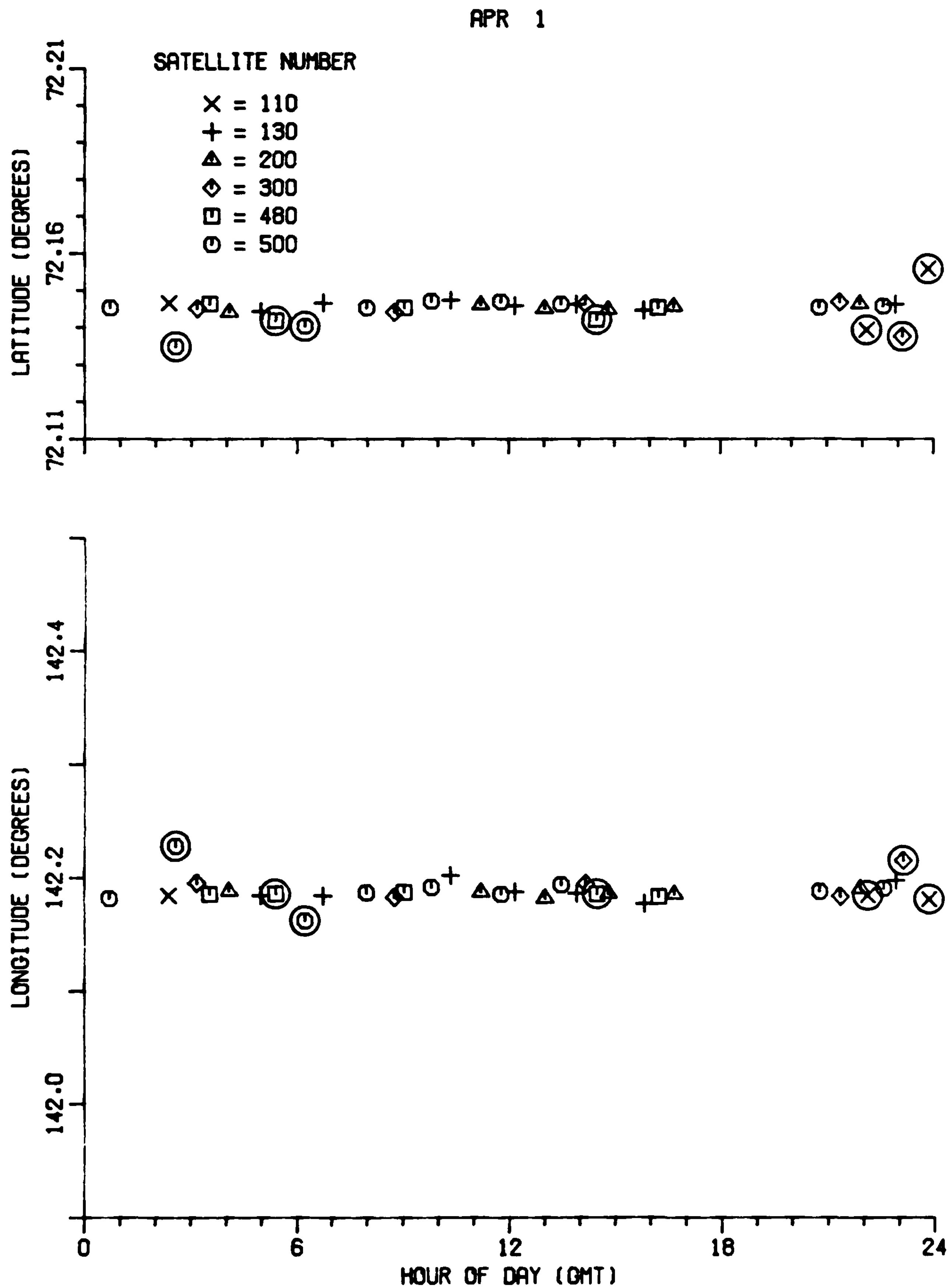

APR 1
SATELLITE NUMBER
× = 110
+ = 130
△ = 200
◇ = 300
□ = 480
○ = 500
LATITUDE (DEGREES)
72.21
72.16
72.11
LONGITUDE (DEGREES)
142.4
142.2
142.0
0
6
12
18
24
HOUR OF DAY (GMT)

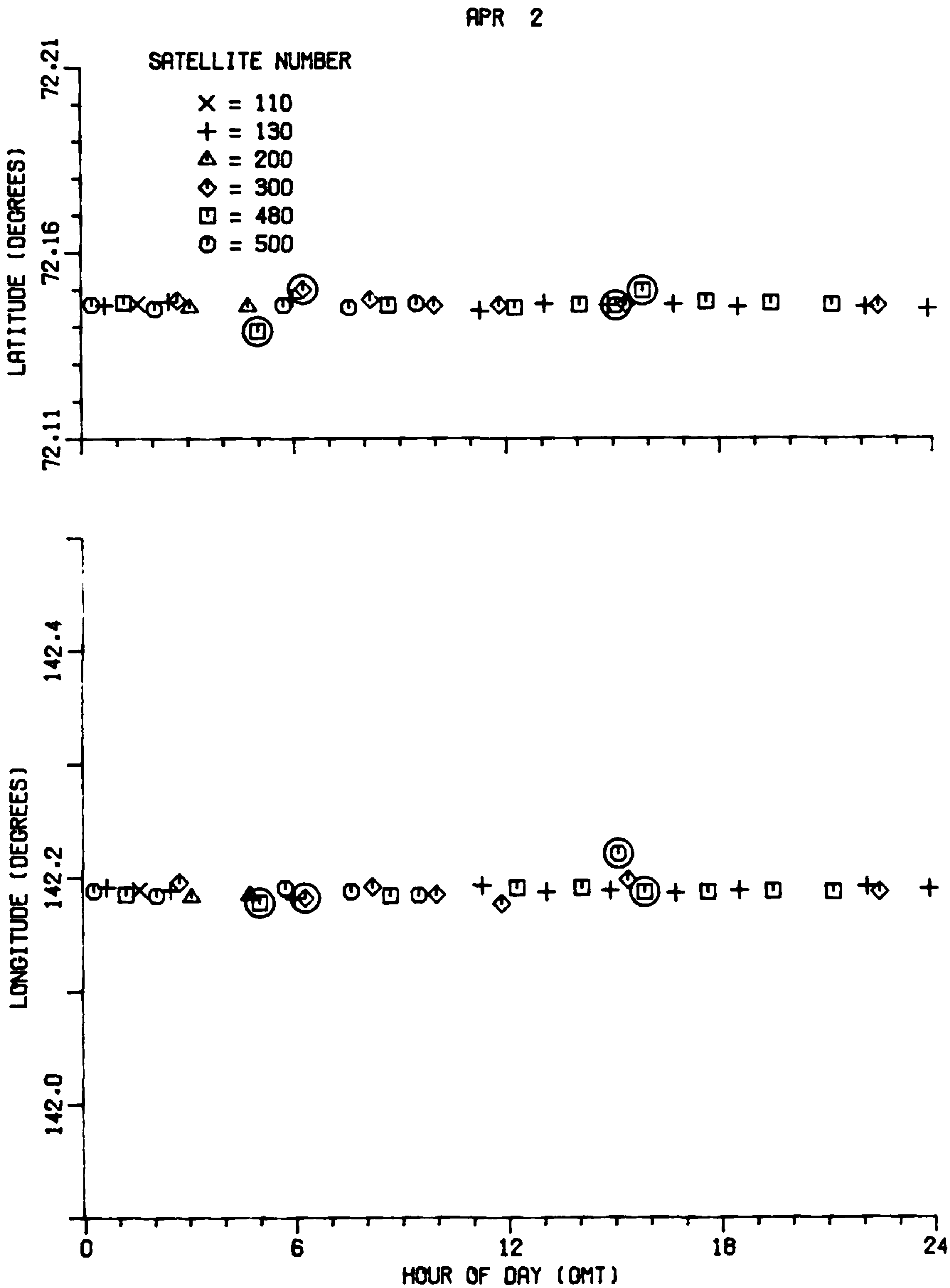
APR 2
SATELLITE NUMBER
X = 110
+ = 130
△ = 200
◇ = 300
□ = 480
⊙ = 500
LATITUDE (DEGREES)
72.21
72.16
72.11
LONGITUDE (DEGREES)
142.4
142.2
142.0
0
6
12
18
24
HOUR OF DAY (GMT)

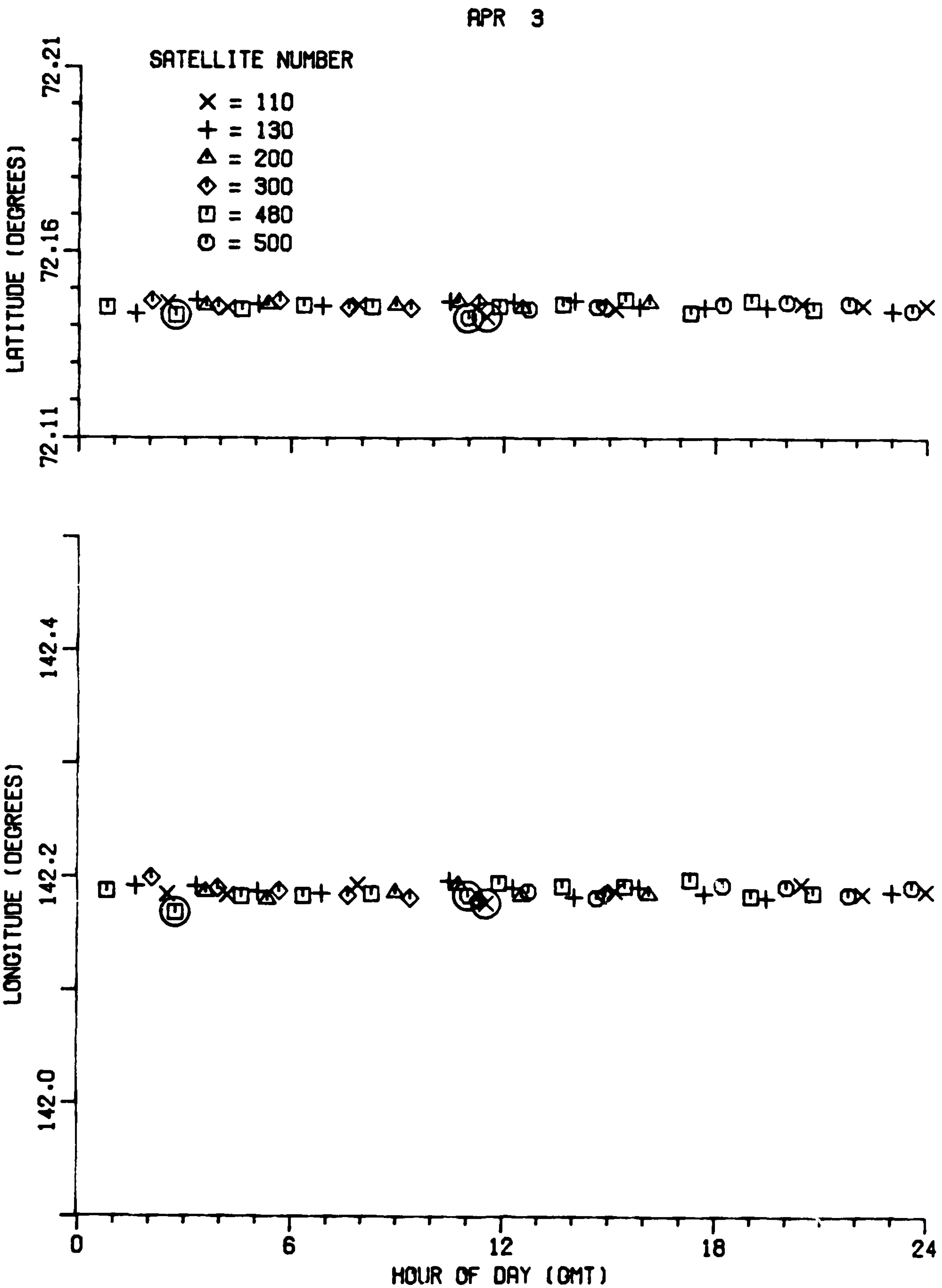
APR 3
SATELLITE NUMBER
X = 110
+ = 130
△ = 200
◇ = 300
□ = 480
○ = 500
LATITUDE (DEGREES)
72.21
72.16
72.11
LONGITUDE (DEGREES)
142.4
142.2
142.0
0
6
12
18
24
HOUR OF DAY (GMT)

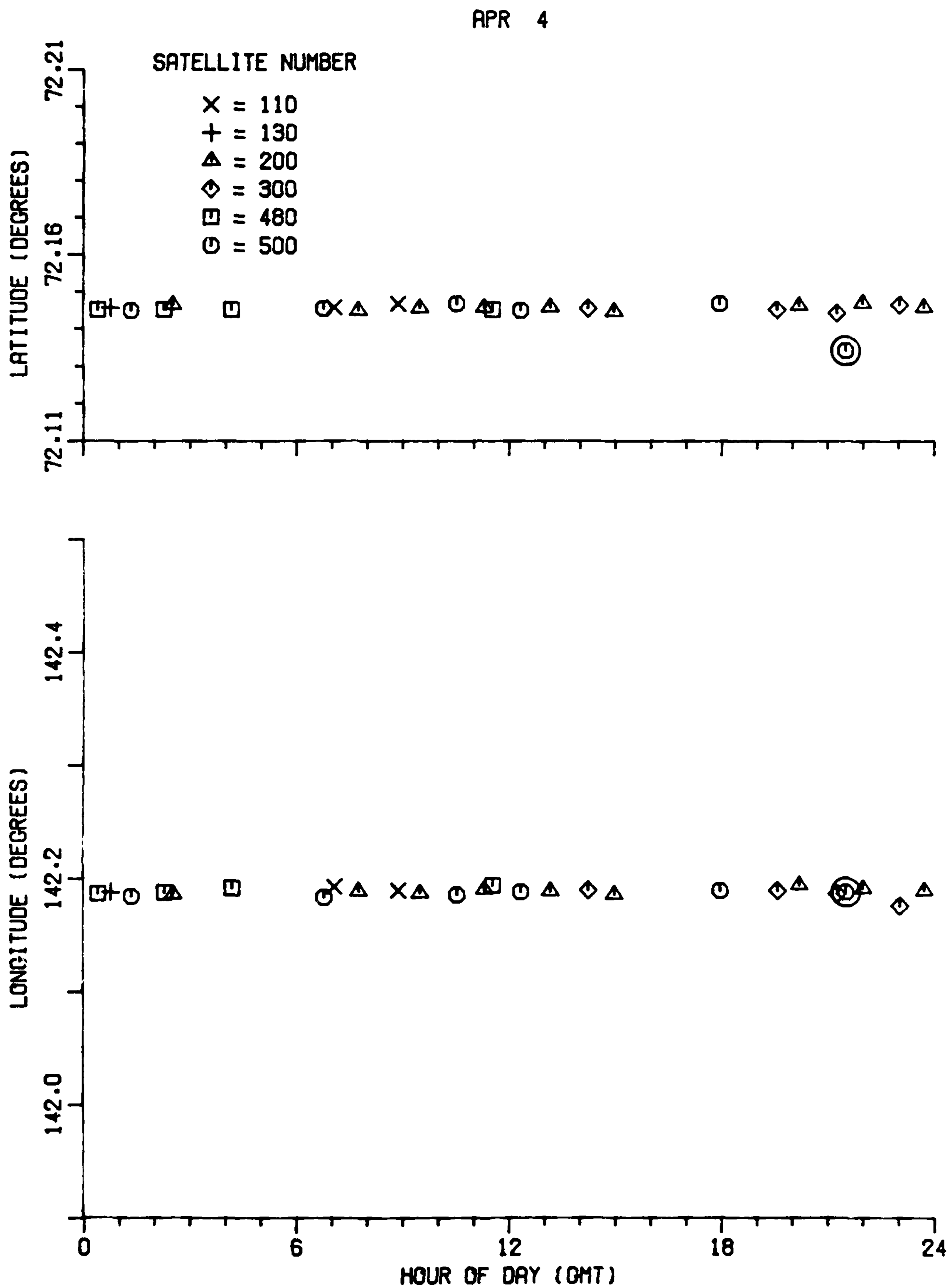
APR 4
SATELLITE NUMBER
X = 110
+ = 130
△ = 200
◇ = 300
⊡ = 480
⊙ = 500
LATITUDE (DEGREES)
72.21
72.16
72.11
LONGITUDE (DEGREES)
142.4
142.2
142.0
0
6
12
18
24
HOUR OF DAY (GMT)

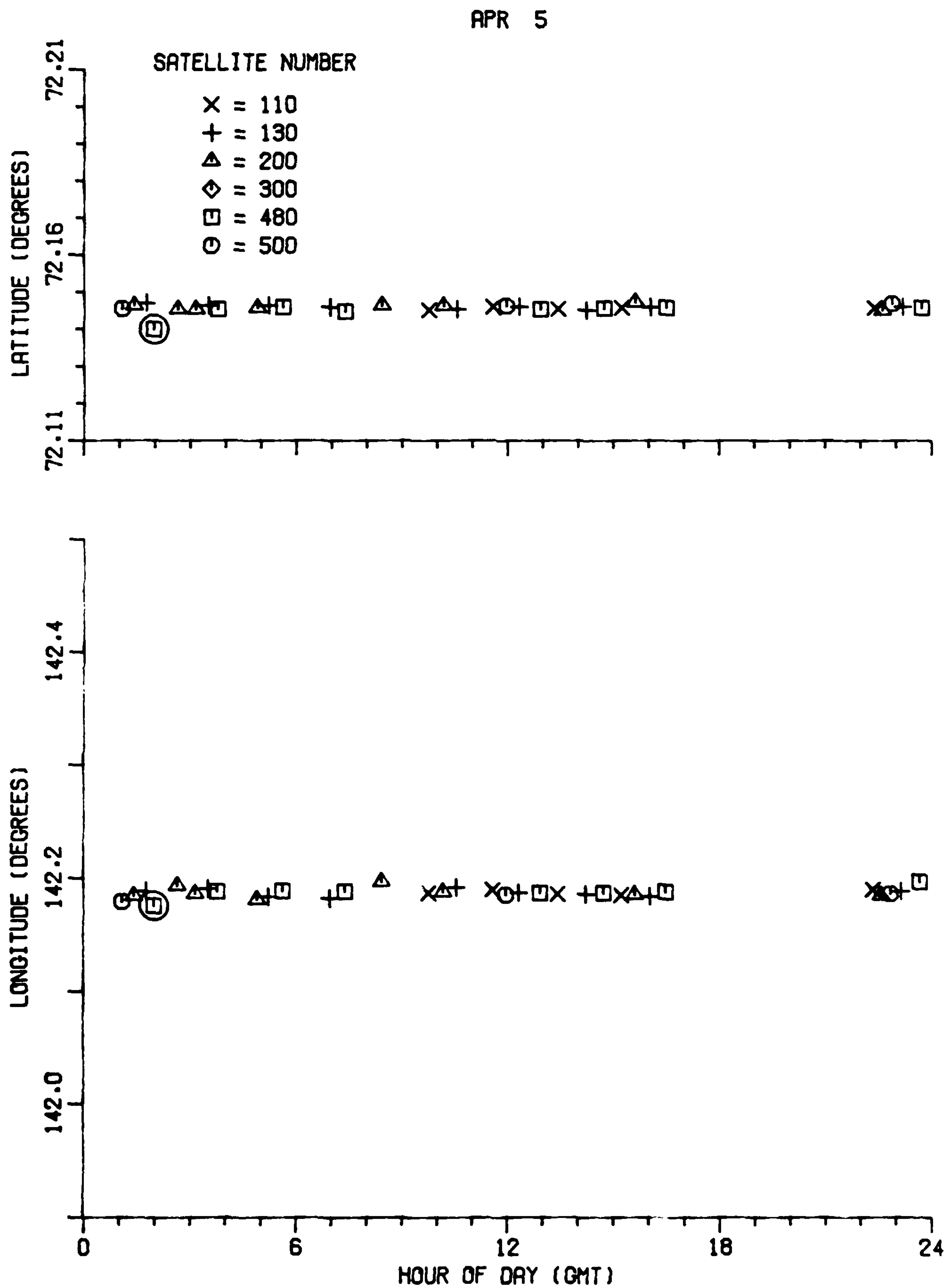
APR 5
SATELLITE NUMBER
× = 110
+ = 130
△ = 200
◇ = 300
□ = 480
⊙ = 500
LATITUDE (DEGREES)
72.21
72.16
72.11
LONGITUDE (DEGREES)
142.4
142.2
142.0
0
6
12
18
24
HOUR OF DAY (GMT)

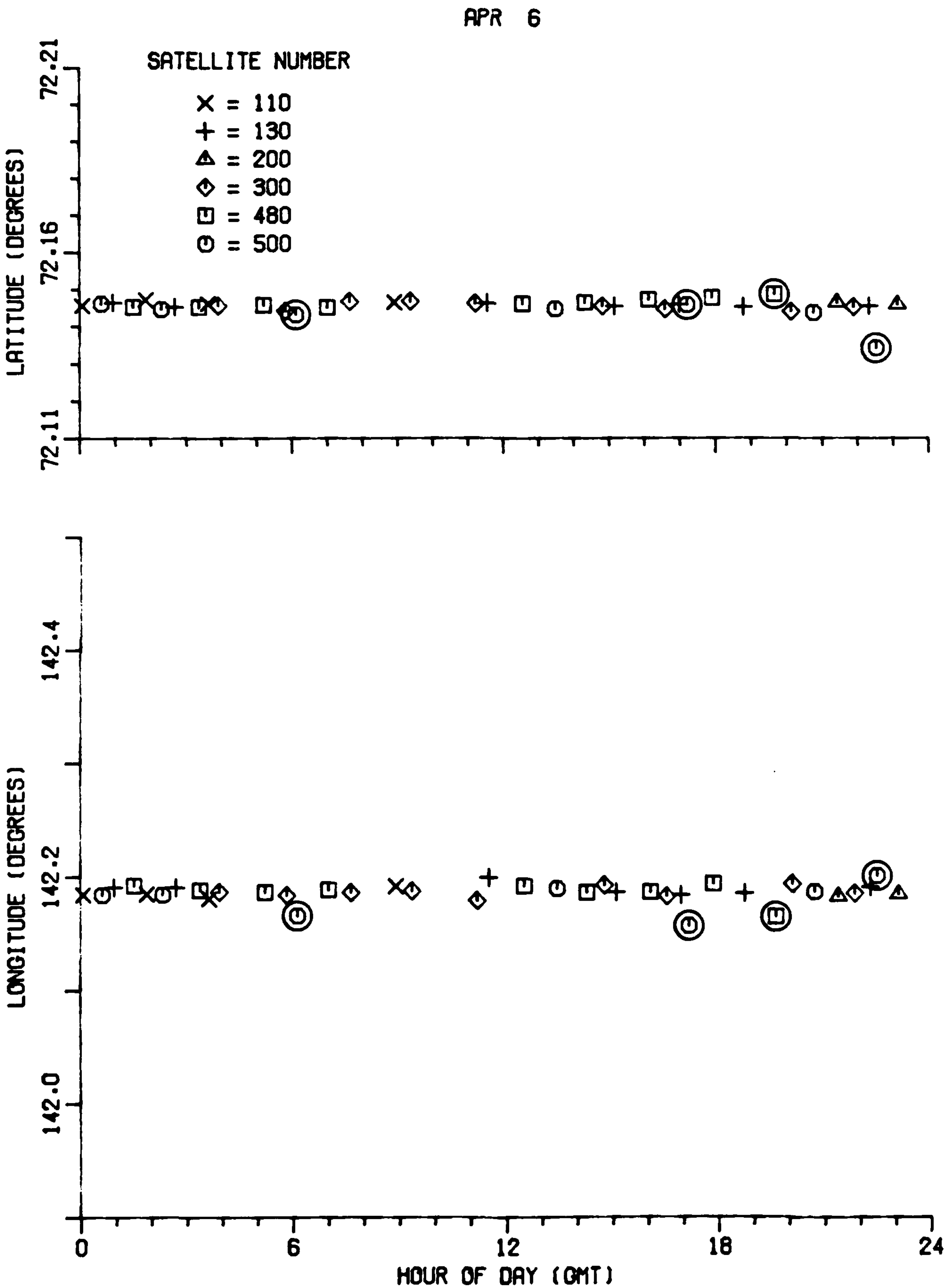
APR 6
SATELLITE NUMBER
X = 110
+ = 130
Δ = 200
◇ = 300
□ = 480
○ = 500
LATITUDE (DEGREES)
72.21
72.16
72.11
LONGITUDE (DEGREES)
142.4
142.2
142.0
0
6
12
18
24
HOUR OF DAY (GMT)

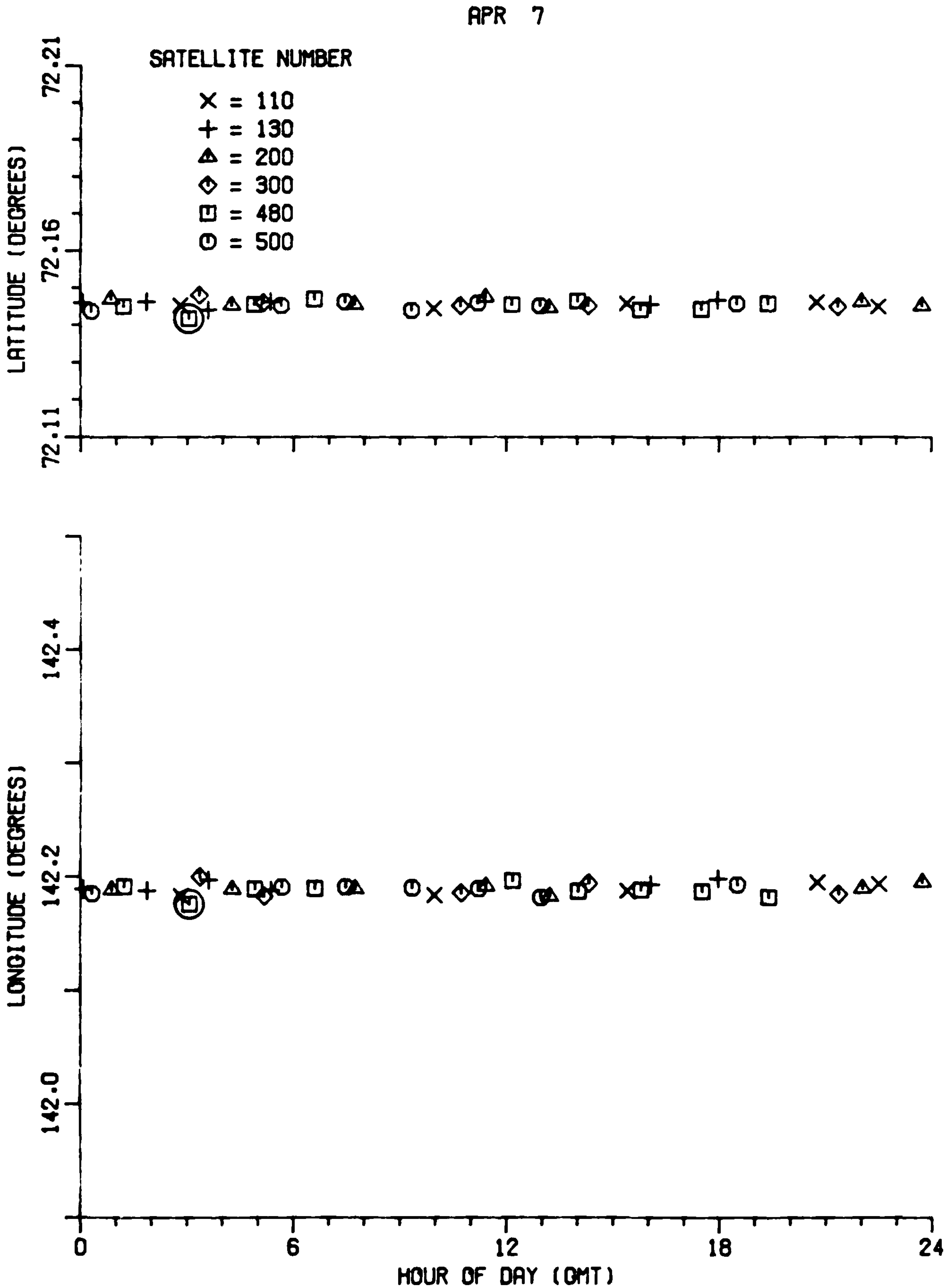

APR 7
SATELLITE NUMBER
× = 110
+ = 130
△ = 200
◇ = 300
□ = 480
⊙ = 500
72.21
72.16
72.11
LATITUDE (DEGREES)
142.4
142.2
142.0
LONGITUDE (DEGREES)
0
6
12
18
24
HOUR OF DAY (GMT)

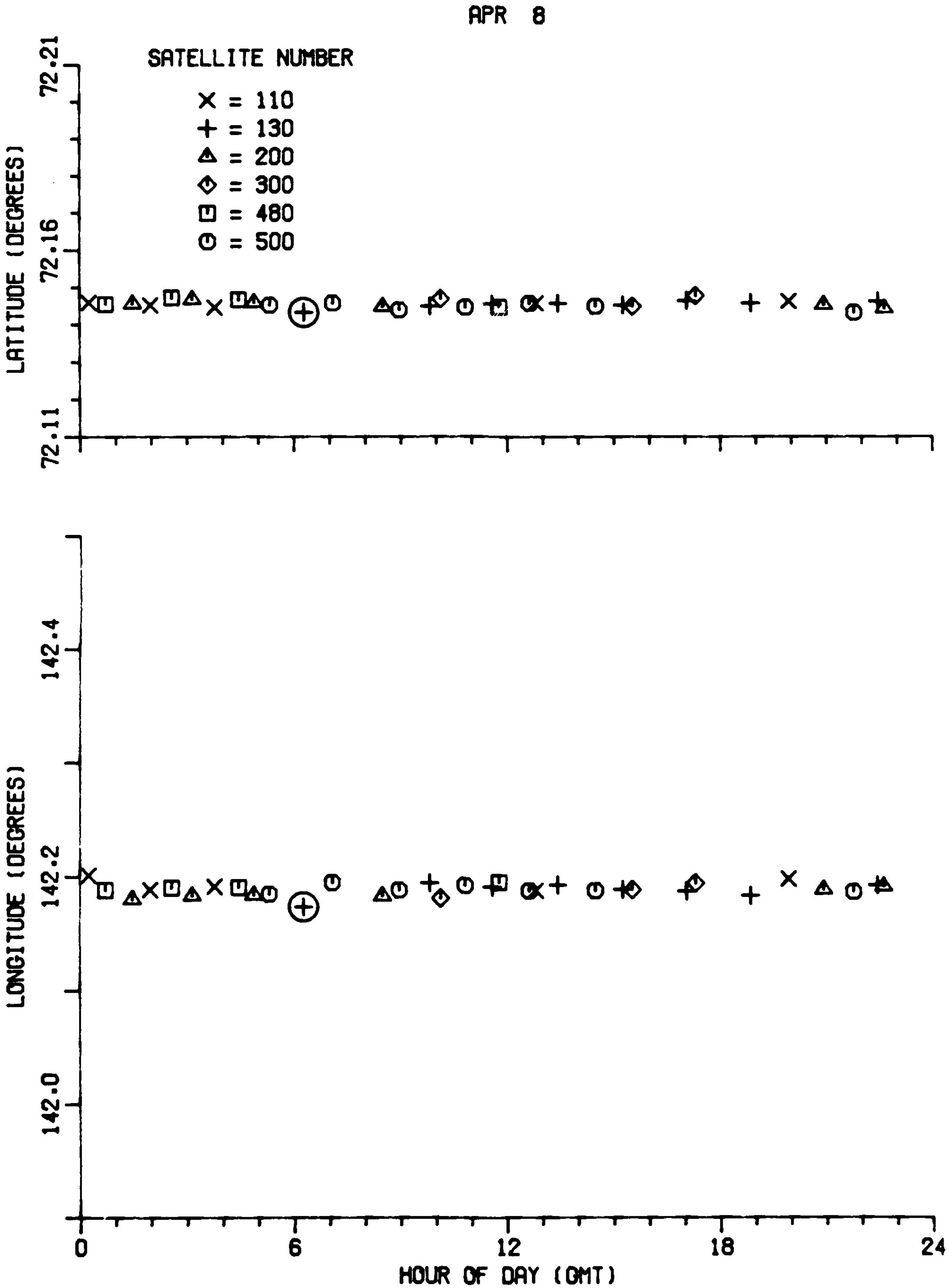
APR 8
SATELLITE NUMBER
X = 110
+ = 130
△ = 200
◇ = 300
⊡ = 480
⊙ = 500
LATITUDE (DEGREES)
72.21
72.16
72.11
LONGITUDE (DEGREES)
142.4
142.2
142.0
0
6
12
18
24
HOUR OF DAY (GMT)

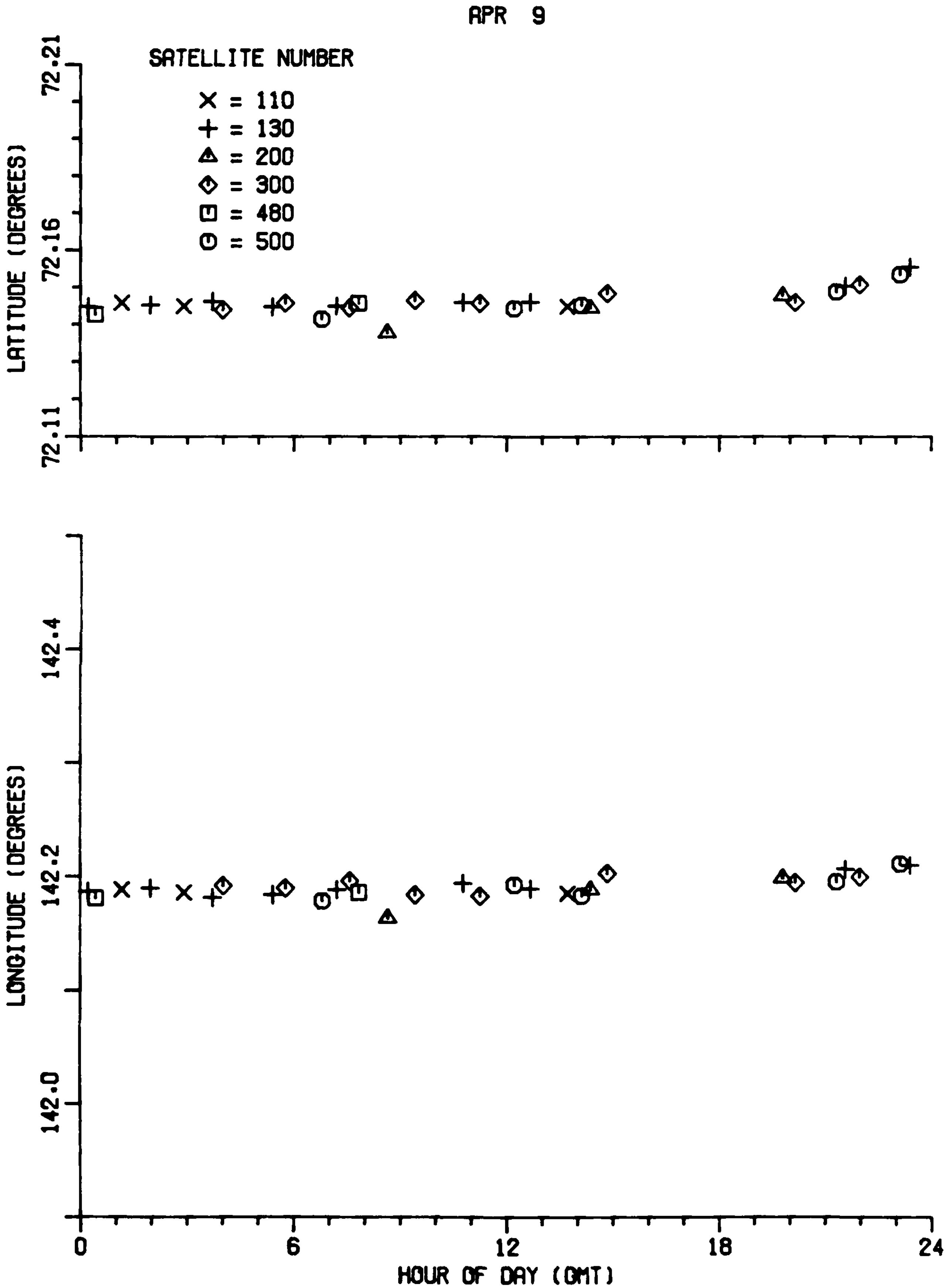
APR 9
SATELLITE NUMBER
X = 110
+ = 130
Δ = 200
◇ = 300
□ = 480
⊙ = 500
LATITUDE (DEGREES)
72.21
72.16
72.11
LONGITUDE (DEGREES)
142.4
142.2
142.0
0
6
12
18
24
HOUR OF DAY (GMT)

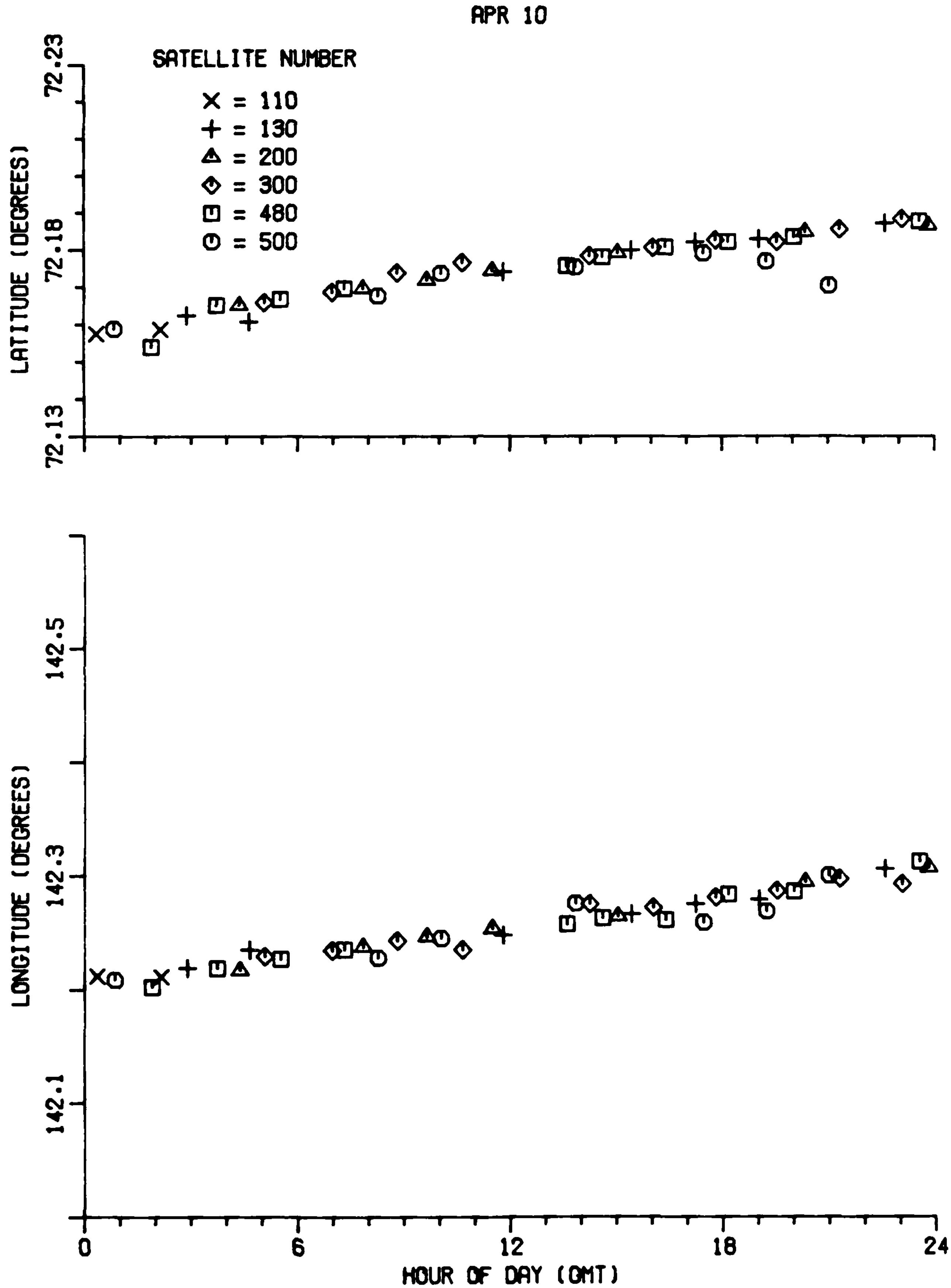
APR 10
SATELLITE NUMBER
X = 110
+ = 130
△ = 200
◇ = 300
□ = 480
⊙ = 500
LATITUDE (DEGREES)
72.23
72.18
72.13
LONGITUDE (DEGREES)
142.5
142.3
142.1
0
6
12
18
24
HOUR OF DAY (GMT)

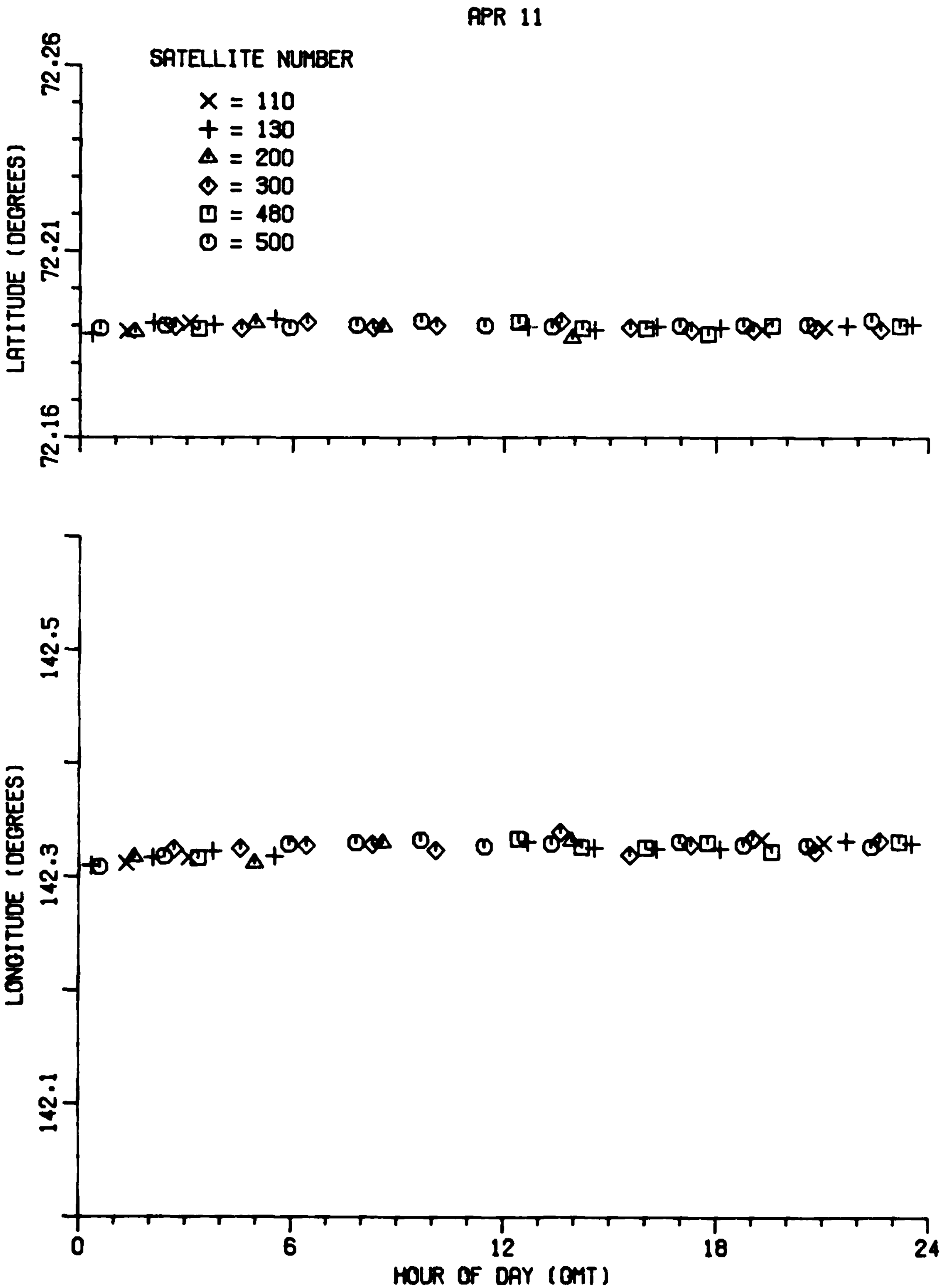
APR 11
SATELLITE NUMBER
X = 110
+ = 130
Δ = 200
◇ = 300
▣ = 480
ⓞ = 500
LATITUDE (DEGREES)
72.26
72.21
72.16
LONGITUDE (DEGREES)
142.5
142.3
142.1
0
6
12
18
24
HOUR OF DAY (GMT)

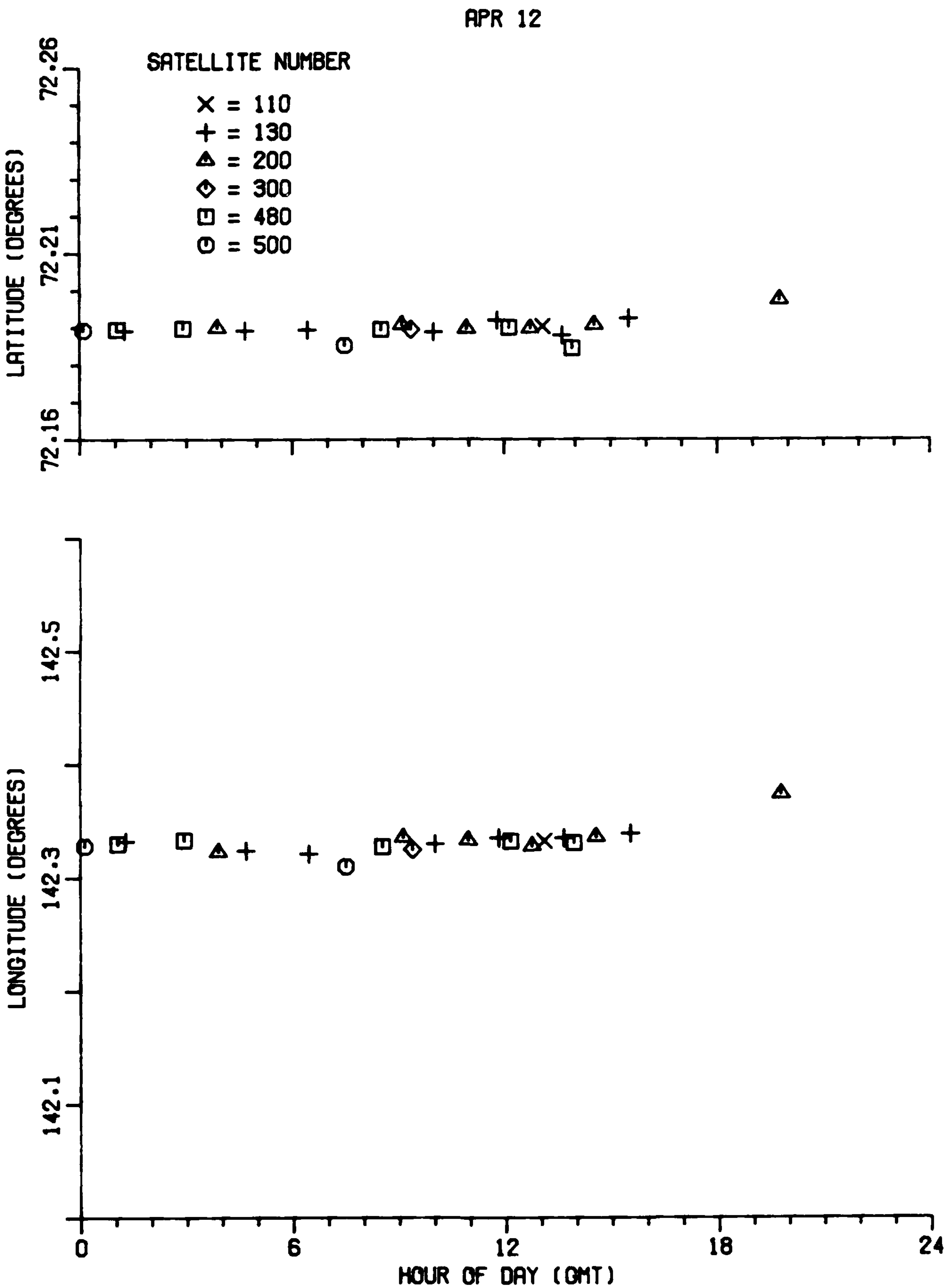
APR 12
SATELLITE NUMBER
× = 110
+ = 130
△ = 200
◇ = 300
□ = 480
○ = 500
LATITUDE (DEGREES)
72.26
72.21
72.16
LONGITUDE (DEGREES)
142.5
142.3
142.1
0
6
12
18
24
HOUR OF DAY (GMT)

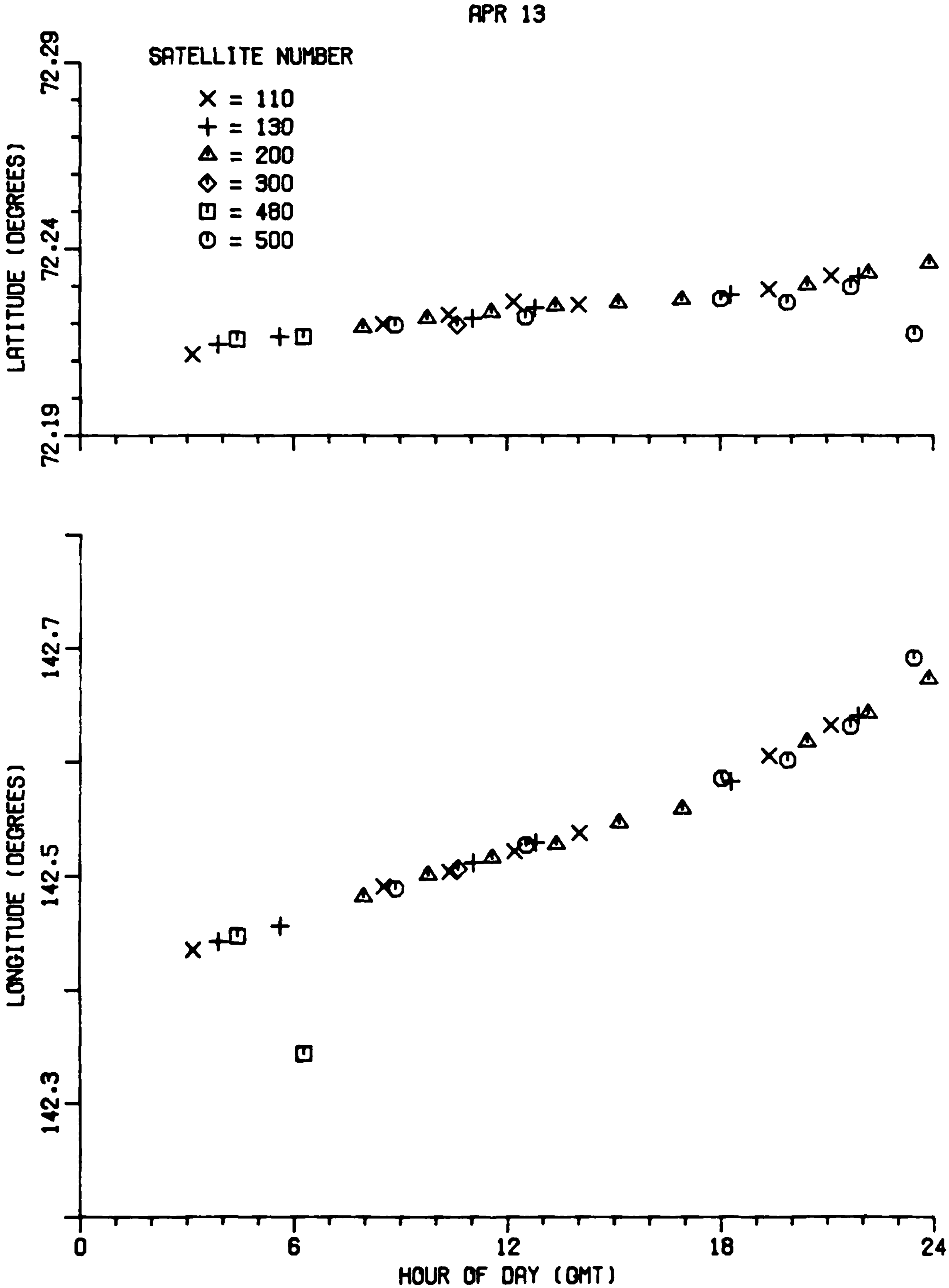

APR 13
SATELLITE NUMBER
× = 110
+ = 130
△ = 200
◇ = 300
□ = 480
○ = 500
LATITUDE (DEGREES)
72.29
72.24
72.19
LONGITUDE (DEGREES)
142.7
142.5
142.3
0
6
12
18
24
HOUR OF DAY (GMT)

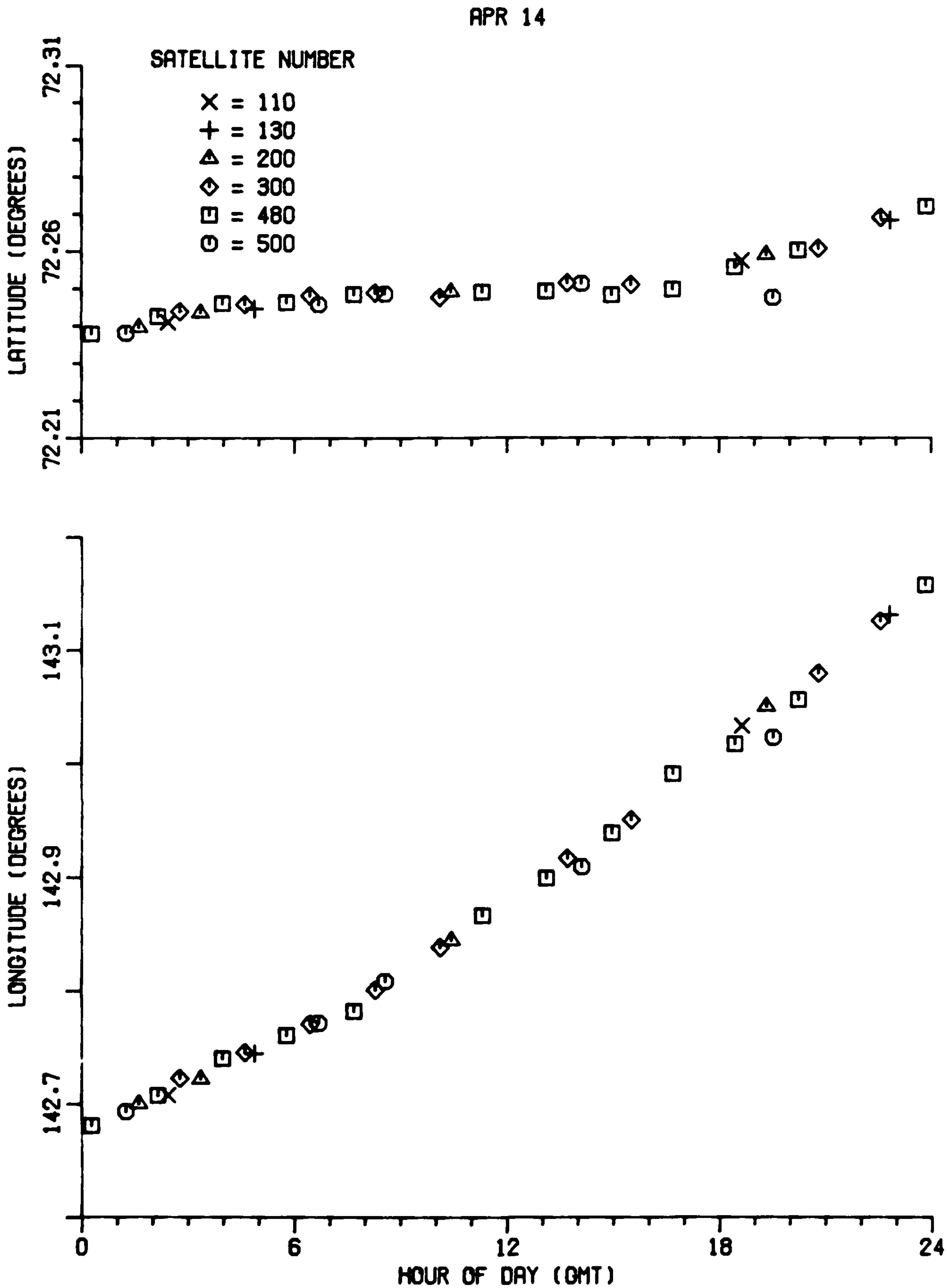
APR 14
SATELLITE NUMBER
X = 110
+ = 130
△ = 200
◇ = 300
⊡ = 480
⊙ = 500
LATITUDE (DEGREES)
72.31
72.26
72.21
LONGITUDE (DEGREES)
143.1
142.9
142.7
0
6
12
18
24
HOUR OF DAY (GMT)

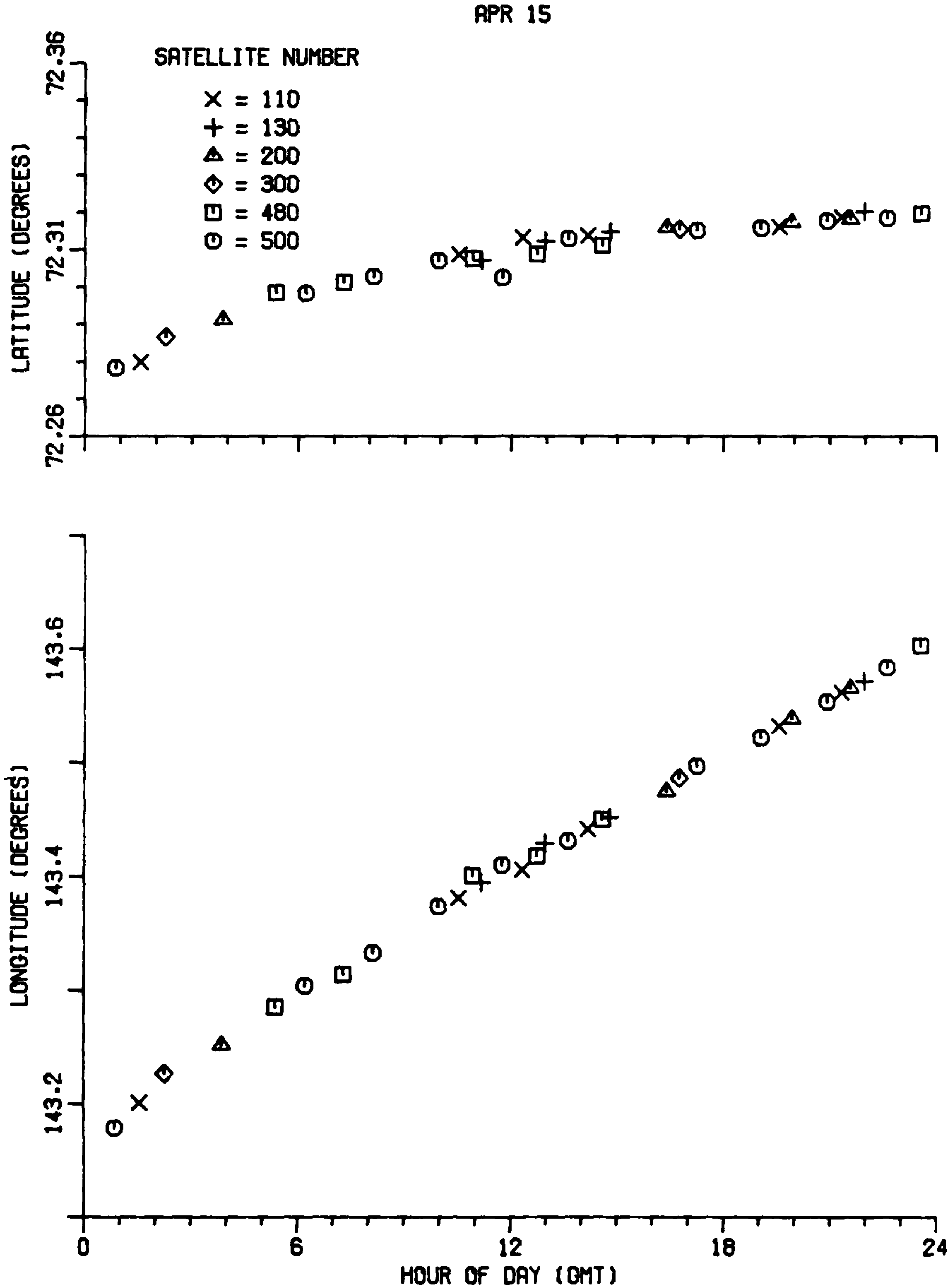

APR 15
SATELLITE NUMBER
× = 110
+ = 130
△ = 200
◇ = 300
⊡ = 480
⊙ = 500
LATITUDE (DEGREES)
72.36
72.31
72.26
LONGITUDE (DEGREES)
143.6
143.4
143.2
0
6
12
18
24
HOUR OF DAY (GMT)

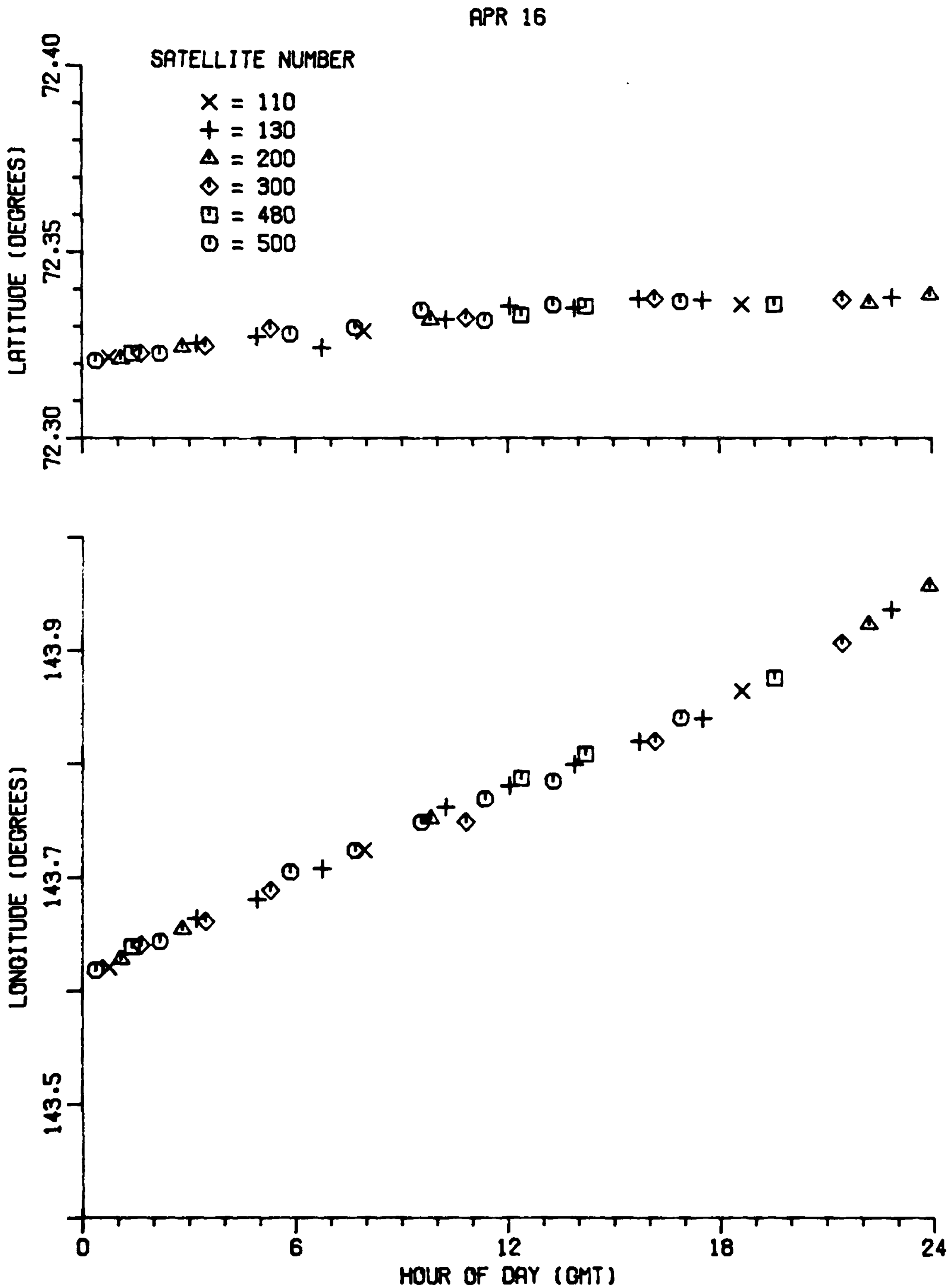
APR 16
SATELLITE NUMBER
X = 110
+ = 130
Δ = 200
◇ = 300
⊡ = 480
⊙ = 500
LATITUDE (DEGREES)
72.40
72.35
72.30
LONGITUDE (DEGREES)
143.9
143.7
143.5
0
6
12
18
24
HOUR OF DAY (GMT)

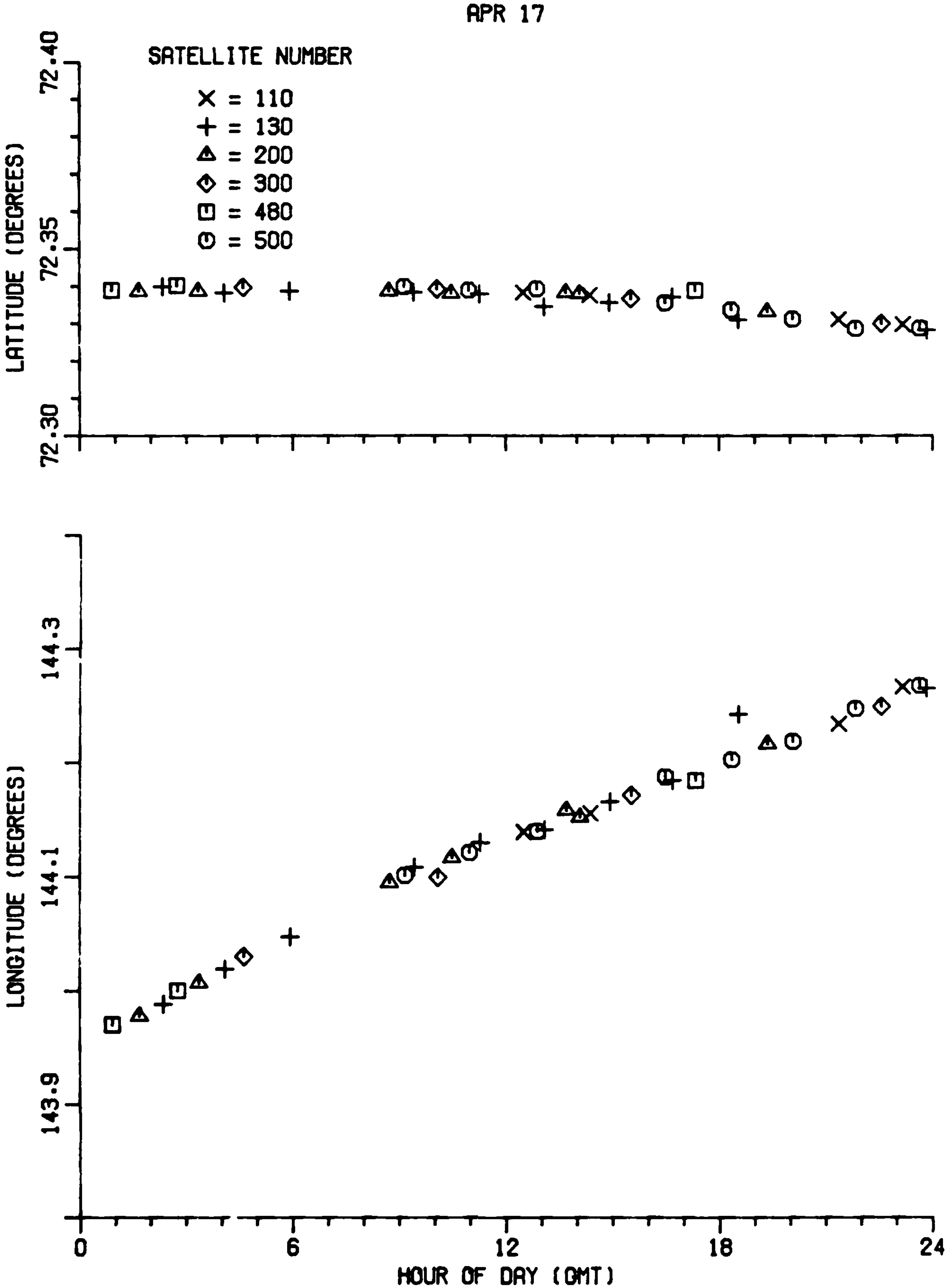

APR 17
SATELLITE NUMBER
X = 110
+ = 130
△ = 200
◇ = 300
□ = 480
○ = 500
LATITUDE (DEGREES)
72.40
72.35
72.30
LONGITUDE (DEGREES)
144.3
144.1
143.9
0
6
12
18
24
HOUR OF DAY (GMT)

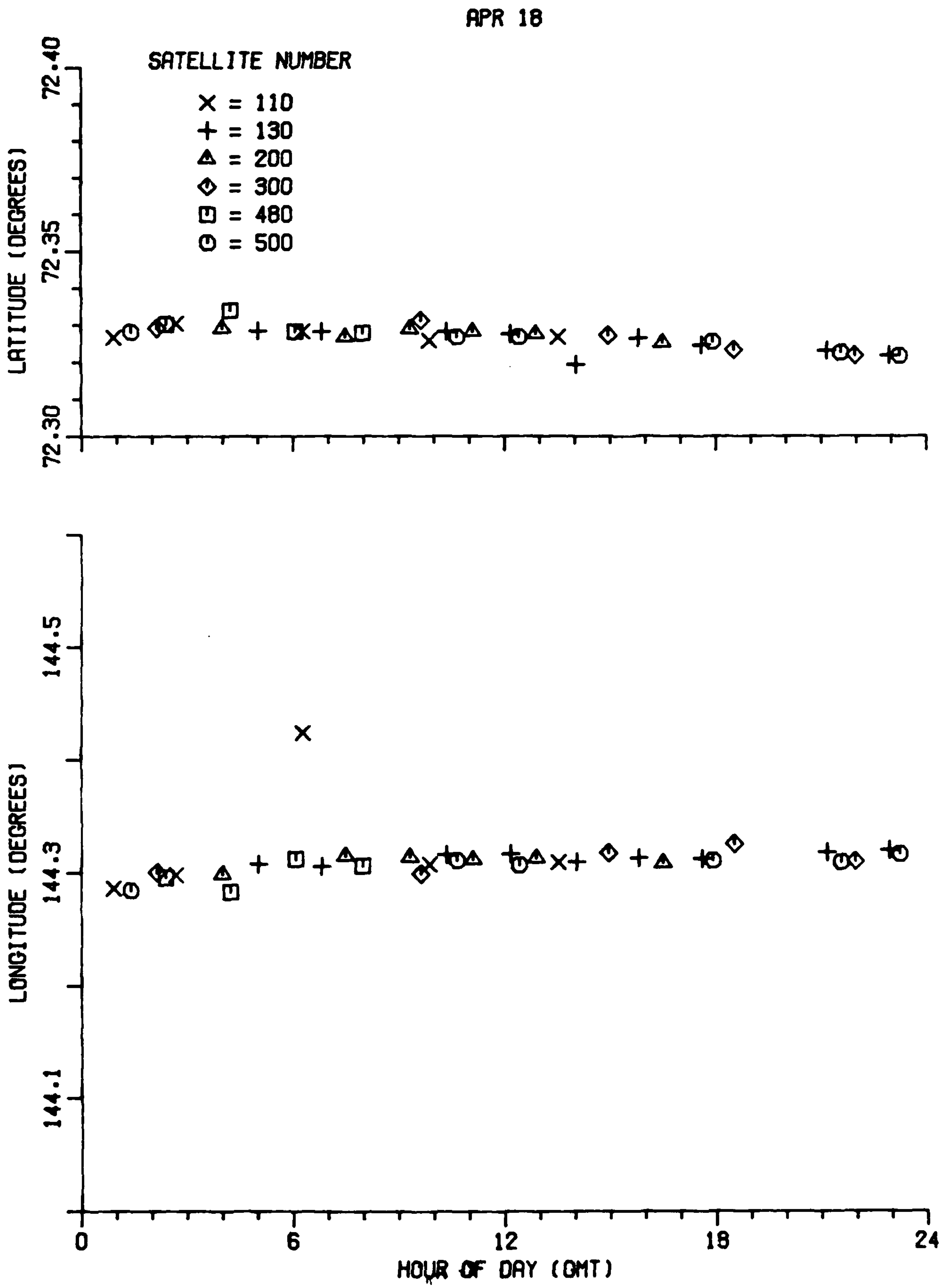
APR 18
SATELLITE NUMBER
× = 110
+ = 130
△ = 200
◇ = 300
⊡ = 480
⊙ = 500
LATITUDE (DEGREES)
72.40
72.35
72.30
LONGITUDE (DEGREES)
144.5
144.3
144.1
0
6
12
18
24
HOUR OF DAY (GMT)

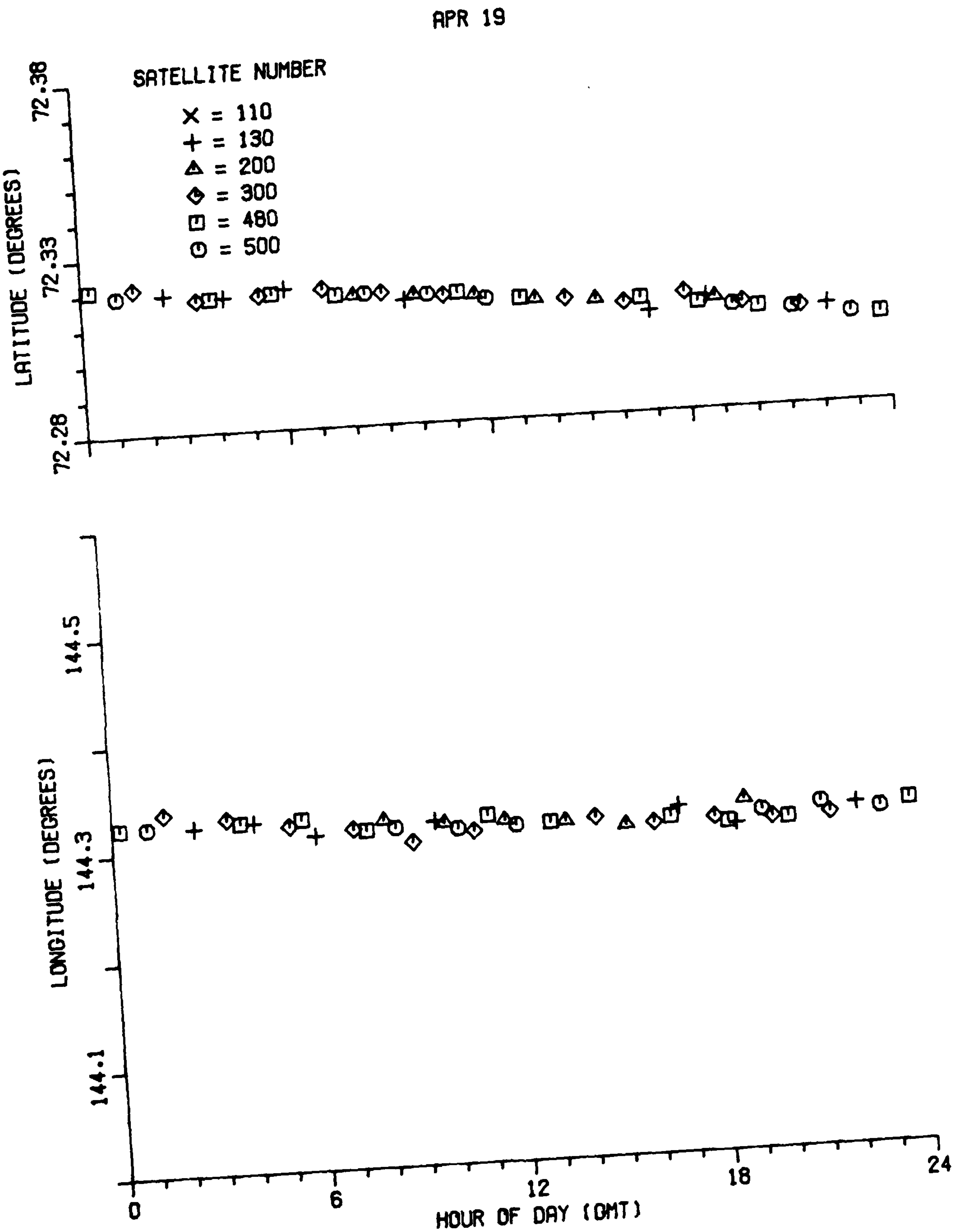
APR 19
SATELLITE NUMBER
X = 110
+ = 130
△ = 200
◇ = 300
□ = 480
○ = 500
72.38
72.33
72.28
LATITUDE (DEGREES)
144.5
144.3
144.1
LONGITUDE (DEGREES)
0
6
12
18
24
HOUR OF DAY (GMT)

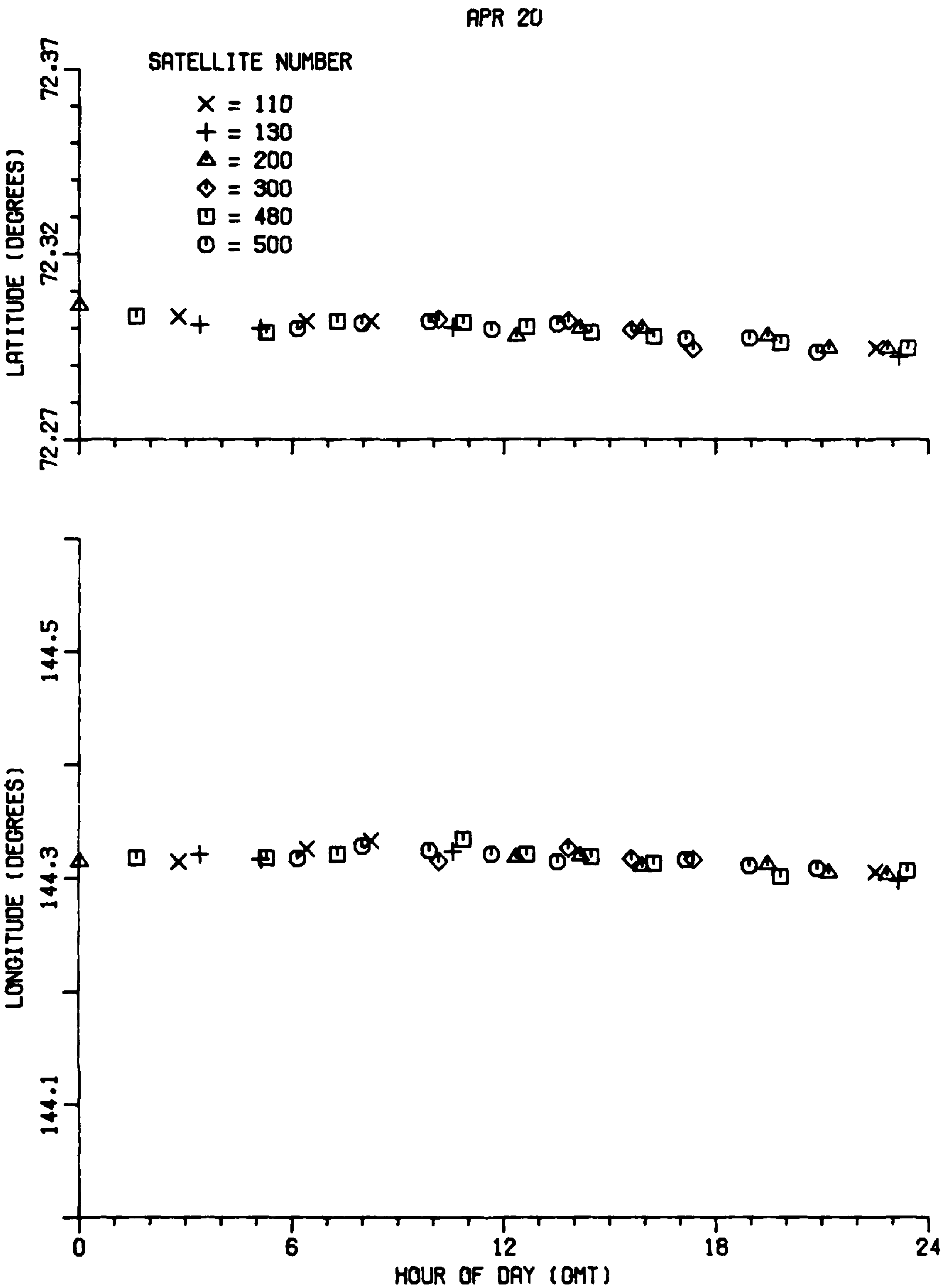
APR 20
SATELLITE NUMBER
X = 110
+ = 130
Δ = 200
◇ = 300
□ = 480
⊙ = 500
LATITUDE (DEGREES)
72.37
72.32
72.27
LONGITUDE (DEGREES)
144.5
144.3
144.1
0
6
12
18
24
HOUR OF DAY (GMT)

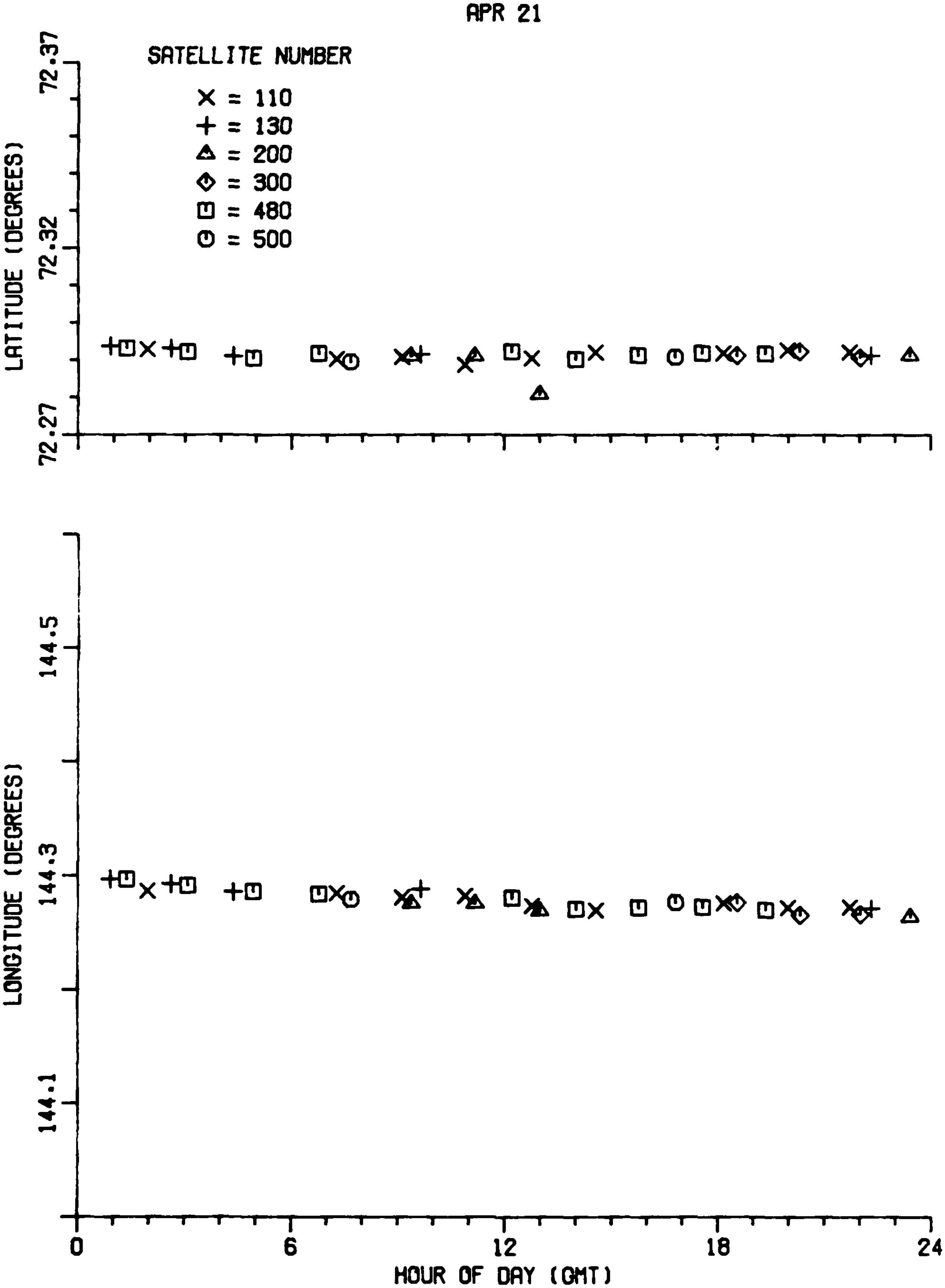
APR 21
SATELLITE NUMBER
X = 110
+ = 130
Δ = 200
◇ = 300
□ = 480
⊙ = 500
LATITUDE (DEGREES)
72.37
72.32
72.27
LONGITUDE (DEGREES)
144.5
144.3
144.1
0
6
12
18
24
HOUR OF DAY (GMT)

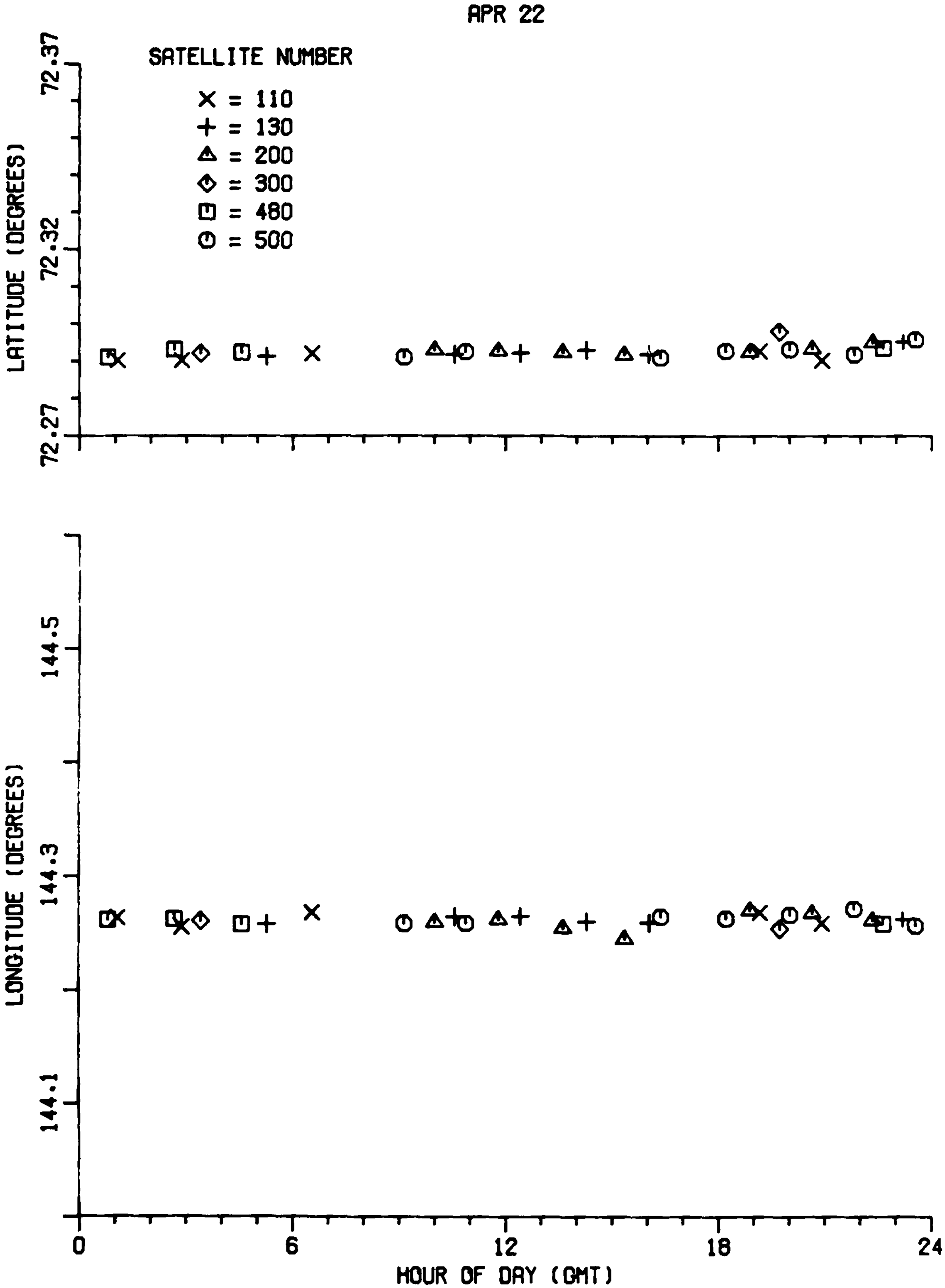
APR 22
SATELLITE NUMBER
X = 110
+ = 130
△ = 200
◇ = 300
□ = 480
⊙ = 500
LATITUDE (DEGREES)
72.37
72.32
72.27
LONGITUDE (DEGREES)
144.5
144.3
144.1
0
6
12
18
24
HOUR OF DAY (GMT)

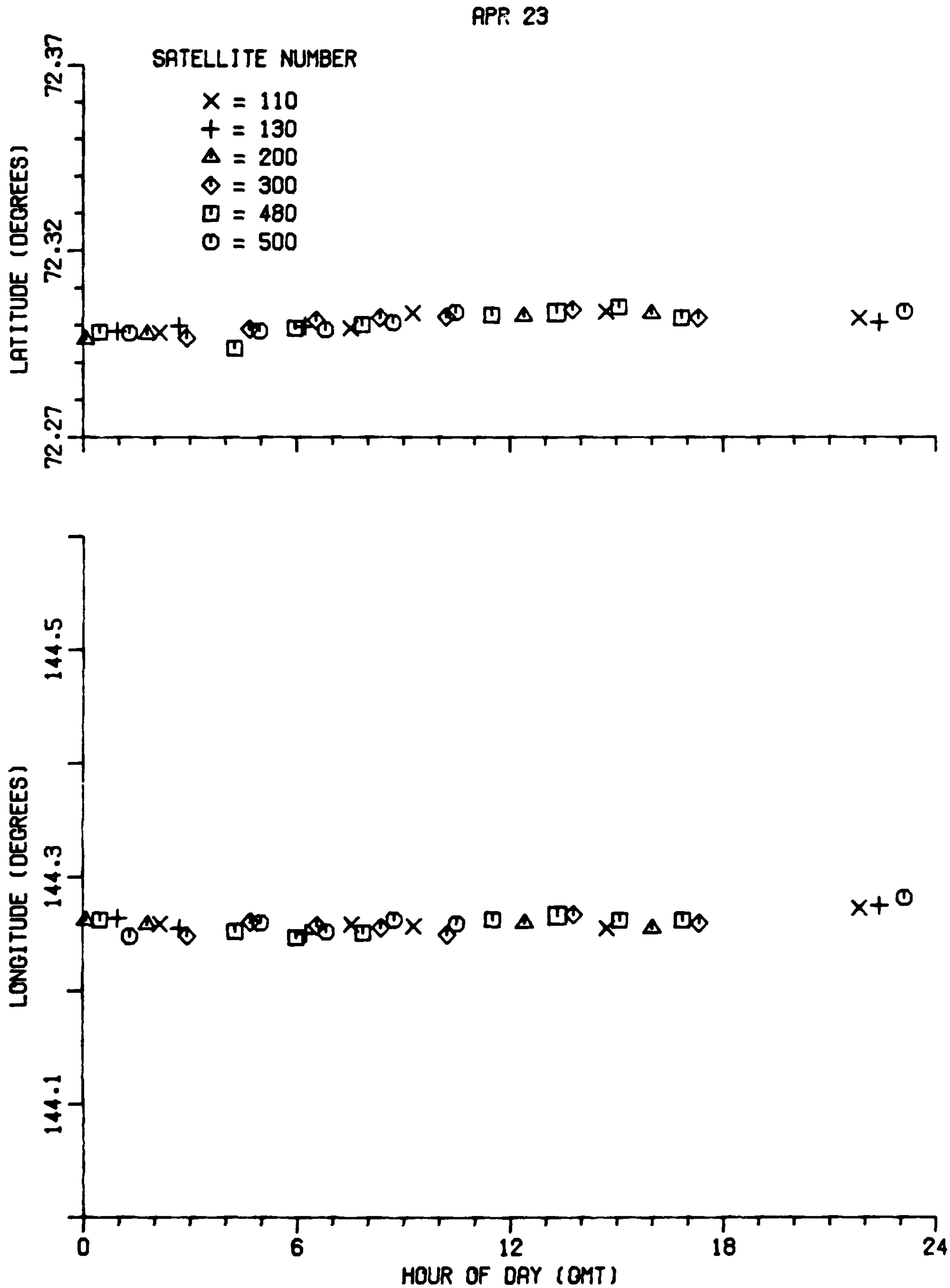
APR 23
SATELLITE NUMBER
X = 110
+ = 130
△ = 200
◇ = 300
⊡ = 480
⊙ = 500
LATITUDE (DEGREES)
72.37
72.32
72.27
LONGITUDE (DEGREES)
144.5
144.3
144.1
0
6
12
18
24
HOUR OF DAY (GMT)

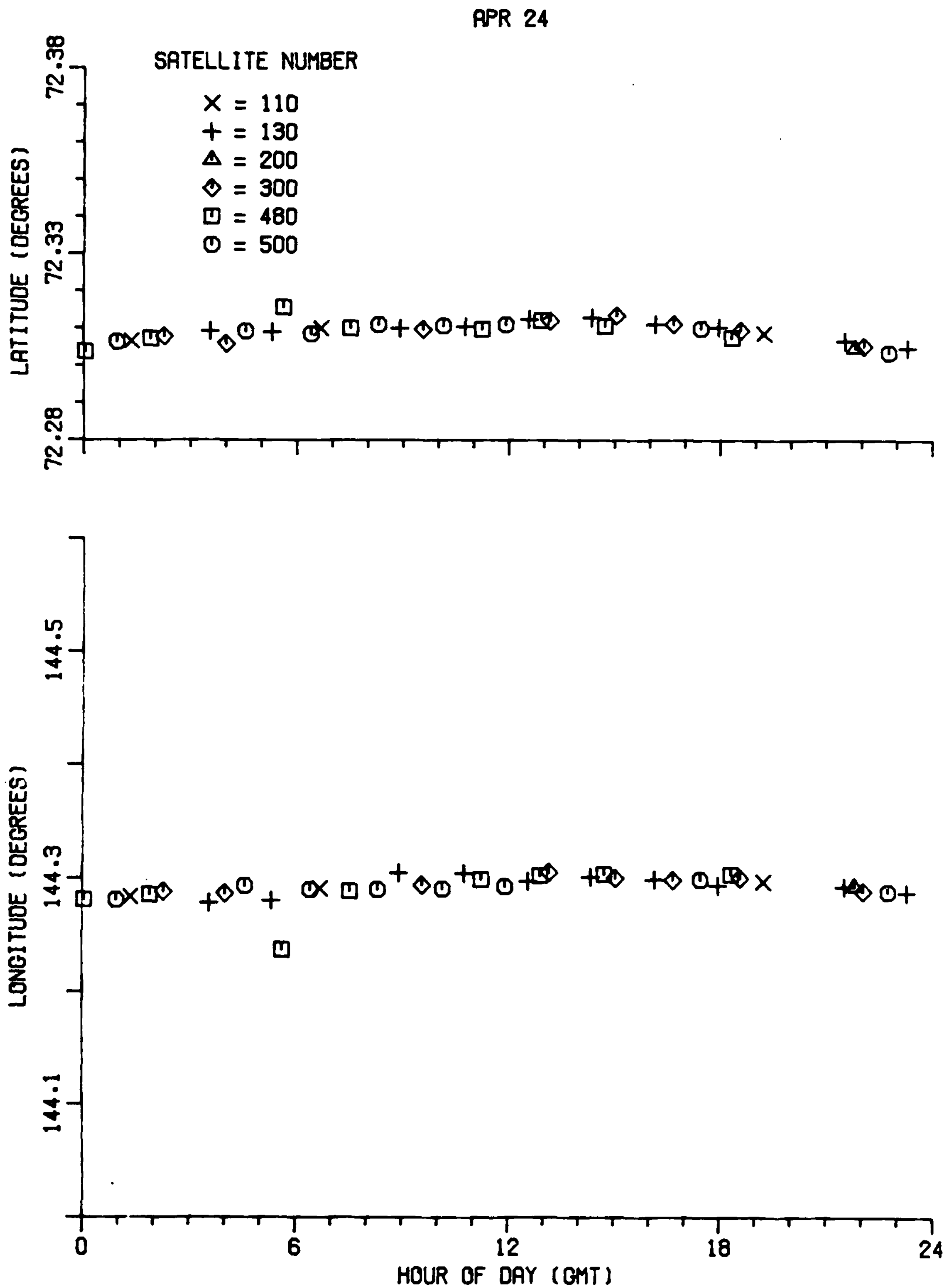

APR 24
SATELLITE NUMBER
X = 110
+ = 130
Δ = 200
◇ = 300
⊡ = 480
⊙ = 500
LATITUDE (DEGREES)
72.38
72.33
72.28
LONGITUDE (DEGREES)
144.5
144.3
144.1
0
6
12
18
24
HOUR OF DAY (GMT)

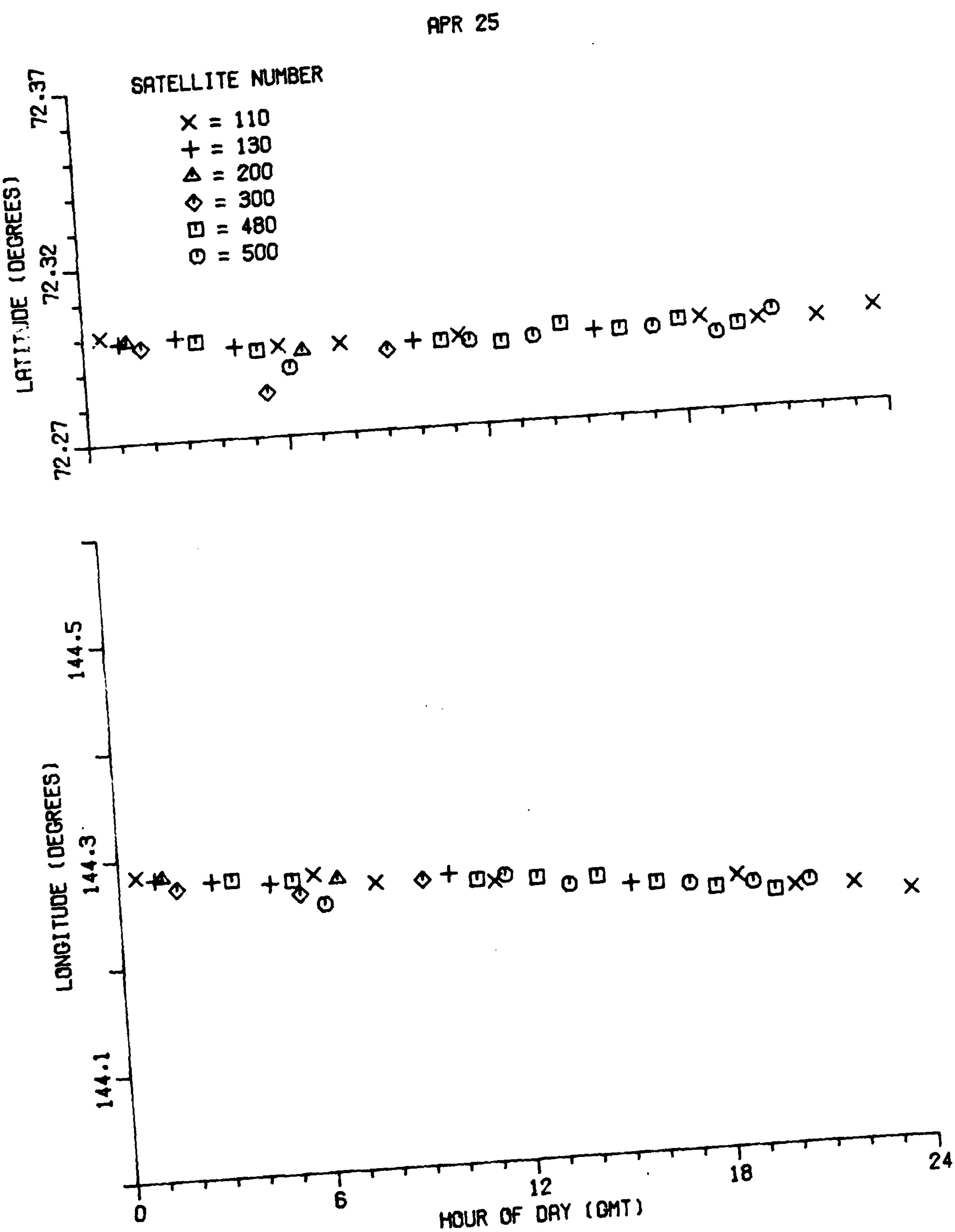
APR 25
SATELLITE NUMBER
X = 110
+ = 130
Δ = 200
◇ = 300
□ = 480
⊙ = 500
LATITUDE (DEGREES)
72.37
72.32
72.27
LONGITUDE (DEGREES)
144.5
144.3
144.1
0
6
12
18
24
HOUR OF DAY (GMT)

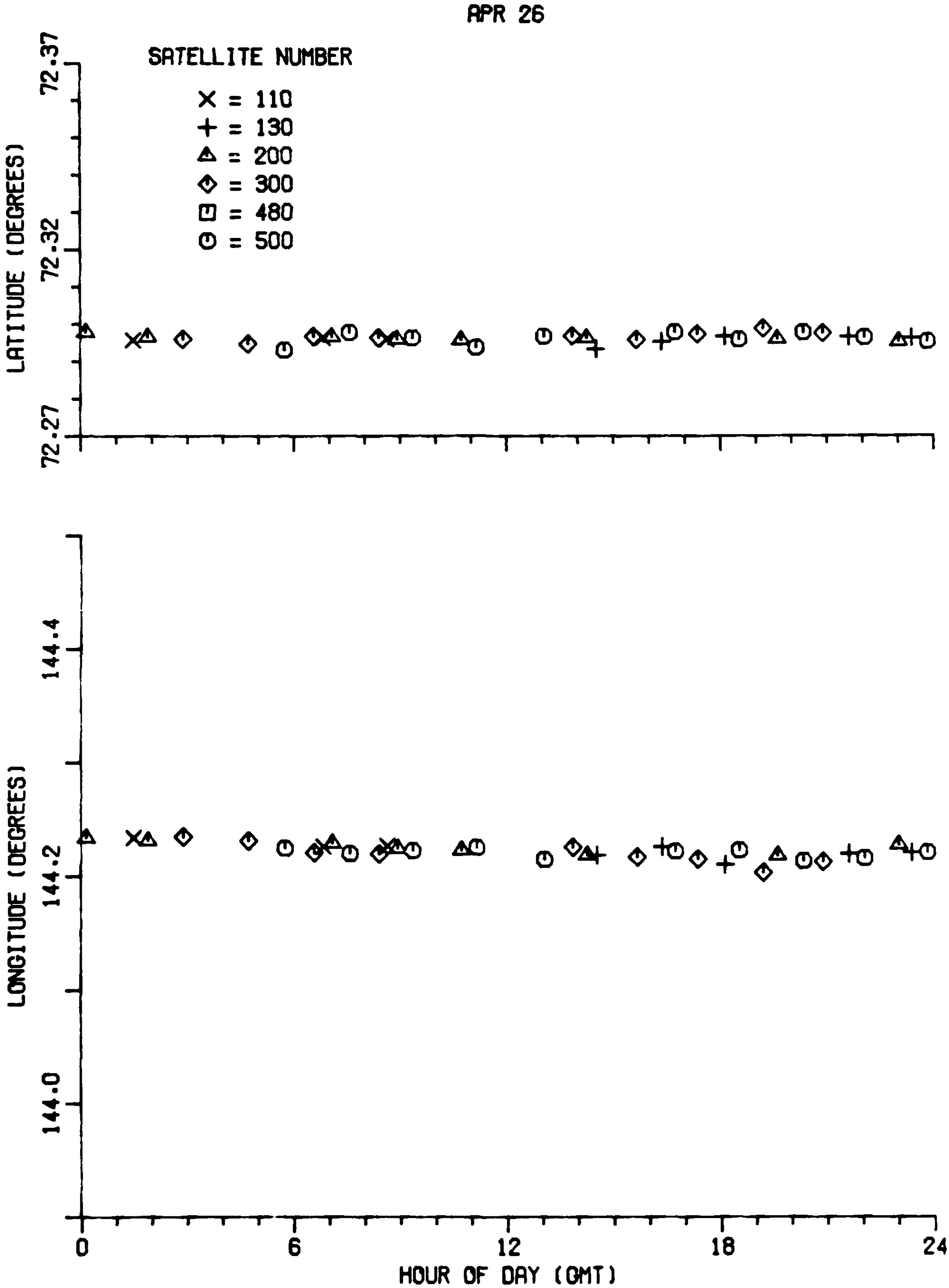

APR 26
SATELLITE NUMBER
× = 110
+ = 130
△ = 200
◇ = 300
⊡ = 480
⊙ = 500
LATITUDE (DEGREES)
72.37
72.32
72.27
LONGITUDE (DEGREES)
144.4
144.2
144.0
0
6
12
18
24
HOUR OF DAY (GMT)

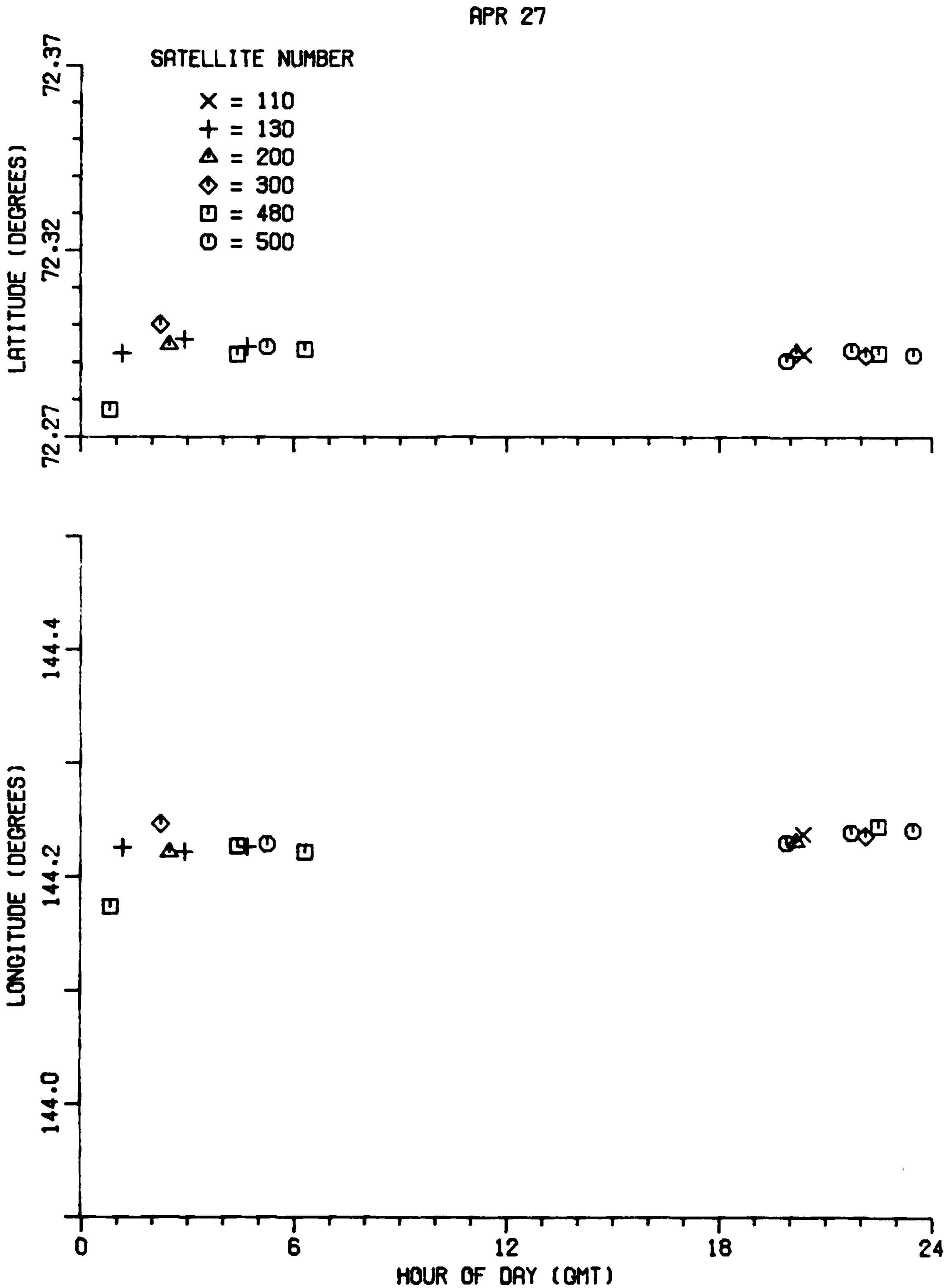
APR 27
SATELLITE NUMBER
X = 110
+ = 130
Δ = 200
◇ = 300
⊡ = 480
⊙ = 500
LATITUDE (DEGREES)
72.37
72.32
72.27
LONGITUDE (DEGREES)
144.4
144.2
144.0
0
6
12
18
24
HOUR OF DAY (GMT)

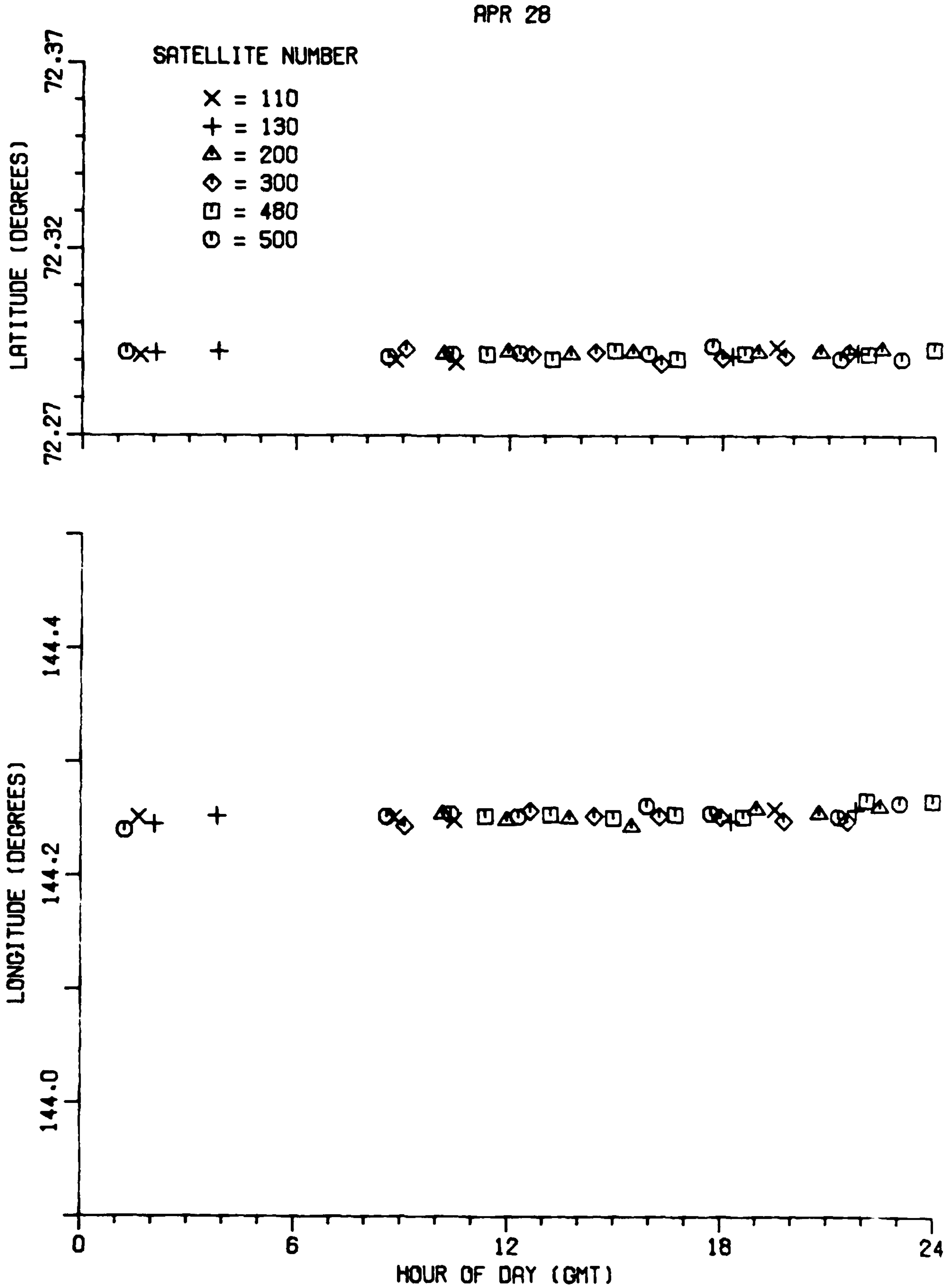

APR 28
SATELLITE NUMBER
× = 110
+ = 130
△ = 200
◇ = 300
□ = 480
○ = 500
LATITUDE (DEGREES)
72.37
72.32
72.27
LONGITUDE (DEGREES)
144.4
144.2
144.0
0
6
12
18
24
HOUR OF DAY (GMT)

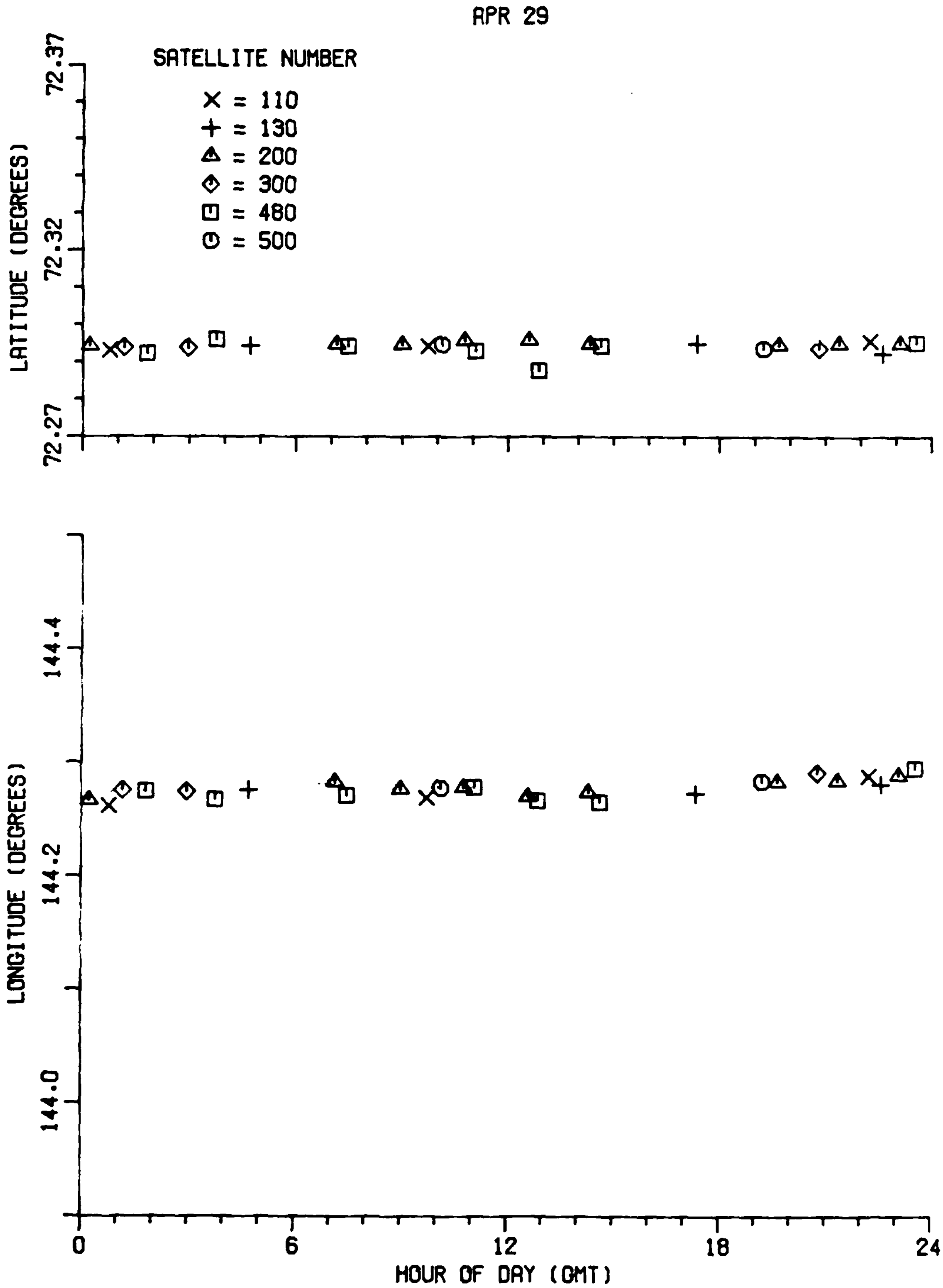
APR 29
SATELLITE NUMBER
X = 110
+ = 130
Δ = 200
◊ = 300
□ = 480
⊙ = 500
LATITUDE (DEGREES)
72.37
72.32
72.27
LONGITUDE (DEGREES)
144.4
144.2
144.0
0
6
12
18
24
HOUR OF DAY (GMT)

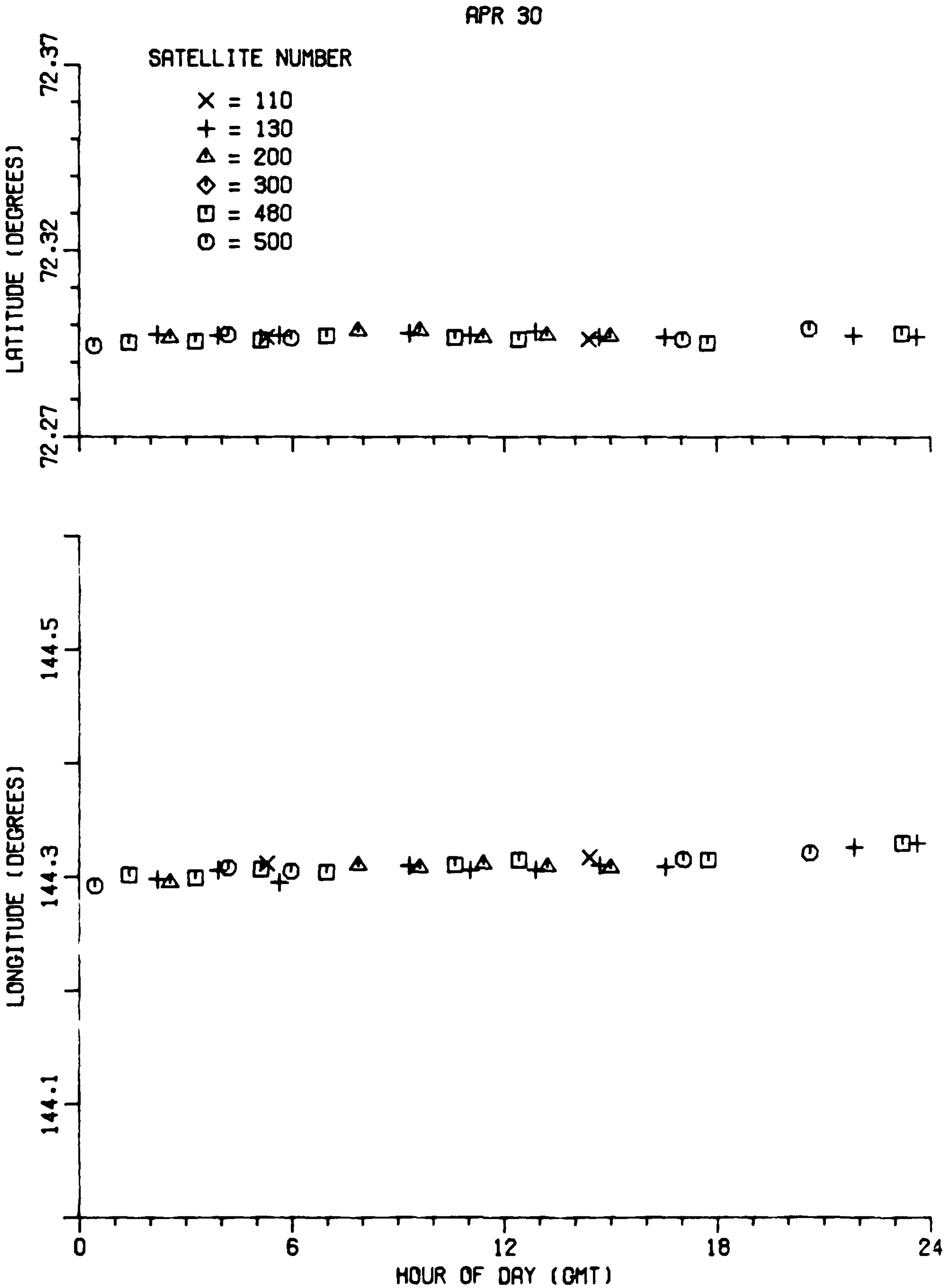
APR 30
SATELLITE NUMBER
X = 110
+ = 130
△ = 200
◇ = 300
□ = 480
⊙ = 500
LATITUDE (DEGREES)
72.37
72.32
72.27
LONGITUDE (DEGREES)
144.5
144.3
144.1
0
6
12
18
24
HOUR OF DAY (GMT)

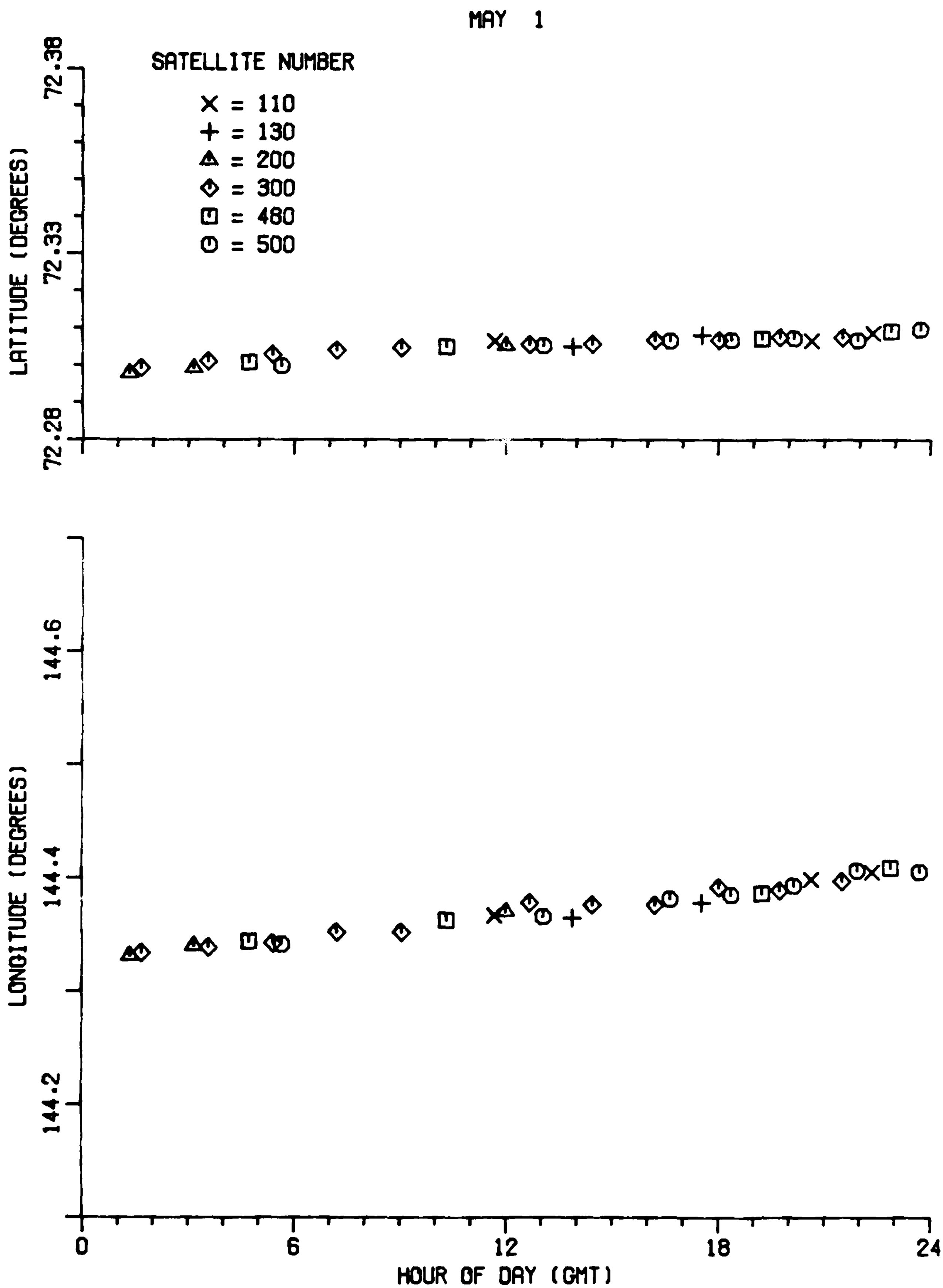
MAY 1
SATELLITE NUMBER
X = 110
+ = 130
Δ = 200
◇ = 300
□ = 480
⊙ = 500
LATITUDE (DEGREES)
72.38
72.33
72.28
LONGITUDE (DEGREES)
144.6
144.4
144.2
0
6
12
18
24
HOUR OF DAY (GMT)

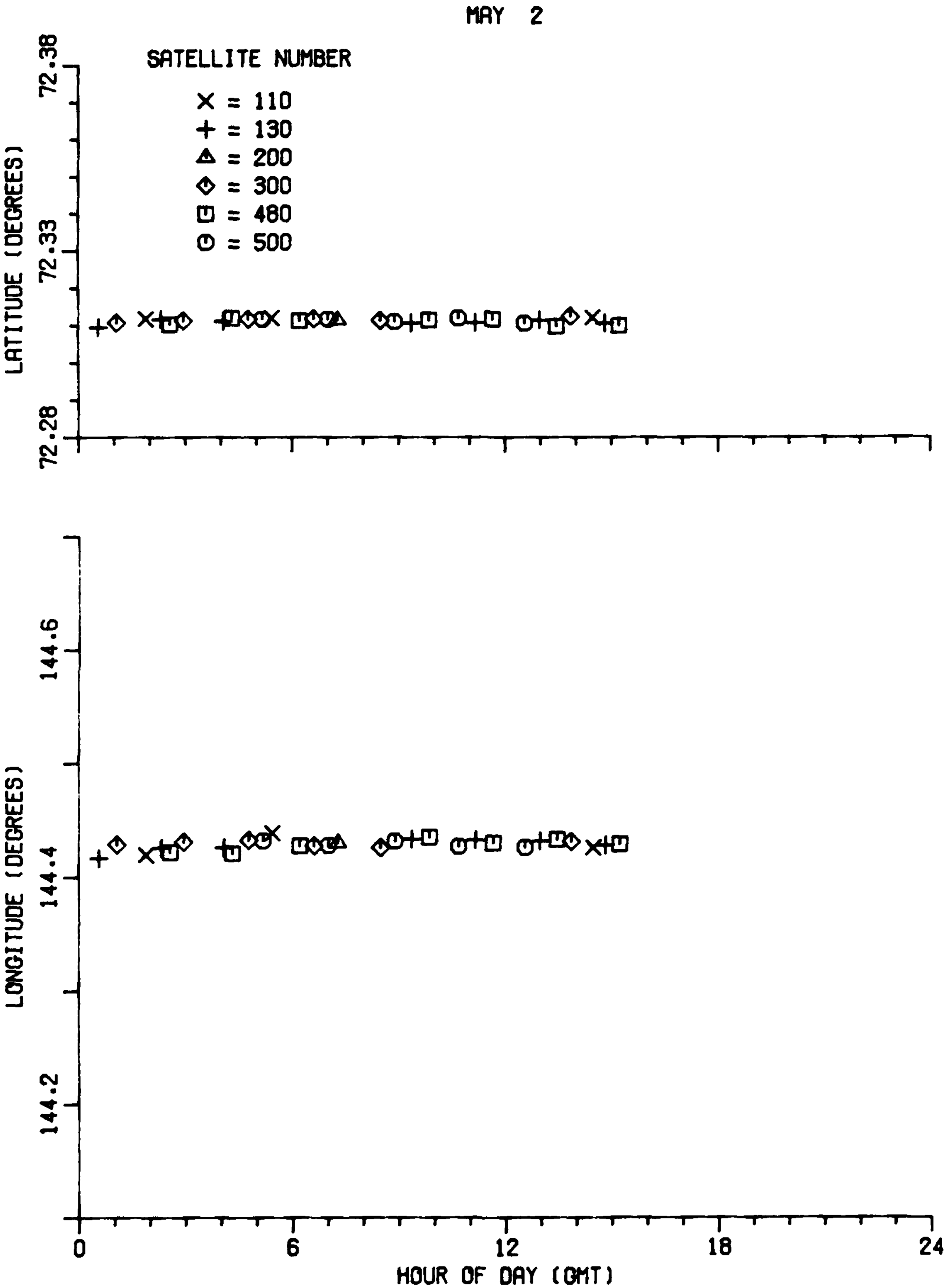
MAY 2
SATELLITE NUMBER
X = 110
+ = 130
Δ = 200
◇ = 300
□ = 460
○ = 500
LATITUDE (DEGREES)
72.38
72.33
72.28
LONGITUDE (DEGREES)
144.6
144.4
144.2
0
6
12
18
24
HOUR OF DAY (GMT)

APPENDIX B

Spring 1986 CTD Measurements

CTD Measurements at the 1986 ice camp

Date	Sta. No.	Local Time	Tape	Sensor Number C	Sensor Number T	Sensor Number D	Max. Depth (m)
Mar 22	3	0600	1	3	429	1653	300
	7	1800					
23	9	0600					
	11	1800					
24	13	0600					
	15	1530					70
	17	1800					300
25	19	0615	2				
	21	1815					
26	23	0600					
27	25	0730					
	27	1644					
28	29	0600					
29	31	0600					
30	33	0600					
	35	1800					
31	37	0600					
	39	1800					
Apr 1	41	0600					
	43	1845					
2	45	0600	3	19	432	1653	
	47	1730					
3	49	1426					
4	51	1430					
5	53	0715	4				
6	55	0645					
7	57	1225					
8	59	0630					
9	61	0630					
10	63	1315					100
11	65	0630					300
12	67	0640					
13	69	0630					
14	71	0645					
15	73	0800	5				300
16	75	0745					
17	77	0930		3	429	1653	
18	79	0545					
19	81	0845					
20	83	0645					
22	85	0815					
23	87	1730					
24	89	1615					
25	91	0815					
	93	2045					100
	Deep Cast	1200	1	16	432	52	1500

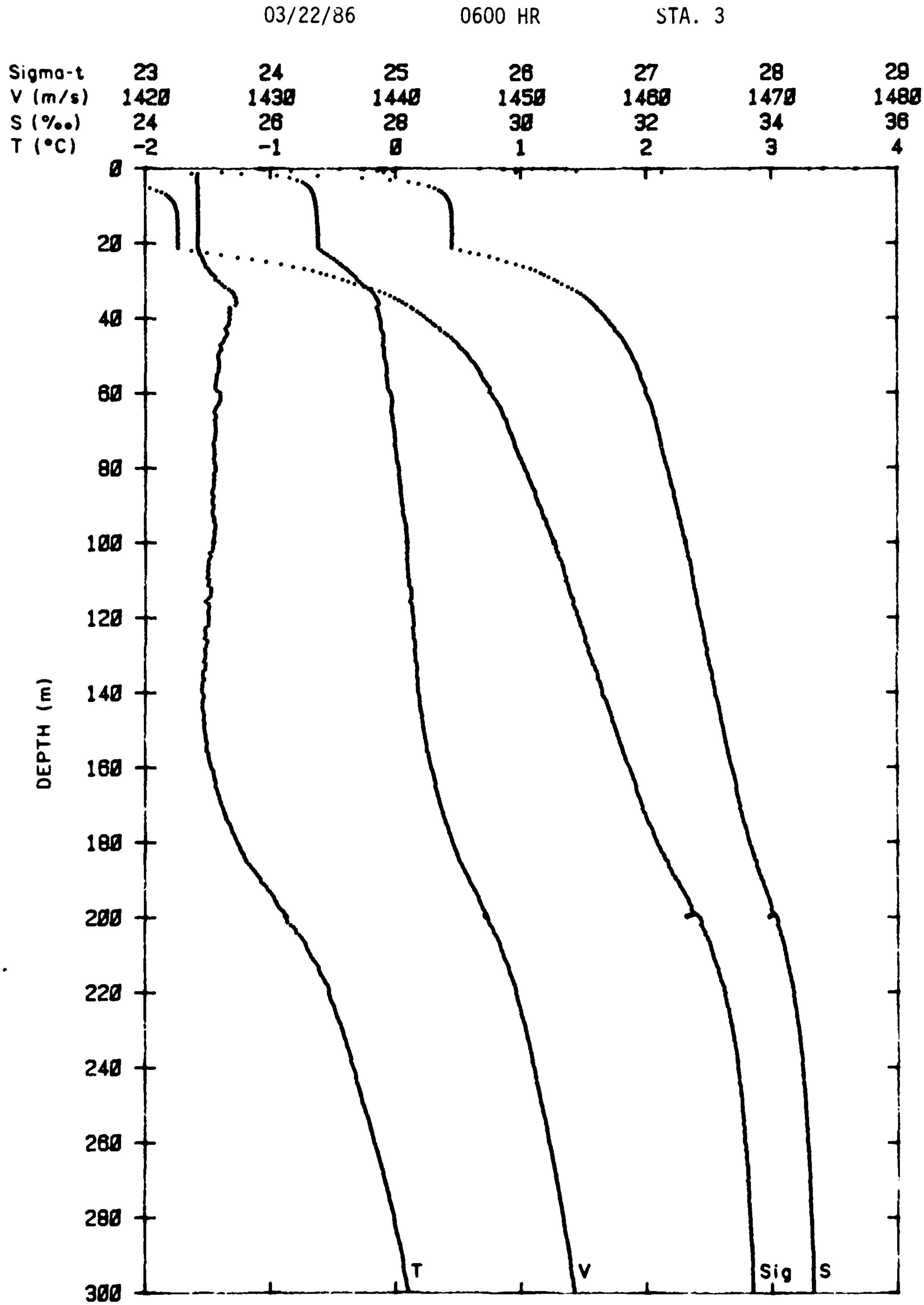

03/22/86
0600 HR
STA. 3
Sigma-t
V (m/s)
S (‰)
T (°C)
23 24 25 26 27 28 29
1420 1430 1440 1450 1460 1470 1480
24 26 28 30 32 34 36
-2 -1 0 1 2 3 4
DEPTH (m)
0 20 40 60 80 100 120 140 160 180 200 220 240 260 280 300
T
V
Sig
S

03/22/86 1800 HR STA. 7

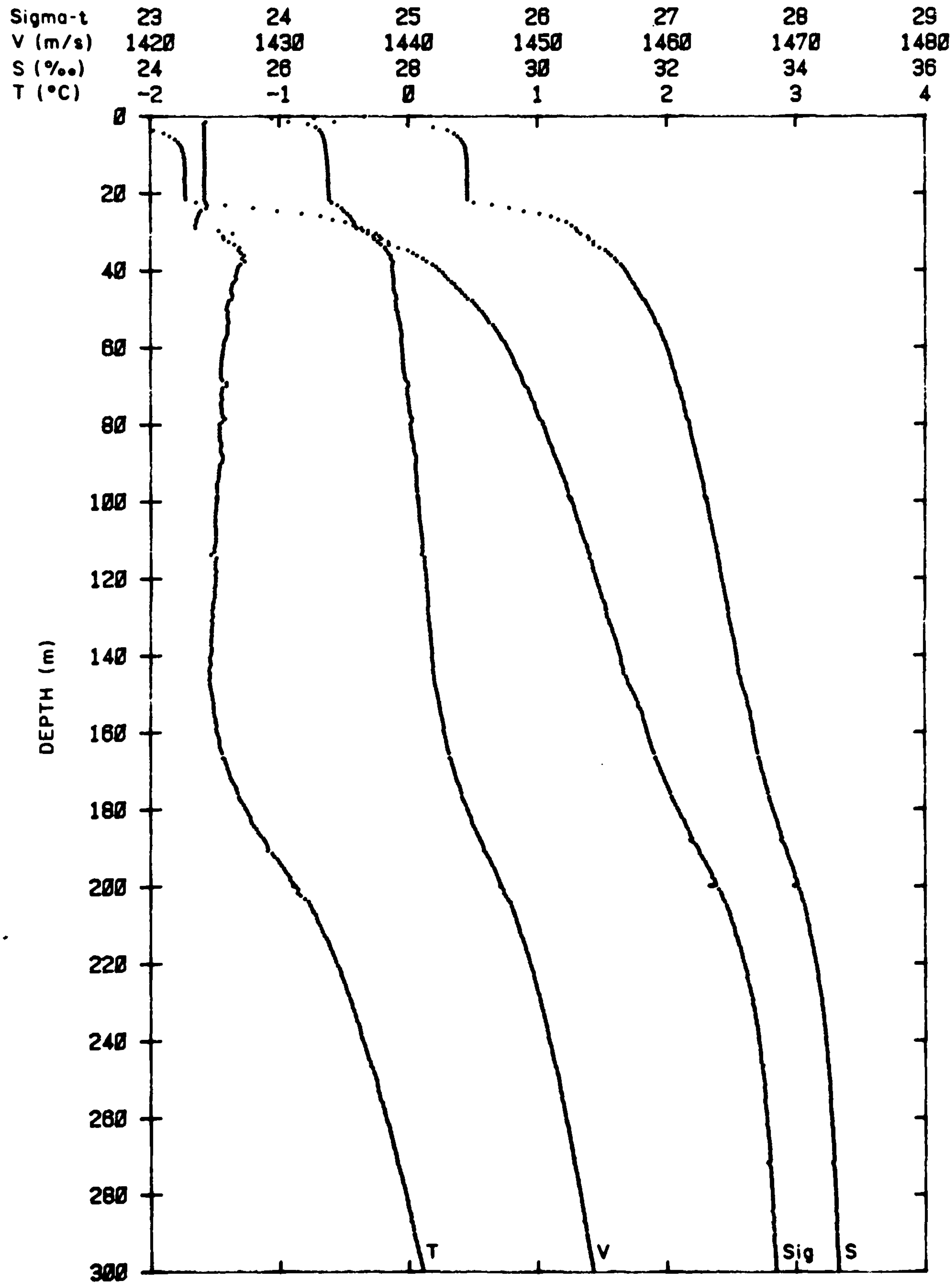

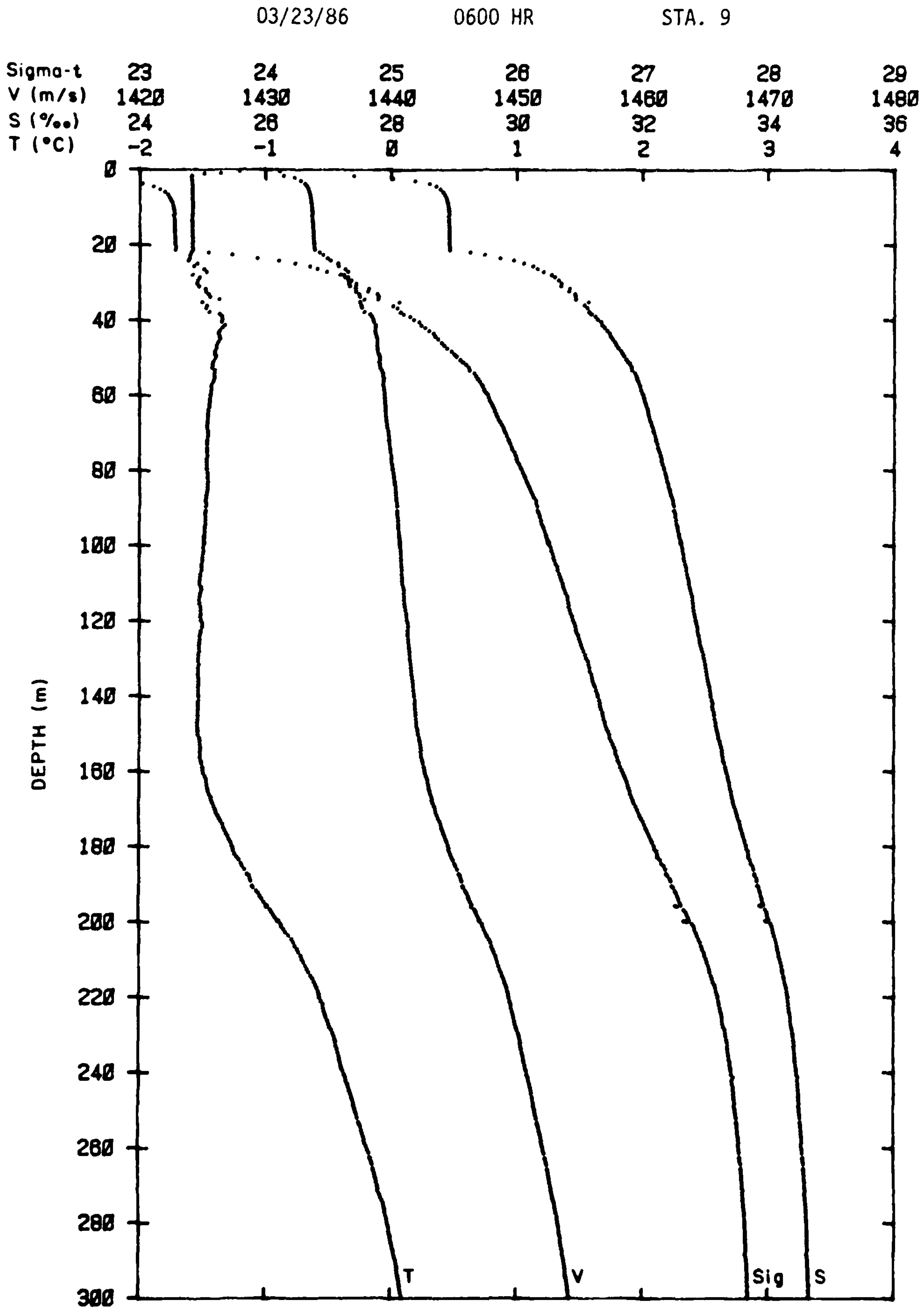
03/23/86 0600 HR STA. 9
Sigma-t 23 24 25 26 27 28 29
V (m/s) 1420 1430 1440 1450 1460 1470 1480
S (‰) 24 26 28 30 32 34 36
T (°C) -2 -1 0 1 2 3 4
DEPTH (m)
0
20
40
60
80
100
120
140
160
180
200
220
240
260
280
300
T
V
Sig
S

03/23/86 1800 HR STA. 11

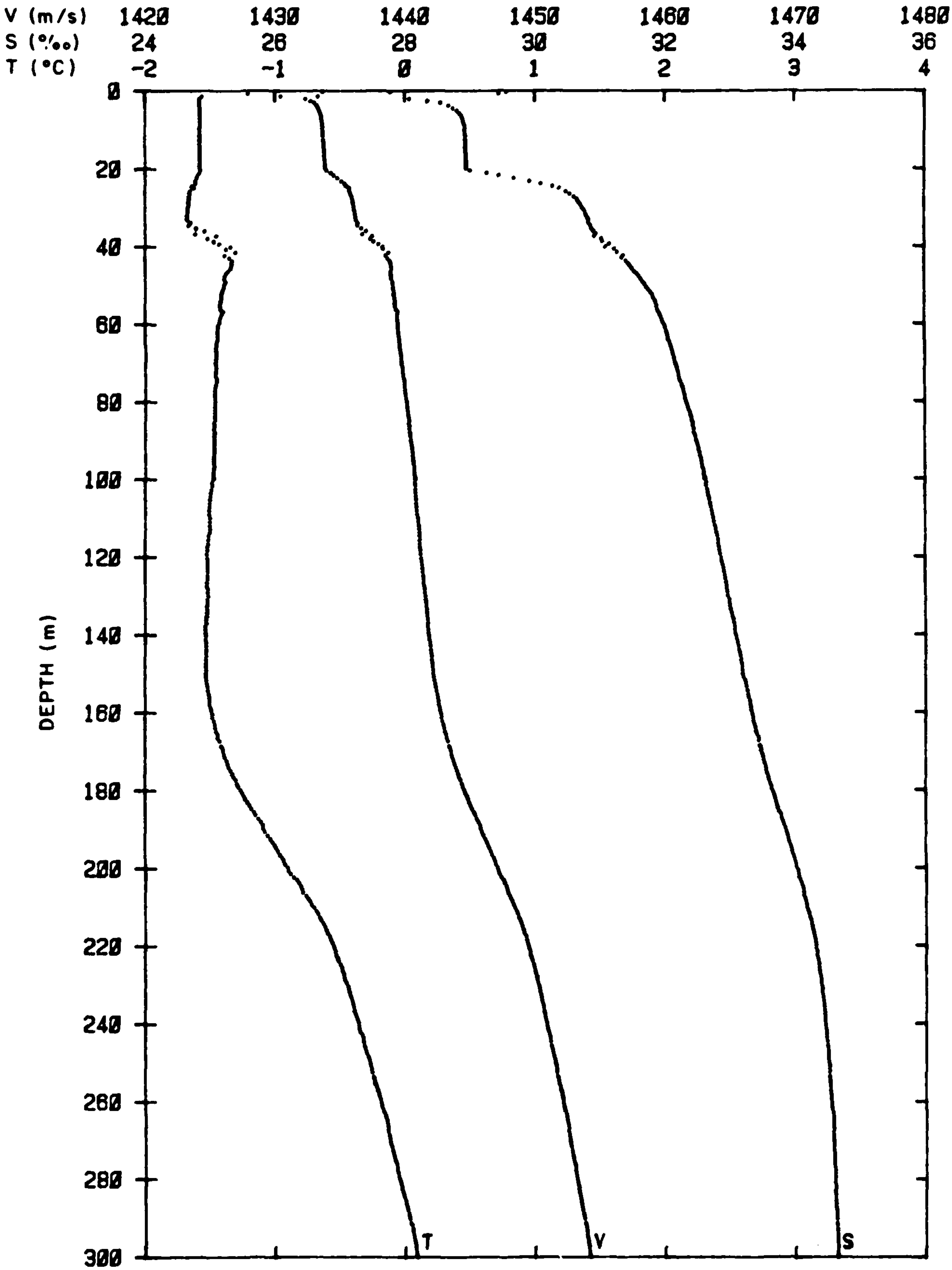

03/24/86 0600 HR STA. 13

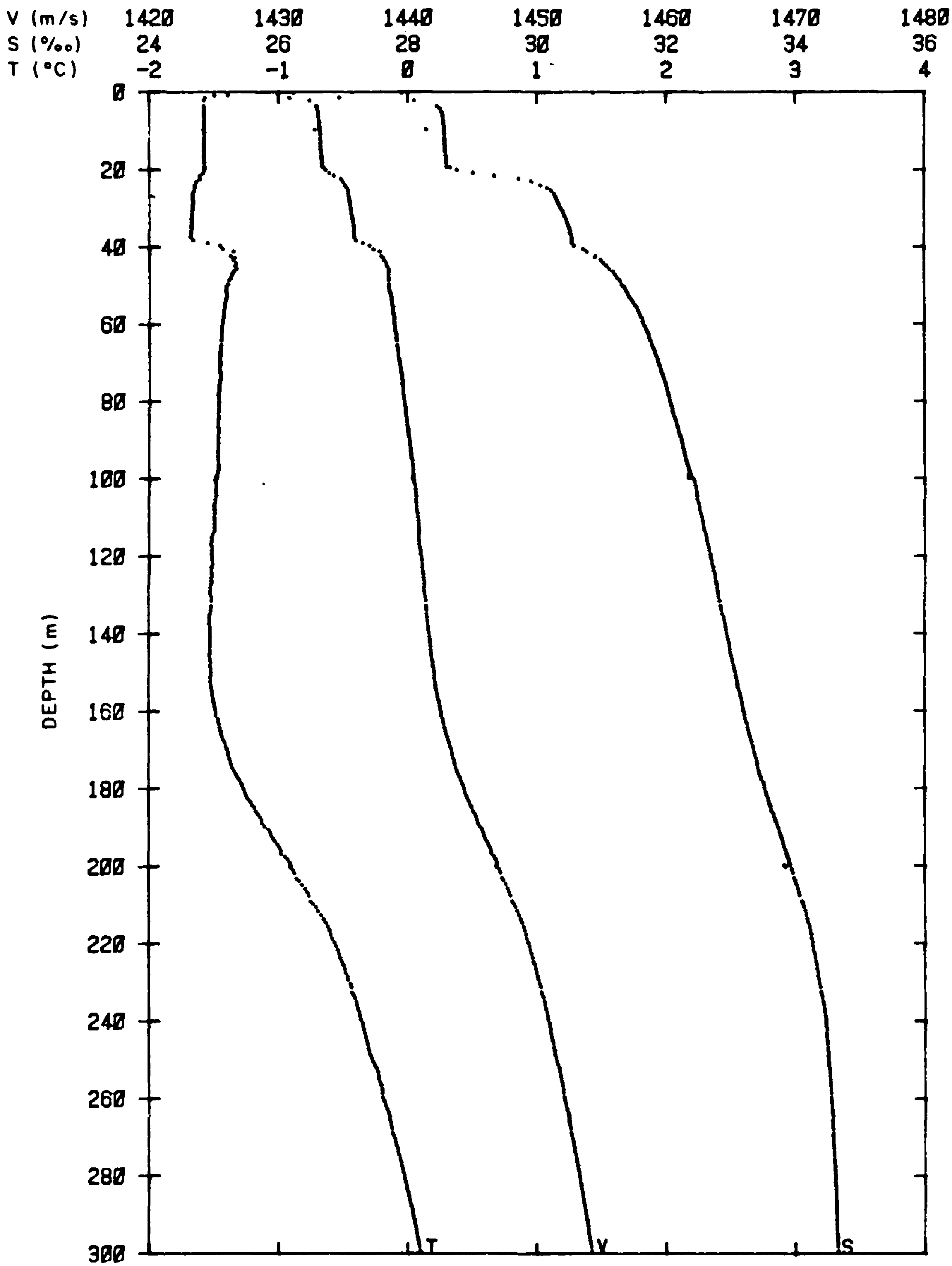

03/24/86 1530 HR STA. 15

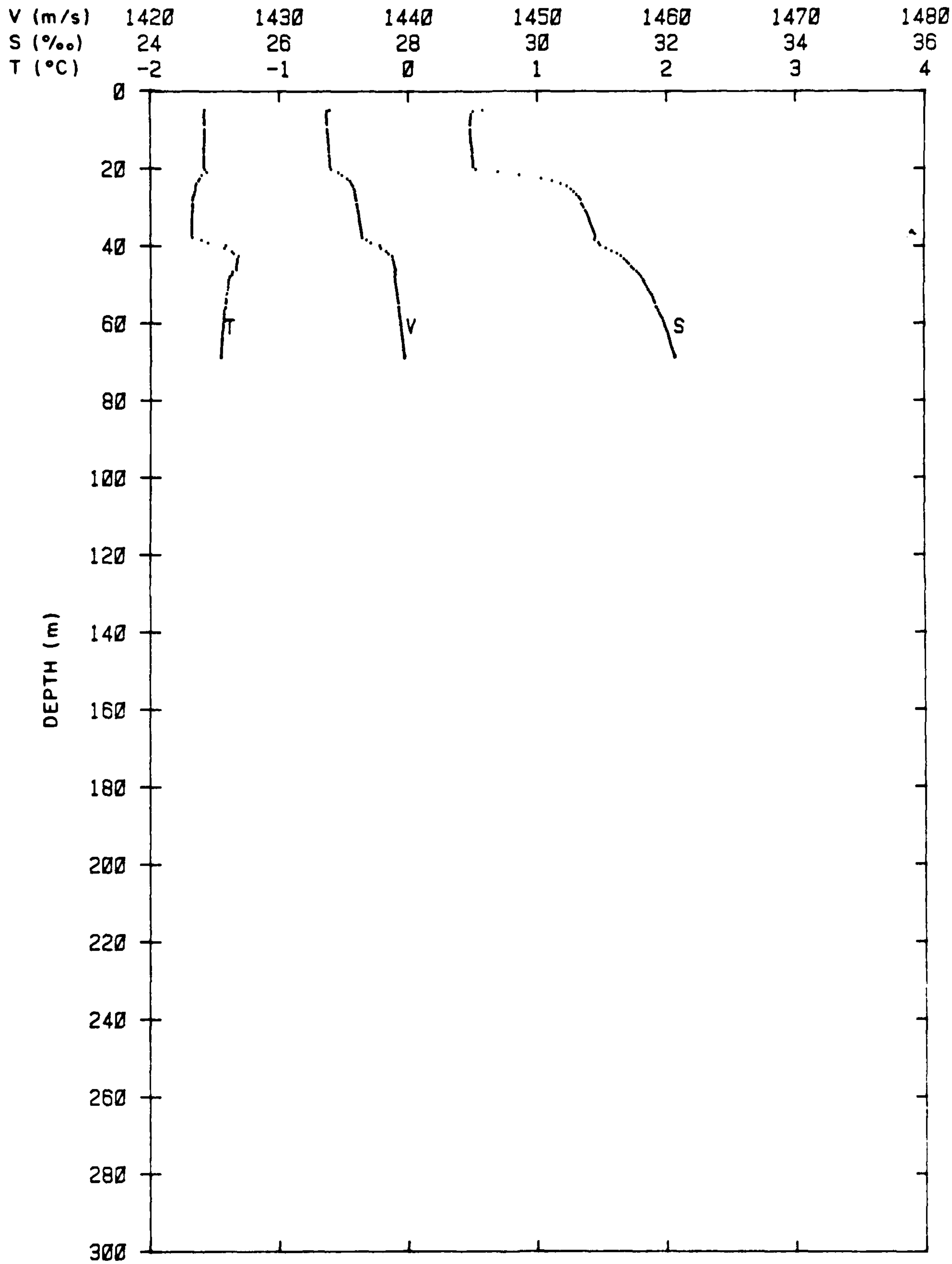

03/24/86 1800 HR STA. 17

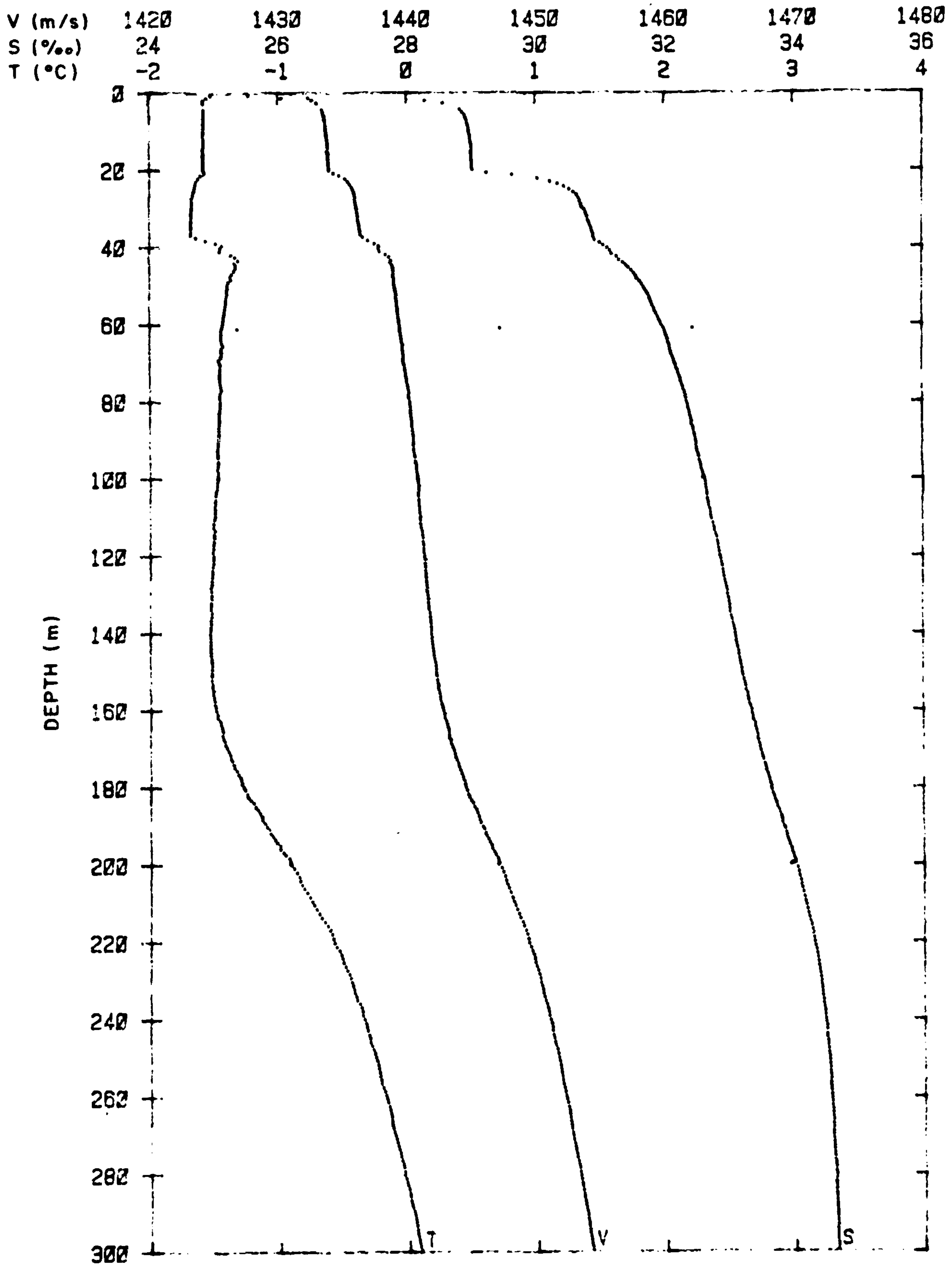

03/25/86 0615 HR STA. 19

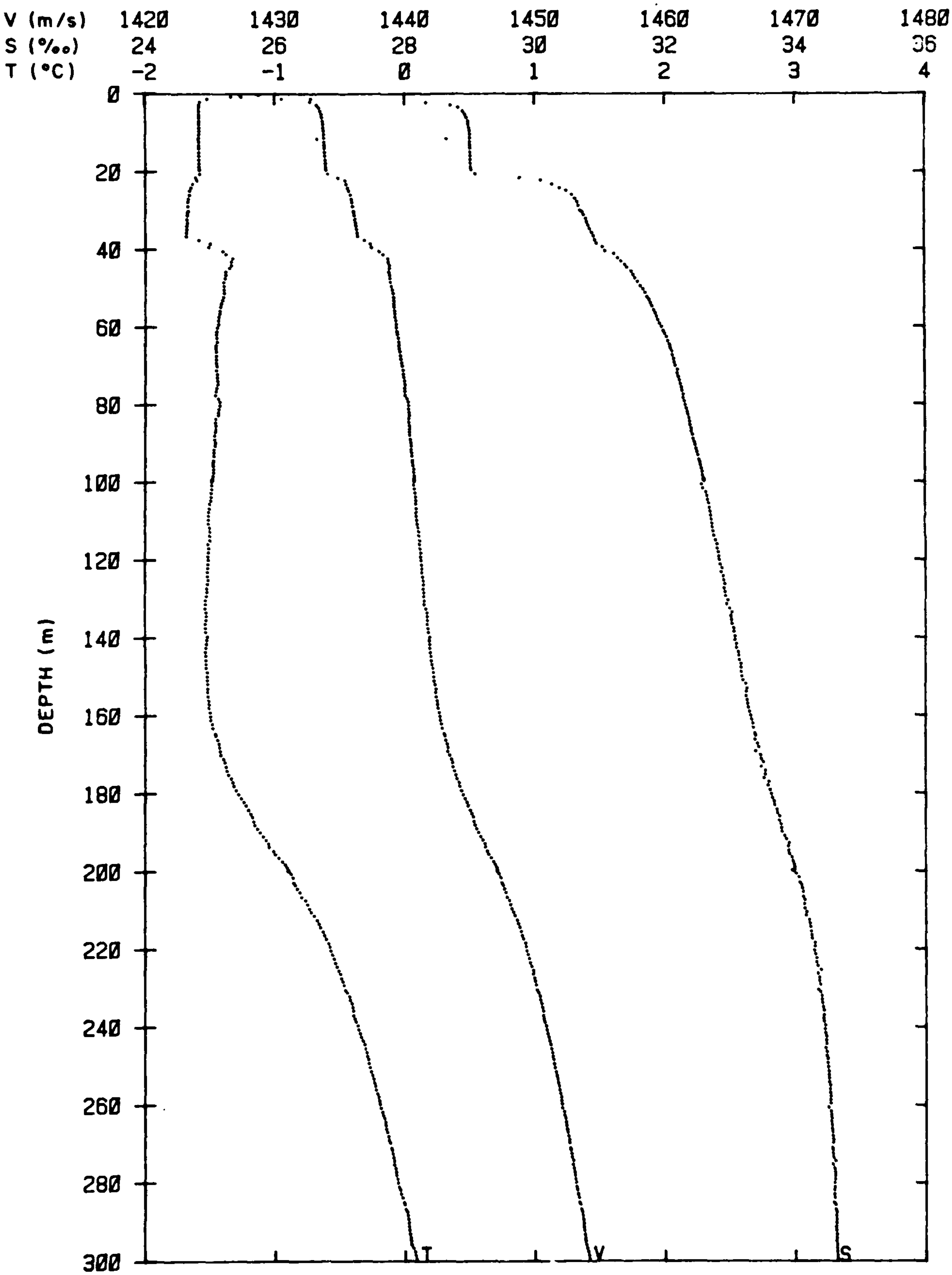

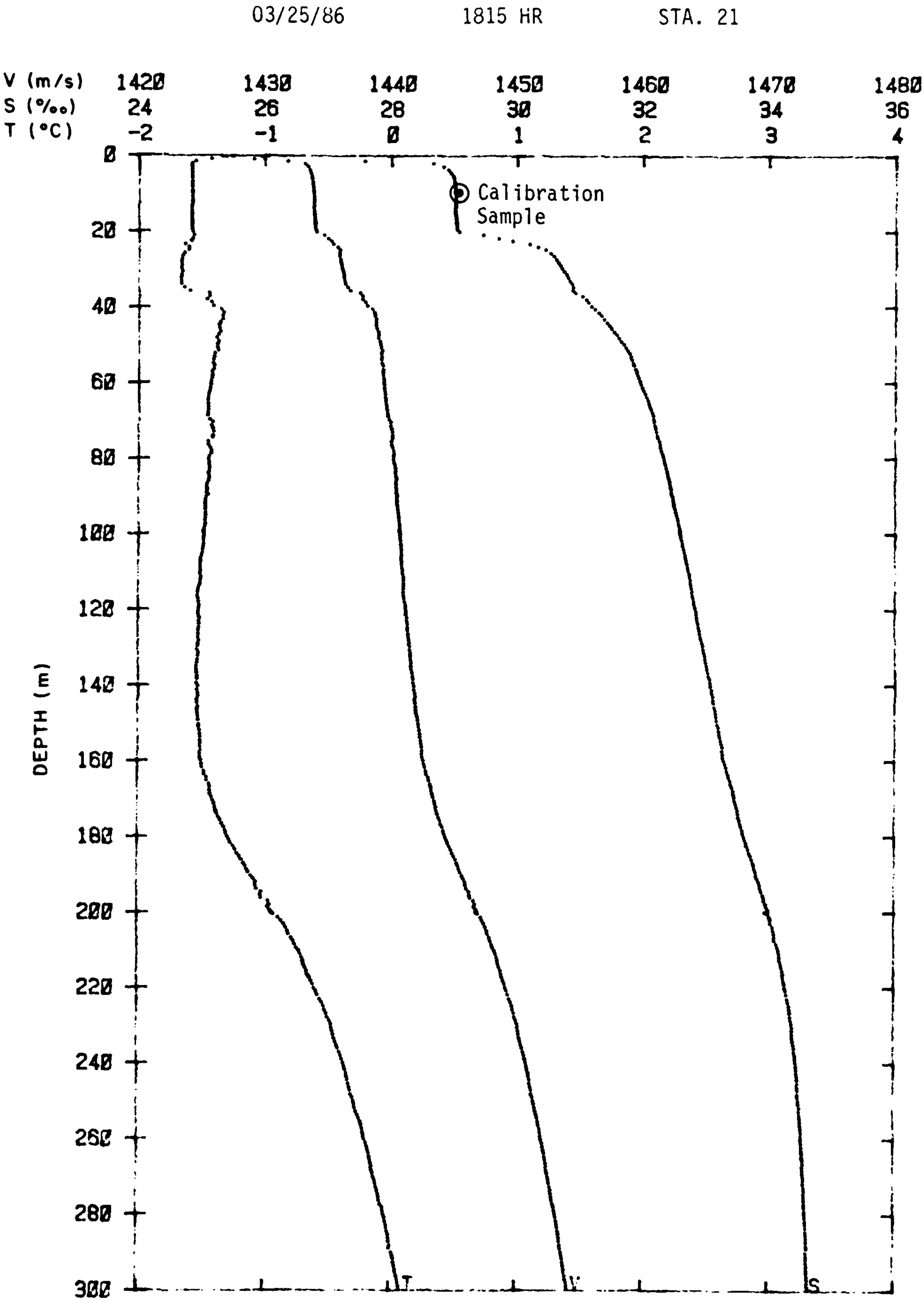
03/25/86
1815 HR
STA. 21
V (m/s) 1420 1430 1440 1450 1460 1470 1480
S (‰) 24 26 28 30 32 34 36
T (°C) -2 -1 0 1 2 3 4
Calibration Sample
DEPTH (m)
0
20
40
60
80
100
120
140
160
180
200
220
240
260
280
300
T
V
S

03/26/86 0600 HR STA. 23

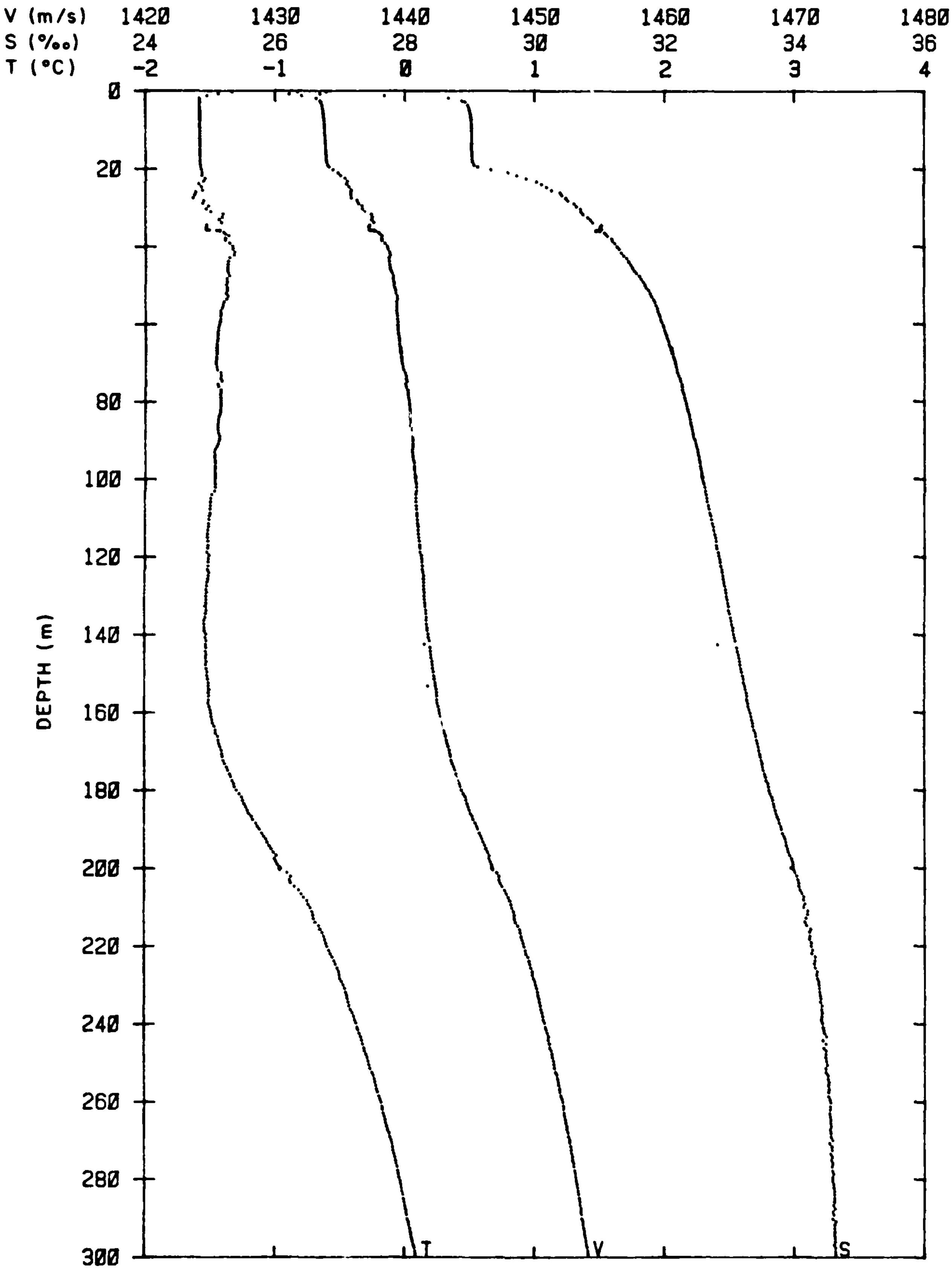

03/27/86 0730 HR STA. 25

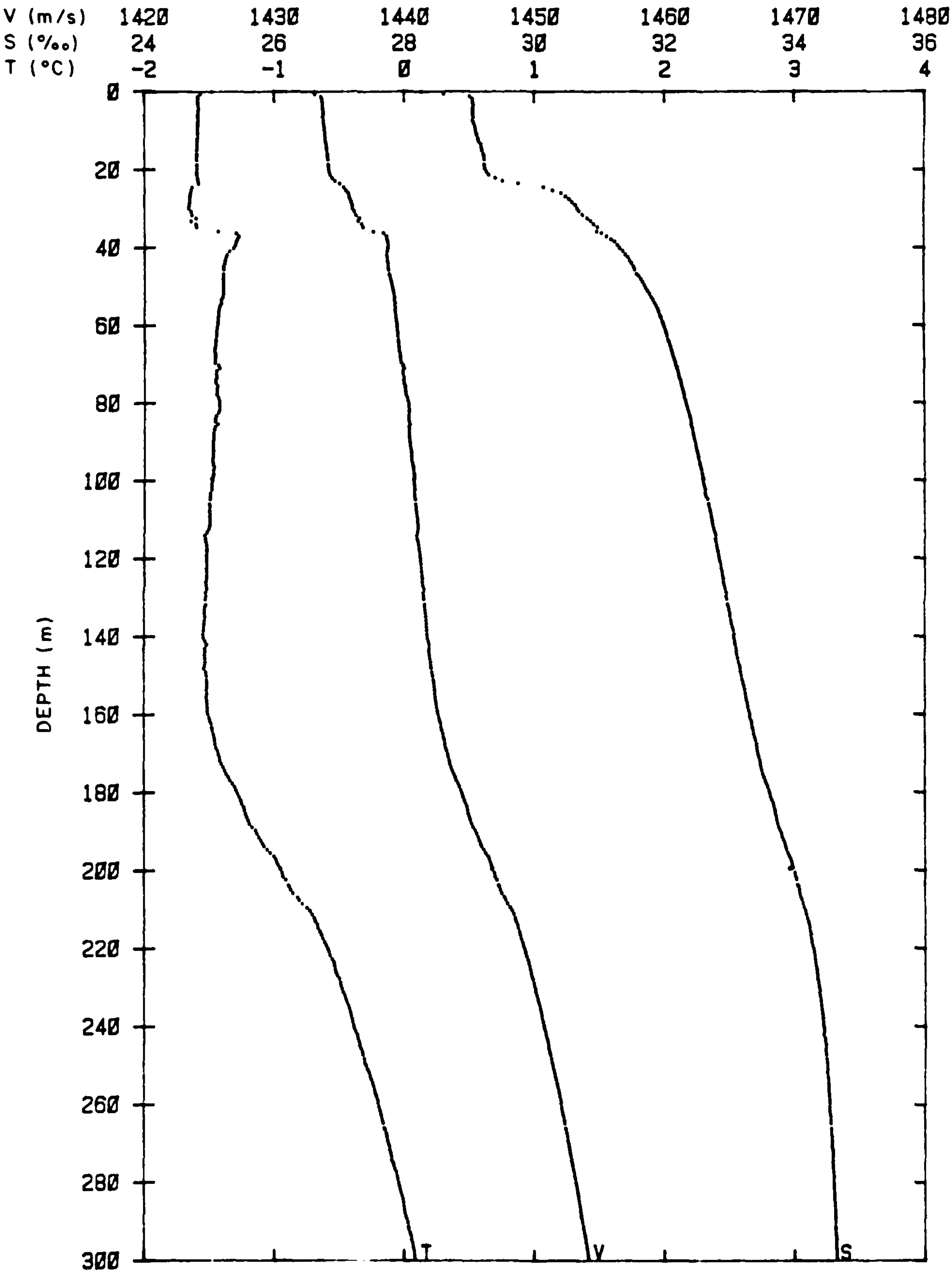

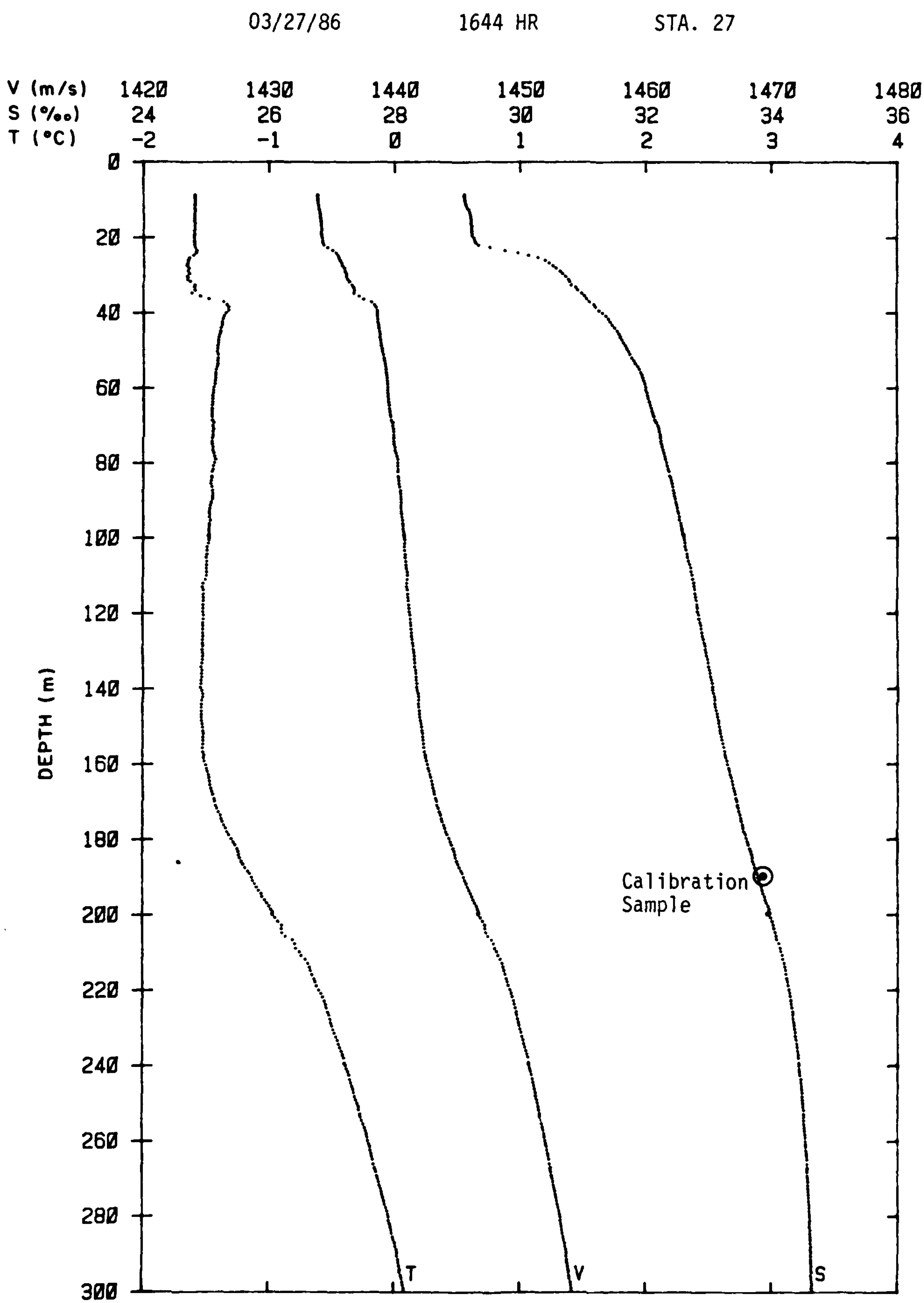
03/27/86
1644 HR
STA. 27
V (m/s) 1420 1430 1440 1450 1460 1470 1480
S (‰) 24 26 28 30 32 34 36
T (°C) -2 -1 0 1 2 3 4
DEPTH (m)
0
20
40
60
80
100
120
140
160
180
200
220
240
260
280
300
Calibration Sample
T
V
S

03/28/86 0600 HR STA. 29

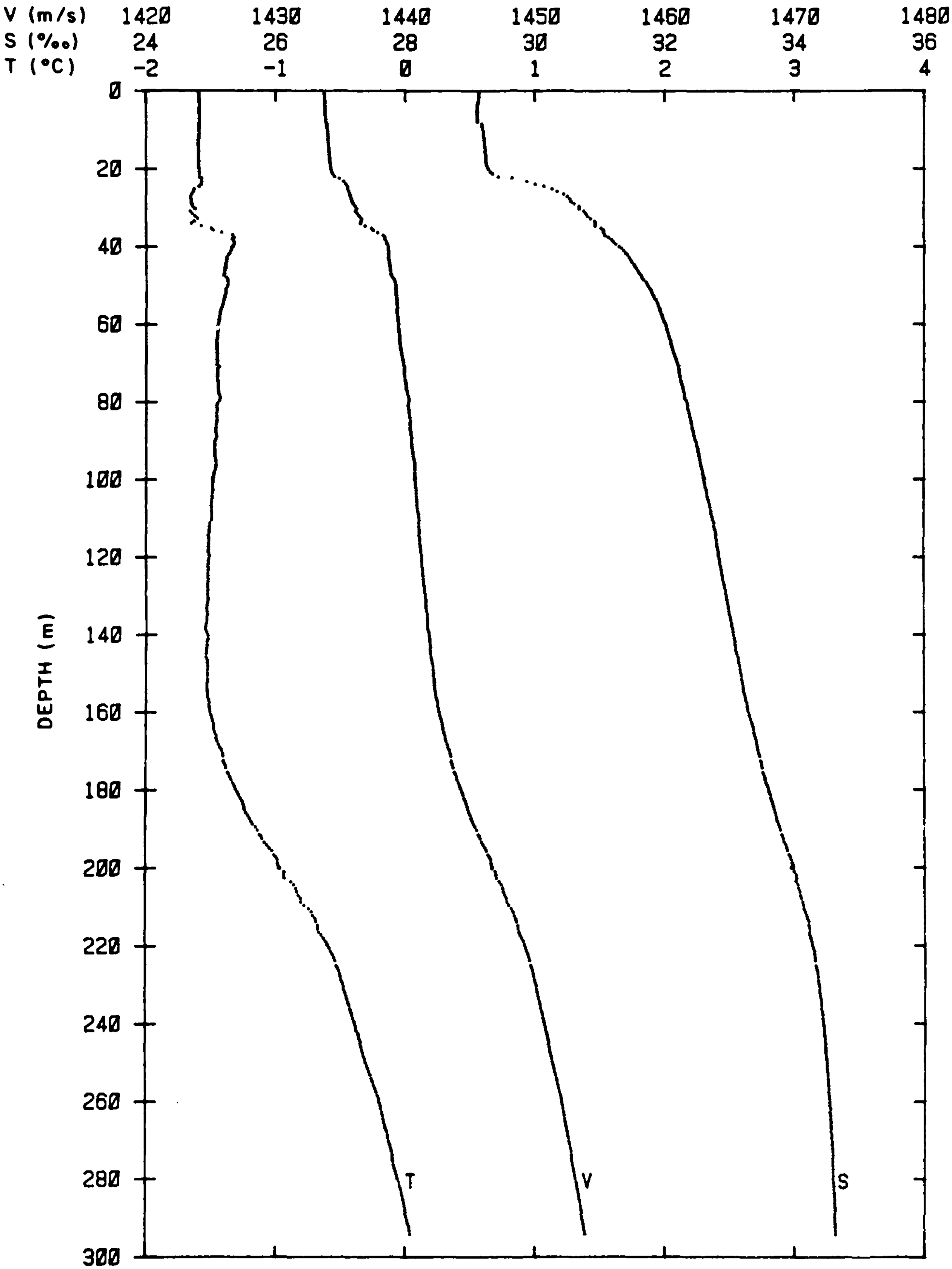

03/29/86 0600 HR STA. 31

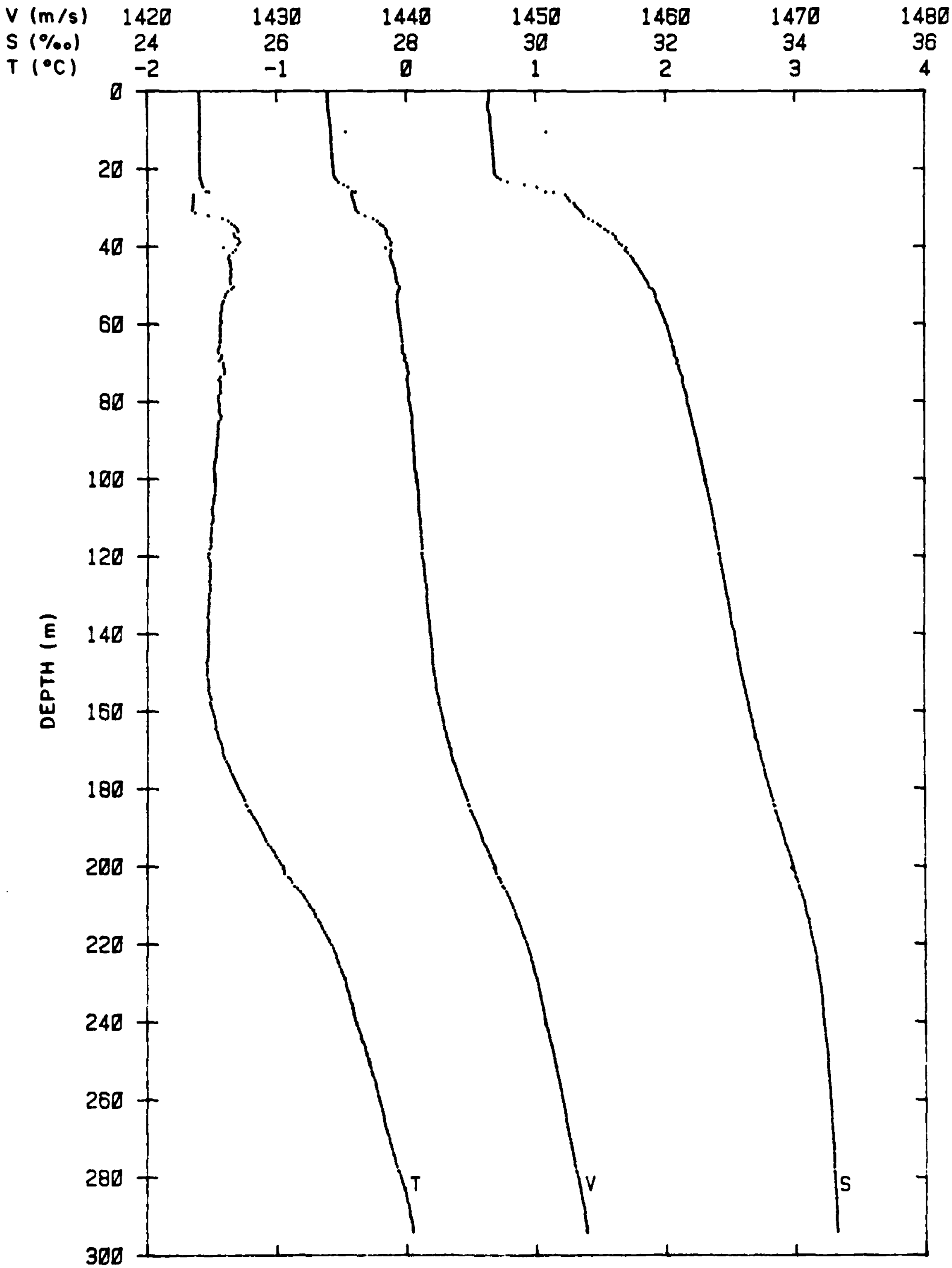

03/30/86 0600 HR STA. 33

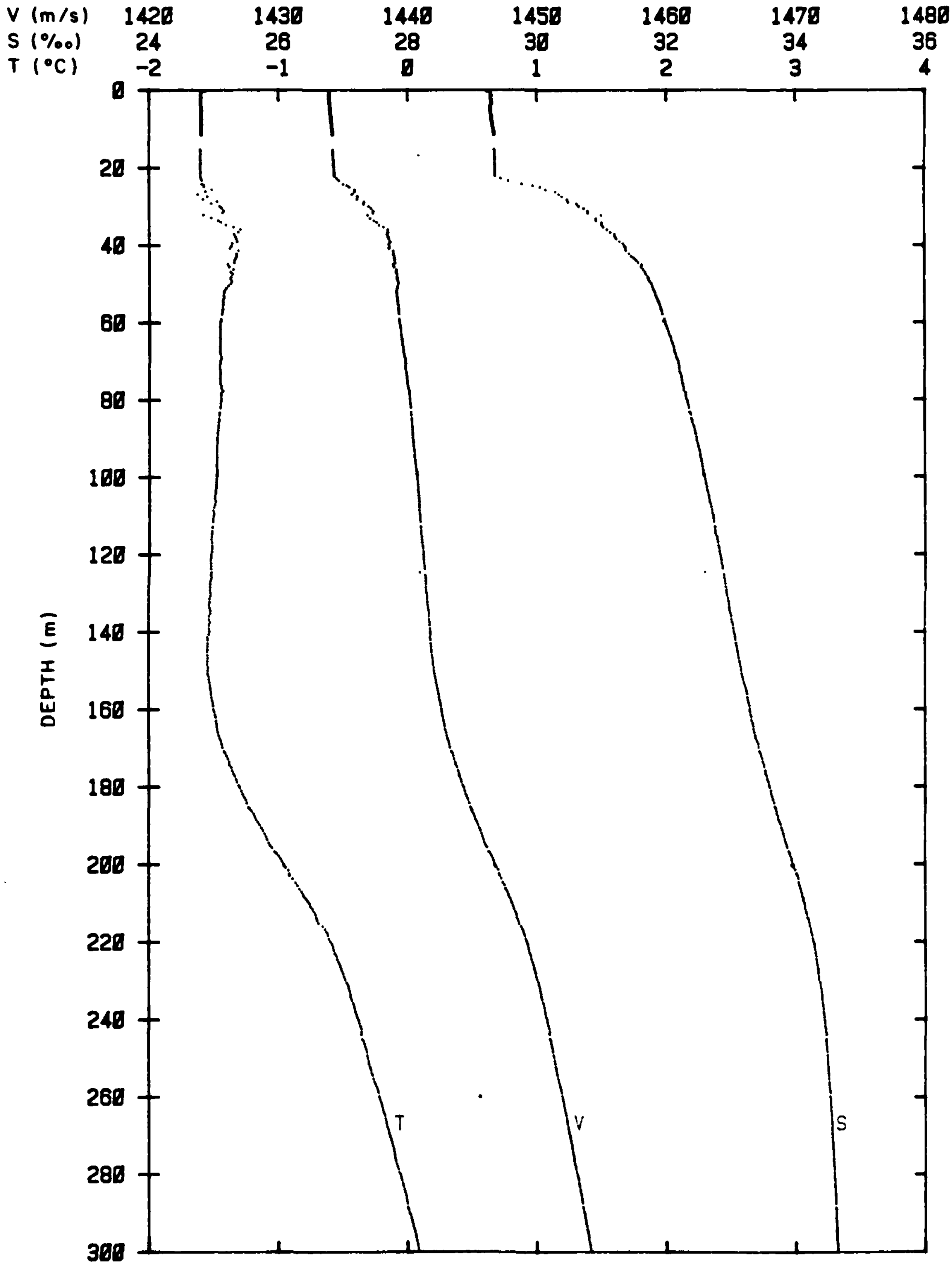

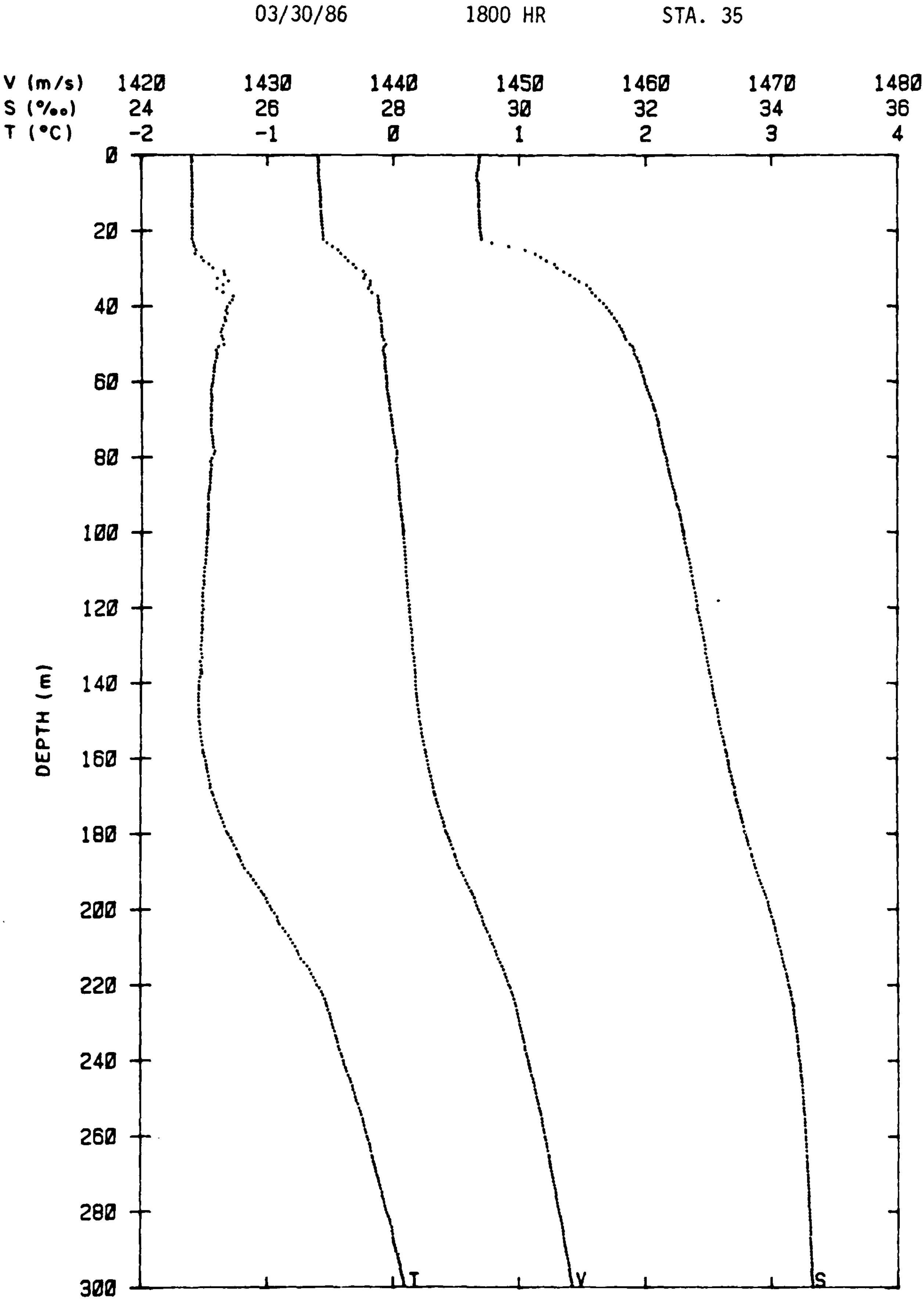
03/30/86
1800 HR
STA. 35
V (m/s) 1420 1430 1440 1450 1460 1470 1480
S (‰) 24 26 28 30 32 34 36
T (°C) -2 -1 0 1 2 3 4
DEPTH (m)
0 20 40 60 80 100 120 140 160 180 200 220 240 260 280 300
T
V
S

03/31/86 0600 HR STA. 37

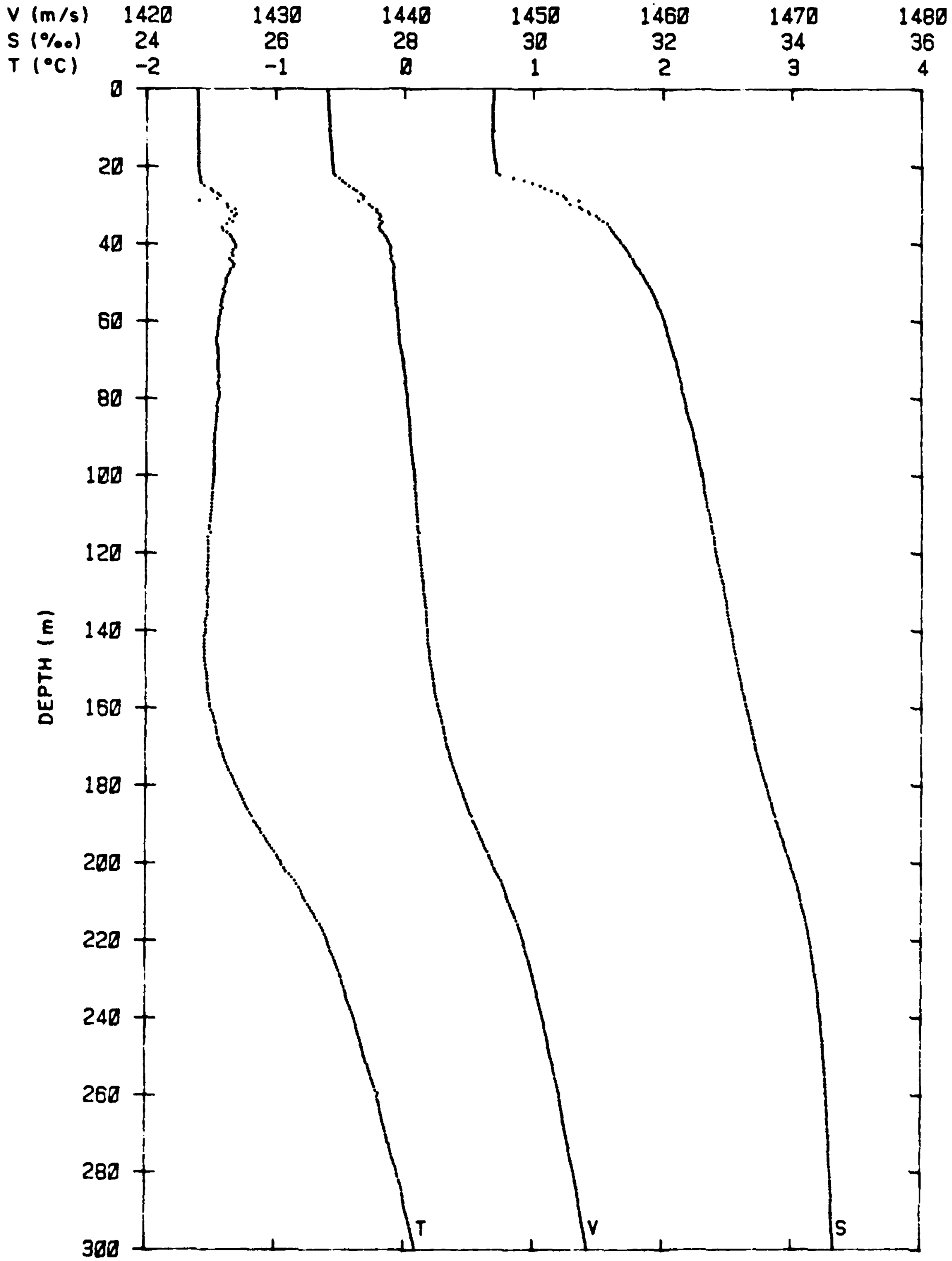

03/31/86 1800 HR STA. 39

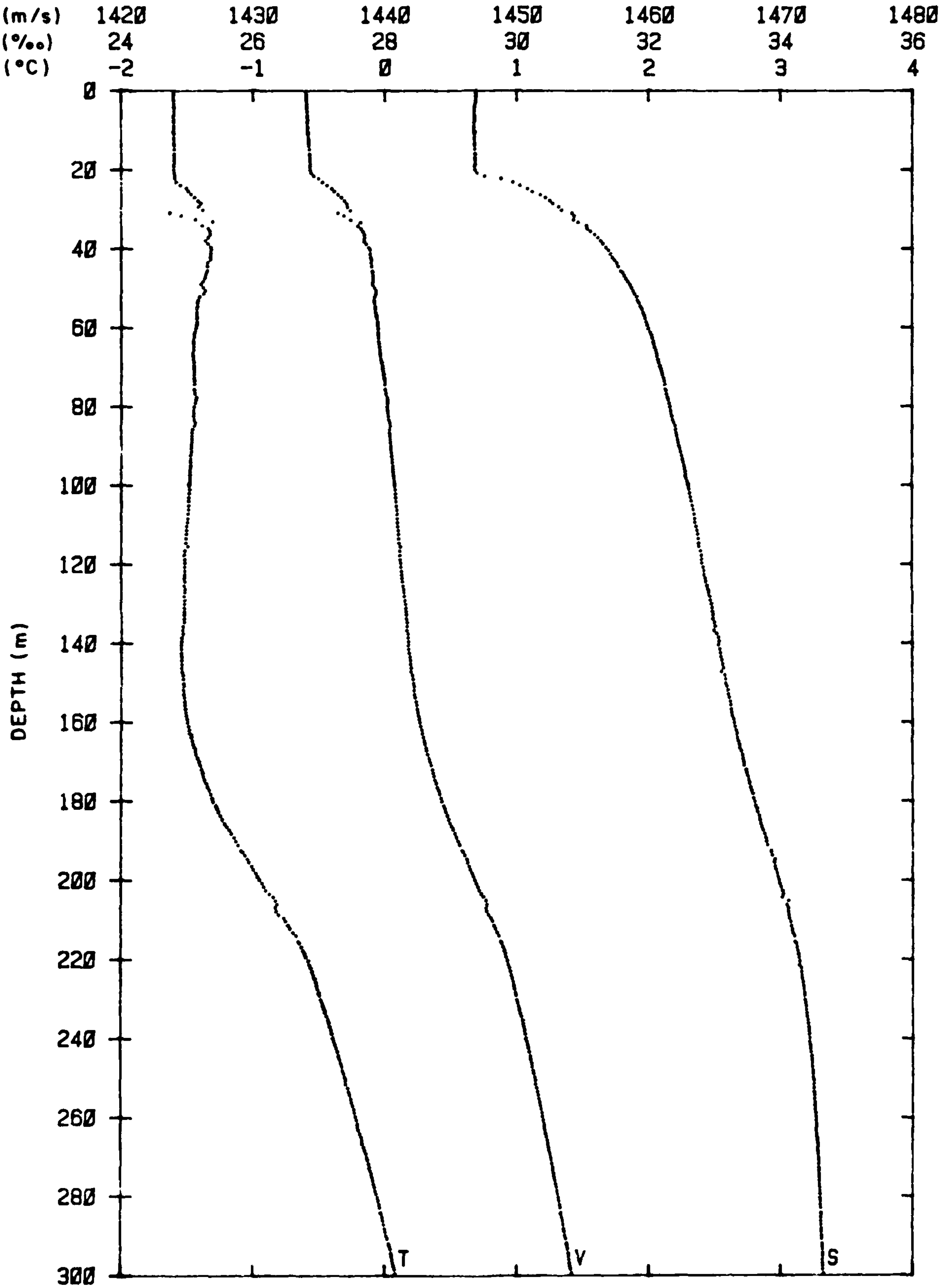

04/01/86 0600 HR STA. 41

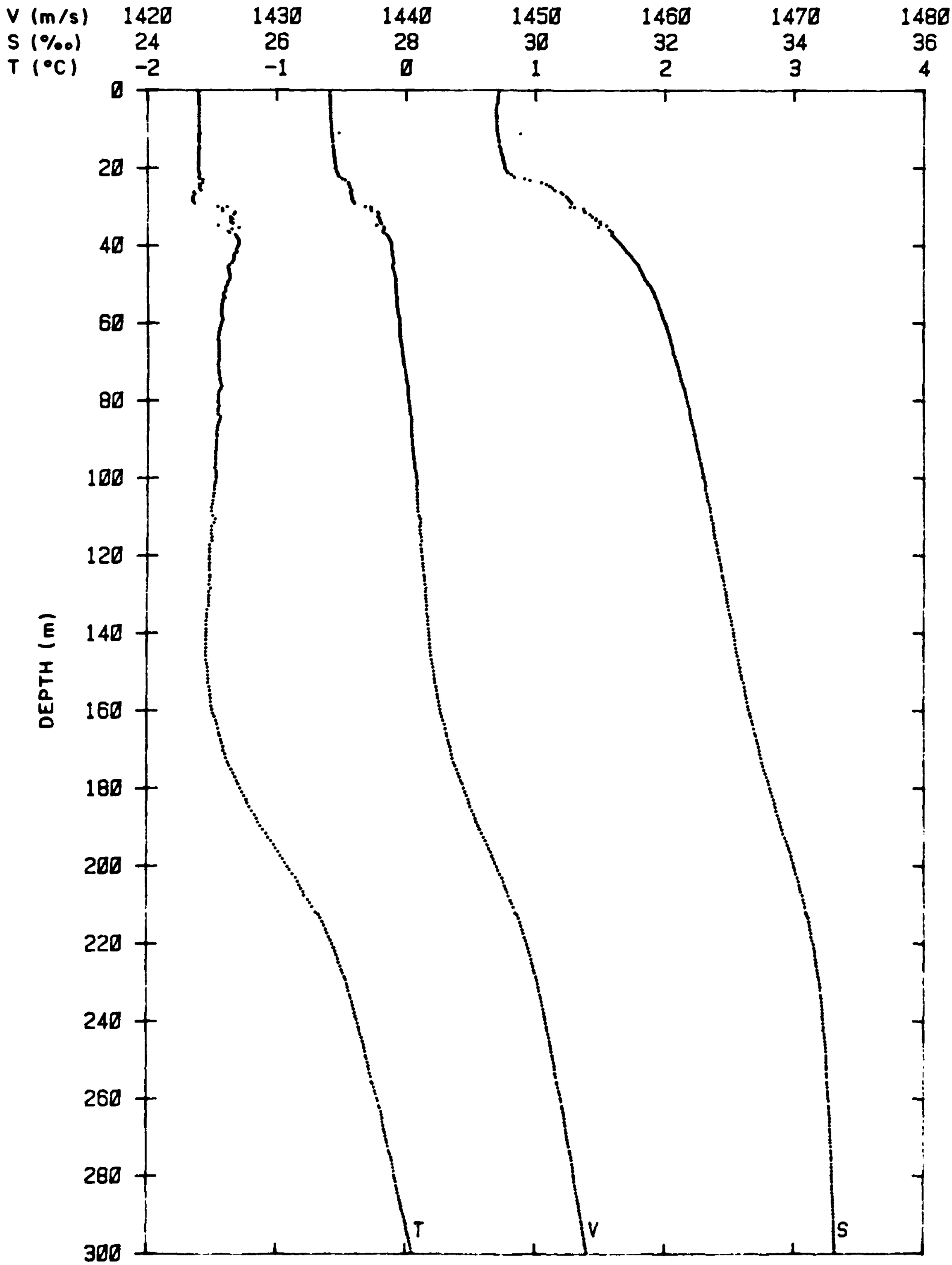

04/01/86 1845 HR STA. 43

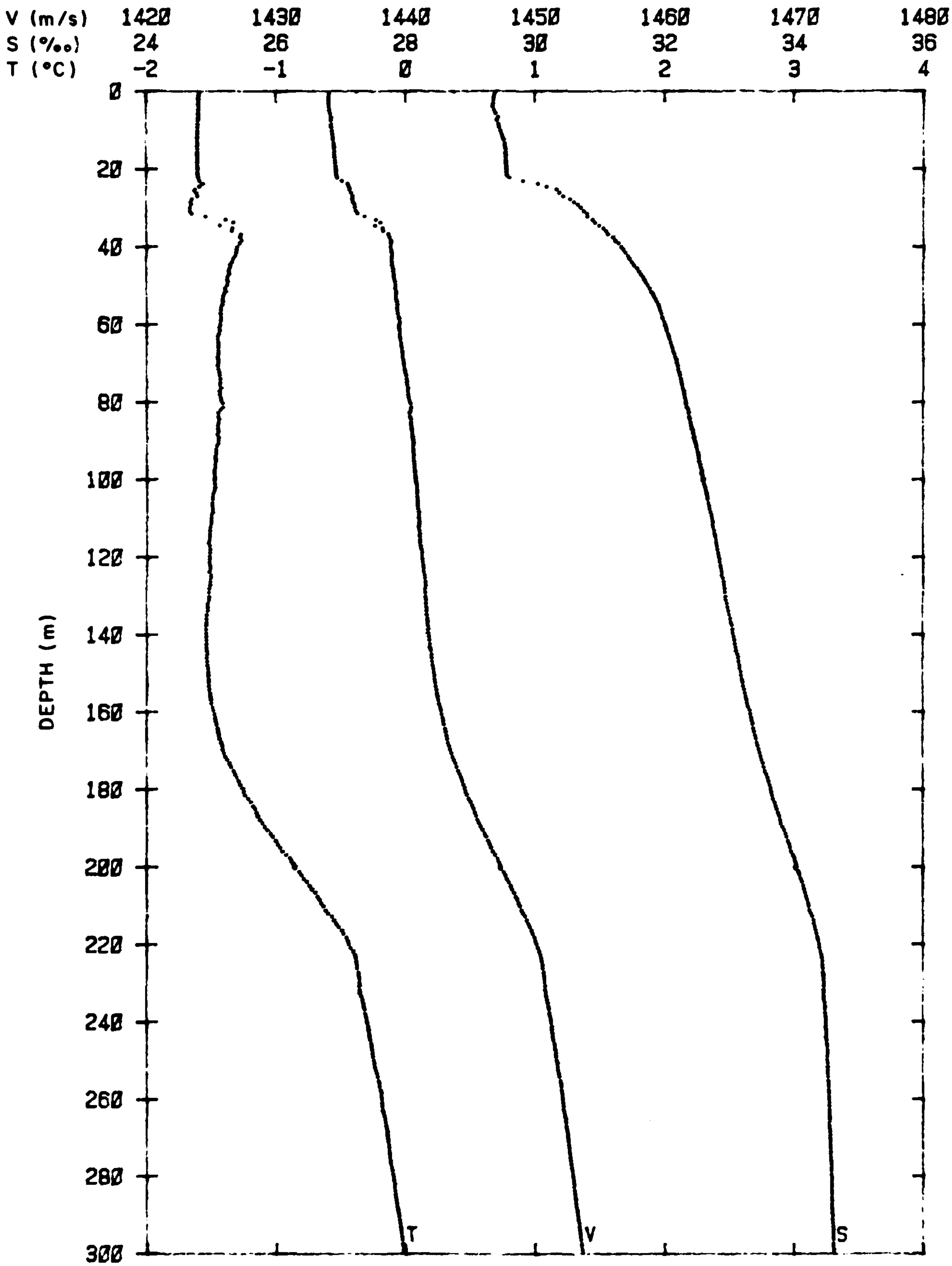

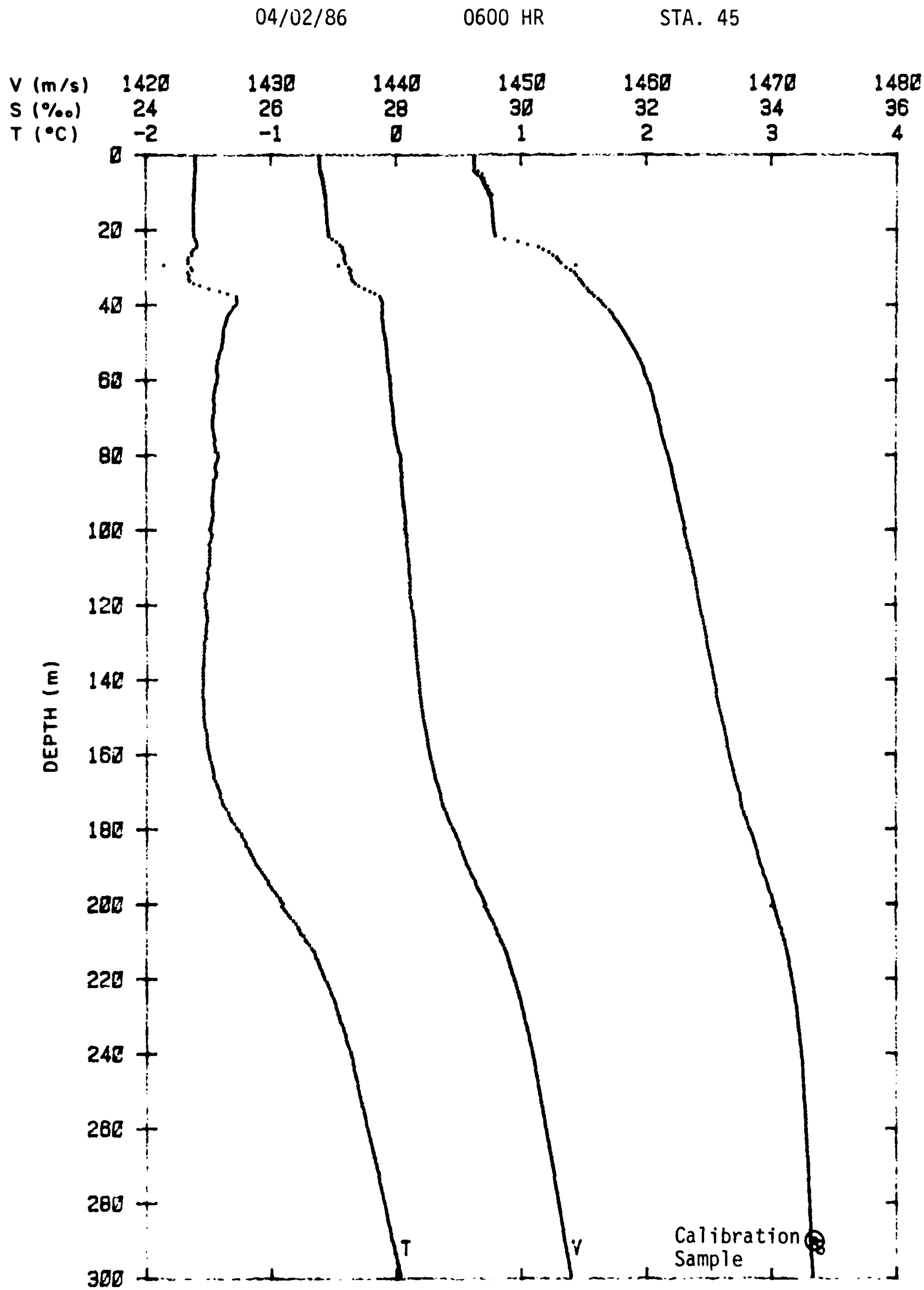

04/02/86
0600 HR
STA. 45
V (m/s) 1420 1430 1440 1450 1460 1470 1480
S (‰) 24 26 28 30 32 34 36
T (°C) -2 -1 0 1 2 3 4
DEPTH (m)
0
20
40
60
80
100
120
140
160
180
200
220
240
260
280
300
T
V
Calibration Sample

04/02/86 1730 HR STA. 47

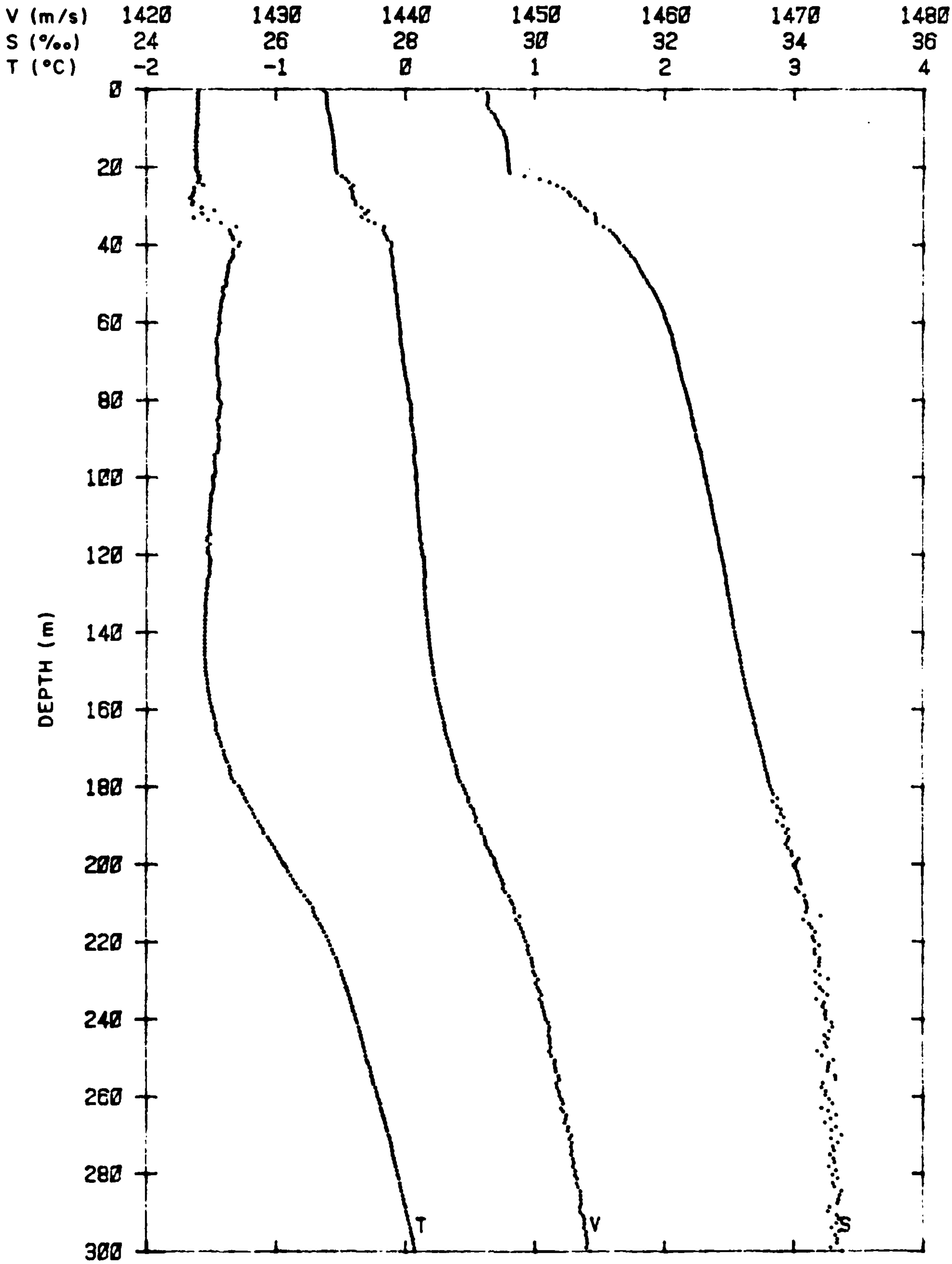

04/03/86 1426 HR STA. 49

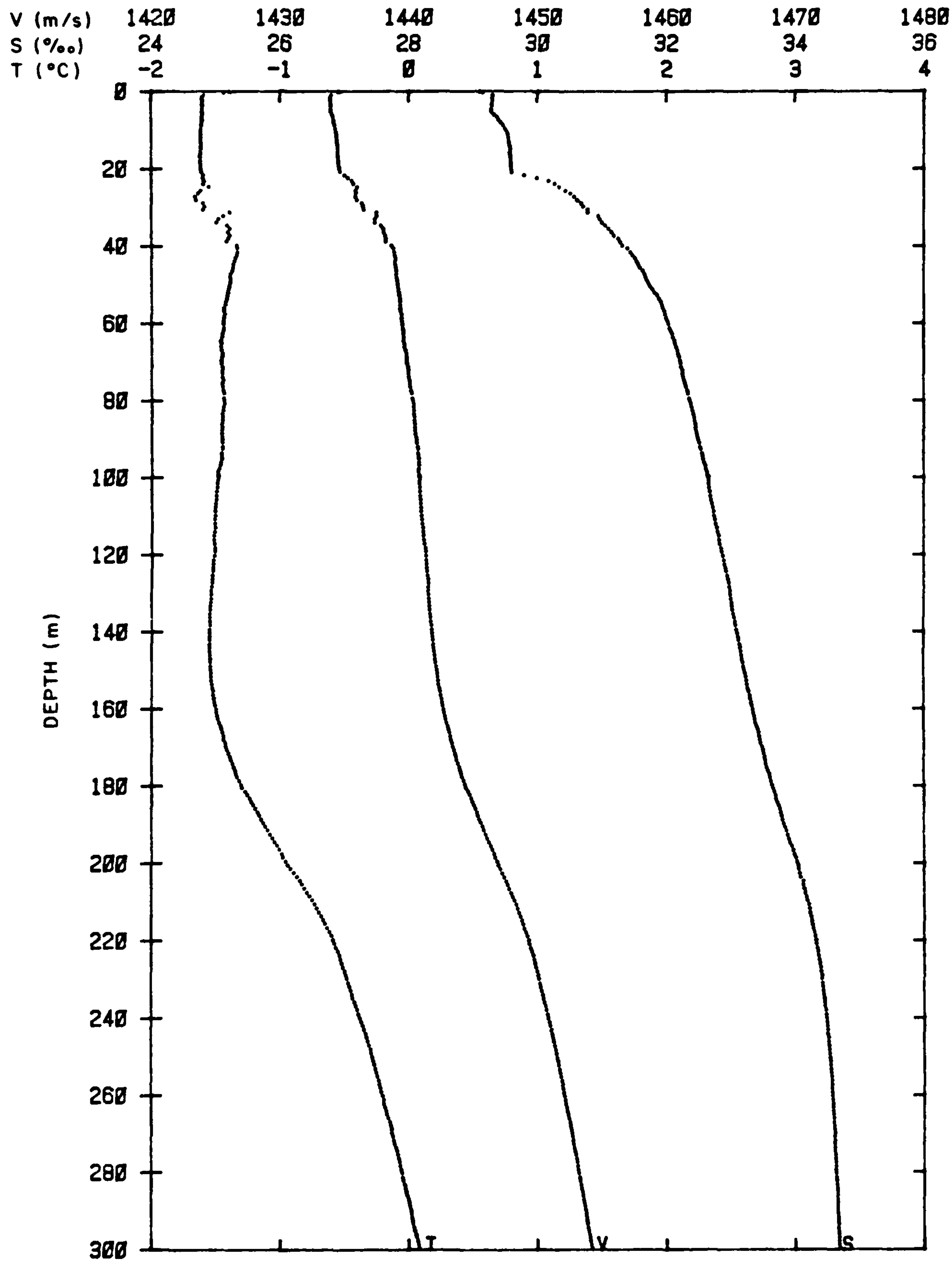

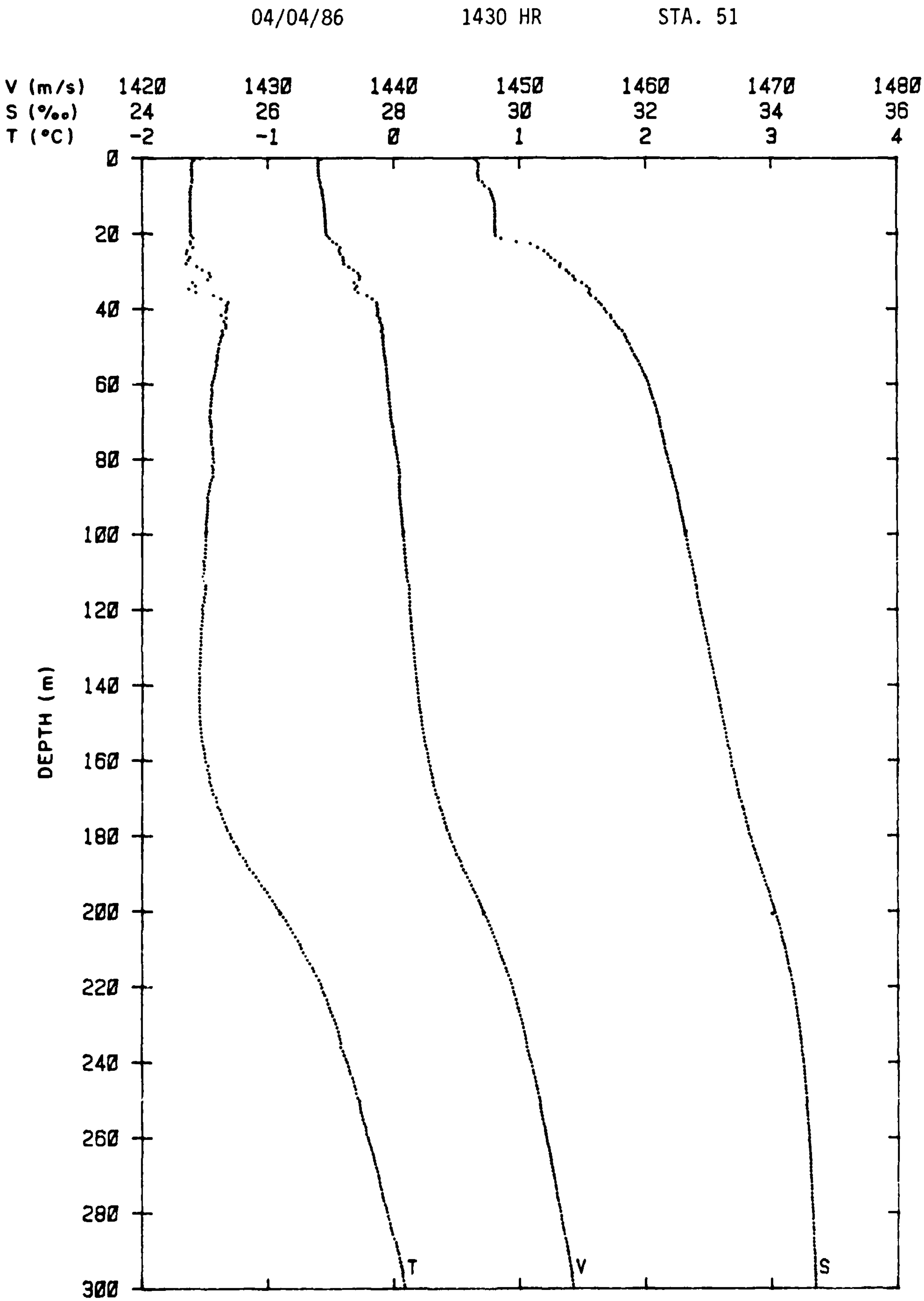
04/04/86
1430 HR
STA. 51
V (m/s) 1420 1430 1440 1450 1460 1470 1480
S (‰) 24 26 28 30 32 34 36
T (°C) -2 -1 0 1 2 3 4
DEPTH (m)
0
20
40
60
80
100
120
140
160
180
200
220
240
260
280
300
T
V
S

04/05/86 0715 HR STA. 53

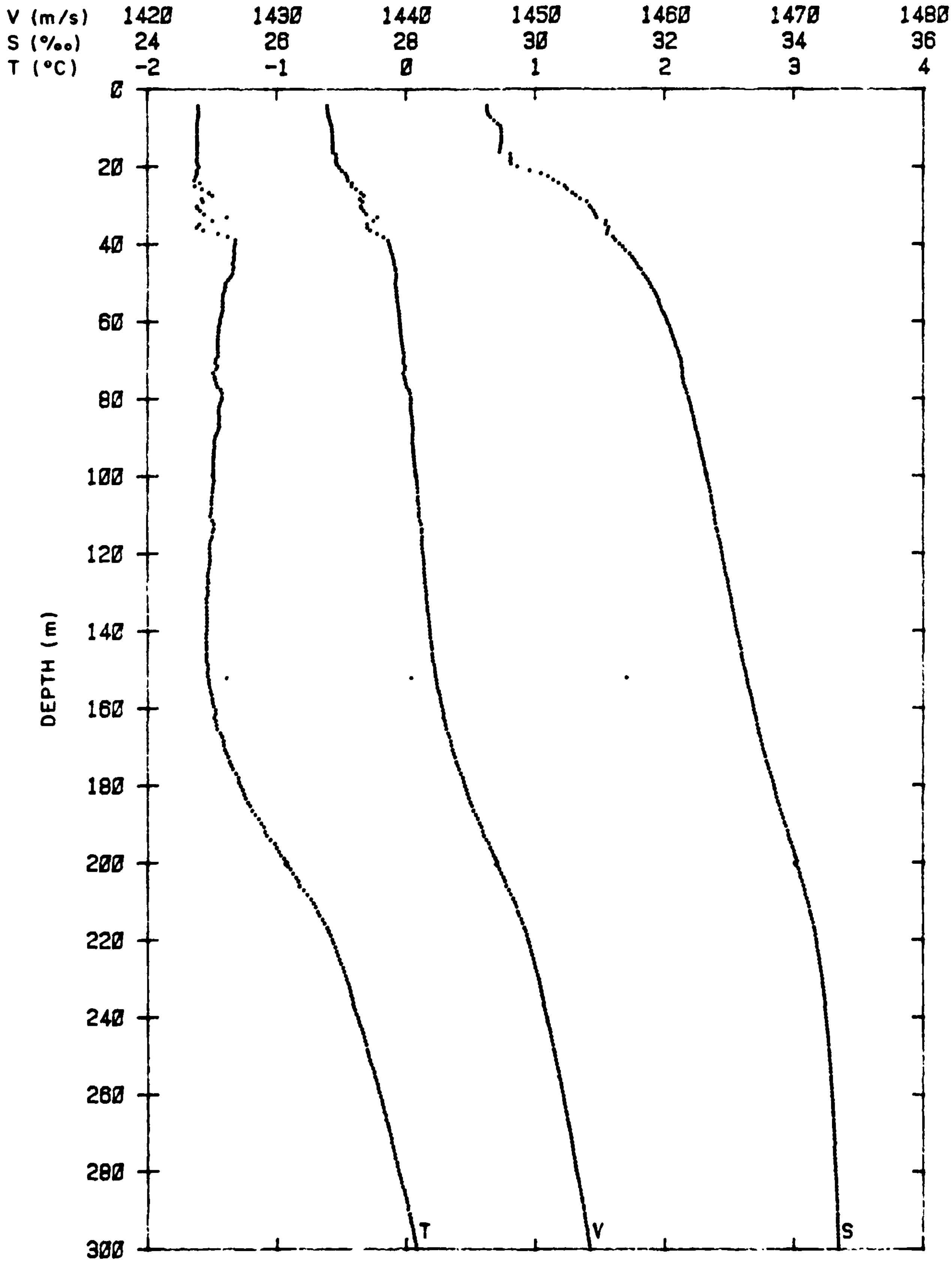

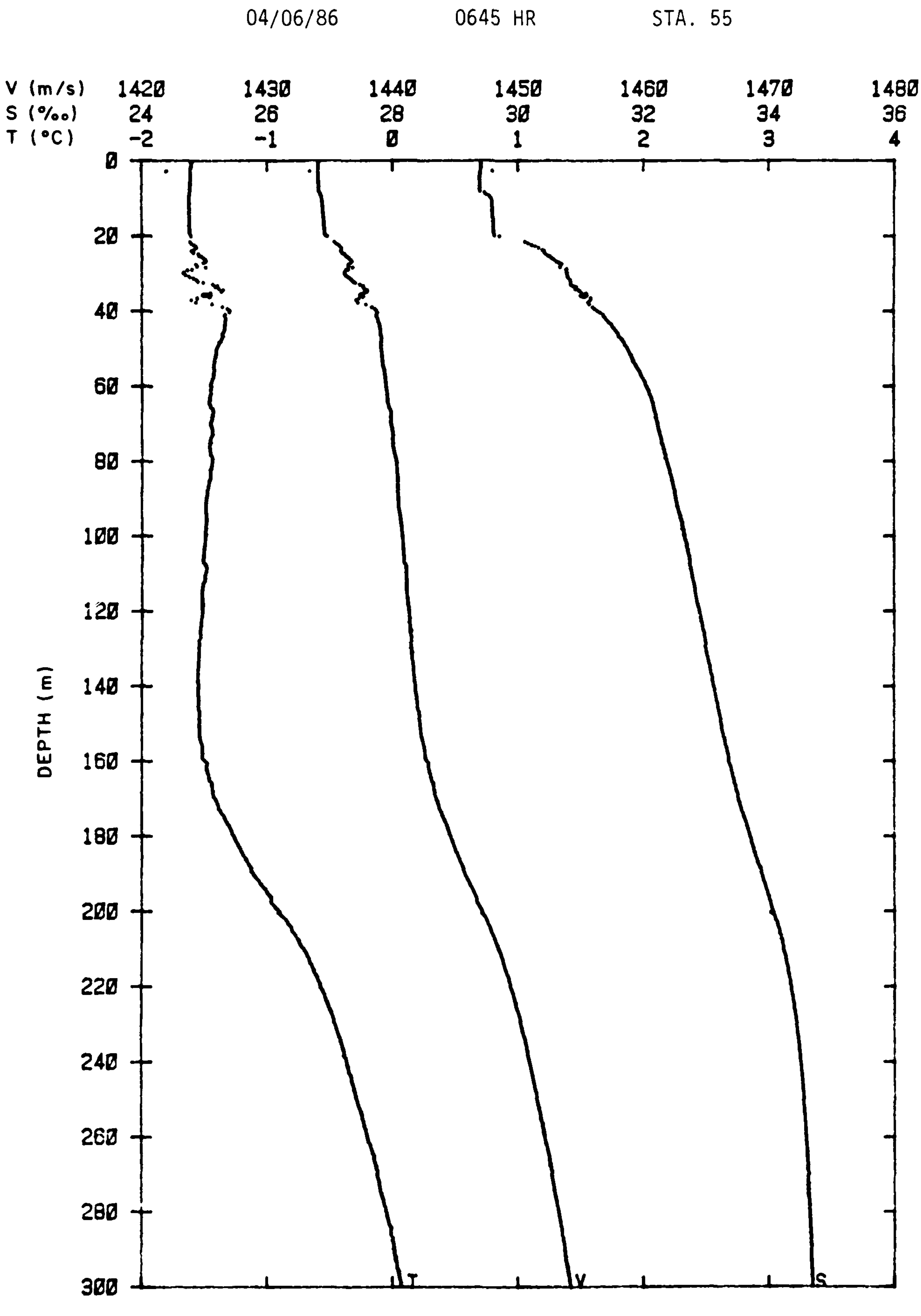
04/06/86
0645 HR
STA. 55
V (m/s) 1420 1430 1440 1450 1460 1470 1480
S (‰) 24 26 28 30 32 34 36
T (°C) -2 -1 0 1 2 3 4
DEPTH (m)
0 20 40 60 80 100 120 140 160 180 200 220 240 260 280 300
T
V
S

04/07/86 1225 HR STA. 57

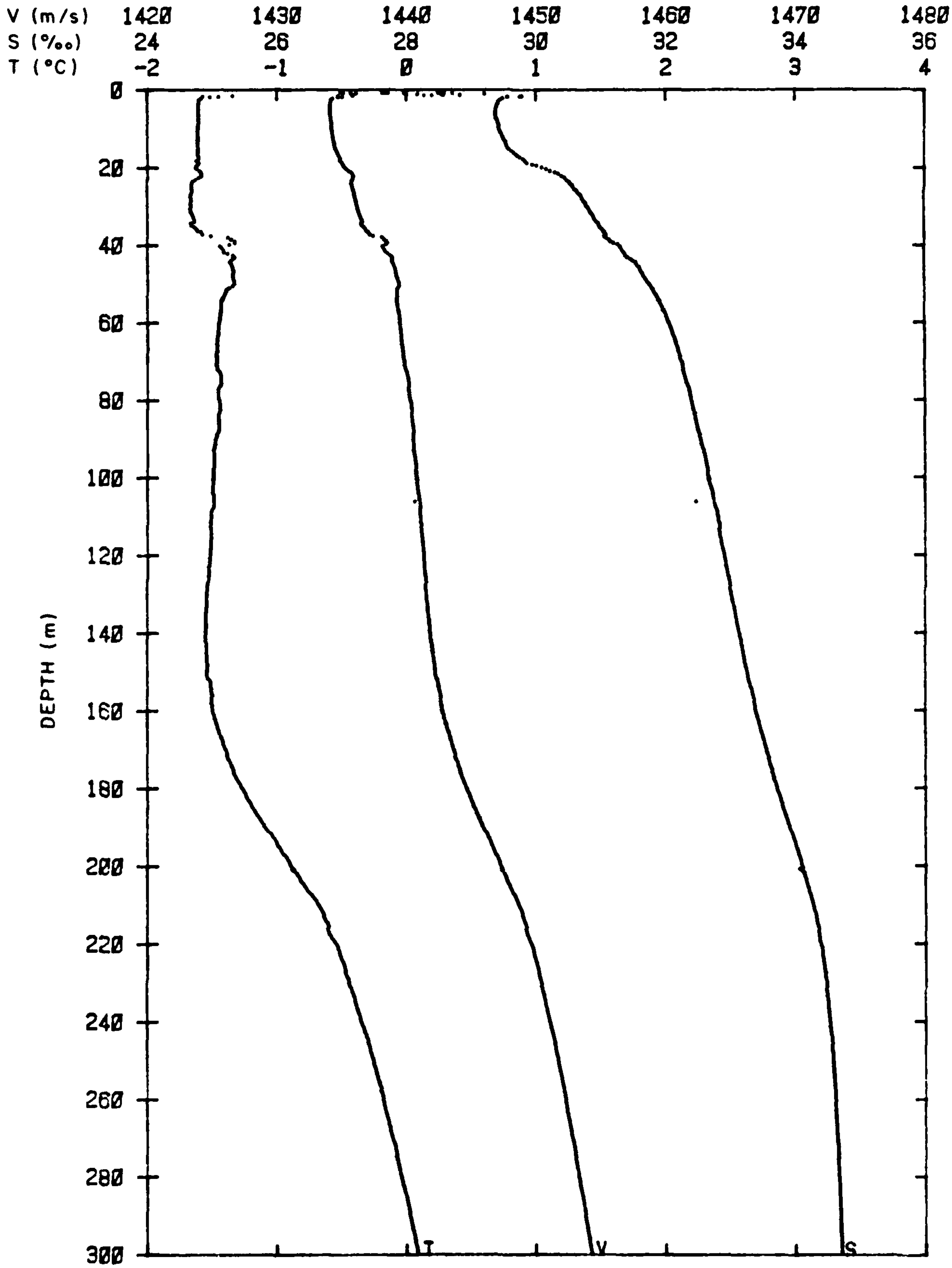

04/08/86 0630 HR STA. 59

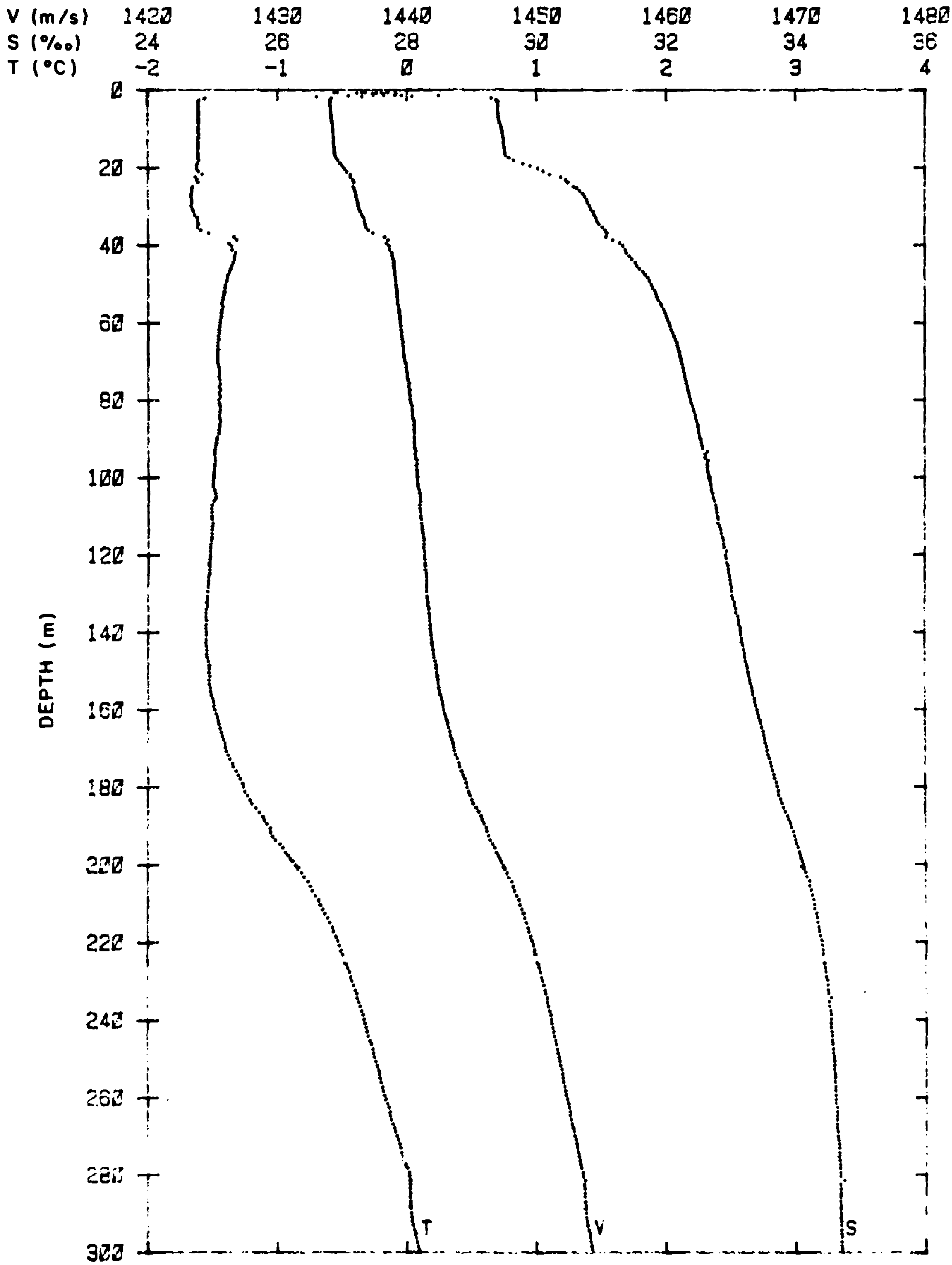

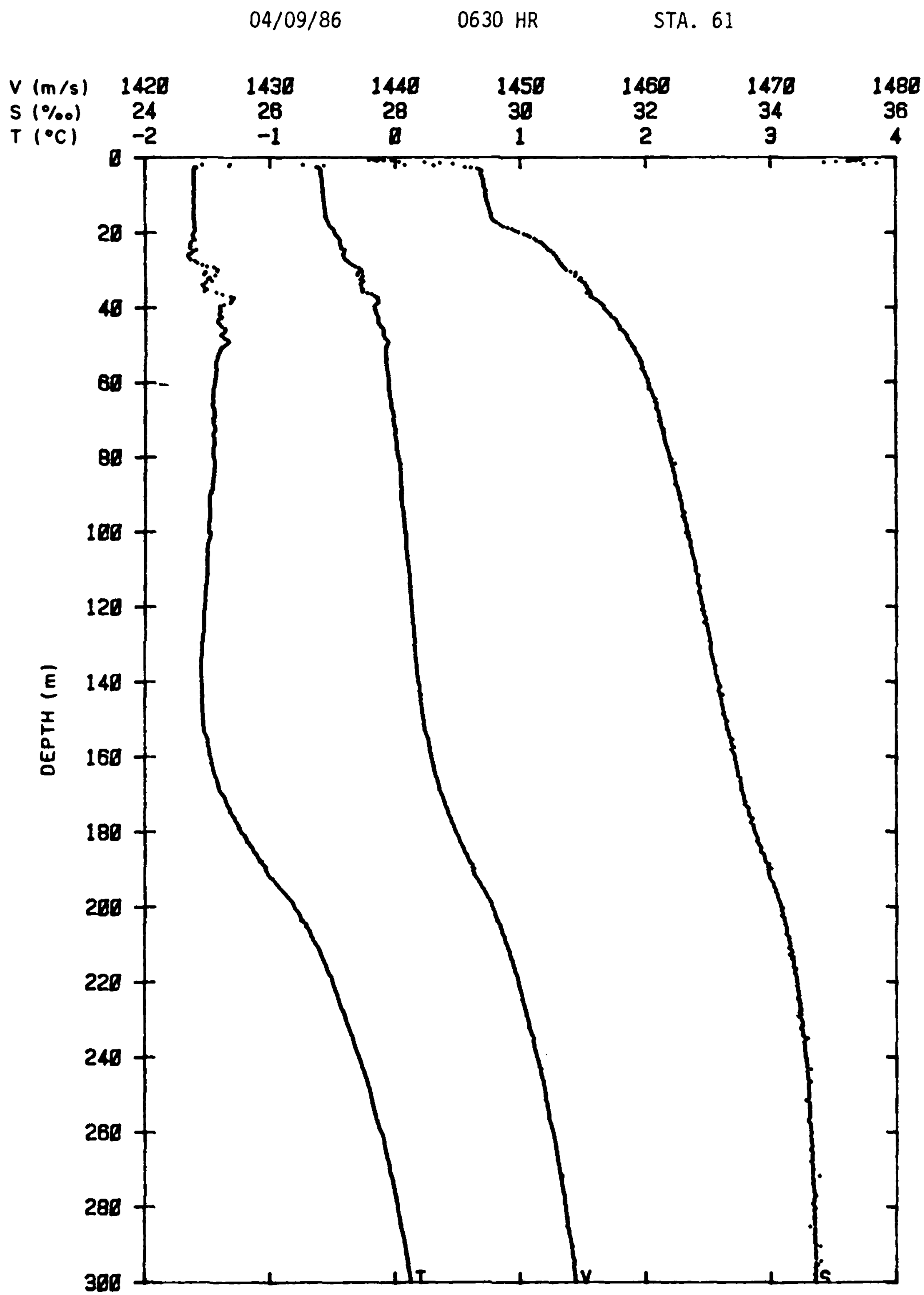

04/09/86
0630 HR
STA. 61
V (m/s) 1420 1430 1440 1450 1460 1470 1480
S (‰) 24 26 28 30 32 34 36
T (°C) -2 -1 0 1 2 3 4
DEPTH (m)
0
20
40
60
80
100
120
140
160
180
200
220
240
260
280
300
T
V
S

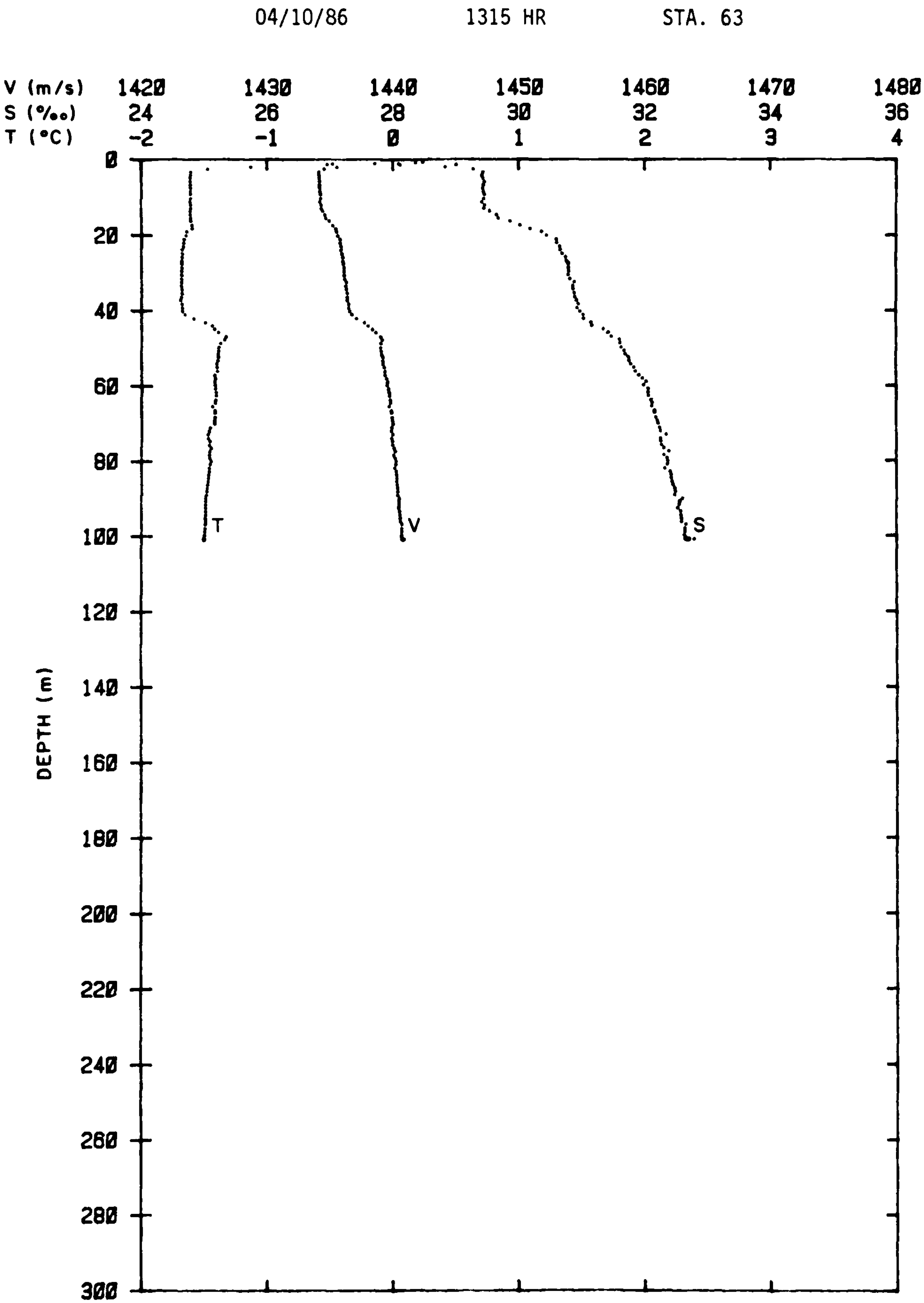
04/10/86
1315 HR
STA. 63
V (m/s) 1420 1430 1440 1450 1460 1470 1480
S (‰) 24 26 28 30 32 34 36
T (°C) -2 -1 0 1 2 3 4
DEPTH (m)
0 20 40 60 80 100 120 140 160 180 200 220 240 260 280 300
T
V
S

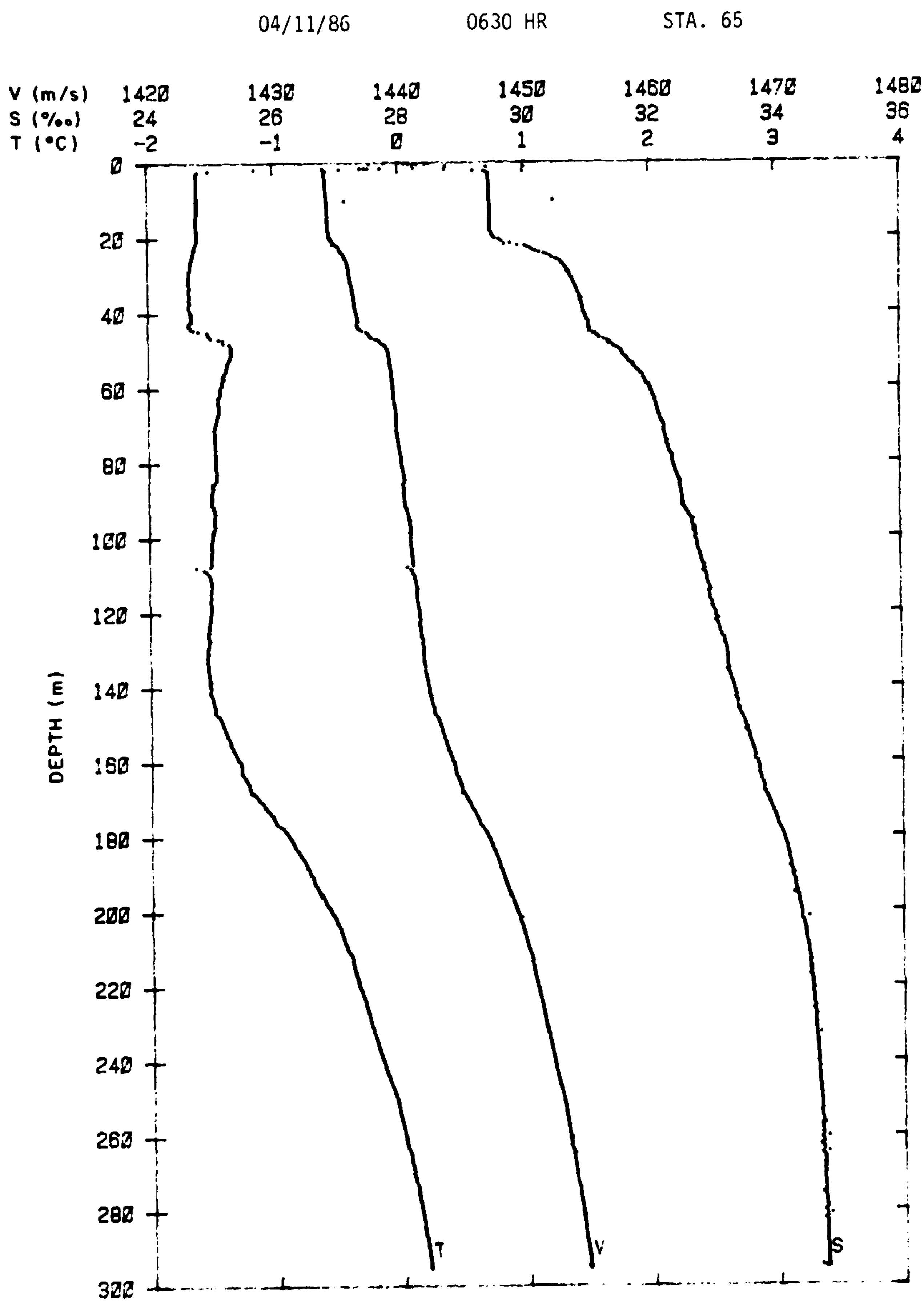
04/11/86
0630 HR
STA. 65
V (m/s) 1420 1430 1440 1450 1460 1470 1480
S (‰) 24 26 28 30 32 34 36
T (°C) -2 -1 0 1 2 3 4
DEPTH (m)
0 20 40 60 80 100 120 140 160 180 200 220 240 260 280 300
T
V
S

04/12/86 0640 HR STA. 67

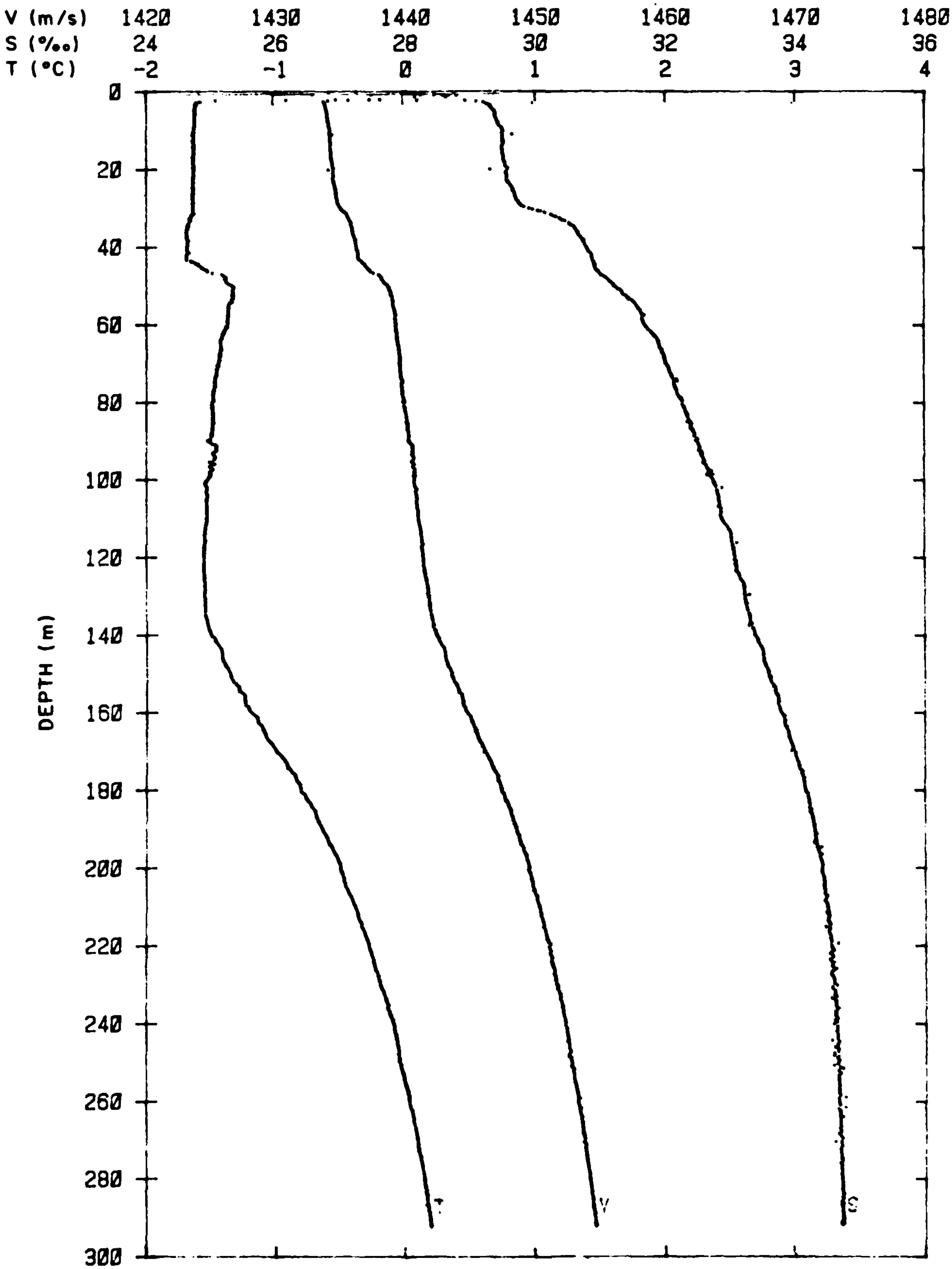

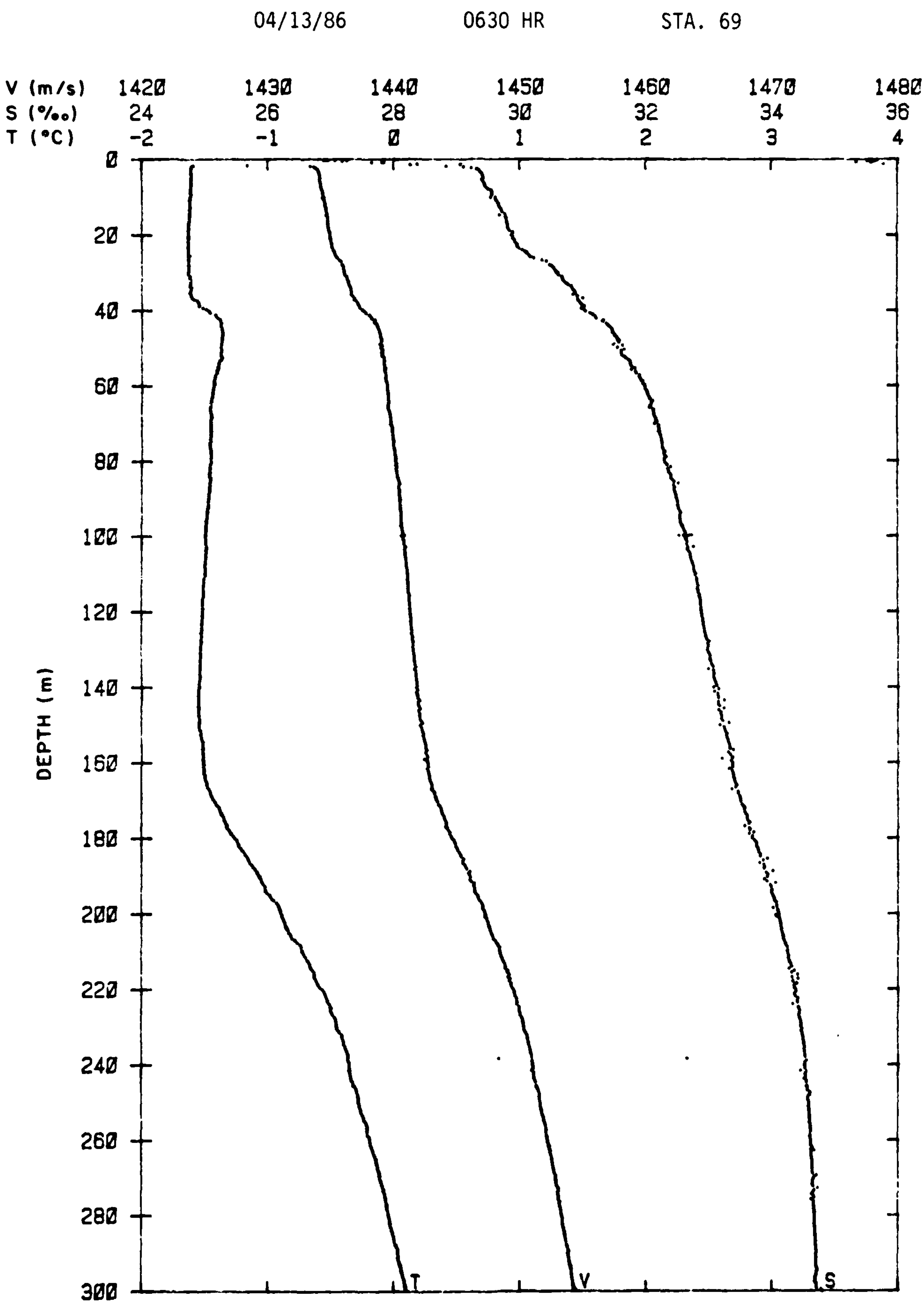
04/13/86
0630 HR
STA. 69
V (m/s) 1420 1430 1440 1450 1460 1470 1480
S (‰) 24 26 28 30 32 34 36
T (°C) -2 -1 0 1 2 3 4
DEPTH (m)
0
20
40
60
80
100
120
140
160
180
200
220
240
260
280
300
T
V
S

04/14/86 0645 HR STA. 71

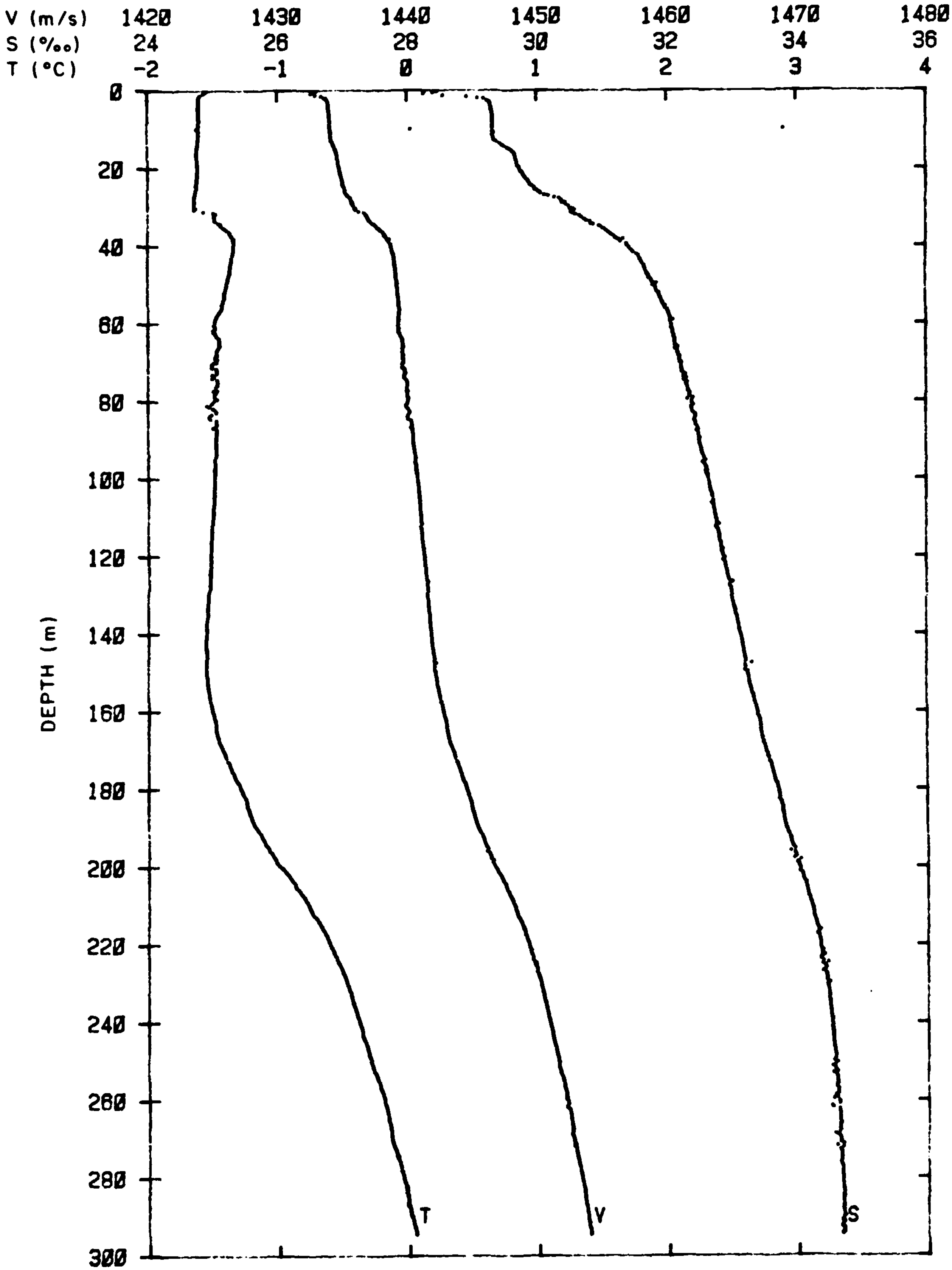

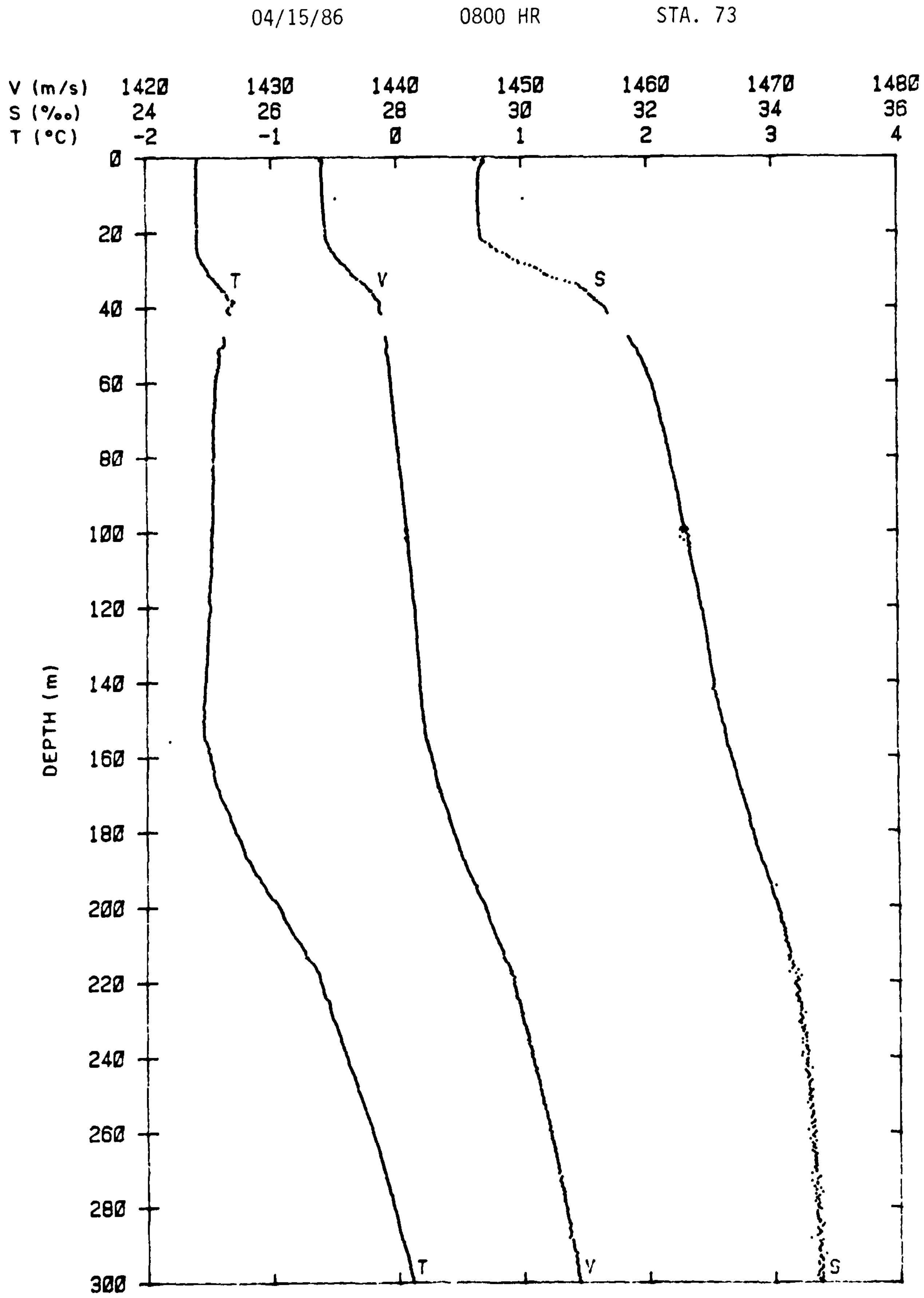
04/15/86
0800 HR
STA. 73
V (m/s) 1420 1430 1440 1450 1460 1470 1480
S (‰) 24 26 28 30 32 34 36
T (°C) -2 -1 0 1 2 3 4
DEPTH (m)
0 20 40 60 80 100 120 140 160 180 200 220 240 260 280 300
T
V
S

04/16/86 0745 HR STA. 75

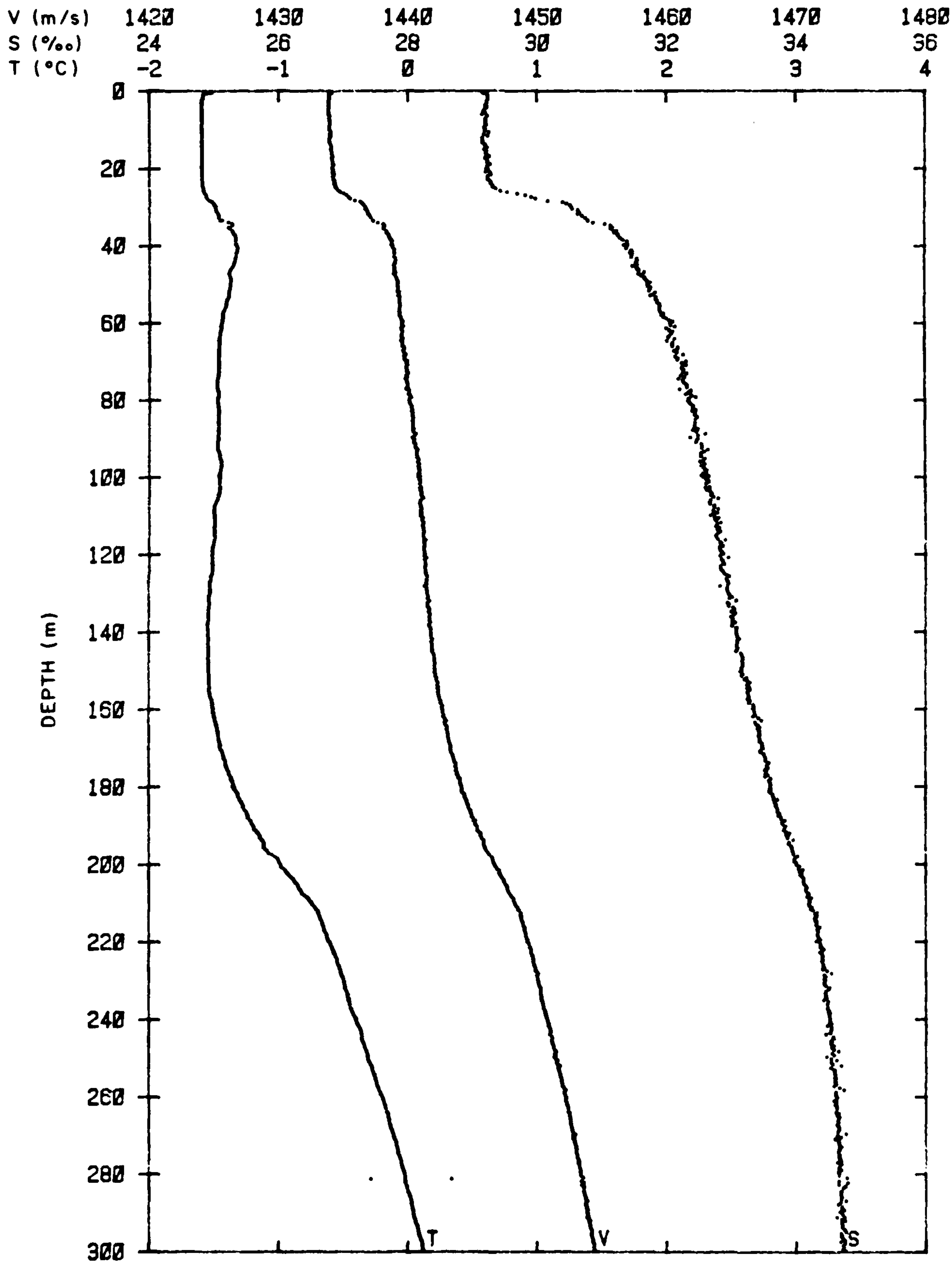

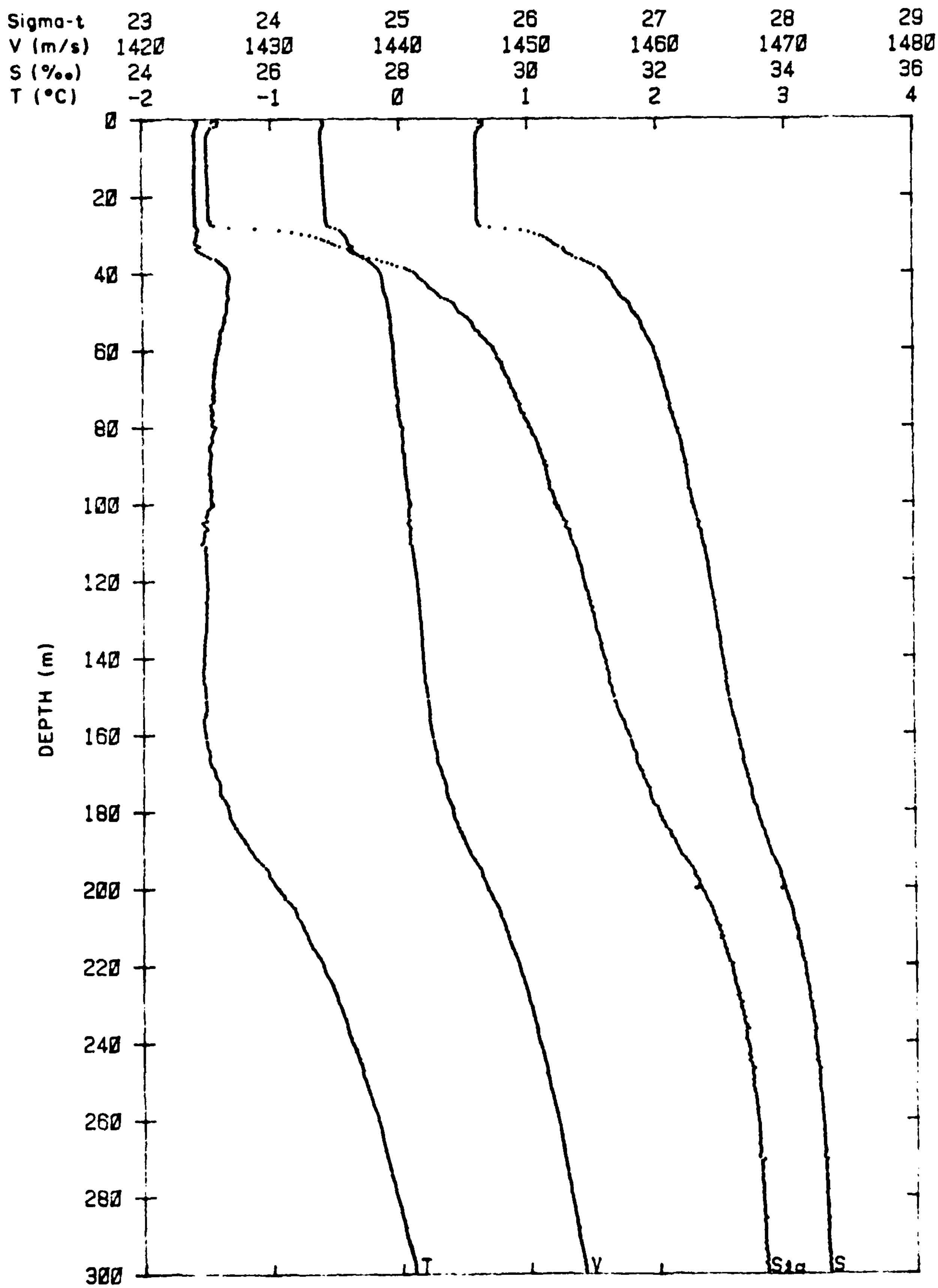
Sigma-t 23 24 25 26 27 28 29
V (m/s) 1420 1430 1440 1450 1460 1470 1480
S (‰) 24 26 28 30 32 34 36
T (°C) -2 -1 0 1 2 3 4
DEPTH (m)
0
20
40
60
80
100
120
140
160
180
200
220
240
260
280
300
T
V
Sig
S

04/18/86 0545 HR STA. 79

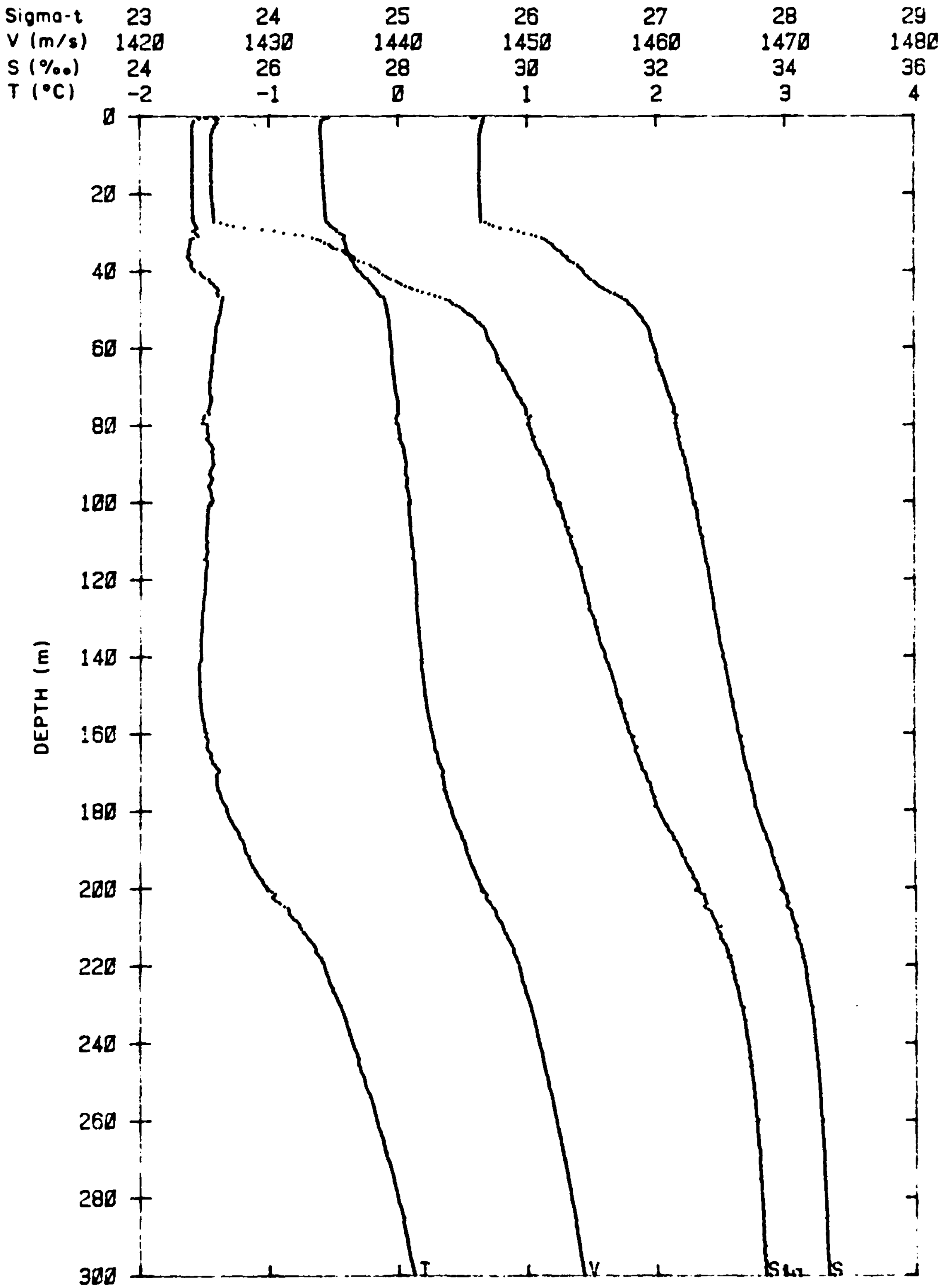

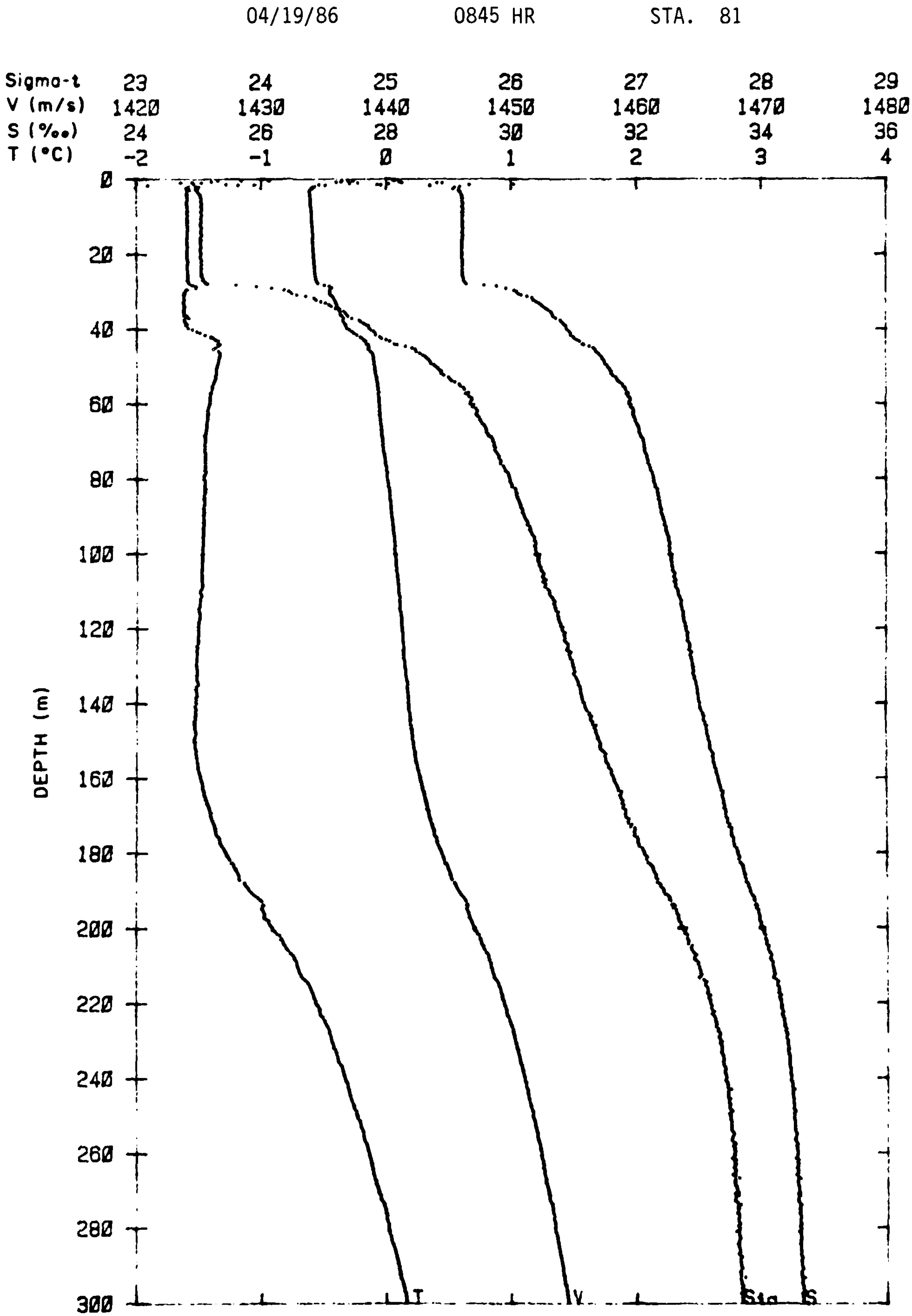
04/19/86
0845 HR
STA. 81
Sigma-t 23 24 25 26 27 28 29
V (m/s) 1420 1430 1440 1450 1460 1470 1480
S (‰) 24 26 28 30 32 34 36
T (°C) -2 -1 0 1 2 3 4
DEPTH (m)
0
20
40
60
80
100
120
140
160
180
200
220
240
260
280
300
T
V
Sig
S

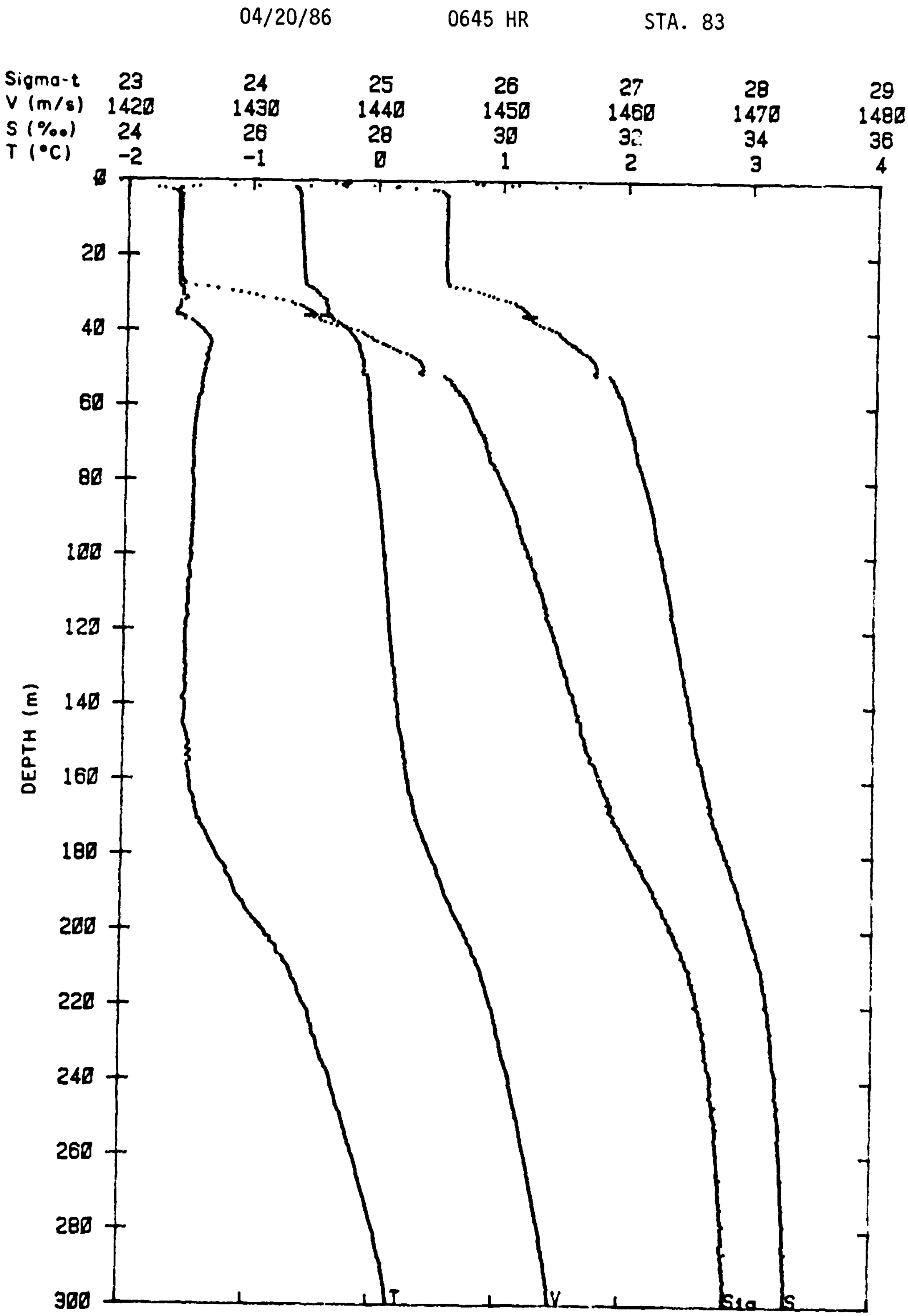
04/20/86
0645 HR
STA. 83
Sigma-t 23 24 25 26 27 28 29
V (m/s) 1420 1430 1440 1450 1460 1470 1480
S (‰) 24 26 28 30 32 34 36
T (°C) -2 -1 0 1 2 3 4
DEPTH (m)
0
20
40
60
80
100
120
140
160
180
200
220
240
260
280
300
T
V
Sig
S

04/22/86 0815 HR STA. 85

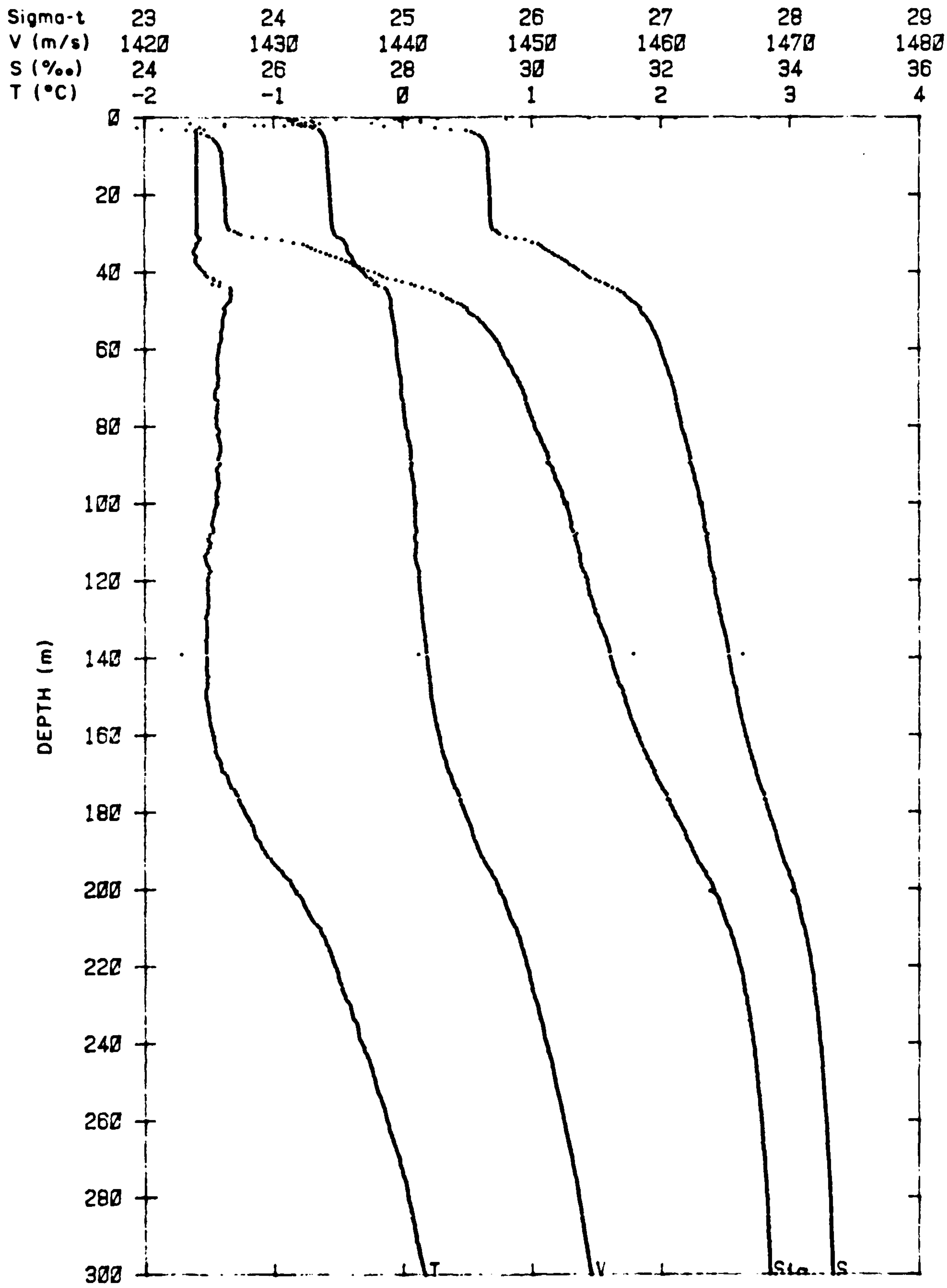

04/23/86 1730 HR STA. 87

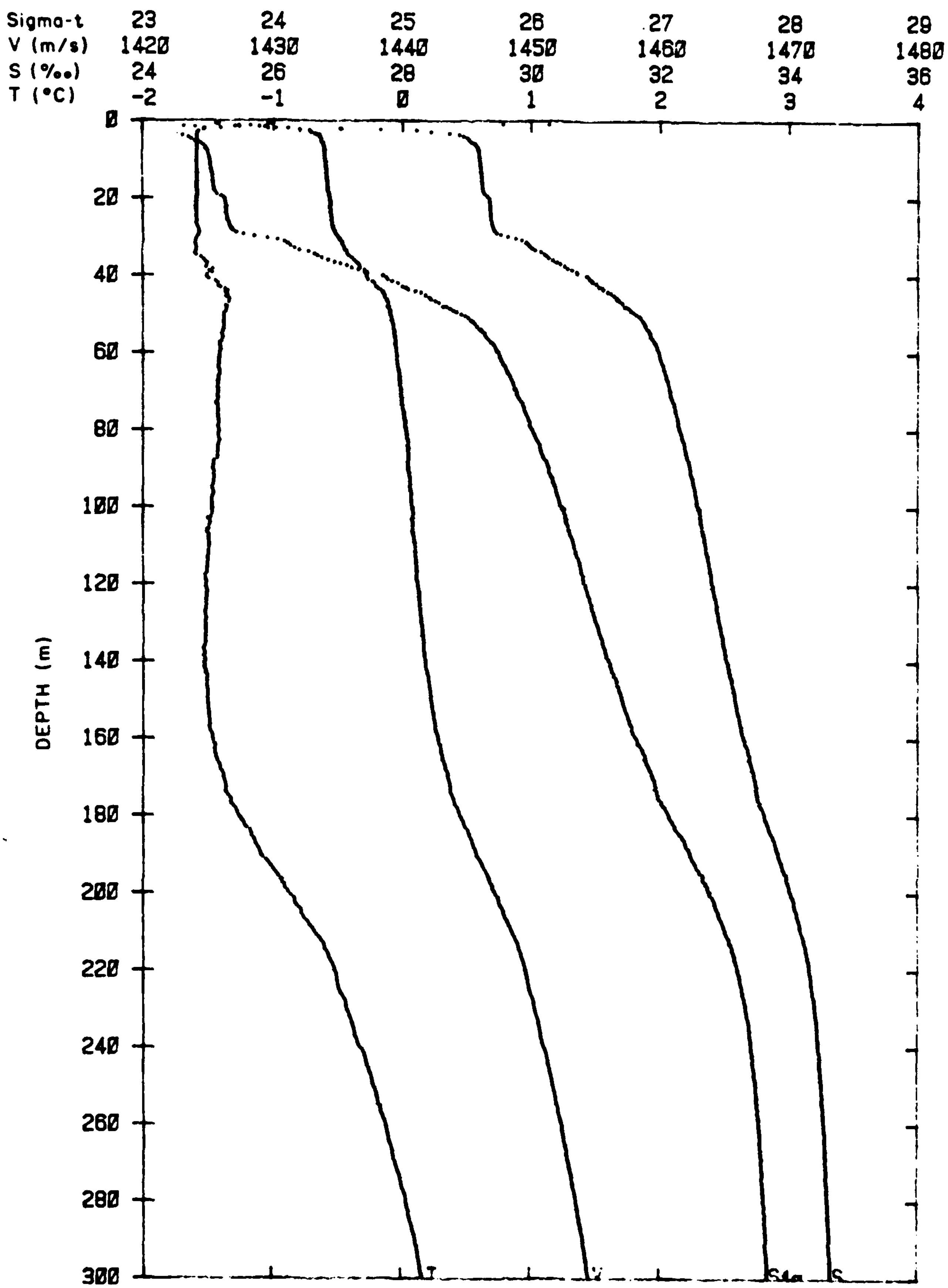

04/24/86 1615 HR STA. 89

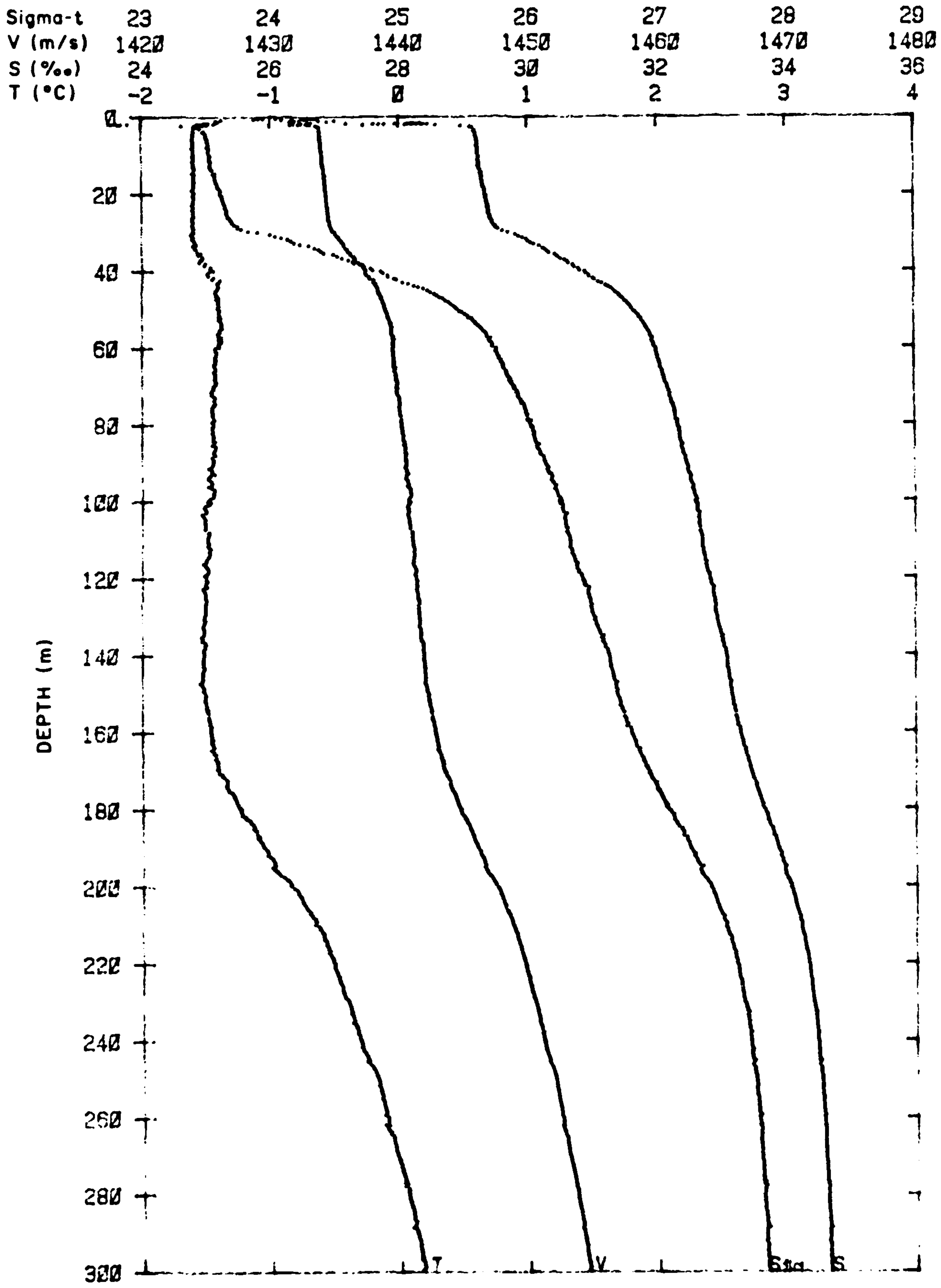

04/25/86 0815 HR STA. 91

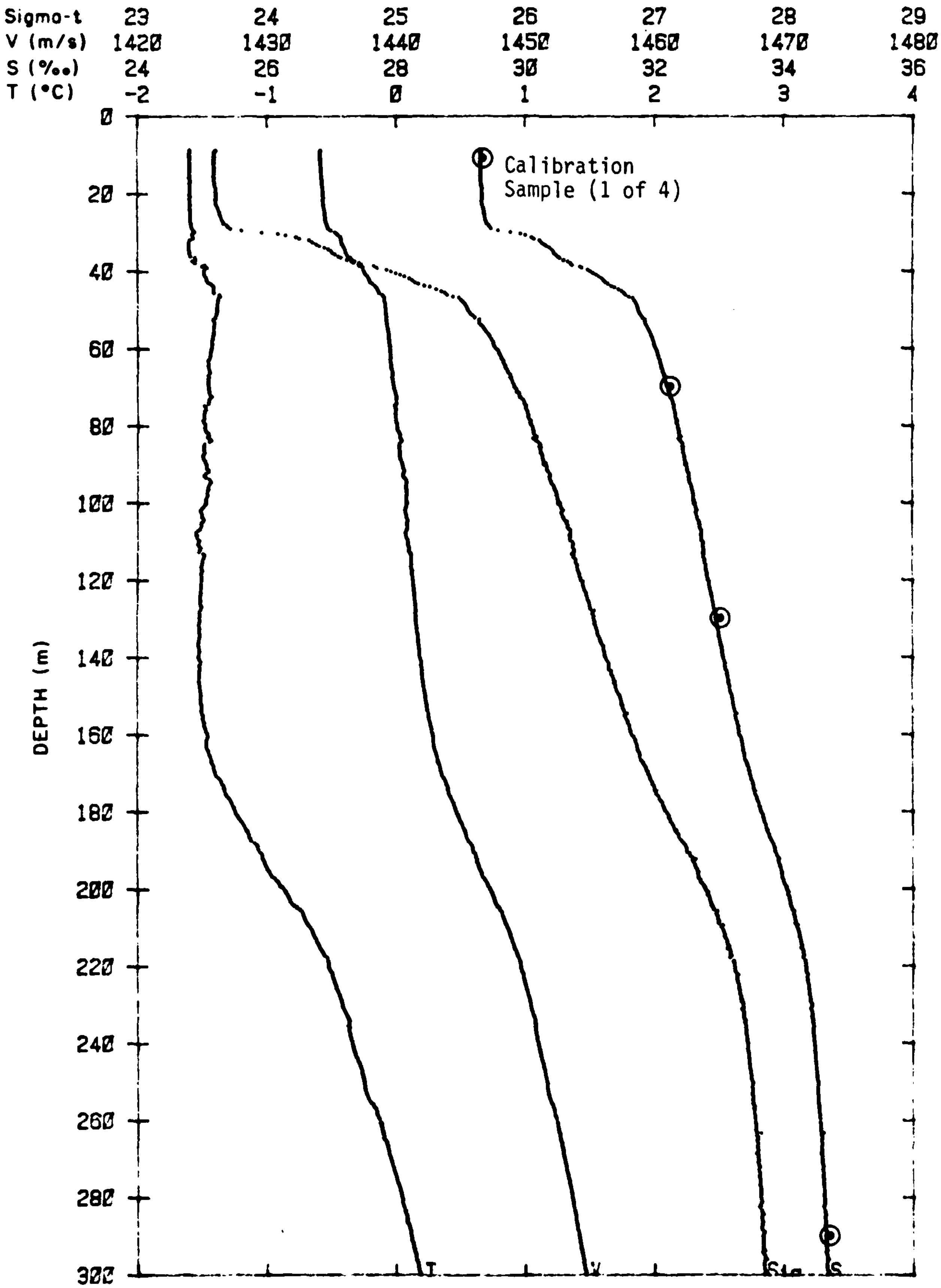

04/25/86 2045 HR STA. 93

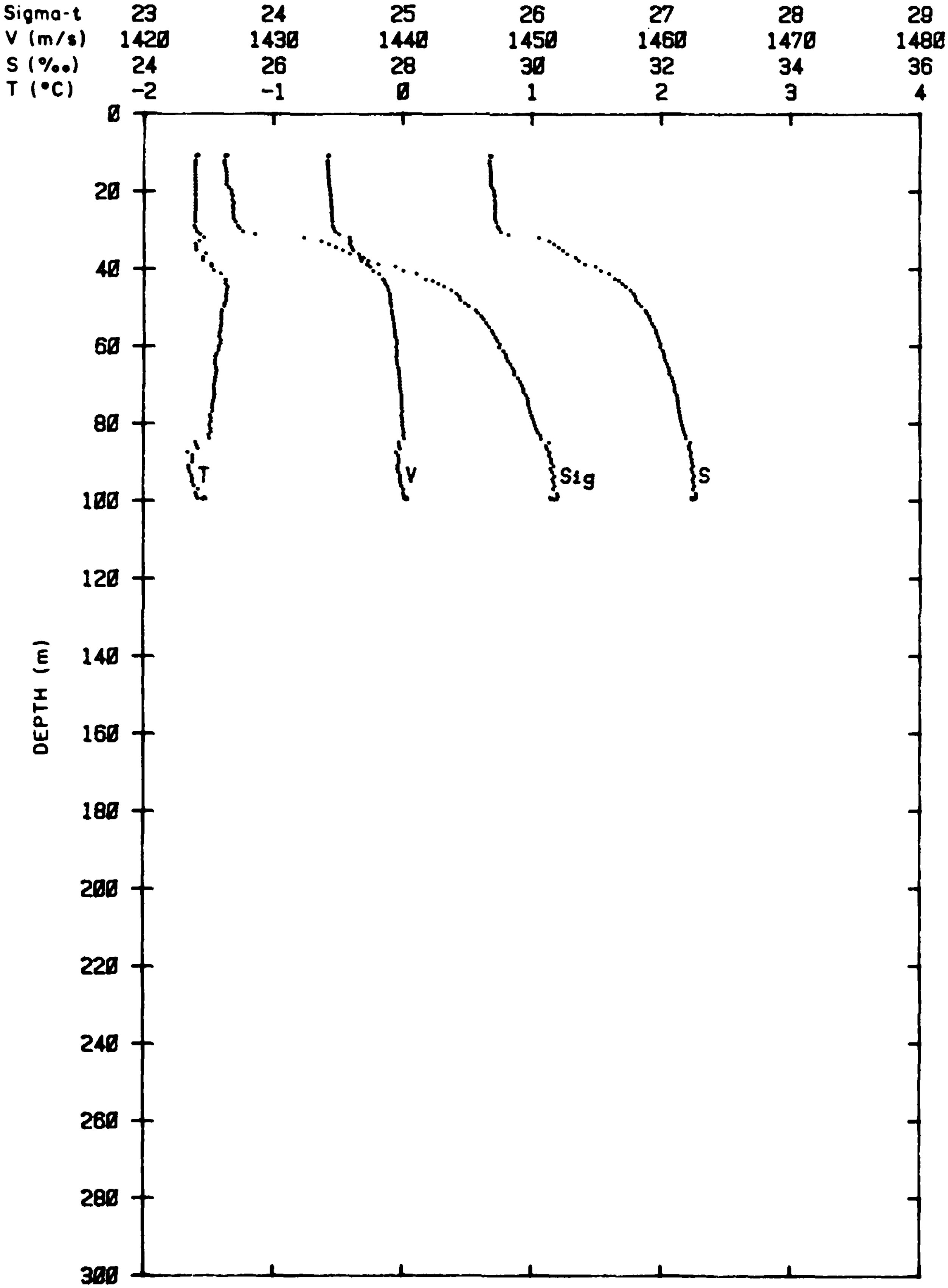

04/25/86 1200 HR DEEP CAST

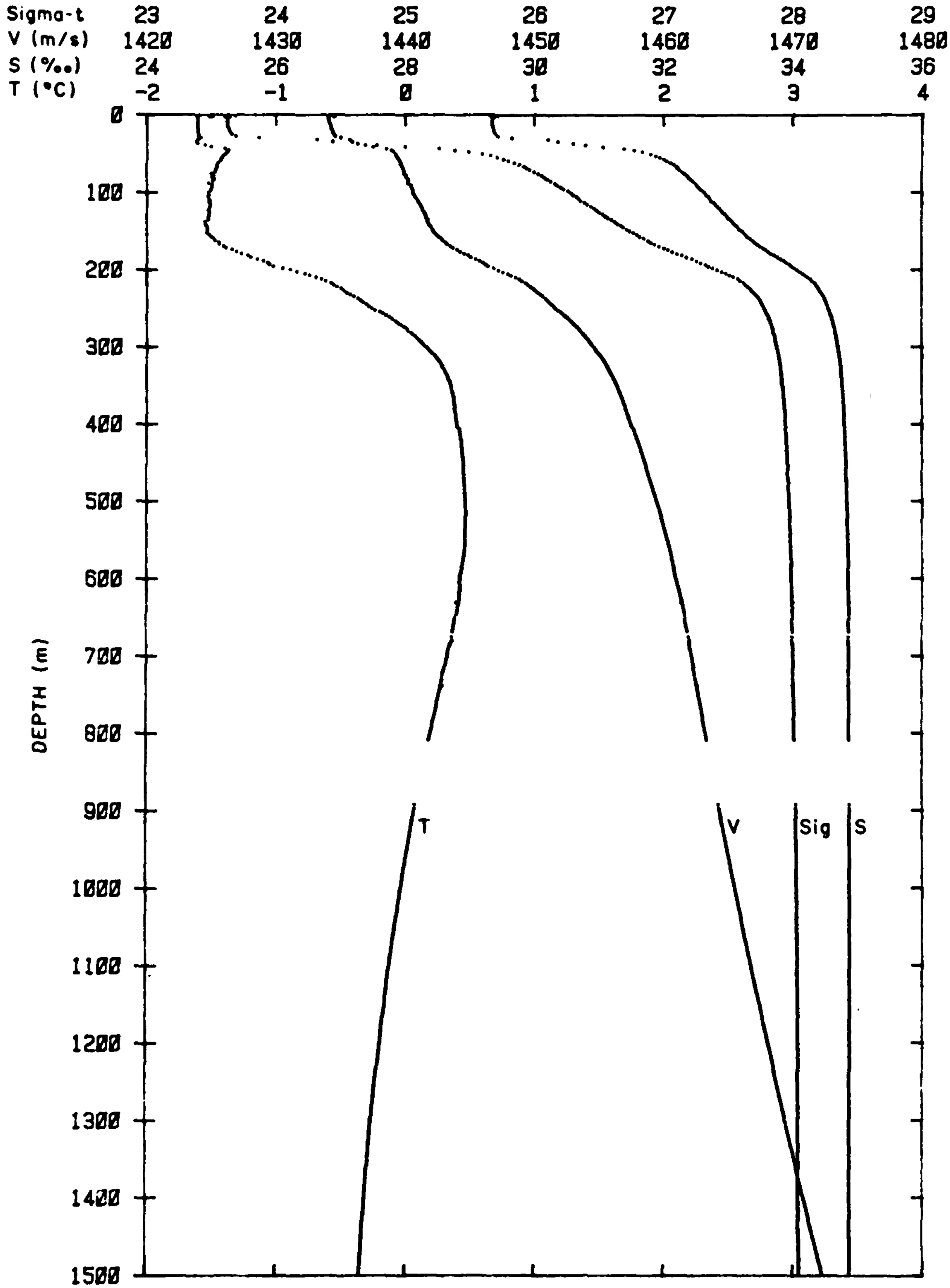

Distribution List

Assistant Secretary of the Navy
(Research, Engineering and Systems)
Department of the Navy
Washington, DC 20350 [2 cp]

Chief of Naval Operations
Department of the Navy
Washington, DC 20350-2000

OP 006D
OP 006T
OP 02
OP 095
OP 098
OP 22
OP 223
OP 951
OP 951B3

Director of Defense Research and Engineering
Office of Assistant Director (Ocean Control)
The Pentagon
Washington, DC 20301

Chief of Naval Research
Department of the Navy
800 North Quincy Street
Arlington, VA 22217

OCNR 00
OCNR 112
OCNR 1125
OCNR 1321 [2 cp]

Office of Naval Research
R. Silverman, Resident Representative
315 University District Bldg., JD-16
1107 N.E. 45th Street
Seattle, WA 98195

Office of Naval Technology
Department of the Navy
Ballston Center Tower #1
800 N. Quincy Street
Arlington, VA 22217

OCNR 22
OCNR 23
OCNR 232
OCNR 234

Commander
Naval Air Systems Command Hq.
Department of the Navy
Washington, DC 20361 [2 cp]

AIR 340L

Commander
Space and Naval Warfare Systems Command (NC1)
(SPAWAR)
Department of the Navy
Washington, DC 20363-5100

SPAWAR 03
SPAWAR 005
PDW-180
PDW-181
PDW-182

Commander
Naval Sea Systems Command
Department of the Navy
Washington, DC 20362

NSEA 05R26
NSEA 06
NSEA 06U
NSEA 63D
Code PMS-402 [2 cp]
Code PMS-407 [2 cp]

Commanding Officer
Naval Underwater Systems Center
Newport, RI 02840

Library [2 cp]
Code 00
Code 01Y [4 cp]
Code 25202
Code 3636
Code 3824

Officer-in-Charge
New London Laboratory
Naval Underwater Systems Center
New London, CT 06320

Library [2 cp]
Code 2111
Code 3211
Code 3422
Code 3423 [2 cp]

Commander
Naval Weapons Center
China Lake, CA 93555

Library

Commander
Naval Ocean Systems Center
San Diego, CA 92152

Library [4 cp]
Code 00
Code 19 [5 cp]
Code 541
Code 614 [3 cp]
Code 844 [3 cp]

Director
Naval Research Laboratory
Washington, DC 20375

Technical Information Division [3 cp]
Acoustics Division (D. Bradley)
Acoustics Division (C. Votaw)

Commanding Officer
Naval Ocean Research and Development Activity
NSTL Station, MS 39529

Library [4 cp]
Code 113
Code 200
Code 242 [3 cp]
Code 243
Code 270

Commanding Officer
Naval Oceanographic Office
Bay St. Louis
NSTL Station, MS 39522

Code 7300 (W. Jobst)
Code 7320 (R. Christensen)

Commander
Naval Air Development Center
Warminster, PA 18974

Library [2 cp]
Code 3031 (A. Horbach)

Commander
David W. Taylor Naval Ship Research
and Development Center
Bethesda, MD 20084

Library
Code 1720.4 (K. Nashida) [2 cp]

Commander
Naval Surface Weapons Center
White Oak
Silver Spring, MD 20910

Library [4 cp]
Code R-01
Code R-43 (J. Scarzello) [2 cp]
Code U-04 (M. Kleinerman)
Code U-13 (B. Moore)
Code U-42 (J. Bacom)
C. McClure
P. Keller

Commanding Officer
Naval Civil Engineering Laboratory
Port Hueneme, CA 93043-5003

Library
Code L43P3 [2 cp]

Commanding Officer
Naval Coastal Systems Center
Panama City, FL 32407

Commander, SECOND Fleet
Fleet Post Office
New York, NY 09501

Commander, THIRD Fleet
Fleet Post Office
San Francisco, CA 96601

Commander Submarine Force
U.S. Atlantic Fleet
Norfolk, VA 23511

Code 00
Code 019
Code N311

Commander Submarine Force
U.S. Pacific Fleet
FPO San Francisco, CA 96601

Code 00
Code N2
Code N21

Commander
Submarine Squadron THREE
Fleet Station Post Office
San Diego, CA 92132

Commander
Submarine Group FIVE
Fleet Station Post Office
San Diego, CA 92132

Commander
Submarine Development Squadron TWELVE
Box 70
Naval Submarine Base - New London
Groton, CT 06340

Code 20

Director
Defense Advanced Research Project Agency
1400 Wilson Boulevard
Arlington, VA 22209

Commanding Officer
Naval Intelligence Support Center
4301 Suitland Road
Washington, DC 20390

Commanding Officer
Naval Submarine School
Box 70
Naval Submarine Base - New London
Groton, CT 06340

Commanding Officer
Naval Polar Oceanographic Center
4301 Suitland Road
Washington, DC 20390

LCDR H. Rosner
AG2 D. Culpepper
Library

Superintendent
Naval Postgraduate School
Monterey, CA 93940

Library [2 cp]
R. Bourke
R. Paquette

Director
Applied Research Laboratory
The Pennsylvania State University
State College, PA 16801

Library
E. Liska
R. Ingram [2 cp]
S. McDaniel
F. Symons, Jr.

Director
Applied Research Laboratories
The University of Texas at Austin
P.O. Box 8029
Austin, TX 78713-8029 [2 cp]

Director
Applied Physics Laboratory
University of Washington
1013 N.E. 40th Street
Seattle, WA 98105

R.L. Colony
J.G. Dworski
T.E. Ewart
R.E. Francois
G.R. Garrison
R.W. Gill
D.R. Jackson
F.W. Karig
J.C. Luby
J.H. Morison
C.G. Sienkiewicz
R.P. Stein
E.I. Thorsos
N. Untersteiner
T. Wen
D.P. Winebrenner
Library

Sandia National Laboratories
Kirtland Air Force Base
P.O. Box 5800
Albuquerque, NM 87185

Library
R. Thomas

Polar Research Laboratory, Inc.
6309 Carpenteria Avenue
Carpenteria, CA 90813

School of Oceanography
University of Washington
Seattle, WA 98195

Library
L. Coachman

National Oceanic and Atmospheric Administration
Pacific Marine Environmental Laboratory
7600 Sand Point Way N.E.
Seattle, WA 98115

K. Aagaard

UNCLASSIFIED

SECURITY CLASSIFICATION OF THIS PAGE (When Data Entered)

REPORT DOCUMENTATION PAGE

READ INSTRUCTIONS BEFORE COMPLETING FORM

1. REPORT NUMBER APL-UW 4-86	2. GOVT ACCESSION NO.	3. RECIPIENT'S CATALOG NUMBER
4. TITLE (and Subtitle) ENVIRONMENTAL MEASUREMENTS IN THE BEAUFORT SEA, SPRING 1986		5. TYPE OF REPORT & PERIOD COVERED Technical
		6. PERFORMING ORG. REPORT NUMBER APL-UW 4-86
7. AUTHOR(s) G.R. Garrison, T. Wen, R.E. Francois, W.J. Felton, M.L. Welch		8. CONTRACT OR GRANT NUMBER(s) N00024-85-C-6264
9. PERFORMING ORGANIZATION NAME AND ADDRESS Applied Physics Laboratory University of Washington 1013 N.E. 40th, Seattle, WA 98105		10. PROGRAM ELEMENT, PROJECT, TASK AREA & WORK UNIT NUMBERS PE 62435N Block RD3A Subproject RJ35I21
11. CONTROLLING OFFICE NAME AND ADDRESS Commander, Space and Naval Warfare Systems Command Code 005, Department of the Navy Washington, DC 20363-5100		12. REPORT DATE January 1987
		13. NUMBER OF PAGES 155
14. MONITORING AGENCY NAME & ADDRESS (if different from Controlling Office) Naval Ocean Research & Development Activity Code 242, NSTL Station Bay St. Louis, MS 39529-5004		15. SECURITY CLASS. (of this report) Unclassified
		15a. DECLASSIFICATION DOWNGRADING SCHEDULE

16. DISTRIBUTION STATEMENT (of this Report)

Approved for public release; distribution is unlimited.

17. DISTRIBUTION STATEMENT (of the abstract entered in Block 20, if different from Report)

18. SUPPLEMENTARY NOTES

19. KEY WORDS (Continue on reverse side if necessary and identify by block number)

Arctic	Currents
Beaufort Sea	Floe drift
CTD profiles	Weather

20. ABSTRACT (Continue on reverse side if necessary and identify by block number)

Environmental measurements at an ice camp in the Beaufort Sea are reported for the period 20 March to 2 May 1986. The measurements include weather, floe movement, CTD profiles, ice properties, currents relative to the floe, and underwater noise.

DD FORM 1 JAN 73 1473 EDITION OF 1 NOV 65 IS OBSOLETE
S/N 0102 LF 014 6601

UNCLASSIFIED

SECURITY CLASSIFICATION OF THIS PAGE (When Data Entered)